



Publicly Accessible Penn Dissertations

1-1-2015

Latency, Expression and Splicing During Infection With HIV

Scott Sherrill-Mix

University of Pennsylvania, shescott@mail.med.upenn.edu

Follow this and additional works at: <http://repository.upenn.edu/edissertations>

 Part of the [Bioinformatics Commons](#), [Biology Commons](#), and the [Virology Commons](#)

Recommended Citation

Sherrill-Mix, Scott, "Latency, Expression and Splicing During Infection With HIV" (2015). *Publicly Accessible Penn Dissertations*. 2008.
<http://repository.upenn.edu/edissertations/2008>

This paper is posted at ScholarlyCommons. <http://repository.upenn.edu/edissertations/2008>
For more information, please contact libraryrepository@pobox.upenn.edu.

Latency, Expression and Splicing During Infection With HIV

Abstract

Over 35 million people are living with human immunodeficiency virus (HIV-1). The mechanisms causing integrated provirus to become latent, the diversity of spliced viral transcripts and the cellular response to infection are not fully characterized and hinder the eradication of HIV-1. We applied high-throughput sequencing to investigate the effects of host chromatin on proviral latency and variation of expression and splicing in both the host and virus during infection.

To evaluate the link between host chromatin and proviral latency, we compared genomic and epigenetic features to HIV-1 integration site data for latent and active provirus from five cell culture models. Latency was associated with chromosomal position within individual models. However, no shared mechanisms of latency were observed between cell culture models. These differences suggest that cell culture models may not completely reflect latency in patients.

We carried out two studies to explore mRNA populations during HIV infection. Single-molecule amplification and sequencing revealed that the clinical isolate HIV89.6 produces at least 109 different spliced mRNAs. Viral message populations differed between cell types, between human donors and longitudinally during infection. We then sequenced mRNA from control and HIV89.6-infected primary human T cells. Over 17 percent of cellular genes showed altered activity associated with infection. These gene expression patterns differed from HIV infection in cell lines but paralleled infections in primary cells. Infection with HIV89.6 increased intron retention in cellular genes and abundance of RNA from human endogenous retroviruses. We also quantified the frequency and location of chimeric HIV-host RNAs. These two studies together provided a detailed accounting of both HIV89.6 and host expression and alternative splicing.

A more cost-effective method of detecting viral load would aid patients with poor access to healthcare. We developed improved methods for assaying HIV-1 RNA using loop-mediated isothermal amplification based on primers targeting regions of the HIV-1 genome conserved across subtypes. Combined with lab-on-a-chip technology, these techniques allow quantitative measurements of viral load in a point-of-care device targeted to resource-limited settings.

This work disclosed novel HIV-host interactions and developed techniques and knowledge that will aid in the study and management of HIV-1 infection.

Degree Type

Dissertation

Degree Name

Doctor of Philosophy (PhD)

Graduate Group

Genomics & Computational Biology

First Advisor

Frederic D. Bushman

Keywords

expression, HIV-1, latency, RNA-Seq, splicing

Subject Categories

Bioinformatics | Biology | Virology

LATENCY, EXPRESSION AND SPLICING DURING INFECTION WITH HIV

Scott Sherrill-Mix

A DISSERTATION

in

Genomics and Computational Biology

Presented to the Faculties of the University of Pennsylvania

in

Partial Fulfillment of the Requirements for the

Degree of Doctor of Philosophy

2015

Supervisor of Dissertation:

Frederic D. Bushman, Ph.D., Professor of Microbiology

Graduate Group Chairperson:

Li-San Wang, Ph.D., Associate Professor of Pathology and Laboratory Medicine

Dissertation Committee:

Nancy Zhang, Ph.D. Associate Professor of Statistics

Yoseph Barash, Ph.D., Assistant Professor of Genetics

Kristen Lynch, Ph.D., Professor of Biochemistry and Biophysics

Michael Malim, Ph.D., Professor of Infectious Diseases, King's College London

LATENCY, EXPRESSION AND SPLICING DURING INFECTION WITH HIV

© COPYRIGHT

2015

Scott A. Sherrill-Mix

This work is licensed under the
Creative Commons Attribution
NonCommercial-ShareAlike 3.0
License

To view a copy of this license, visit

<http://creativecommons.org/licenses/by-nc-sa/3.0/>

Dedicated to William Maurer, Gayle Maurer & Michele Sherrill-Mix

ACKNOWLEDGEMENTS

I would like to thank Rick Bushman for being a great advisor and mentor. My committee—Nancy Zhang, Yoseph Barash, Kristen Lynch and Michael Malim—also provided guidance and encouragement. I am also grateful to many of the faculty of GCB for teaching and advice and my fellow GCB students—especially Fan Li, Paul Ryvkin, Nathan Berkowitz, Hannah Dueck, Yih-Chii Hwang and Sarah Middleton—for camaraderie and class and prelim prep. My previous advisors Ram Myers and Mike James provided a foundation for this research. I would also like to thank Hannah Chervitz, Tiffany Barlow, Mali Skotheim, Caitlin Greig and Laurie Zimmerman for organizing and managing everything.

The Bushman lab was like a second home with labmates that were both good friends and good colleagues. My fellow (or former) GCB students—Christel Chehoud, Erik Clarke, Serena Dolliva and Rithun Mukherjee—provided genomic and computational biological conversations and commiserations. Christian Hoffman tutored my wet bench skills. I had productive collaborations with Kyle Bittinger, Alexandra Bryson, Rebecca Custers-Allen, Stephanie Grunberg, Brendan Kelly, Nirav Malani, Karen Ocwieja, Greg Peterfreund, Rohini Sinha, Sesh Sundararaman and Young Hwang. Aubrey Bailey kept the servers humming and the office cheerful. Arwa Abbas, Alice Laughlin, Frances Male and Jacque Young brought the lab together. Troy Brady, Emily Charlson, Anatoly Dryga, Sam Minot, Christopher Nobles, Eric Sherman, Vesa Turkki and Yinghua Wu were great to work with.

The HIV Immune Networks Team (HINT) consortium P01 AI090935 and NRSA computational genomics training grant T32 HG000046 provided funding for this research.

Finally and most importantly, thanks to my wife and son for providing support and inspiration.

ABSTRACT

LATENCY, EXPRESSION AND SPLICING DURING INFECTION WITH HIV

Scott Sherrill-Mix

Frederic D. Bushman, Ph.D.

Over 35 million people are living with human immunodeficiency virus (HIV-1). The mechanisms causing integrated provirus to become latent, the diversity of spliced viral transcripts and the cellular response to infection are not fully characterized and hinder the eradication of HIV-1. We applied high-throughput sequencing to investigate the effects of host chromatin on proviral latency and variation of expression and splicing in both the host and virus during infection.

To evaluate the link between host chromatin and proviral latency, we compared genomic and epigenetic features to HIV-1 integration site data for latent and active provirus from five cell culture models. Latency was associated with chromosomal position within individual models. However, no shared mechanisms of latency were observed between cell culture models. These differences suggest that cell culture models may not completely reflect latency in patients.

We carried out two studies to explore mRNA populations during HIV infection. Single-molecule amplification and sequencing revealed that the clinical isolate HIV_{89.6} produces at least 109 different spliced mRNAs. Viral message populations differed between cell types, between human donors and longitudinally during infection. We then sequenced mRNA from control and HIV_{89.6}-infected primary human T cells. Over 17 percent of cellular genes showed altered activity associated with infection. These gene expression patterns differed from HIV infection in cell lines but paralleled infections in primary cells. Infection with HIV_{89.6} increased intron retention in cellular genes and abundance of RNA from human endogenous retroviruses. We also quantified the frequency and location of chimeric HIV-host RNAs. These two studies together provided a detailed accounting of both HIV_{89.6} and host

expression and alternative splicing.

A more cost-effective method of detecting viral load would aid patients with poor access to healthcare. We developed improved methods for assaying HIV-1 RNA using loop-mediated isothermal amplification based on primers targeting regions of the HIV-1 genome conserved across subtypes. Combined with lab-on-a-chip technology, these techniques allow quantitative measurements of viral load in a point-of-care device targeted to resource-limited settings.

This work disclosed novel HIV-host interactions and developed techniques and knowledge that will aid in the study and management of HIV-1 infection.

TABLE OF CONTENTS

ABSTRACT	v
TABLE OF CONTENTS	vii
LIST OF TABLES	ix
LIST OF ILLUSTRATIONS	x
CHAPTER 1 : Introduction	1
1.1 The HIV epidemic	1
1.2 The HIV virus	4
1.3 HIV detection	10
1.4 Contributions	11
CHAPTER 2 : HIV latency and integration site placement in five cell-based models	12
2.1 Abstract	12
2.2 Background	13
2.3 Methods	15
2.4 Results	19
2.5 Conclusions	30
2.6 Availability of supporting data	32
2.7 Acknowledgements	32
CHAPTER 3 : Dynamic regulation of HIV-1 mRNA populations analyzed by single- molecule enrichment and long-read sequencing	33
3.1 Abstract	33
3.2 Introduction	34
3.3 Materials and methods	36
3.4 Results	43
3.5 Discussion	49
3.6 Acknowledgements	53
CHAPTER 4 : Gene activity in primary T cells infected with HIV _{89.6} : intron reten- tion and induction of distinctive genomic repeats	54
4.1 Abstract	54
4.2 Background	55
4.3 Methods	57
4.4 Results	61
4.5 Discussion	78
4.6 Conclusions	82
4.7 Availability of supporting data	83
4.8 Acknowledgements	83

CHAPTER 5 : A reverse transcription loop-mediated isothermal amplification assay optimized to detect multiple HIV subtypes	84
5.1 Abstract	84
5.2 Introduction.....	85
5.3 Methods	86
5.4 Results.....	88
5.5 Testing different primer designs	92
5.6 Discussion	96
5.7 Acknowledgments.....	98
CHAPTER 6 : Conclusions and future directions.....	99
6.1 Latency and integration location	99
6.2 HIV-1 alternative splicing.....	100
6.3 Host expression during HIV infection	103
6.4 LAMP PCR and lab-on-a-chip	104
APPENDICES	108
A.1 Generalized linear models of changes in use of mutually exclusive HIV-1 splice acceptors	108
A.2 Reproducible report of HIV integration sites and latency analysis	114
BIBLIOGRAPHY	144

LIST OF TABLES

TABLE 2.1 : Integrations from <i>in vitro</i> models of latency	18
TABLE 2.2 : Genomic data available for comaprison to integration sites	20
TABLE 4.1 : Samples and sequencing coverage.....	61
TABLE 4.2 : Data used for meta-analysis of expression changes during HIV infection	63
TABLE 5.1 : Primer set ACeIN-26	93

LIST OF ILLUSTRATIONS

FIGURE 1.1 : The HIV replication cycle.....	4
FIGURE 1.2 : The HIV-1 genome	8
FIGURE 2.1 : Correlations of genomic features and latency	21
FIGURE 2.2 : Lasso regressions predicting latency	22
FIGURE 2.3 : Cellular expression and latency	24
FIGURE 2.4 : Strand orientation and latency	25
FIGURE 2.5 : Genes and latency	26
FIGURE 2.6 : Aliphoid repeats and latency	27
FIGURE 2.7 : Acetylation and latency	29
FIGURE 2.8 : Shared expression status between near neighbors	29
FIGURE 3.1 : Mapping the splice donors and acceptors of HIV _{89.6}	35
FIGURE 3.2 : Spliced transcripts produced from HIV _{89.6}	42
FIGURE 3.3 : Novel transcripts utilizing acceptor A8c	47
FIGURE 3.4 : Temporal, cell type and donor variability in accumulation of HIV-1 messages.....	50
FIGURE 4.1 : Comparisons among studies quantifying cellular gene expression after HIV infection	64
FIGURE 4.2 : Comparisons of the effect of HIV infection on cellular gene expression to additional studies comparing transcription in subsets of immune cells	66
FIGURE 4.3 : Changes in the abundance of intronic regions with HIV infection ...	67
FIGURE 4.4 : Repeat categories enriched upon infection with HIV	69
FIGURE 4.5 : Characteristics of LTR12C sequences associated with induction upon infection of primary T cells with HIV _{89.6}	71
FIGURE 4.6 : Estimating relative abundance of HIV _{89.6} message size classes using RNA-Seq data	73
FIGURE 4.7 : Transcription and splicing of the HIV _{89.6} RNA	74
FIGURE 4.8 : Chimeric RNA sequences containing both human and HIV sequences	78
FIGURE 5.1 : Amplification results for all RT-LAMP primer sets tested	90
FIGURE 5.2 : Subtype-agnostic RT-LAMP primers design	91
FIGURE 5.3 : Performance of the AceIN-26 primer set with different starting RNA concentrations	94
FIGURE 5.4 : Replicate tests of the ACeIN-26 primer set over six HIV subtypes..	95
FIGURE 6.1 : Ebola RT-LAMP primers design	107

CHAPTER 1: Introduction

1.1 The HIV epidemic

In 1981, physicians began to notice a mysterious increase, often clustered in men who had sex with men or intravenous drug users, in the occurrences of Kaposi's sarcoma and pneumocystis pneumonia¹⁻⁶.

Kaposi's sarcoma was, until 1981, a rare cancer in the US found largely in elderly men with Jewish or Mediterranean ancestry⁷. Kaposi's sarcoma had also been seen in immunocompromised individuals⁸⁻¹⁰ and there were suggestions that it was a virus-associated cancer¹¹ although the causative human herpesvirus would not be discovered for another decade^{12,13}.

Pneumocystis pneumonia was known to be caused by infection of the alveoli with the yeast-like fungus *Pneumocystis jirovecii*^{14,15}. Pneumocystis pneumonia was almost exclusively seen in patients with suppressed immune systems or immune disorders and rarely, if ever, in immunocompetent individuals¹⁵.

The mechanism for this spike of opportunistic infections was clarified when researchers found severe T cells depletion and decreases in cellular immunity in these patients^{4-6,16,17}. This disease was eventually labeled acquired immunodeficiency syndrome (AIDS). However, the underlying cause remained unclear.

Potential transmissions by transfusion¹⁸⁻²⁰, injection drug use^{4,17,21}, maternal transmission²² and both homosexual^{16,23} and heterosexual^{17,24} contact pointed towards an infectious agent. In 1983, a virus later named human immunodeficiency virus type 1 (HIV-1) was isolated from patient samples²⁵⁻²⁸ and soon detected in most immunodeficient patients²⁸⁻³¹.

Reports of AIDS and associated opportunistic infections in sub-Saharan Africa soon revealed widespread endemic infection³²⁻³⁵ and a great diversity of viruses³⁶⁻⁴¹. Retrospective studies suggested that the virus had been present, at least sporadically, in Europe and the USA for decades^{42,43} and circulating for even longer in Africa^{33,44-48}. Archived patient samples

containing HIV-1 genome fragments from as early as 1959 were found in what is now Kinshasa, in the Democratic Republic of Congo⁴⁶. These samples showed extensive genome diversification already present in the 1960s, suggesting that HIV-1 had been circulating in humans for some time^{47,48}. Phylogenetic analyses adding in contemporary HIV-1 type M sequences estimated a most recent common ancestor in the early 1900s⁴⁸⁻⁵³.

A virus similar to HIV causing AIDS in monkeys was soon discovered in macaques^{54,55} and many other primates⁵⁶. HIV-1 appeared most similar to a virus found in chimpanzees^{55,57} and surveys of wild chimpanzees in Africa revealed a closely related simian immunodeficiency virus infecting chimpanzees in central Africa⁵⁸⁻⁶⁰.

Thus, the ancestor of HIV-1 was likely transmitted from a chimpanzee to a human, likely during harvest of chimpanzees for food⁶¹⁻⁶⁶, in the forests of southeastern Cameroon. The virus was probably transported down the Sangha River⁶⁷ to the city of Kinshasa, where HIV-1 began its global spread^{38,48,53,68}. A combination of social upheaval, increased mobility, urbanization and mass vaccination campaigns with unsterilized needles appear to have provided fuel for the growing epidemic^{53,69-71}. A virus appears to have been carried from Africa to Haiti in the 1960s, perhaps by workers returning home from an exchange program^{35,68}, and then into the US in the 1970s⁷² before being detected in the US in 1981. In the past 34 years, HIV-1 has spread to over 78 million people and caused over 35 million deaths⁷³.

In the early days of the epidemic, there were no tests to detect the virus, and no treatments. The presence of the virus was often revealed by the onset of AIDS. Opportunistic infections⁷⁴ and death usually followed soon after. The median survival time after diagnosis with AIDS was about 1 year^{75,76}.

Isolation of the virus allowed the detection of HIV infection through assays of antibody response to viral proteins. Testing revealed that patients had a median survival time of around a decade from initial infection⁷⁷⁻⁸⁰.

In 1987, the successful trial of the reverse transcriptase inhibitor azidothymidine provided the first hope for treatment^{81–83} but it soon became apparent that the fast mutation rate of HIV^{84–90} and strong selection by drug therapy could quickly create drug-resistant forms of virus in patients receiving single drug therapy^{91–100}. Even with therapy, median survival time from AIDS diagnosis rose to only about 2 years^{76,82,101,102}.

Additional antiretrovirals, again targeting reverse transcriptase, were developed¹⁰³. Sequential or alternating administration of different antiretroviral drugs did not greatly improve prognosis^{104–108}. Simultaneous treatment with two reverse transcriptase inhibitor offered modest benefits but viral escape was still common^{109–113}.

Development of drugs targeting other stages of the HIV replication cycle allowed synergistic combinations of antiretroviral drugs^{114–119}. The difficulty for HIV to evolve multiple drug resistant mutations^{120,121} meant that therapy using simultaneous combinations of drugs finally began to offer patients more hope of long term survival^{122–126}. With early triple therapy, median survival time rose to 20 years^{79,127} and, with further development, now approaches the life expectancy of control populations^{128–131}.

However although antiretrovirals effectively suppress HIV, there is currently no practicable cure^{132,133}. If a patient, even a patient who had the virus suppressed to undetectable levels for years, stops treatment, then virus abundance quickly rebounds to pretreatment levels^{134–136}.

Upon infection, latent HIV are quickly^{137,138} established in resting CD4⁺ T cells and macrophages. These latent provirus are long-lived and resistant to therapy and immune response^{139,140}. Resting CD4⁺ cells have half-lives of up to 40 months^{141,142} meaning significant proportions of HIV will remain latent for decades yet can be stimulated at any time by activity in their host cell to reactivate and restart viral replication^{134–136,140,141,143,144}.

Latently infected cells are one of the most significant barriers to curing HIV¹⁴⁵. If the latent proviruses could be induced into activity and their host cells eliminated then the virus might

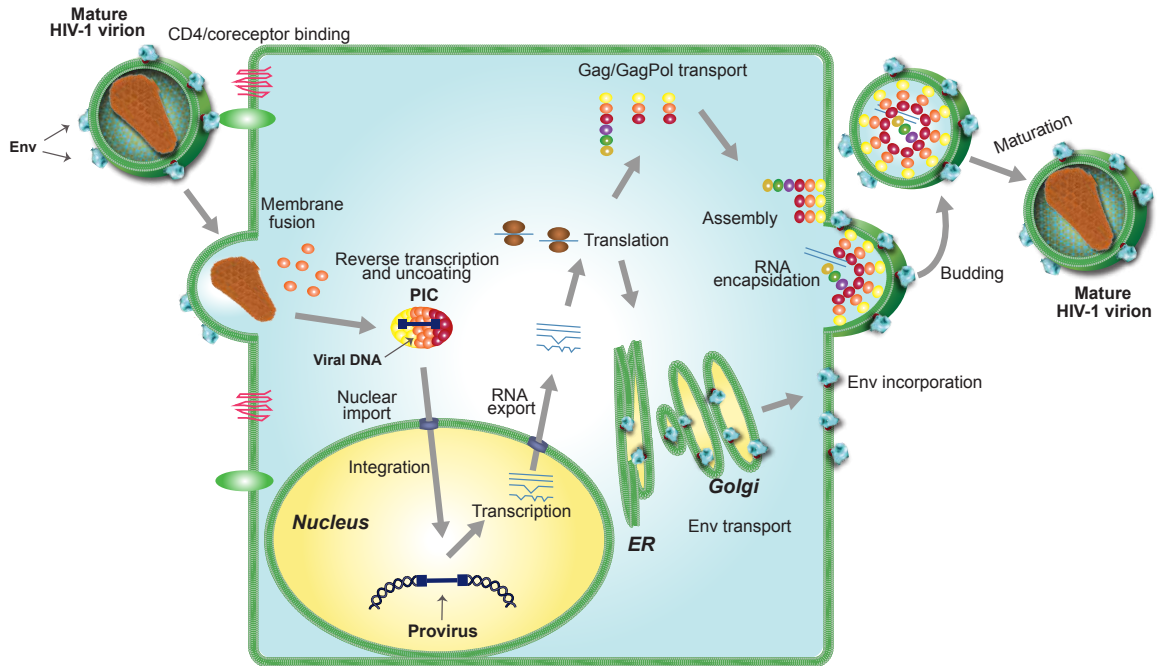


Figure 1.1: The HIV replication cycle

be eradicated from its host^{146–149}. Cell models of latency are used to study this problem in the lab^{150–152}. In Chapter 2, we compare latent and active provirus among these cell models to see if latency relates to the chromosomal position of integration and whether models share the same drivers of latency.

1.2 The HIV virus

HIV is an enveloped, single-strand positive-sense retrovirus (Figure 1.1). To replicate, the virion gains access into a host cell through cellular receptors^{153–160}. The viral RNA genome is reverse transcribed to create a DNA intermediate that is integrated into a host cell chromosome^{161–164}. Host polymerase then transcribes viral messenger RNAs which are translated in the cytoplasm. Full length RNA is packaged into budding particles along with expressed viral proteins and the virion buds from the cell.

The HIV genome encodes genes for at least two polyproteins and seven proteins:

Gag (group specific antigens) is a myristoylated membrane protein which is anchored on

the virion surface and cleaved by viral protease after virion budding to produce matrix, capsid, nucleocapsid and p6 protein along with two small spacer peptides SP1 and SP2.

MA p17 (matrix) is a trimeric protein that supports the inside of the viral lipid bilayer to stabilize the virion¹⁶⁵. It also aids in transport of the genome to the nucleus through a nuclear localization signal¹⁶⁶ and in nuclear import in non-dividing cells¹⁶⁷.

CA p24 (capsid) proteins assemble to form a protective shell around the RNA genome of the virus. The viral capsid is composed of around 1500 copies of CA arranged into hexameric rings interspersed with 12 pentameric rings to form a fullerene cone^{168–171}. CA binds cellular CPSF6¹⁷², cyclophilin A^{173,174} and RanBP2¹⁷⁵, perhaps to gain access to the nucleus^{175,176} and to avoid premature uncoating and exposure of the viral genome to innate immune factors¹⁷⁷.

NC p7 (nucleocapsid) recognizes the ψ packaging element of the viral genome¹⁷⁸ through two zinc-finger motifs and is packaged together with the RNA into virions¹⁷⁹.

p6 (protein 6 kDa) is a small protein which appears to primarily recruit cellular proteins to allow virion budding from the cell membrane^{180–182} and aid in the packaging of Vpr in to particles¹⁸³.

Pol (polymerase) is cleaved by viral protease to produce reverse transcriptase, integrase and HIV protease. The Pol protein is generated when a ribosome translating *gag* meets a stem-loop in the HIV mRNA¹⁸⁴, stutters and moves back a base, causing a -1 nucleotide frameshift when it continues translation¹⁸⁵. Translational frameshifting happens in about $\frac{1}{20}$ of translations¹⁸⁶.

RT p51 (reverse transcriptase)¹⁸⁷ generates DNA from an RNA template^{161,162}.

Retrovirus package two copies of RNA in each virion^{188–190}. If two different virus infect the same cell then interstrand transfer during the reverse transcription step allows recombination between strains^{191–193}. A lack of proofreading in the RT step leads to the high mutation rate of around 2×10^{-5} mutations per base per replication^{84–90}.

IN p31 (integrase) is a dimeric enzyme which integrates the retroviral DNA into host chromatin^{164,194–197}. Integrase removes two nucleotides from from the 3' ends of the viral DNA and inserts the pair of viral ends into host DNA¹⁹⁸.

PR (protease) is a dimeric aspartyl protease¹⁹⁹ that cleaves viral polyproteins Gag and Pol^{200,201}.

Env gp160 (envelope) is a trimeric transmembrane protein that mediates entry through fusion of viral and cellular membrane by binding its receptor CD4^{153–157} and coreceptors CXCR4¹⁵⁸, CCR3 or CCR5^{159,160}. gp160 is cleaved into its active form, consisting of two subunits gp41 and gp120²⁰², by cellular furin protease²⁰³. The envelope protein is highly glycosylated to form a mutable 'glycan shield' against host adaptive immune response²⁰⁴. There are about 14 Env proteins per virion²⁰⁵. Env sequence is highly variable within and between patients^{206,207} due to positive selection from host immune recognition^{208–210}.

Tat (trans-activator of transcription) protein is a transactivator of expression from the HIV-1 long terminal repeat^{211–213}. The virus does not replicate efficiently without this transactivation²¹⁴. Tat may also regulate cellular expression such as downregulation of major histocompatibility complex type I expression²¹⁵. Tat may suppress miRNA silencing pathway^{216–218} but this remains controversial²¹⁹.

Rev (regulator of expression of virion proteins) is a transactivator protein that shuttles between the nucleus and cytoplasm²²⁰ and causes the export of partially spliced and unspliced viral transcripts^{221–225} from the nucleus through the recognition of a rev

response element^{226,227}.

Nef (negative factor) is a myristoylated membrane-associated protein²²⁸ that is involved in multiple functions. Nef causes endocytosis of the viral entry receptors CD4^{229–233} and CCR5²³⁴ and major histocompatibility complex molecules^{235–238}. Nef also induces T cell activation through interactions with signaling kinases and the T cell receptor^{239–243}. In contrast, Nef in most other primate lentiviruses inhibits activation and inflammation²⁴⁴ perhaps indicating that the gain of *vpu* in HIV-1 and its simian relatives allowed the loss of the immune inhibitory traits of *nef* and thus contributes to the increased pathogenicity of these viruses^{245,246}.

Vpr (viral protein R) is a 15 kDa protein^{247,248} with diverse functions. Vpr arrests the cell in the G2 phase of the cell cycle^{249–253} and aids in transport of the viral genome to the nucleus¹⁶⁶. Vpr protein may disrupt nuclear membrane integrity²⁵³. Vpr also appears to transactivate viral expression^{254,255} and induce apoptosis^{256,257} but these may be linked to conditions caused by cell cycle arrest. Vpr is incorporated into virions^{258,259}.

Vif (virion infectivity factor) counteracts the cellular restriction factor APOBEC3G²⁶⁰ by excluding APOBEC3G from incorporation into the virion²⁶¹ and causing APOBEC3G to be ubiquitinated and degraded^{262–264}. APOBEC3G is otherwise packaged into virions²⁶⁵ and deaminates the HIV genome during reverse transcription causing G-to-A hypermutation^{265–268}.

Vpu (viral protein U)^{269,270} is a small integral membrane protein which has two known functions; degradation of CD4 and downregulation of BST-2 from the cell membrane. Vpu causes cellular CD4 to be ubiquitinated and degraded^{271,272} which prevents interactions between progeny virus and host cell CD4 receptor^{232,233,273,274} and superinfection by other viruses²³⁰ while also releasing Env proteins from CD4 interactions in the endoplasmic reticulum^{275,276}. Vpu also counteracts the cellular restriction factor BST-2, which would otherwise interfere with viral budding^{277,278}. Vpu does not appear

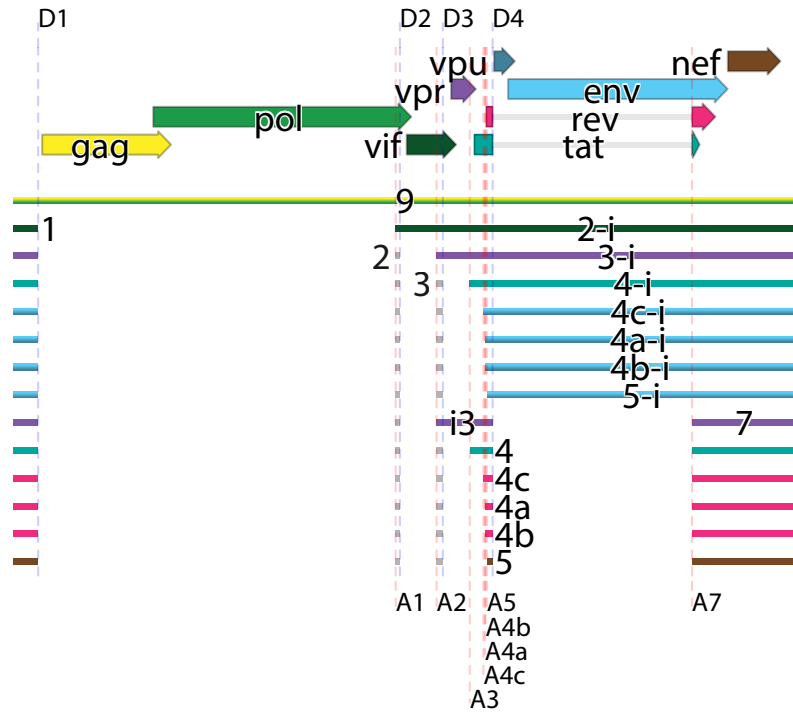


Figure 1.2: The HIV-1 genome. Arrows indicate open reading frames. Dashed lines show major splice acceptors (red) and donors (blue). Major spliceforms are shown as thin rectangles and colored according to their corresponding open reading frame.

to be found in the virion²⁷⁹.

A strong selective pressure for genome compactness^{280–282} pushes HIV and other lentiviruses to subvert host cell alternative splicing pathways to allow tighter packing of their genetic information. Through weak splice sites²⁸³ and overlapping reading frames (Figure 1.2), the virus manages to produce regulated quantities of these nine proteins and polyproteins from its single transcription start site and less than 10 kilobase genome²⁸⁴.

In HIV, splicing occurs between at least four splice donors and eight splice acceptors²⁸⁴. Two splice donors, D1 and D4, are relatively strong while the remaining donors and all acceptors are fairly weak²⁸⁵. The weak acceptors seem balanced with Rev’s nuclear export activity²⁸³. Several exonic splicing silencers^{286,287} and exon splicing enhancers^{288,289} and a single intronic splicing silencer²⁹⁰ in the viral genome interact with many human splicing factors, including hnRNPs A1^{287,290} H, F, 2H9, and A2²⁹¹ and SR proteins SRp40^{288,292}, SRp75²⁹², ASF/SF2²⁸⁸ and SC35²⁹¹, to alter viral splicing^{284,293}.

In Chapter 3, we investigate viral splicing and reveal unappreciated splice sites, novel proteins

and dynamic changes in viral splicing between human subjects, over time and between cell types.

Inclusion and exclusion of a particular stretch of RNA into an mRNA is determined by a balance of RNA secondary structure^{291,294,295}, chromatin structure²⁹⁶, nucleosome positioning²⁹⁷, histone marks²⁹⁸, previous splicings²⁹⁹, order of intron removal^{300,301} and enhancers³⁰² and suppressors³⁰³ that bind specific motifs³⁰⁴. Together these factors create a controllable splicing code³⁰⁵⁻³⁰⁷.

Alternative splicing may also play an unappreciated role in HIV-host interactions. Viral proteins interact with components of the cellular splicing complex³⁰⁸⁻³¹⁰. These interactions have been reported to change splicing in viral^{309,311,312} and cellular transcripts^{313,314} and raise the possibility that the virus has evolved to alter host splicing. Although infection has been shown to cause genome-wide changes in the expression of cellular genes³¹⁵⁻³¹⁹, no genome-wide study of cellular alternative splicing during HIV infection has ever been reported.

Several viral proteins affect mRNA abundances. Rev causes export of unspliced viral mRNA that would otherwise be trapped in the nucleus³²⁰ to be exported^{321,322} and may also interact with splicing factors to alter viral splicing³⁰⁸. The HIV protein Tat is best known for its trans-activation of viral transcription^{211,323} and triggering apoptosis in uninfected cells^{324,325} but Tat also appears to independently affect alternative splicing of viral transcripts^{309,311,312,326}. Viral protein Vpr is known to cause cell cycle arrest²⁵² with corresponding changes in expression. Vpr also appears to alter alternative splicing of some cellular transcripts^{313,314} and interact with the SMN complex³¹⁰, which assembles spliceosomal snRNP³²⁷. Although all three of these proteins modify viral splicing, whether they also cause widespread alterations in cellular splicing is unknown.

HIV infection also appears to induce the expression of certain human endogenous retroviruses (HERVs)³²⁸⁻³³³ and retrotransposons³³⁴. These HERV and retrotransposon mRNA and

their translated proteins offer potential markers of infection and vaccine targets³³⁵⁻³⁴⁰ but no genome-wide screen of the effects of HIV infection on the transcription of these elements has been reported.

In Chapter 4, we investigate splicing and expression during HIV infection and report global changes in intron retention and in the expression of endogenous retrovirus and retrotransposons.

1.3 HIV detection

Immunoassays are the current standard of care for the detection of HIV infection. These tests are based on the enzyme-linked immunosorbent assay (ELISA), using an enzyme linked to an antibody to produce a detectable signal only in the presence of antigen³⁴¹⁻³⁴³.

The isolation of HIV²⁵⁻²⁸ allowed the production of large quantities of virions that could be used as antigen. These virions were bound to a substrate, sera from patients added and any patients antibodies sensitive to HIV allowed to bind. Any unbound antibodies were washed away. Then a peroxidase enzyme-labeled antibody targeted to human antibody was added, allowed to bind and the unbound antibodies again washed away. Any HIV-targeted patient antibodies would bind the antigen and be bound in turn by the peroxidase-labeled antibody so that the peroxidase would change the color of media^{30,31,344}. These tests had a large false positive rate and the standard procedure was to perform multiple ELISA tests follow by a Western blot test before informing patients^{345,346} but false positives were still prevalent³⁴⁷. More conservative criteria and cleaner lab procedures reduced false positives³⁴⁸. Four generations of development³⁴⁹ have resulted in more sensitive and specific detection of patient antibodies along with earlier detection using antibodies directly able to detect the HIV capsid protein^{350,351}.

Rapid immunoassays with less specificity but able to provide results in 30 minutes have been developed to allow point-of-care testing. Immediate results reduce patient stress and reduces the number of patients lost to follow up prior to delivery of results³⁵²⁻³⁵⁴. Rapid

tests detecting HIV in oral fluids have been developed and obviate the need for a blood draw^{355–357} and allow self testing at home^{358,359}.

Immunoassays provide robust and affordable point-of-care detection of HIV but no viable point-of-care assays for viral load exist³⁶⁰. Existing laboratory-based tests are relatively expensive and require specialized equipment making access difficult in resource-limited settings^{361,362}. Without viral load measures, CD4⁺ T cell counts or clinical presentation are used to infer the emergence of viral drug resistance. These criteria are not specific nor sensitive enough without viral load measures so many patients are unnecessarily switched to second line therapy^{363,364} or switched too late leading to accumulations of drug resistant mutations³⁶⁵. Medecins Sans Frontieres describe point-of-care viral load tests as “desperately needed”³⁶⁰. In Chapter 5, we design loop-mediated isothermal amplification methods that can be used with microfluidics to create a point-of-care assay viral load in resource-limited settings.

1.4 Contributions

Much of this work was performed as part of a large collaboration. It would not tell a complete story in isolation. Therefore, I have preserved the chapters in published form and detailed my contribution to each project at the start of the chapter.

CHAPTER 2: HIV latency and integration site placement in five cell-based models

This chapter was originally published as:

S Sherrill-Mix, MK Lewinski, M Famiglietti, A Bosque, N Malani, KE Ocwieja, CC Berry, D Looney, L Shan et al. 2013. HIV latency and integration site placement in five cell-based models. *Retrovirology*, 10:90. doi: 10.1186/1742-4690-10-90

I led the computational analysis, with assistance from CC Berry and N Malani. MK Lewinski, D Looney and J Guatelli analyzed integration sites using IonTorrent sequencing. M Famiglietti, A Bosque and V Planelles prepared DNA from latent and activated T cells using the Central Memory CD4 + model. L Shan, RF Siliciano, MJ Pace, LM Agosto, KE Ocwieja and U O'Doherty contributed data and suggestions. FD Bushman and I planned the overall study. I produced the figures. FD Bushman and I wrote the paper.

Additional files are available at <http://www.retrovirology.com/content/10/1/90/additional>

2.1 Abstract

Background: HIV infection can be treated effectively with antiretroviral agents, but the persistence of a latent reservoir of integrated proviruses prevents eradication of HIV from infected individuals. The chromosomal environment of integrated proviruses has been proposed to influence HIV latency, but the determinants of transcriptional repression have not been fully clarified, and it is unclear whether the same molecular mechanisms drive latency in different cell culture models.

Results: Here we compare data from five different *in vitro* models of latency based on primary human T cells or a T cell line. Cells were infected in vitro and separated into

fractions containing proviruses that were either expressed or silent/inducible, and integration site populations sequenced from each. We compared the locations of 6,252 expressed proviruses to those of 6,184 silent/inducible proviruses with respect to 140 forms of genomic annotation, many analyzed over chromosomal intervals of multiple lengths. A regularized logistic regression model linking proviral expression status to genomic features revealed no predictors of latency that performed better than chance, though several genomic features were significantly associated with proviral expression in individual models. Proviruses in the same chromosomal region did tend to share the same expressed or silent/inducible status if they were from the same cell culture model, but not if they were from different models.

Conclusions: The silent/inducible phenotype appears to be associated with chromosomal position, but the molecular basis is not fully clarified and may differ among *in vitro* models of latency.

2.2 Background

Highly active antiretroviral therapy (HAART) can suppress HIV-1 replication in infected patients, but the ability of HIV to persist as an inducible reservoir of latent proviruses^{134,140,143} obstructs eradication of the virus and functional cure¹⁴⁵. These latent proviruses are long lived^{141,142} and relatively invisible to the immune system^{139,140}. The potential for even a single virus to restart infection despite successful antiviral therapy means that it may be necessary to eliminate all latent proviruses to eradicate HIV from an infected person.

After integration, a positive feedback loop of Tat transactivation appears to partition proviral gene activity into either of two stable states³⁶⁷⁻³⁶⁹—abundant Tat driving high proviral expression or little Tat leading to quiescent latency. Similar to the positional effect variegation observed in fruit fly chromosomal rearrangements^{370,371}, studies on cell clones with single integrations show that differing integration sites can have large differences in proviral expression³⁷²⁻³⁷⁴. These data suggest that integration site location, along with the cellular environment³⁷⁴⁻³⁷⁷, influences the balance between latency and proviral expression.

Associations between latency and genomic features have also been reported in collections of integration sites from cell culture models although the consistency of these effects across model systems and their relationships to latency in patients remains uncertain. Lewinski et al.¹⁵⁰ reported that proviruses integrated in gene deserts, aliphoid repeats and highly expressed genes are more likely to have low expression. Shan et al.¹⁵¹ reported an association between latency and integration in the same transcriptional orientation as host genes. Pace et al.¹⁵² found that silent and expressed provirus integration sites differed in the abundance and expression levels of nearby genes, GC content, CpG islands and aliphoid repeats. In model systems with defined integration sites, Lenasi et al.³⁷⁸ reported decreased and Han et al.³⁷⁹ reported increased viral transcription when the provirus is downstream of a highly expressed host gene.

Cell-based models of latency are important for many aspects of HIV research, including screening small molecules that can reverse latency and potentially allow eradication^{380,381}. Location-driven differences in expression are preserved even after demethylation and histone deacetylase treatment³⁷², which suggests that integration location has the potential to confound “shock and kill” anti-latency treatments^{382,383}. A greater understanding of the effects of integration site location on latency could thus affect antiretroviral development.

To search for features of integration site associated with latency, we generated a set of inducible and expressed integration sites using a primary central memory CD4⁺ T cell model of latency^{384,385}, collected four previously reported integration site datasets and modeled the effects of genomic features near the integration site on the expression status of these proviruses. Although some genomic features associated with latency in individual models, no feature was consistently associated with proviral expression across all five cell culture models. However, closely neighboring proviruses within the same cellular model shared the same latency status much more often than expected by chance suggesting that chromosomal position of integration affects latency but that the mechanism remains unclear or differs between cell culture models. Thus these data help inform the design of experiments in HIV

eradication research.

2.3 Methods

2.3.1 Integration sites

Naive CD4⁺ T cells were purified by negative selection from peripheral blood mononuclear cells. The cells were activated with anti-CD3 and anti-CD28 (+TGF-beta, anti-IL-12, and anti-IL-4) to generate “non-polarized” cells (the in vitro equivalent of central memory T cells). Five days after isolation, cells were infected with an NL4-3-based virus with GFP in place of Nef and the LAI envelope (X4) provided in trans at a concentration of 500 ng of p24 as measured by ELISA per million cells. Based on previous experience with this model, this amount of p24 should produce an MOI of approximately 0.15. Cells were cultured in the presence of IL-2. Two days post-infection, cells were sorted for GFP⁺; this active population expresses GFP even when treated with flavopiridol, although for this study they were not treated. The inducible population was the set of GFP negative cells from the initial sort that, 9 days post-infection, were activated with anti-CD3 and anti-CD28 and sorted for GFP production.

Genomic DNA from the inducible and expressed populations was digested with MseI, ligated to an adapter, and amplified by ligation-mediated PCR essentially as in Wu et al.³⁸⁶ and Mitchell et al.³⁸⁷ except that the nested PCR primers included sequence for the Ion Torrent P1 adapter and adapter A sequence with a 5 base barcode sequence specific to the inducible or expressed conditions. Amplicons were sequenced using an Ion Torrent Personal Genome Machine (PGM) according to manufacturer’s instructions using an Ion 316 chip and the Ion PGM 200 Sequencing kit (Life Technologies). The sequence reads were sorted into samples by barcode. All reads were required to match the expected 5’ sequence with a Levenshtein edit distance less than 3 from the expected barcode, 5’ primer and HIV long terminal repeat (LTR). The 5’ primer and HIV sequence, along with the 3’ primer if present, were trimmed from the read. Sequences with less than 24 bases remaining or containing any eight base

window with an average quality less than 15 were discarded. Duplicate reads and reads forming an exact substring of a longer read were removed.

2.3.2 Analysis

All statistical analysis was performed in R 2.15.2³⁸⁸. The analyses are described in a reproducible report (Appendix A.2). The annotated integration site data necessary to perform the analyses and the compilable code to generate this reproducible report are provided as supplemental information³⁶⁶. The new Central Memory CD4⁺ data set was analyzed as in Berry et al.³⁸⁹. The integration patterns appeared similar to previously reported HIV integration site datasets³⁹⁰.

2.3.3 Previously published data

We collected integration sites from three previously reported studies (Table 2.1), for a total of four expressed versus silent/inducible pairs of samples. These studies used primary CD4⁺ T cells or Jurkat cells infected with HIV or HIV-derived constructs as cell culture models of latency. Flow cytometry allowed cells expressing viral encoded proteins to be sorted from non-expressing cells. In two of the studies, these non-expressing populations were stimulated to ensure that the provirus could be aroused from latency. Specific differences in protocol between the study sets are summarized below.

Jurkat Lewinski et al.¹⁵⁰ infected Jurkat cells with a VSV-G pseudotyped, GFP-expressing pEV731 HIV construct (LTR-Tat-IRES-GFP)³⁷² at an MOI of 0.1. The cells were sorted into GFP+ and GFP- two to four days after infection. GFP+ cells were sorted again two weeks after infection and cells that were again GFP+ were collected for integration site sequencing. GFP- cells were sorted for GFP negativity twice more then stimulated with TNF α . Cells that were GFP+ after stimulation were collected for integration site sequencing. DNA was digested with MseI or a combination of NheI, SpeI and XbaI, ligated to adapters for nested PCR, amplified and sequenced by Sanger capillary electrophoresis.

Bcl-2 transduced CD4⁺ Shan et al.¹⁵¹ transduced CD4⁺ T cells with Bcl-2, costimulated with bound anti-CD3 and soluble anti-CD28 antibodies, interleukin-2 and T cell growth factor and then infected with X4-pseudotyped GFP-expressing NL4-3- δ 6-drEGFP construct³⁹¹ at an MOI of less than 0.1. DNA was extracted, digested with PstI and circularized³⁹². HIV-human junctions were amplified by reverse PCR and sequenced using Sanger capillary electrophoresis.

Active CD4⁺ & Resting CD4⁺ Pace et al.¹⁵² spinoculated CD4⁺ T cells with HIV NL4-3 at an MOI of 0.1. After 96 hours, the cells were stained for intracellular Gag CD25, CD69 and HLA-DR and sorted into four subpopulations based on activation state and Gag expression; activated Gag-, activated Gag+, resting Gag- and resting Gag+. The ability of the viruses to reactivate was not tested although previous studies have shown that the majority are likely inducible³⁹³. Genomic DNA was extracted and digested with restriction enzymes MseI and Tsp509 and ligated to adapters. Proviral LTR-host genome junctions were sequenced by 454 pyrosequencing after nested PCR.

All datasets were processed using the hiReadsProcessor R package³⁹⁴. Adaptor trimmed reads were aligned to UCSC freeze hg19 using BLAT³⁹⁵. Genomic alignments were scored and required to start within the first three bases of a read with 98% identity. Alignments for a given read with a BLAT score less than the maximum score for that read were discarded. Reads giving rise to multiple best scoring genomic alignments were excluded, while reads with a single best hit were dereplicated and converged if within 5bp of each other. The Bcl-2 transduced CD4⁺ sample was sequenced from U3 in the 5' HIV LTR while the other samples were sequenced from U5 in the 3' LTR. To account for the 5 base duplication of host DNA caused by HIV integration, the chromosomal coordinates of the Bcl-2 transduced CD4⁺ sample were adjusted by ± 4 bases.

To allow for alignment difficulties in the analysis of genomic repeats, reads with multiple best scoring alignments, along with the single best hit reads used above, were included in the repeat analyses. If any best scoring alignment for a read fell within a repeat, then that

Title	Cell type	Virus	Time of harvest after infection	Sequencing	Generation of expressed vs. silent/inducible	Citation	Silent/inducible unique sites	Expressed unique sites
Jurkat	Jurkat cells	HIV vector pEV731 (LTR-Tat-IRES-GFP)	2 weeks	Sanger	TNF α , GFP expression	Lewinski et al. ¹⁵⁰	463 inducible	643
Bcl-2 transduced CD4 ⁺	Primary CD4 ⁺ T cells (Bcl-2 transduced)	HIV NL4-3- δ 6-drEGFP (inactivated <i>gag</i> , <i>vif</i> , <i>vpr</i> , <i>vpu</i> , <i>nef</i> and <i>env</i> replaced by GFP)	3 days + 3-4 weeks + 3 days	Sanger	anti-CD3, anti-CD28 antibodies, GFP expression	Shan et al. ¹⁵¹	446 inducible	273
Active CD4 ⁺	Primary active CD4 ⁺ T cells	HIV NL4-3	3 days	454	high vs. low Gag	Pace et al. ¹⁵²	1604 silent	1274
Resting CD4 ⁺	Primary resting CD4 ⁺ T cells	HIV NL4-3	3 days	454	high vs. low Gag	Pace et al. ¹⁵²	1942 silent	784
Central Memory CD4 ⁺	Primary central memory CD4 ⁺ T cells	HIV NL4-3 Δ Nef GFP	2 days/9 days	Ion-Torrent	anti-CD3, anti-CD28 antibodies, GFP expression	This paper	1729 inducible	3278

Table 2.1: HIV-1 integration datasets from *in vitro* models of latency where the proviruses were determined to be silent/inducible or expressed

read was considered to map to that repeat.

2.3.4 Genomic features

A total of 140 whole genome features for CD4⁺ T-cells were gathered from data sources indicated in Table 2.2. For features encoded as peaks or hotspots, the log of the distance of each integration site to the nearest border was used for modeling. Integration sites from HIV 89.6 infection in primary CD4⁺ T cells³⁹⁶ were used to count nearby integrations and determine a ± 20 bp position weight matrix for integration targets. Illumina RNA-Seq from active CD4⁺ cells (Chapter 4) was used to estimate raw cellular expression and fragments per kilobase of transcript per million mapped reads for genes as calculated by Cufflinks³⁹⁷. For sequence-based data like RNA-Seq and ChIP-Seq, the number of reads aligned within a $\pm 50, 500, 5,000, 50,000$ and $500,000$ bp windows of each integration site were counted and log transformed. In addition, chromatin state classifications derived from a hidden

Markov model based on histone marks and a few binding factors³⁹⁸ were included as binary variables. All data from previous genomic freezes were converted to hg19 using liftover³⁹⁹.

2.4 Results

The combination of integration site data newly reported here (set named “Central Memory CD4⁺”) with previously published data (sets named “Jurkat”, “Bcl-2 transduced CD4⁺”, “Active CD4⁺”, and “Resting CD4⁺”) provides a collection of 12,436 integration sites (Table 2.1) where the expression status of the provirus—silent/inducible or expressed—is known. In three of the datasets, Jurkat, Central Memory CD4⁺ and Bcl-2 transduced CD4⁺, the proviruses were sorted based on inducibility. In the Resting CD4⁺ and Active CD4⁺ datasets, cells were sorted only based on proviral expression. Previous studies have shown that most silent proviruses in this model system are inducible³⁹³.

2.4.1 Global model

If a genomic feature and latency are monotonically related then we should be able to detect this relationship using Spearman rank correlation. In addition if a feature has a consistent effect across models we should see a consistent pattern in the direction of correlation. A simple first look for correlation between genomic features (Table 2.2) and latency status yielded inconsistent results among the five samples with no variables having a significant Spearman rank correlation across all, or even four out of five, of the samples (Figure 2.1). This suggests that there is not a consistent simple monotonic relationship between the genomic variable and latency, or that any such correlations are modest and not detectable across all studies given the available statistical power. We return to some of the stronger trends below.

To investigate whether a combination of variables may affect latency, we fit a lasso-regularized logistic regression, as implemented in the R package `glmnet`⁴⁰⁸, to predict latency using the genomic variables. The relationship between silent/inducible status and each genomic variable was allowed to vary between models by including the interaction of genomic features

Group	Type	Source	Number	Types
T cell expression	RNA-Seq	Chapter 4	1	RNA
Jurkat expression	RNA-Seq	Encode ⁴⁰⁰	1	wgEncodeHudsonalphaRnaSeq
Integration sites	Locations	Berry et al. ³⁹⁶	1	sites
DNase sensitivity	DNA-Seq/peaks	Encode ⁴⁰⁰	1	wgEncodeOpenChromDnase
Methylation	DNA-Seq	401	1	Methyl
CpG	Locations	UCSC ⁴⁰²	1	cpGIslandExt
Sequence-based	Continuous	—	4	% GC, HIV PWM score, distance to centrosome, chromosomal position
Repeats	Locations	UCSC ⁴⁰²	16	DNA, LINE, Low_complexity, LTR, Other, RC, RNA, rRNA, Satellite, scRNA, Simple_repeat, SINE, snRNA, srpRNA, tRNA, alphoid
Histone features	ChIP-Seq/Peaks	Wang et al. ⁴⁰³	18	H2AK5ac, H2AK9ac, H2BK120ac, H2BK12ac, H2BK20ac, H2BK5ac, H3K14ac, H3K18ac, H3K23ac, H3K27ac, H3K36ac, H3K4ac, H3K9ac, H4K12ac, H4K16ac, H4K5ac, H4K8ac, H4K91ac
Histone features	ChIP-Seq/Peaks	Barski et al. ⁴⁰⁴	23	CTCF, H2AZ, H2BK5me1, H3K27me1, H3K27me2, H3K27me3, H3K36me1, H3K36me3, H3K4me1, H3K4me2, H3K4me3, H3K79me1, H3K79me2, H3K79me3, H3K9me1, H3K9me2, H3K9me3, H3R2me1, H3R2me2, H4K20me1, H4K20me3, H4R3me2, PolII
Chromatin state	Binary	Ernst and Kellis ³⁹⁸	51	state ₁ ,state ₂ ,...,state ₅₁
HATs and HDACs	ChIP-Seq	Wang et al. ⁴⁰⁵	11	Resting-HDAC1, Resting-HDAC2, Resting-HDAC3, Resting-HDAC6, Resting-p300, Resting-CBP, Resting-MOF, Resting-PCAF, Resting-Tip60, Active-HDAC6, Active-Tip60
Nucleosome	ChIP-Seq	Schones et al. ⁴⁰⁶	2	Resting-Nucleosomes, Active Nucleosomes
UCSC genes	Locations	Hsu et al. ⁴⁰⁷	4	in gene, in gene (same strand), gene count, distance to nearest gene, in exon, in intron

Table 2.2: Genomic data available for comparison to HIV integration sites

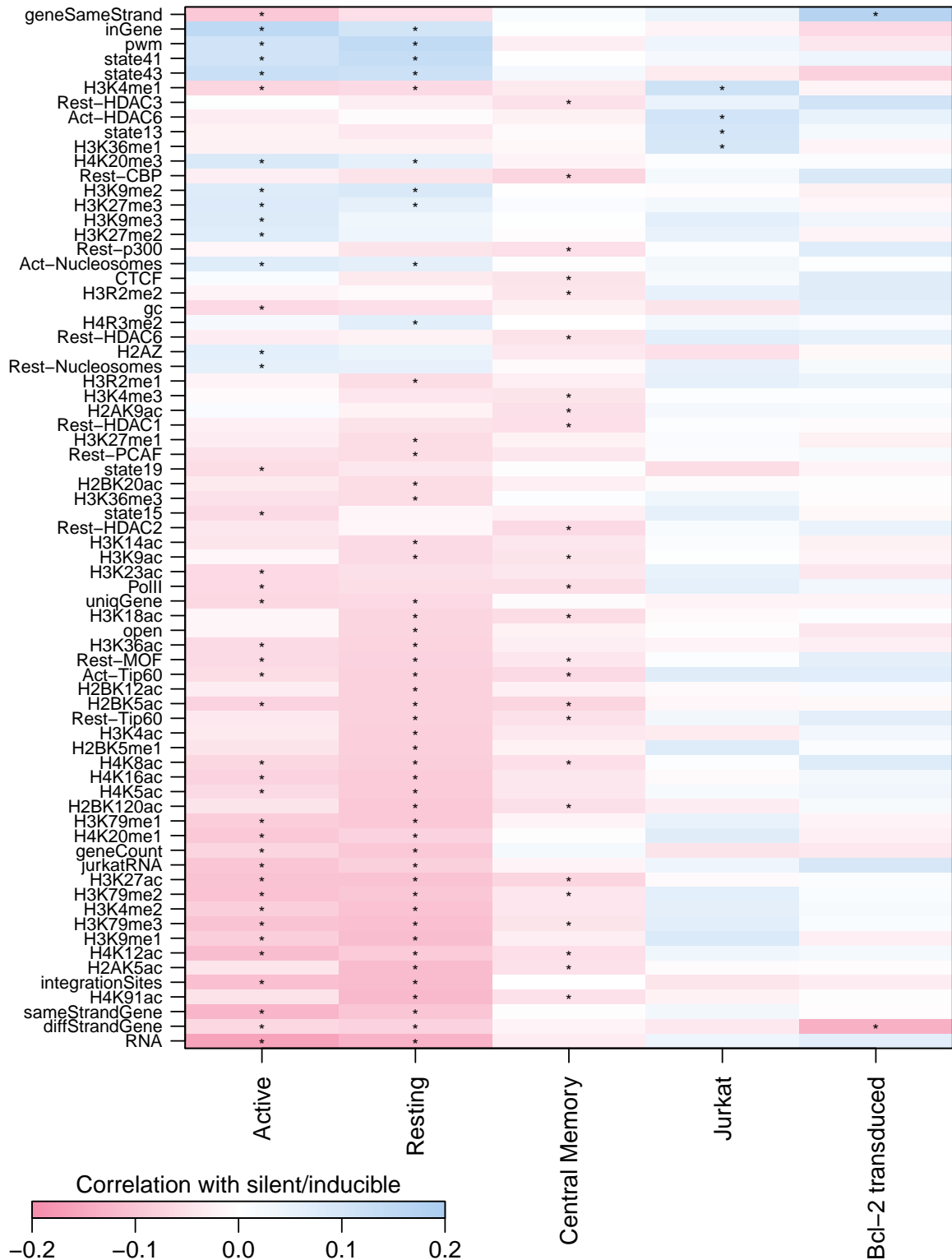


Figure 2.1: Spearman rank correlation between proviral expression status and genomic features. Only genomic features with at least one correlation with latency with a false discovery rate q -value < 0.01 (marked by asterisks) are shown.

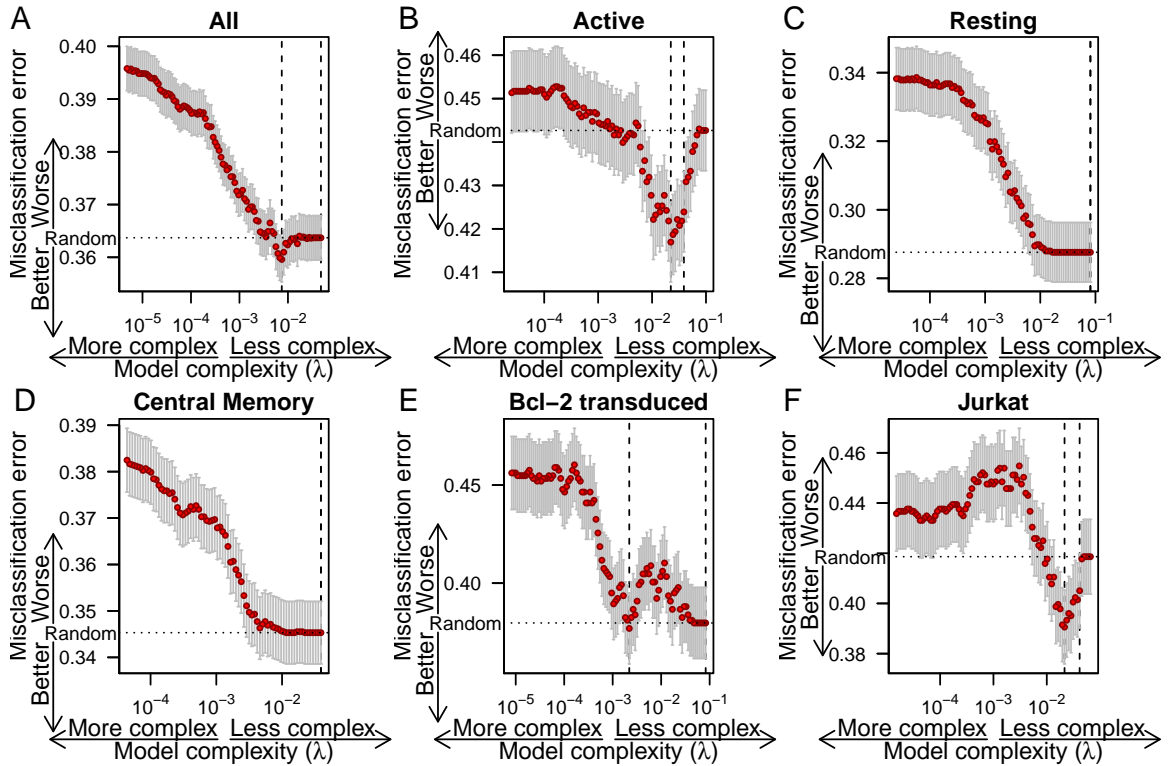


Figure 2.2: Misclassification error from cross validation for lasso regressions of silent/inducible status on genomic features as a function of λ , the regularization coefficient for the lasso regression, for all cell culture models combined and each individual cell culture model. The number of variables included and size of coefficients in the model increases to the left. Whiskers show the standard error of mean misclassification error. Dashed vertical lines indicate the minimum misclassification error and the simplest model within one standard error. Dotted horizontal line indicates the misclassification error expected from random guessing.

with dummy variables indicating cellular model. The λ smoothing parameter of the lasso regression was optimized by finding the λ with lowest classification error in 480-fold cross validation and finding the simplest model with misclassification error within one standard error.

The proportion of silent/inducible sites varied between the samples. To avoid the model overfitting on this source of variation, an indicator variable for each sample was included in the base model. The base model with no genomic variables was selected as the best model by cross validation (Figure 2.2A). This suggest that there is not a consistent linear relationship between an additive combination of genomic variables and latency across all models.

When each dataset was fit individually with leave-one-out cross validation, improvements in cross-validated misclassification error were only observed in the Active CD4⁺ (5.8% decrease in misclassification error, standard error: 2.1) and Jurkat (6.7% decrease in misclassification error, standard error: 3.5) samples (Figure 2.2B-F). There was no overlap in variables selected for the Active CD4⁺ and Jurkat samples.

Finding little global association between latency and genomic features, we investigated whether predictors of latency reported previously by single studies were consistently associated with latency across studies.

2.4.2 Cellular transcription

Model systems with defined integration sites show upstream transcription can interfere with viral transcription⁴⁰⁹ and that cellular transcription in the same orientation may interfere with viral transcription³⁷⁸ or increase viral transcription³⁷⁹ and in opposite orientations may decrease transcription³⁷⁹. In integration site studies, integration outside genes appears to increase latency¹⁵⁰ but high transcription of nearby host cell genes may cause increased latency^{150,151}. In addition, Tat or other viral proteins may affect cellular transcription^{319,410}.

To look at transcription and latency, we ran a logistic regression of silent/inducible status on a quartic function of RNA expression, as determined by RNA-Seq reads within 5,000 bases in Jurkat cells for the Jurkat sample or CD4⁺ T cells for the remaining samples, interacted with indicator variables encoding cell culture model. There appears to be little agreement between samples (Figure 2.3). The Resting CD4⁺ and Active CD4⁺ datasets show an enrichment in silent proviruses in regions with low gene expression. The other three studies show the opposite or no relationship for low expression regions. The two samples showing increased silence in areas of low expression (Resting CD4⁺ and Active CD4⁺) are from a study that did not check whether inactive viruses could be activated. One possible explanation is that regions with low gene transcription may harbor proviruses that are not easily activated, though some other discrepancy between *in vitro* systems could also explain

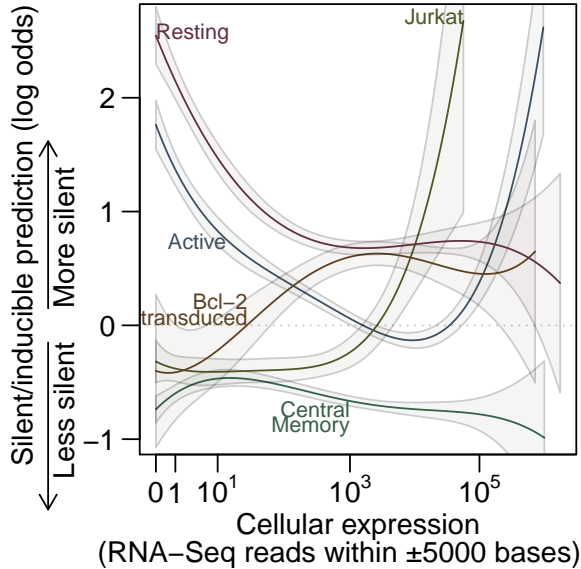


Figure 2.3: Predictions from a logistic regression of silent/inducible status on cellular RNA expression. High y-axis values are predicted to be silent/inducible. Dashed line shows where equal odds of silent/inducible and expressed are predicted. Solid lines show predictions from the regression for each sample and shaded regions indicate one standard error from the modeled predictions.

the difference. Both the Jurkat and Active CD4⁺ samples appear to increase in latency with increasing expression while the remaining three studies did not show a strong trend.

2.4.3 Orientation bias

Shan et al.¹⁵¹ reported that inducible proviruses were oriented in the same strand as the host cell genes into which they had integrated more often than chance. This orientation bias was still reproduced after our reprocessing of the Bcl-2 transduced CD4⁺ sample from Shan et al.¹⁵¹. However, the proportion of provirus oriented in the same strand as host genes did not differ significantly from 50% in the other samples (Figure 2.4). Perhaps orientation bias and transcriptional interference are especially sensitive to parameters of the model system.

2.4.4 Gene deserts

Lewinski et al.¹⁵⁰ reported increased latency in gene deserts. In the collected data, integration outside known genes was associated with latency (Fisher's exact test, $p < 10^{-6}$). This seemed to largely be driven by the Active CD4⁺ and Resting CD4⁺ samples with significant association found individually in only those two samples (both $p < 10^{-8}$) and no significant association observed in the other three samples (Figure 2.5A). Looking only at integration sites outside genes, silent sites in the Resting CD4⁺ sample had a mean distance to the

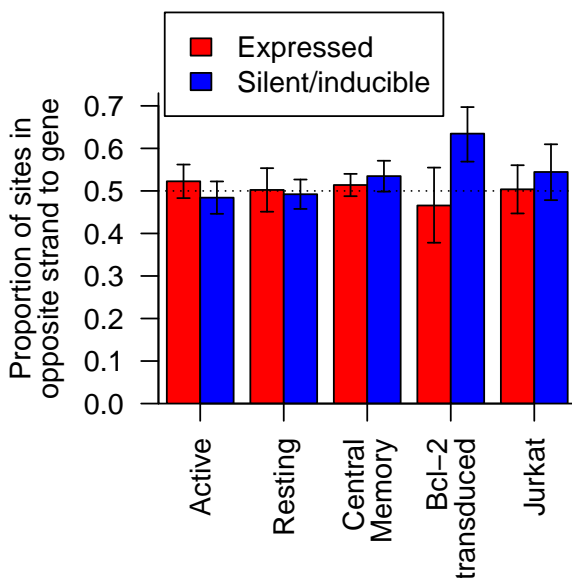


Figure 2.4: The proportion of provirus integrated in the opposite strand compared to cellular genes in silent/inducible (blue) and expressed (red) samples. Error bars show the 95% Clopper-Pearson binomial confidence interval.

nearest gene 2.5 times greater than that of expressed sites (95% CI: 2.2–6.2 \times , $p < 10^{-6}$, Welch two sample t-test on log transformed distance) (Figure 2.5B). The Active CD4⁺ sample had a small difference that did not survive Bonferroni correction.

Lewinski et al.¹⁵⁰ also reported decreased latency near CpG islands and reasoned this was tied to the increased latency in gene deserts. In the Resting CD4⁺ sample, silent sites were on average further from CpG islands than expressed sites (Bonferroni corrected Welch’s two sample T test, $p = 0.006$), but there was no significant relationship between silent/inducible status and log distance to CpG island after Bonferroni correction if the integration site’s location inside or outside of a gene was accounted for first (analysis of deviance).

2.4.5 Alphoid repeats

Alphoid repeats are repetitive DNA sequences found largely in the heterochromatin of centromeres⁴¹¹. Integration near heterochromatic alphoid repeats has been reported to associate with latency^{150,152,373}. Looking only at uniquely mapping sites, there was no statistically significant association between latency and location inside an alphoid repeat in pooled or individual samples (Fisher’s exact test).

Since alphoid repeats are both problematic to assemble in genomes and difficult to map

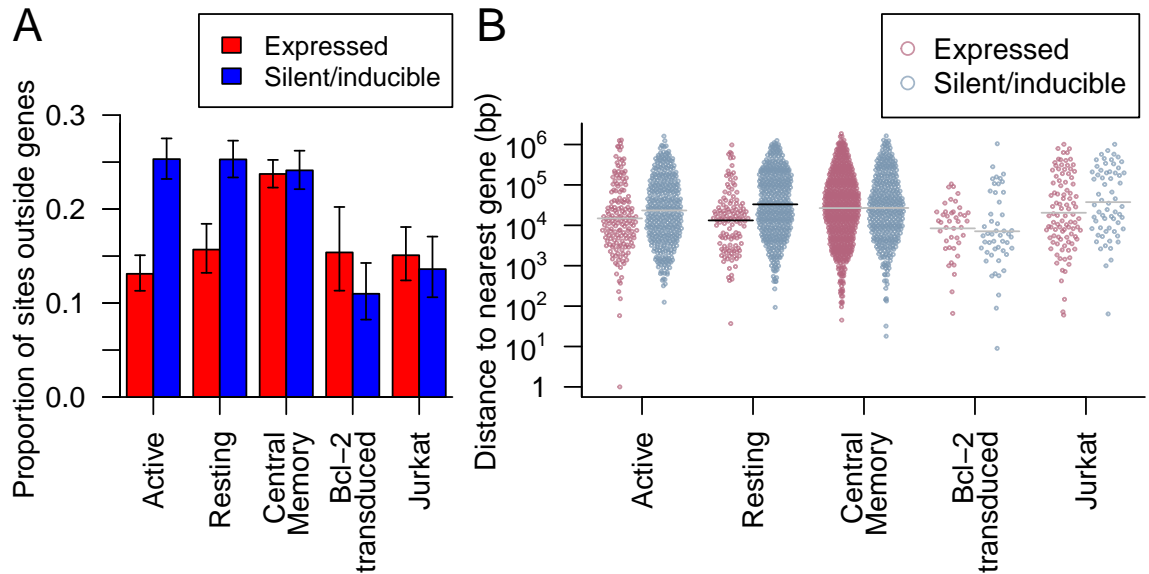


Figure 2.5: (A) The proportion of provirus integrated outside genes in silent/inducible (blue) and expressed (red) samples. Error bars show the 95% Clopper-Pearson binomial confidence interval. (B) The nearest distance to any gene for integration sites (points) outside genes in the five samples. Points are spread in proportion to kernel density estimates. Horizontal lines indicate sample means where there was a significant difference in means between silent/inducible and expressed provirus (black) or no significant difference (grey).

onto, we reasoned that some aliphoid hits might be lost or miscounted in the filtering procedures of the standard workup. To counteract this, we treated each sequence read as an independent observation of a proviral integration and included sequence reads with more than one best scoring alignment. For multiply aligned reads, we considered the read to have been inside an aliphoid repeat if any of its best scoring alignments fell within a repeat. We found 74 reads with potential aliphoid mappings. Integration inside aliphoid repeats was significantly associated with the expression status of a provirus in the Resting CD4⁺, Jurkat and Central Memory CD4⁺ datasets (Bonferroni corrected Fisher's exact test, all $p < 0.05$) and approached significance in the Active CD4⁺ dataset ($p = 0.053$) (Figure 2.6). The Bcl-2 transduced CD4⁺ data did not contain any integration sites in aliphoid repeats, probably due to 1) the relatively low number of integration sites in the dataset and 2) to the requirement for cleavage at two Pst1 restriction sites, which are not found in the consensus sequence of aliphoid repeats⁴¹². Of the 1340 repeat types in the RepeatMasker database⁴¹², only aliphoid repeats achieved a significant association with proviral expression in more than two datasets.

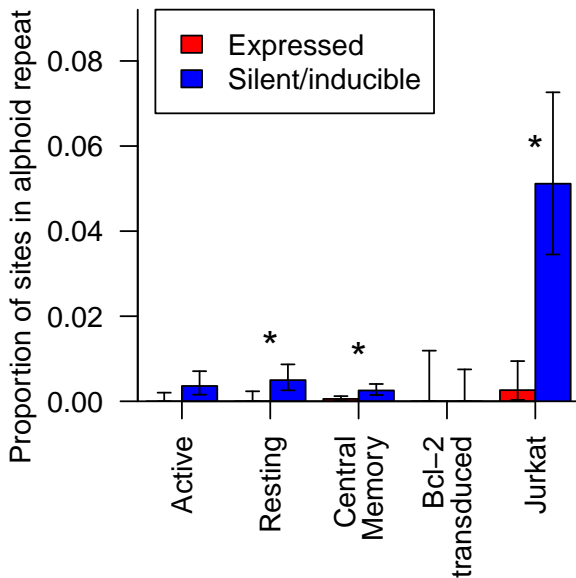


Figure 2.6: The proportion of integration sites with matches in alphoid repeats in silent/inducible (blue) and expressed (red) cells in five samples. Error bars show the 95% Clopper-Pearson binomial confidence interval. Asterisks indicate significant associations between integrations within an alphoid repeat and proviral expression status (Bonferroni corrected Fisher’s exact test $p < 0.05$).

2.4.6 Acetylation

Histone marks or chromatin remodeling, especially involving the key “Nuc-1” histone near the transcription start site in the viral LTR, appear to affect viral expression^{374,413,414}. Based on this effect, histone deacetylase inhibitors have been developed as potential HIV treatments and show some promise in disrupting latency³⁸³. In these genome-wide datasets, we do not have information on the state of individual LTR nucleosomes. However, repressive chromatin does seem to spread to nearby locations if not blocked by insulators^{370,371} and the state of neighboring chromatin could affect proviral transcription independently of provirus-associated histones.

We found that the number of ChIP-seq reads near an integration site from several histone acetylation marks (Figure 2.1) were associated with efficient expression in the Active CD4⁺, Resting CD4⁺ and Central Memory CD4⁺ samples. H4K12ac had the strongest association (Bonferroni corrected Fisher’s method combination of Spearman’s ρ , $p < 10^{-25}$) with silence/latency (Figure 2.7A).

Although the appearance of several significantly associated acetylation marks might suggest acetylation exerts a considerable effect on the expression of a provirus, there are strong

correlations among these marks, so their effects may not be independent. To account for the correlations between these variables, we performed a principal component analysis (PCA) to convert the correlated acetylation marks into a series of uncorrelated principal components that capture much of the variance within a few components. Here, the first principal component explained 59% of the variance and the first ten components 84%. Several of these principal components again displayed significant associations with latency in the Active CD4⁺, Resting CD4⁺ and Central Memory CD4⁺ samples but no significant correlations in the Bcl-2 transduced CD4⁺ or Jurkat samples (Figure 2.7B). A logistic regression of expression status on the first ten principal components and sample did not reduce misclassification error from a base model including only sample in 480-fold cross validation (base model misclassification error: 36.4%, PCA model: 36.5%). This suggests that acetylation of neighboring chromatin does not exert strong effects on latency in all samples.

2.4.7 Clustering

We reasoned that if there was a strong relationship between latency and chromosomal position, then integration sites that are near one another on the same chromosome should share the same expression status more often than expected by chance. To test this, we compared how often pairs of proviruses shared the same expression status in relation to the distance between the two sites (Figure 2.8). Pairs of sites with little distance between integration locations did share the same expression status more often than expected by chance (e.g. neighbors closer than 100bp, Fisher exact test $p = 0.0002$). Breaking out the data to separate between sample and within sample pairings showed that this matching was limited to neighbors within the same experimental model (Figure 2.8), emphasizing that chromosomal environment does appear to influence latency, but the factors involved differ among experimental models of latency.

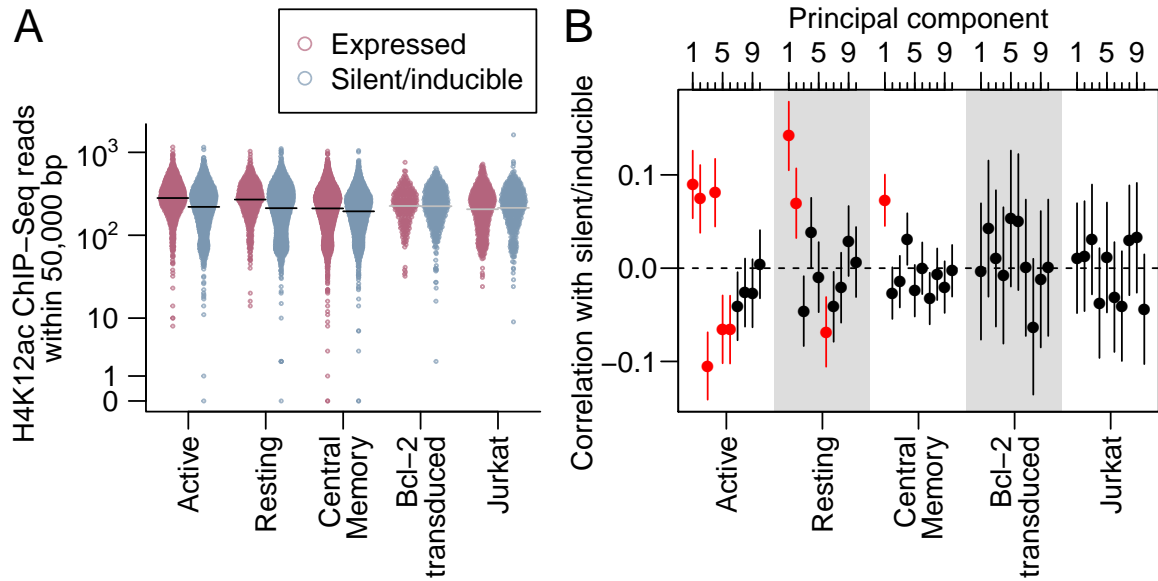


Figure 2.7: (A) The number of ChIP-seq reads for H4K12ac, the histone mark with the lowest Fisher’s method p -value for correlation with latency, within 50,000 bases across the five samples. Integration sites (points) are spread in proportion to kernel density estimates. Horizontal lines indicate sample means where there was a significant difference (black) in means between silent/inducible and expressed provirus or no significant difference (grey). (B) The correlation (points) and its 95% confidence interval (vertical lines) between principal components of acetylation and silent/inducible status for each of the five samples. Red indicates correlations with a Bonferroni-corrected p -value < 0.05 .

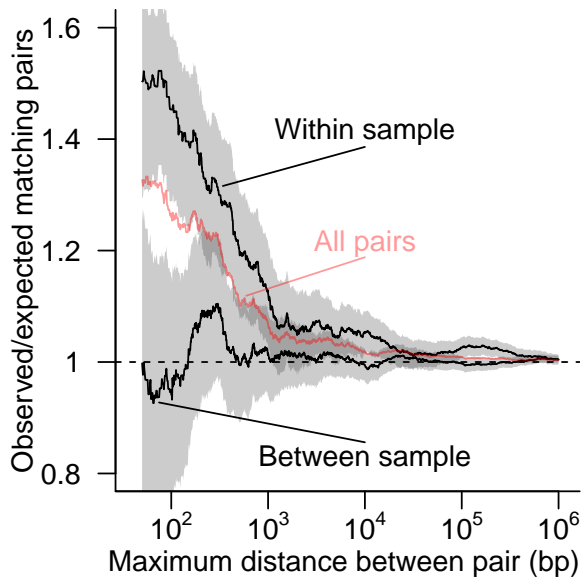


Figure 2.8: The ratio of the number of pairs of proviruses with matching expression status to the number of matches expected by random pairings given the frequency of silent/inducible proviruses. All possible pairs of proviruses integrated within a given distance of each other on the same chromosome (red line) were separated into two sets; one with both proviruses from within the same cell culture model and one with proviruses paired between two different cell culture models (black lines). The shaded region shows the 95% Clopper-Pearson binomial confidence interval for within and between sample pairings. The dashed horizontal line shows the ratio of 1 expected if there is no association between the expression status of neighboring proviruses.

2.5 Conclusions

Here we compared the latency status of HIV-1 proviruses in five model systems with the genomic features surrounding their integration sites. Surprisingly, no relationships between genomic features near the integration location and latency achieved significance in all models. Proviruses from the same cellular model integrated in nearby positions did share the same latency status much more often than predicted by chance, indicating the existence of local features influencing latency, but these were not consistent among models. This suggests that whatever features are affecting latency are highly local and model-specific, and that we may not have access to all relevant chromosomal features e.g. ^{415–418}.

In addition to differences in experimental conditions, methodological issues have the potential to obscure patterns. Examples include multiply infected cells, inactivated viruses and inaccurate assessment of HIV gene activity—each of these are discussed below.

A latent provirus integrated into the same cell as an expressed provirus will be erroneously sorted as expressed, potentially confounding analysis. A low multiplicity of infection (MOI) will help to avoid this problem, but there is still the potential for a significant proportion of the cells studied to contain multiple integrations. This problem arises because although cells with multiple integrations form a small proportion of total cells, most of the total are cells lacking an integrated provirus and thus are excluded by experimental design. For example, assuming integrations are Poisson distributed with an MOI of 0.1 (1 integration per 10 cells), 90.5% of cells will not contain a provirus, 9% of cells will contain one proviral integration and 0.5% of cells will contain multiple integrations. The cells without an integration are not amplified by HIV-targeted PCR leaving only 9.5% of the total cells. Of these cells actually under study, 4.9% will contain multiple integrations. Thus the signal from expressed proviruses may be muted by the presence of latent proviruses in the expressed population.

The replication cycle of HIV is error prone, and a significant proportion of virions contain mutated genomes⁸⁷. In studies that do not check for inducibility, mutant proviruses

integrated in regions of the genome otherwise favorable to proviral expression can be sorted into the latent pool due to mutational inactivation. This problem of inactivated provirus is worse when latent provirus are rare and exacerbated further when looking at latency in the cells of HIV patients due to selective enrichment of inactivated proviruses incapable of spreading infection¹⁴⁰. Here, the effects of mutation are minimized in the datasets that required inducible viral expression (Jurkat, Bcl-2 transduced CD4⁺, Central Memory CD4⁺) but may be a confounder in the two datasets that were sorted based on lack of viral expression only (Active CD4⁺, Resting CD4⁺).

Inaccurate staining or leaky markers may also result in misclassification of proviruses. False positives and false negatives will result in incorrectly sorted latent and expressed integrations. For example, if 5% of cells not containing Gag are labeled as Gag+ and there are an equal amount of latent and expressed integration sites, then 4.8% of integrations labeled expressed will actually be latent. If a category is rare, false staining has even greater potential to cause error. For example, if only 5% of sites are latent and a Gag stain has a false negative rate of 5%, then we would expect 48.7% of sites classified as latent to actually be mislabeled expressed integrations.

Attempts to induce latent proviruses in patients have so far focused on using histone deacetylase inhibitors, raising interest in associations with histone acetylation in these data. An important caveat in results from these genome-wide data is that histone modification near the integrated provirus may not be representative of modification within the provirus at the key “Nuc-1” nucleosome of the transcription start site⁴¹⁴, though local correlations in chromatin states are well established from studies of position effect variegation^{370,371}. We found that some histone acetylation marks were significantly associated with viral expression in some but not all samples (Figures 2.1, 2.7). This lack of association may be due to a lack of power in these studies, but the confidence intervals suggest that any correlations between acetylations and latency are unlikely to be strong. These weak correlations raise the possibility that there are populations of latent proviruses that are not associated with

acetylation and may not be inducible by histone deacetylase inhibitors.

This study highlights that the choice of model system can have a large effect on measurements of latency. Further studies are needed to determine which *in vitro* models best reflect latency *in vivo*. Different cell models may report genuinely different mechanisms of latency. While we did see some relationship between histone acetylation and latency, paralleling a recent clinical trial of SAHA³⁸³, associations with histone acetylation did not explain a large fraction of the difference between latent and expressed proviruses in any of the five models. One possible explanation is that there may be multiple mechanisms that maintain proviruses in a latent state. To be successful, shock-and-kill treatments must induce and destroy all latent proviruses to eliminate HIV from an infected individual, raising the question of whether multiple simultaneous inducing treatments will be necessary.

2.6 Availability of supporting data

Sequence reads from the Central Memory CD4⁺ sample reported here, the Resting CD4⁺ and Active CD4⁺ data reported by Pace et al.¹⁵², the Bcl-2 transduced CD4⁺ data reported by Shan et al.¹⁵¹ and reprocessed data originally reported by Lewinski et al.¹⁵⁰ are available at the Sequence Read Archive under accession number SRP028573.

2.7 Acknowledgements

We would like to thank Werner Witke for assistance with IonTorrent sequencing. This work was supported in part by NIH grants R01 AI 052845-11 to FDB, R21AI 096993 and K02AI078766 to UO'D, 5T32HG000046 to SS-M, AI087508 to VP and R01AI038201 to JG, the Penn Genome Frontiers Institute, the University of Pennsylvania Center for AIDS Research (CFAR) P30 AI 045008 and the University of California, San Diego, CFAR P30 AI036214.

CHAPTER 3: Dynamic regulation of HIV-1 mRNA populations analyzed by single-molecule enrichment and long-read sequencing

This chapter was originally published as:

KE Ocwieja, S Sherrill-Mix, R Mukherjee, R Custers-Allen, P David, M Brown, S Wang, DR Link, J Olson et al. 2012. Dynamic regulation of HIV-1 mRNA populations analyzed by single-molecule enrichment and long-read sequencing. *Nucleic Acids Res*, 40:10345–10355. doi: 10.1093/nar/gks753

FD Bushman, K Travers, DR Link, E Schadt, KE Ocwieja and R Mukherjee conceived and designed the experiment. KE Ocwieja and R Custers-Allen carried out sample preparation and experimental validation. P David and J Olson performed single-molecule amplification. K Travers and S Wang performed sequencing. KE Ocwieja, M Brown and I analyzed the data. KE Ocwieja and I produced the figures. KE Ocwieja, FD Bushman and I wrote the manuscript.

Supplementary data are available at <http://nar.oxfordjournals.org/content/40/20/10345/suppl/DC1>

3.1 Abstract

Alternative RNA splicing greatly expands the repertoire of proteins encoded by genomes. Next-generation sequencing (NGS) is attractive for studying alternative splicing because of the efficiency and low cost per base, but short reads typical of NGS only report mRNA fragments containing one or few splice junctions. Here, we used single-molecule amplification and long-read sequencing to study the HIV-1 provirus, which is only 9700 bp in length, but encodes nine major proteins via alternative splicing. Our data showed that the clinical isolate HIV_{89.6} produces at least 109 different spliced RNAs, including a previously unappreciated ~1 kb class of messages, two of which encode new proteins. HIV-1 message populations

differed between cell types, longitudinally during infection, and among T cells from different human donors. These findings open a new window on a little studied aspect of HIV-1 replication, suggest therapeutic opportunities and provide advanced tools for the study of alternative splicing.

3.2 Introduction

Alternative splicing greatly expands the information content of genomes by producing multiple mRNAs from individual transcription units. Approximately 95% of human genes with multiple exons encode RNA transcripts that are alternatively spliced, and mutations that affect alternative splicing are associated with diseases ranging from cystic fibrosis to chronic lymphoproliferative leukemia^{420–424}. Work to decipher an RNA ‘splicing code’ has revealed that multiple interactions between trans-acting factors and RNA elements determine splicing patterns, though regulation is little understood for most genes³⁰⁵.

The integrated HIV-1 provirus is ~9700 bp in length and has a single transcription start site, but according to the published literature yields at least 47 different mRNAs encoding 9 proteins or polyproteins, making HIV an attractive model for studies of alternative splicing⁴²⁵. HIV mRNAs fall into three classes: the unspliced RNA genome, which encodes Gag/Gag-Pol; partially spliced transcripts, ~4 kb in length, encoding Vif, Vpr, a one-exon version of Tat, and Env/Vpu; and completely spliced mRNAs of roughly 2 kb encoding Tat, Rev and Nef (Figure 3.1A). Additional rare ‘cryptic’ splice donors (5’ splice sites) and acceptors (3’ splice sites) contribute even more mRNAs^{426–431}. A complex array of positive and negative cis-acting elements surrounding each splice site regulates the relative abundance of the HIV-1 mRNAs, and disrupting the balance of message ratios impairs viral replication in several models^{284,432–438}. Studies have suggested strain-specific splicing patterns may exist^{425,439,440}. However, detailed studies of complete message populations have not been reported for clinical isolates of HIV-1.

Several groups have demonstrated tissue- and differentiation-specific splicing of cellular

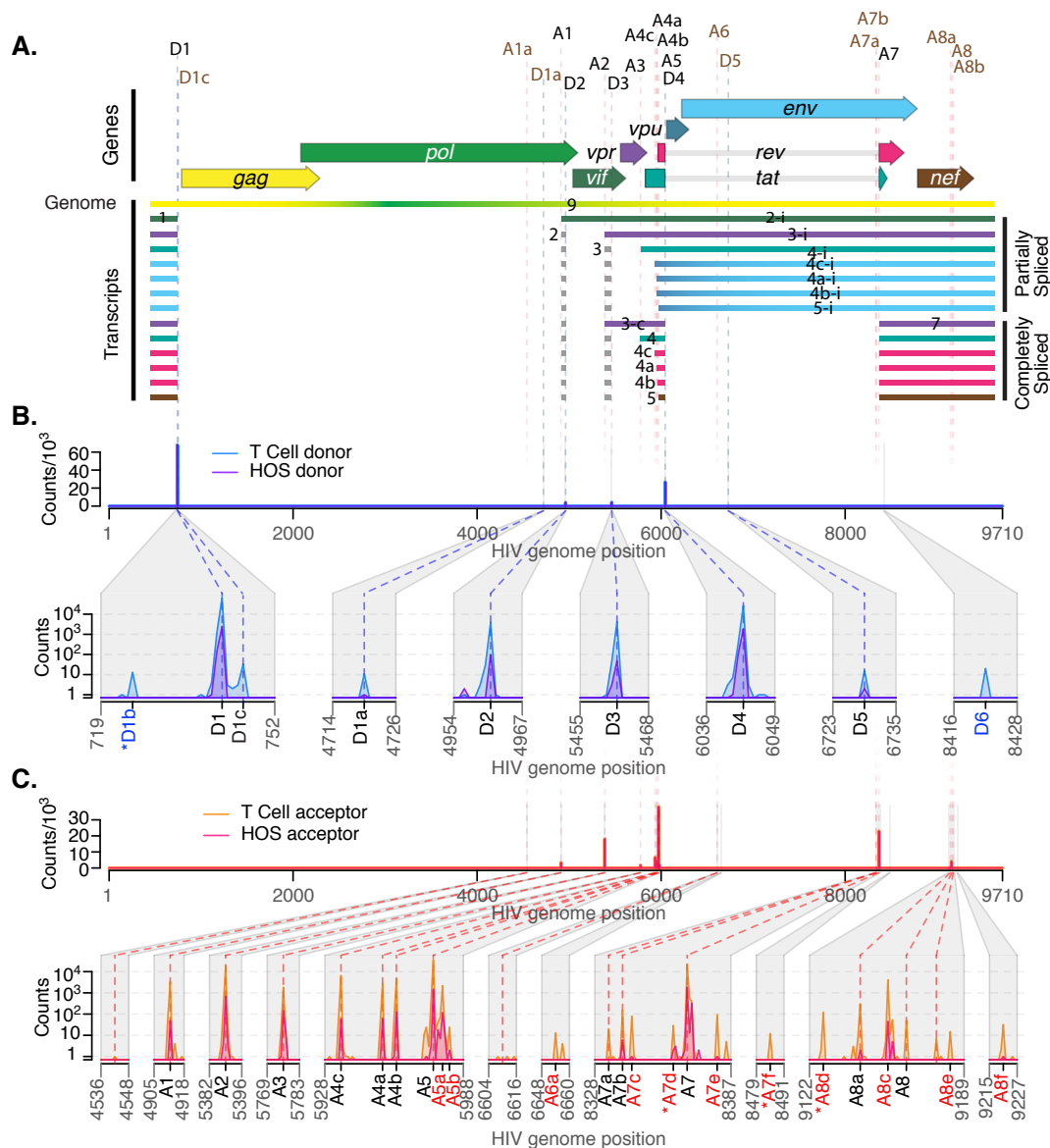


Figure 3.1: Mapping the splice donors and acceptors of HIV_{89.6}. PacBio sequence reads of HIV_{89.6} cDNA from infected HOS-CD4-CCR5 (HOS) and CD4⁺ T cells were aligned to the HIV_{89.6} genome shown in (A). Exons of the conserved HIV-1 transcripts are colored according to the encoded gene. Conserved (black) and published cryptic (brown) splice donors ('D') and acceptors ('A') are shown. Gaps in HIV-1 sequence alignments with at least one end located at a published or verified splice donor or acceptor were defined as introns. For each base of the HIV_{89.6} genome, the number of sequence reads in which that base occurred at the 5'-end (B) or 3'-end (C) of an intron is plotted for each cell type. Putative splice donors and acceptors were defined as loci that were found in at least 10 reads at the 5'- and 3'-ends of introns in sequence alignments from T-cell infections. Regions containing splice sites are enlarged for clarity. Asterisks indicate putative splice sites that are adjacent to dinucleotides other than the consensus GT and AG.

genes^{421,441,442}. Importantly for HIV, these include changes during T-cell activation^{443,444}, raising the question of how cell-specific splicing affects HIV replication. While most studies of HIV-1 splicing have been conducted in cell lines using lab-adapted viral strains, limited works in PBMCs from infected patients, monocytes and macrophages have suggested that differences may indeed exist in relevant cell types^{427,439,445,446}. Moreover, human splicing patterns differ between individuals, but such polymorphisms have not been investigated in the context of HIV infection^{447,448}.

Here, we use deep sequencing to comprehensively characterize the transcriptome of an early passage clinical isolate, HIV_{89.6}⁴⁴⁹, in primary CD4⁺ T cells from seven human donors and in the human osteosarcoma (HOS) cell line. Many deep sequencing techniques provide short reads, which rarely query more than a single exon-exon junction. To distinguish the full structure of HIV-1 mRNAs, which can contain several splice junctions, we used Pacific Biosciences (PacBio) sequencing technology, which yields read lengths up to 10 kb⁴⁵⁰. We used RainDance Technologies single-molecule PCR enrichment to preserve ratios of RNAs during preparation of sequencing templates. We identified previously published and novel HIV-1 transcripts and determined that HIV_{89.6} encodes a minimum of 109 different splice forms. These included a new size class of transcripts, some of which contain novel open reading frames (ORFs) that encode new proteins. We also found significant variation between cell types, over time during infection of HOS cells and among individuals. These data reveal unanticipated complexity and dynamics in HIV-1 message populations, begin to clarify a little studied dimension of HIV-1 replication and suggest possible targets for therapeutic interventions.

3.3 Materials and methods

3.3.1 Cell culture and viral infections

HIV_{89.6} was generated by transfection and subsequent expansion in SupT1 cells. Primary T cells were isolated by the University of Pennsylvania Center for AIDS Research Im-

munology core and confirmed to be homozygous for the wild-type CCR5 allele as shown in Supplementary Table S1 and described in Supplementary Methods. HOS-CD4-CCR5 cells^{451,452} were obtained through the AIDS Research and Reference Reagent Program, Division of AIDS, NIAID, NIH from Dr Nathaniel Landau. Single round infections in T cells and HOS-CD4-CCR5 cells were performed using standard methods (see Supplementary Methods).

3.3.2 RNA and reverse transcription

Total cellular RNA was purified using the Illustra RNA kit (GE Life Sciences, Fairfield, CT, USA) from 5×10^6 cells per infection. Viral cDNA was made using a reverse transcription primer complementary to a sequence in U3 (RTprime, Supplementary Table S2). We used Superscript III reverse transcriptase (Invitrogen) in the presence of RNaseOUT (Invitrogen) to conduct first-strand cDNA synthesis from equal amounts of total cellular RNA from each HOS-CD4-CCR5 time point (15.2 μ g) and from each T-cell infection (3 μ g) according to the manufacturer's instructions for gene-specific priming of long cDNAs, and then treated with RNaseH (Invitrogen). We checked for full reverse transcription of the longest (unspliced) viral cDNAs by PCR using primers that bind in the first major intron of HIV_{89.6} (keo003, keo004, Supplementary Table S2, data not shown).

3.3.3 Bulk RT-PCR and cloning

Transcripts were amplified from cellular RNA using the Onestep RT-PCR kit (Qiagen) with primer pairs keo056/keo057 and keo058/keo059 (Supplementary Table S2) with the following amplification: 5 cycles of 30 s at 94°C, 12 s at 56°C, 40 s at 72°C; then 30 cycles of 30 s at 94°C, 14 s at 56°C, 40 s at 72°C; and finally 10 min at 72°C. For verification of dynamic changes, primers F1.2 and R1.2 were used with 35 cycles of 30 s at 94°C, 30 s at 56°C and 45 s at 72°C followed by 10 min at 72°C. Products were resolved on agarose gels (Nusieve 3:1, Lonza for verification of dynamic changes, Invitrogen for cloning) stained with ethidium-bromide (Sigma) for visualization, or SYBR Safe DNA gel stain (Invitrogen) for

cloning (keo056/keo057 amplified material). DNA was purified using Qiaquick gel extraction kit (Qiagen) and cloned using the TOPO TA cloning kit (Invitrogen). Plasmid DNA was prepared using Qiaprep Spin Miniprep kit (Qiagen). Inserts were identified and verified using Sanger sequencing. The cDNAs for *tat*^{8c}, *tat* (1 and 2 exon), *ref*, *rev* and *nef*, and the transcript with exon structure 1-5-8c were cloned into the expression vector pIRES2-AcGFP1 (Clontech) as described in Supplementary Methods.

3.3.4 Assays of protein activity and HIV replication

Activity and HIV replication assays were performed as described in Supplementary Methods. Tat activity expressed from each cDNA was measured in TZM-bl cells²⁰⁴ (gift of Dr Robert W. Doms). Rev activity was assayed in HEK-293T cells co-transfected with pCMVGagPol-RRE-R, a reporter plasmid from which Gag and Pol are expressed in a Rev-dependent manner (gift of David Rekosh)⁴⁵³. Intracellular and released supernatant p24 was measured from cells transfected with expression constructs and infected with HIV_{89.6}.

3.3.5 Western blotting

HEK-293T cells were transfected with expression constructs and treated with MG132 (EMD Chemicals) to inhibit the proteasome or DMSO (Supplementary Methods). Proteins were detected by immunoblotting using a mouse antibody that recognizes the carboxy terminus of HIV-1 Nef diluted 1:1000 in 5% milk (gift of Dr James Hoxie)⁴⁵⁴. Horseradish peroxidase (HRP)-conjugated secondary rabbit-anti-mouse antibody (p0260, DAKO) was used for detection with SuperSignal West Pico Chemiluminescent Substrate (Thermo Scientific). Beta-tubulin was used as a loading control, detected by the HRP-conjugated antibody (ab21058, Abcam).

3.3.6 Single-molecule amplification

Amplification was performed by RainDance Technologies using a protocol similar to that previously reported (detailed description in Supplementary Methods)⁴⁵⁵. Amplification

was carried out in droplets to suppress competition between amplicons. PCR droplets were generated on the RDT 1000 (RainDance Technologies) using the manufacturer's recommended protocol. The custom primer libraries for this study contained 18 (HOS-CD4-CCR5 cells) or 20 (primary T cells) PCR primer pairs designed to amplify different HIV RNA isoforms (Supplementary Table S2).

3.3.7 Single-molecule sequencing

DNA amplification products from the RainDance PCR droplets were converted to SMRTbell templates using the PacBio RS DNA Template Preparation Kit. Sequencing was performed by Pacific Biosciences using the PacBio SMRT sequencing technology as described⁴⁵⁰. Sequence information was acquired during real time as the immobilized DNA polymerase translocated along the template molecule. Prior to sequence acquisition, hairpin adapters were ligated to each DNA template end so that DNA polymerase could traverse DNA molecules multiple times during rolling circle replication (SMRTbell template sequencing⁴⁵⁶), allowing error control by calculating the consensus ('circular consensus sequence' or CCS). For raw reads, the average length was 2860 nt, and 10% were > 5000 nt. After condensing into consensus reads, the mean read length was 249.5 nt, due to the use of a shorter Pacific Biosciences sequencing protocol to accommodate the small size of many amplicons. Consensus reads of 1% were > 1100 nt. Sequencing data were collected in 45-min movies.

3.3.8 Data analysis

Raw reads were processed to produce CCSs. Raw reads were also retained to help in primer identification and to avoid biasing against long reads. Reads were aligned against the human genome using Blat³⁹⁵. Misprimed reads matching the RT primer, reads with a CCS length shorter than 40 nt or raw length shorter than 100 nt and reads matching the human genome were discarded. Filtered reads were aligned against the HIV_{89.6} reference genome. Potential novel donors and acceptors were found by filtering putative splice junctions in the Blat hits for a perfect sequence match 20 bases up- and downstream of the junction, ignoring

homopolymer errors, and requiring that one end of the junction be a known splice site. Local maximums within a 5-nt span with > 9 such junctions were called as novel splice sites.

Filter-passed reads were aligned against all expected fragments based on primers and known and novel junctions. Primers were identified in CCS reads by an edit distance ≤ 1 from the primer in the start or end of the read, in raw reads by an edit distance ≤ 5 from a concatenation of the primer, hairpin adapter and the reverse complement of the primer, and in both types of reads by a Blat hit spanning an entire expected fragment.

Gaps in Blat hits were ignored if ≤ 10 bases long or in regions of likely poor read quality ≤ 20 bases long where an inferred insertion of unmatched bases in the read occurred at the same location as skipped bases in the reference. Any Blat hits with a gap > 10 nt remaining in the query read were discarded. If HIV sequence was repeated in a given read (likely due to PacBio circular sequencing), the alignments were collapsed into the union of the coverage. Gaps in the HIV sequence found in uninterrupted query sequence were called as tentative introns. Splice junctions were assigned to conserved or previously identified (published or in this work) splice sites and reads appearing to contain donors or acceptors further than 5 nt away from these sites were discarded. Reads with Blat hits outside the expected primer range were discarded from that primer grouping. The assigned primer pair, observed junctions and exonic sequence were used to assign each read to a given spliceform (specific transcript structure) or set of possible spliceforms. Partial sequences that did not extend through both primers were assigned to specific transcripts if the read contained enough information to rule out all other spliceforms or if all other possible spliceforms contained rare ($< 1\%$ usage) donors or acceptors (Supplementary Table S3). Otherwise, the read was called indeterminate.

To calculate the ratios of transcripts within the partially spliced class, we counted the number of reads for each assigned spliceform amplified by primer pair 1.3 and divided by the total number of assigned partially spliced reads amplified with these primers (Supplementary Figure S1 and Supplementary Table S2). Assigned sequences amplified with primer pairs

1.4 and 4.1 (full-length cDNAs, T cells only) were used to calculate ratios of transcripts within each of the two completely splice classes (~2 and ~1 kb). To compare ratios of ~2 kb transcripts calculated within reads from primer pairs 1.4 and 4.1, we normalized ratios from pair 4.1 to the *nef* 2 transcript (containing exons 1, 5 and 7). Due to size biases inherent in the approach, we did not compare across size classes, and unspliced transcripts were not included in ratio analysis. For all ratio analysis, transcripts including cryptic or novel junctions were counted only if they appeared in at least five reads, otherwise they were excluded from the analysis and from the count of total assigned reads.

To estimate the minimum total number of transcripts present, partial sequence reads were included. Each exon-exon junction occurring in at least five reads and not previously assigned to a particular transcript (Figure 3.2) was counted as evidence of an additional transcript (47 additional junctions were detected, see Supplementary Table S4). If two such junctions could conceivably occur in a single mRNA, we counted only one unless we could verify from sequence reads that they were amplified from separate cDNAs, resulting in 31 additional transcripts. The minimum transcript number calculated by a greedy algorithm treating introns as events in a scheduling problem agreed with the above calculation.

Several groups have demonstrated tissue- and differentiation-specific splicing of cellular genes^{421,441,442}. Importantly for HIV, these include changes during T-cell activation^{443,444}, raising the question of how cell-specific splicing affects HIV replication. While most studies of HIV-1 splicing have been conducted in cell lines using lab-adapted viral strains, limited works in PBMCs from infected patients, monocytes and macrophages have suggested that differences may indeed exist in relevant cell types^{427,439,445,446}. Moreover, human splicing patterns differ between individuals, but such polymorphisms have not been investigated in the context of HIV infection^{447,448}.

For studies of transcript dynamics, reads from primer pairs 1.2, 1.3 and 1.4 containing junctions between D1 or any donor and each of five mutually exclusive acceptors, A3, A4c, A4a, A4b, A5 and A5a, were collected and their ratios calculated.

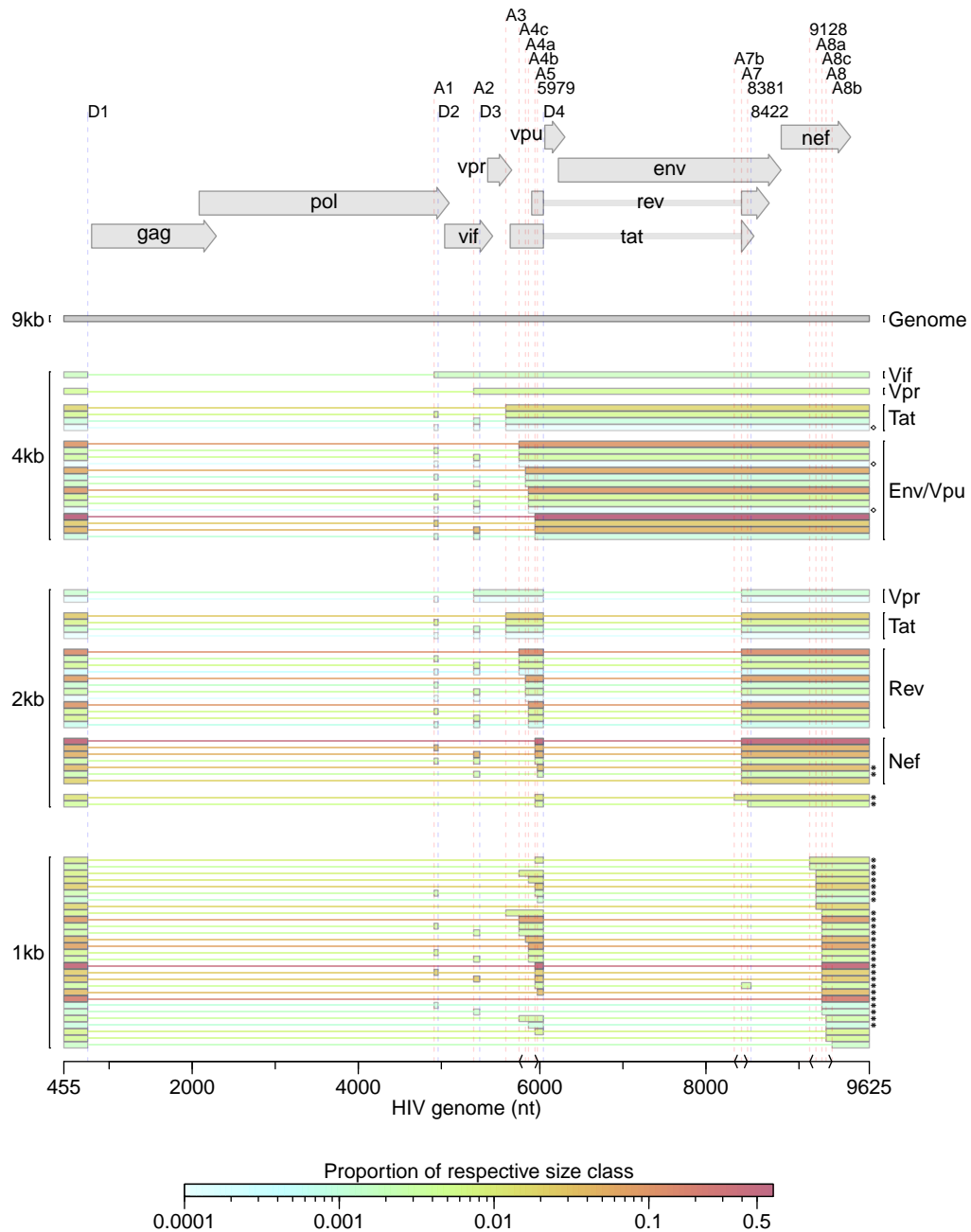


Figure 3.2: HIV_{89.6} transcripts in T cells for which the full message structure was determined are shown arranged by size class. Thick bars correspond to exons and thin lines to excised introns. For the well-conserved transcripts, encoded proteins are indicated. The relative abundance of each transcript within its size class is indicated by color. Asterisks denote transcripts that have not been reported previously to our knowledge. Of the 47 conserved HIV-1 transcripts, three were detected in fewer than five reads (indicated with \diamond) and two messages were not detected and are not shown (one encoding Vpr and one encoding Env/Vpu). Depicted non-conserved transcripts (using novel or cryptic splice sites) were each detected in at least five independent sequence reads across samples from at least two different human T-cell donors.

3.3.9 Statistical analysis

Statistical modeling was performed using generalized linear modeling as described in Appendix A.1. All analyses were performed in R 2.14.0 (R Development Core)³⁸⁸.

3.3.10 Data access

Sequence data is available in the SRA database with the following accession numbers: SRP014319.

3.4 Results

3.4.1 Sequencing HIV-1 transcripts produced in primary T cells and HOS cells

In order to characterize HIV-1 transcript populations, we prepared viral cDNA from primary CD4⁺ T cells of seven different healthy human donors infected in vitro with HIV_{89.6}, an early passage dual-tropic clade-B clinical isolate (Supplementary Figure S1, human donor data in Supplementary Table S1)⁴⁴⁹. We also studied HIV messages produced in infected HOS cells engineered to express CD4 and CCR5 (HOS-CD4-CCR5) because these cells support efficient HIV replication and engineered variants are widely used in HIV research. HOS cells were harvested at 18, 24 and 48 hours post infection (hpi) to investigate longitudinal changes during infection, and for comparison to 48 h infected T cells.

To preserve the relative proportions of template molecules while amplifying the cDNA, we used RainDance Technologies' single-molecule micro-droplet based PCR⁴⁵⁵. Droplet libraries containing multiple overlapping primer pairs were designed to query all message forms and allow later calculation of relative abundance (Supplementary Table S2 and Supplementary Figure S1). Each primer was unique so that sequences could be assigned to a specific primer pair, which helped reconstruct the origin of sequence reads and deduce message structures. Amplified DNA products were sequenced using Single Molecule Real-Time (SMRT) technology from Pacific Biosciences^{450,456}. We obtained 847 492 filtered reads of amplified HIV-1 transcripts in primary CD4⁺ T cells and 89 350 in HOS cells. The longest

sequenced continuous stretch of HIV-1 cDNA was 2629 bp.

3.4.2 Splice donors and acceptors

We aligned PacBio reads containing HIV sequences to the HIV_{89.6} genome and identified candidate introns as recurring gaps in our sequences. Using this approach, we observed splicing at each of the widely conserved major splice donors and acceptors and several published cryptic sites (Figure 3.1A, hereafter referred to by their identifications shown in this figure, ‘D’ for donors, ‘A’ for acceptors).

In addition, we identified 13 putative novel splice sites: 2 donors and 11 acceptors (Figure 3.1 and Supplementary Table S3). In order to be selected as a bona fide splice site and remove artifacts possibly created by recombination during sample preparation, we required that the new acceptor or donor was observed spliced to previously reported splice donors or acceptors in > 10 sequence reads in CD4⁺ T cells. The most frequently used novel splice site was an acceptor that we have termed A8c because it lies near A8, A8a and A8b (discussed in detail below). Additional novel sites are further discussed in Supplementary Report S1.

Most of the new splice sites adhered to consensus sequences for the standard spliceosome (Supplementary Table S3). However, there appeared to be one splice donor upstream of D1 with a cytidine in place of the usual uracil 2 nt downstream of the splice site. Similar ‘GC donors’ appear in 1% of known splice junctions in humans⁴⁵⁷. Of the novel splice acceptors, three were preceded by dinucleotides other than the consensus AG. Alternative dinucleotides are used infrequently as splice acceptors^{458–461}; however, it is possible that our deep sequencing method allowed us to observe rare events.

3.4.3 Structures of spliced HIV_{89.6} RNAs

To quantify the populations of HIV-1 transcripts, we aligned all reads to the collection of 47 well-established spliced HIV-1 transcripts and detected 45 of them (Figure 3.2). We additionally aligned reads to the HIV_{89.6} genome allowing all possible combinations of splice

junctions—canonical, cryptic or novel—determined from the sequencing data (Figure 3.1), yielding an additional 32 complete transcripts, 19 of which were novel. The data also provide evidence for more novel splice junctions but in incomplete sequences, implying the existence of additional new transcripts (Supplementary Table S4 and Supplementary Report S1). The full data set taken together provides evidence for least 109 different HIV_{89.6} transcripts in primary T cells.

Amplification primers that isolated the two main classes of spliced messages allowed us to determine the ratios of mRNAs in each (Figure 3.2 and Supplementary Table S5). Within the partially spliced class of transcripts, *env/vpu*, *tat* (1-exon), *vpr* and *vif* messages existed in an average ratio of 96:4:< 1:< 1 in CD4⁺ T cells. The ratio of *nef:rev:tat:vpr* within the ~2 kb transcript class was 64:33:3:< 1. Consistent with previous reports, the most abundant transcript in each class contained the splice junction from D1 to A5 (D1[^]A5)—an *env/vpu* transcript contributing 64% of the partially spliced class, and a completely spliced *nef* transcript contributing 47% of ~2 kb messages (Figure 3.2)^{425,462}. The relatively low abundance of transcripts encoding Tat suggests that Tat sufficiently stimulates HIV transcription elongation at low concentrations, or that the *tat* transcripts must be efficiently translated. Due to biases inherent in the reverse transcription step, we could only compare transcripts within each size class, and we note that our methods have not been validated for empirical quantification. However, the ratios were roughly confirmed using overlapping sequence reads obtained with alternate primer pairs and by end point RT-PCR analysis of HIV-1 RNAs (data not shown).

Exons 2 and 3 are non-coding exons whose inclusion in transcripts other than *vif* and *vpr* has no known function. We found that they were included in other messages infrequently, each in ~7–8% of transcripts in the ~2 kb completely spliced class of transcripts and 5% of partially spliced transcripts accumulating in T cells. This is consistent with previous measurements in the partially spliced class but much lower than has been estimated for completely spliced transcripts in HeLa cells, suggesting cell-type-specific splicing patterns

may influence inclusion of these exons⁴²⁵.

3.4.4 A novel ~1 kb class of completely spliced transcripts

Primers placed near the 5'- and 3'-ends of the HIV_{89.6} genome amplified a second class of completely spliced transcripts ~1 kb in length. In place of A7, these transcripts use a set of little studied splice acceptors located ~800 bp downstream within the 3'-TR. Two groups have previously observed splicing from D1 to acceptors A8, A8a and A8b in this region, yielding messages of this size class in patient samples; however, none of these could be translated to a protein of significant length^{427,431}. We determined the complete structure of 29 members of the 1-kb class (Figure 3.2 and Supplementary Table S5). The most abundant messages observed in this class use the novel acceptor A8c to define their terminal exon. For HIV_{89.6}, acceptor A8c was used nearly as frequently as A7, which gives us the 2-kb class of transcripts (Supplementary Table S3), and this was supported by end point RT-PCR analysis (data not shown).

Acceptor A8c is not well conserved in HIV-1/SIVcpz (14%), although it is conserved in clade G viruses (> 95%) and most HIV-2/SIVsmm genomes (86%)⁴⁶³. This is due to the poor conservation of an adenosine at the wobble base position of the 123rd codon (proline) of the Nef reading frame, which creates the AG dinucleotide generally required at splice acceptors. Since any base at this position would code for proline, there does not seem to be strong selection for a splice acceptor here. However, A8c is displaced from nearby well-conserved (> 90%) cryptic acceptors A8a and A8b by multiples of 3 bp (12 and 21 bp, respectively), so splicing to any of these three acceptors would create similar ORFs. All HIVs and SIVs maintain at least one of these three acceptors, suggesting possible function⁴⁶³. We confirmed that the 1 kb transcripts using A8a, A8b and A8c were present in infected HOS and T cells by end point RT-PCR using additional primer pairs and by Sanger sequencing of cloned transcripts (Figure 3.3A and B; data not shown).

The 1-kb transcript containing exons 1, 4 and 8c (1-4-8c, where exon 8c begins at A8c

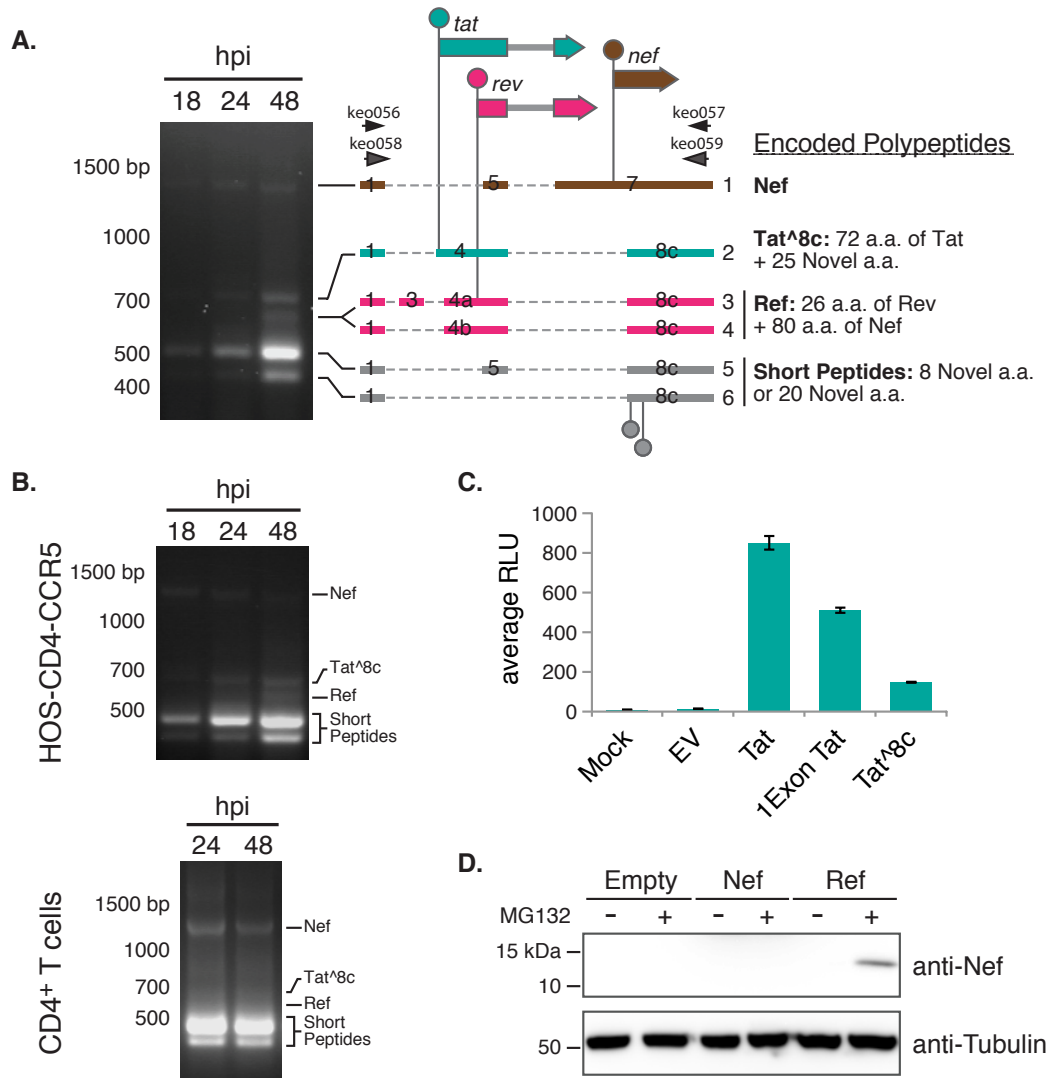


Figure 3.3: HIV_{89.6} transcripts were amplified by RT-PCR using RNA from infected HOS-CD4-CCR5 cells with primers keo056 and keo057. Major bands detected after gel electrophoresis were cloned from the 48 hpi sample and message structures determined by Sanger sequencing. Thick bars represent exons and dashed lines excised introns. Genes are shown above (not to scale) with start codons indicated by circles. Messages 1, 2, 4 and 5 were cloned into expression plasmids for activity assays. (B) Confirmation of presence of the ~1 kb message RNAs in HOS-CD4-CCR5 and primary CD4⁺ T cells (human donor 1, harvested 24 and 48 hpi). An independent primer pair (keo058 and keo059) was used to amplify transcripts by RT-PCR. (C) Tat activity was measured in Tzm-bl cells as Tat-dependent luciferase production after transient transfection with expression plasmids. (D) Western blot showing expression of protein of the predicted size for Ref (12.5 kb) in cells transfected with the Ref expression construct and treated with proteasome inhibitor MG132, detected by an antibody recognizing the carboxy-terminus of Nef. Expression plasmid encoding Nef was included to control for possible expression of partial Nef peptides or breakdown products from the Nef ORF.

and extends to the poly-adenylation site) encodes the first exon of Tat followed by 25 novel amino acids (termed Tat^{8c}). Tat^{8c} showed activity when overexpressed in cells containing a Tat reporter construct (Figure 3.3C, nucleotide and amino acid sequences in Supplementary Table S6). Transcripts with exon structures 1-4a/b/c-8c encode a novel fusion of the amino-terminal 26 amino acids of Rev and the carboxy-terminal 80 amino acids of Nef, hereafter referred to as Ref. We did not detect Rev activity on overexpression of the *ref* transcript, and Ref did not appear to interfere with the normal function of Rev or with HIV replication (Supplementary Figure S2). Ref was detectable by western blot using antibodies targeting the C terminus of Nef after inhibition of the proteasome, suggesting that the fusion is expressed but not stable (Figure 3.3D). Thus, Ref has the potential to encode a new epitope potentially relevant in immune detection of HIV. The transcripts with exon structures 1-5-8c and 1-8c encode at most a short peptide, and so are candidates for acting as regulatory RNAs.

3.4.5 Temporal dynamics of transcript populations

To assess longitudinal variation, we investigated HIV_{89.6} transcript populations during the course of a single round of infection in HOS-CD4-CCR5 cells. A sensitive method for comparison among conditions involves quantifying utilization of six mutually exclusive splice acceptors A3, A4c, A4a, A4b, A5 and a novel acceptor just downstream of A5 termed A5a. Splicing at these acceptors determines the relative levels of messages encoding Tat and Env/Vpu in the partially spliced class and messages encoding Tat, Rev and Nef in the completely spliced class.

We observed longitudinal changes in the levels of these messages in HOS cells over 12–48 h that were statistically significant ($p < 10^{-10}$; generalized linear model described in Appendix A.1). This pattern was especially evident in junctions involving donor 1 spliced to each of these acceptors (Figure 3.4A). Most dramatically, transcripts with splicing junctions between D1 and A3 (tat messages) increased with time ($p < 10^{-10}$), while D1[^]A4b junctions (used in *env/vpu* or *rev* messages) were used reciprocally less ($p < 10^{-10}$). Such kinetic changes

affecting specific transcripts both with and without the Rev-response element cannot be explained by the accumulation of Rev, and they may reflect differential transcript stability or HIV-induced alterations to the host splicing machinery. Temporal changes in HOS cells were confirmed using end point RT-PCR and analysis after electrophoresis on ethidium-stained gels (Figure 3.4B).

3.4.6 Cell-type-specific splicing patterns

We also compared splicing between T cells and HOS cells and found significant cell type differences ($p < 10^{-10}$). For example, while transcripts with D1[^]A5 junctions were dominant in both cell types, messages using the D1[^]A4c splice junction (encoding Env/Vpu or Rev) made up the bulk of the remaining transcripts in T cells but were a minor species in HOS-CD4-CCR5 cells. Likewise, Tat messages (using A3), which were quite abundant in HOS cells at all time points, contributed relatively little to populations of transcripts in primary T cells harvested at 48 hpi (Figure 3.4A). We also used end point PCR and analysis on ethidium-bromide-stained gels to confirm that the relative ratios of transcripts containing junctions to A3, A4a, A4b and A4c were different in HOS and T cells (Figure 3.4B).

3.4.7 Human variation in HIV-1 splicing

Quantitative comparisons also revealed modest differences in splicing between primary CD4⁺ T cells isolated from different human donors that were statistically significant ($p < 10^{-10}$) under a generalized linear model (Figure 3.4A). The magnitudes of predicted differences were small, all $< 33\%$ and most $< 10\%$.

3.5 Discussion

Use of single-molecule enrichment and long-read single-molecule sequencing has made possible the most complete study to date of the composition of HIV-1 message populations, revealing several new layers of regulation. Studies of the low-passage HIV89.6 isolate in a relevant cell type showed numerous differences from studies of lab-adapted HIV strains in transformed

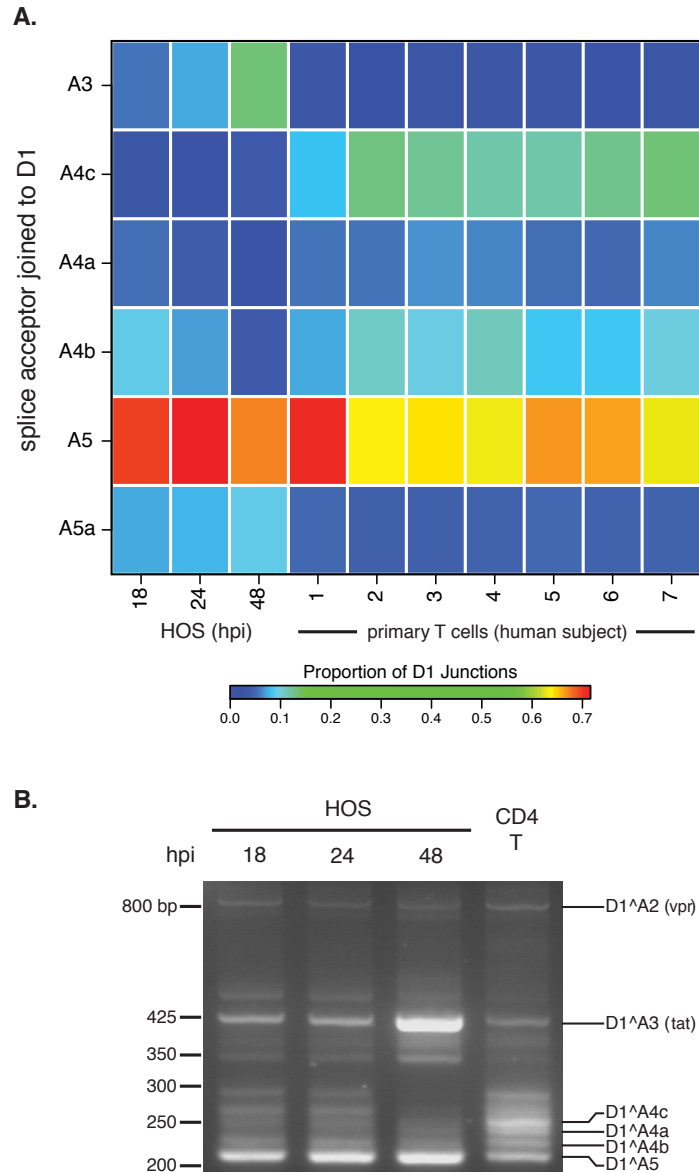


Figure 3.4: Temporal, cell type and donor variability in accumulation of HIV-1 messages. (A) In order to highlight changes in ratios of HIV-1 transcripts accumulating over time during infection and between HOS-CD4-CCR5 cells and primary T cells, we used PacBio read counts to calculate proportions of transcripts with splicing from the first major splice donor, D1, to each of the mutually exclusive acceptors: A3, A4c, A4a, A4c, A5 and the novel putative acceptor A5a. The heat map shows average data for T cell and HOS cell samples in columns with the color tiles indicating the proportion of D1 splicing to each of the mutually exclusive acceptors (rows), according to the color scale shown. (B) Reverse transcription and bulk PCR amplification of HIV_{89,6} transcripts from HOS cells and primary T cells from one human subject (subject 3) resolved by agarose gel electrophoresis and stained with ethidium bromide verified temporal and cell type changes shown in (A).

cell lines, highlighting the importance of studying the most relevant models. These data also illustrate the limitations of gel-based assays for studying HIV-1 message population. Multiple different combinations of HIV-1 exons yield mRNAs of similar sizes that are easily confused in typical assays using gel electrophoresis. Thus, in many settings the more detailed information provided by single-molecule amplification and single-molecule DNA sequencing is more useful.

Using these methods, we have detected significant variations between HIV message populations generated in T cells from different human donors. The differences were modest compared to those observed between cell types or time points, perhaps not surprisingly since any human polymorphisms strongly affecting mRNA processing might interfere with normal gene expression. However, because tight calibration of message levels is important to HIV-1, the observed differences in message ratios might affect HIV-1 acquisition or disease progression. The variation in observed transcripts could also be affected by different kinetics of infection in T cells from the different donors. In either case, these data suggest that human polymorphisms may exist that affect HIV-1 message populations in infected individuals, providing a new candidate mechanism connecting human genetic variation with measures of HIV disease.

Sequences from the 89.6 viral strain revealed a class of small (~1 kb) completely spliced transcripts, most contributed by splicing to a new poorly conserved acceptor A8c. These encoded two new proteins, one of which had Tat activity, and we showed that another, a Rev-Nef fusion termed Ref, could be detected in cells. HIV_{89.6} is a particularly cytotoxic virus isolated from the CSF of a patient, and it forms unusually large syncytia in macrophages⁴⁴⁹. The abundance of 1-kb transcripts produced by this virus provides a possible explanation for its unique properties. In addition to the novel acceptor A8c, we have also identified 3 putative novel splice donors and 11 putative novel acceptors, which require further studied to clarify possible functions.

The wealth of new messages found here in HIV_{89.6} and in other HIV-1 isolates suggests

there may be ongoing evolution of novel splice sites and new ORFs. Because splice acceptors in HIV-1 are weak²⁸⁴, mutations creating sequences that even slightly resemble the 3' splice site consensus may be occasionally recruited as novel acceptors, creating new mRNAs. In fact, new splice signals may evolve with relative ease—it has been estimated that reasonable matches to the consensus for splice donors, acceptors and branch-point sites occur within random sequence every 290, 490 and 24 bp, respectively⁴⁶⁴, though sequence substitutions in HIV are usually also constrained by overlapping viral coding regions. We and others have observed appearance of novel exons within the major HIV-1 introns^{426,428,429}. Such long stretches of RNA relatively devoid of competing splice sites may be particularly poised to evolve new signals. On the other hand, most of the putative novel splice acceptors we observed clustered near previously identified acceptors in HIV-1, suggesting that conserved cis-acting splicing signals may recruit factors that act promiscuously on new nearby sequences. Clusters of splice sites might also provide redundancies that protect vital messages, as suggested previously^{465,466}. Frequent evolution of new splice sites may allow viruses to test out new combinations of exons, potentially yielding new RNAs and proteins, like those reported here. However, such novelty must compete with immune constraints—unstable novel polypeptides like Ref can be targeted to the proteasome and presented on MHC molecules as new epitopes for immune recognition.

HIV has likely evolved to produce calibrated message populations in T cells which seem to be altered with relative ease, as in infection in HOS cells, suggesting that therapeutic disruption of correct splicing may be feasible. A few studies have begun to explore small molecule therapy to disrupt HIV-1 splicing^{432,436}. Several factors could be responsible for the differences we observed between HOS and T cells, including hnRNP A/B and H, SC35, SF2/ASF and SRp40^{288,467}. Inhibition of SF2/ASF has already been shown to abrogate HIV-1 replication in vitro⁴³². Thus the lability seen here for function of these factors suggests they may be attractive antiretroviral targets.

3.6 Acknowledgements

We would like to thank the University of Pennsylvania Center for AIDS Research (CFAR) for preparation of viral stocks and isolation of primary CD4⁺ T cells; James A. Hoxie, Ronald G. Collman, Jianxin You, Robert W. Doms, Paul Bates, David Rekosh and members of the Bushman laboratory for reagents, helpful discussion and technical expertise.

CHAPTER 4: Gene activity in primary T cells infected with HIV_{89.6}: intron retention and induction of distinctive genomic repeats

This chapter is under review as:

S Sherrill-Mix, K Ocwieja and F Bushman. Under Review.
Gene activity in primary T cells infected with HIV_{89.6}: in-
tron retention and induction of distinctive genomic repeats.
Retrovirology

KE Ocwieja performed the infections and sequencing. I analyzed the data.
KE Ocwieja, FD Bushman and I planned the overall study. I produced
the figures. FD Bushman and I wrote the paper.

4.1 Abstract

Background: HIV infection has been reported to alter cellular gene activity, but published studies have commonly assayed transformed cell lines and lab-adapted HIV strains, yielding inconsistent results. Here we carried out a deep RNA-Seq analysis of primary human T cells infected with the low passage HIV isolate HIV_{89.6}.

Results: Seventeen percent of cellular genes showed altered activity 48 hours after infection. In a meta-analysis including four other studies, our data differed from studies of HIV infection in cell lines but showed more parallels with infections of primary cells. We found a global trend toward retention of introns after infection, suggestive of a novel cellular response to infection. HIV_{89.6} infection was also associated with activation of several human endogenous retroviruses (HERVs) and retrotransposons, of interest as possible novel antigens that could serve as vaccine targets. The most highly activated group of HERVs was a subset of the ERV-9. Analysis showed that activation was associated with a particular variant of ERV-9 long terminal repeats that contains an indel near the U3-R border. These data also allowed quantification of >70 splice forms of the HIV_{89.6} RNA and specified the main types of chimeric HIV_{89.6}-host RNAs. Comparison to over 100,000 integration site sequences from

the same infected cell populations allowed quantification of authentic versus artifactual chimeric reads, showing that 5' read-in, splicing out of HIV_{89.6} from the D4 donor and 3' read-through were the most common HIV_{89.6}-host cell chimeric RNA forms.

Conclusions: Analysis of RNA abundance after infection of primary T cells with the low passage HIV_{89.6} isolate disclosed multiple novel features of HIV-host interactions, notably intron retention and induction of transcription of retrotransposons and endogenous retroviruses.

4.2 Background

HIV replication requires integration of a cDNA copy of the viral RNA genome into cellular chromosomes, followed by transcription and splicing to yield viral mRNA. Alternative splicing allows the small 9.1 kb HIV genome to generate at least 108 mRNA transcripts encoding at least 9 proteins and polyproteins^{284,419,425,430,469,470}. During replication, HIV also reprograms cellular transcription and splicing. For example, the virus-encoded Vpr protein arrests the cell cycle^{249,251,252,254} and the viral Tat protein binds to P-TEFb and alters transcription at the HIV promoter and some cellular promoters as well⁴⁷¹⁻⁴⁷⁶.

Changes in host cell gene expression have been reported during HIV infection^{317-319,477-485} and differences in expression have been observed associated with the stage⁴⁸⁶ and progression⁴⁸⁷ of disease. Multiple studies suggest that cells detect HIV infection, in part through the recognition of cytoplasmic DNA in abortive infections^{177,488,489}, and respond by inducing interferon-regulated, apoptotic and stress response pathways^{319,477-481,483-485}. Several studies have also suggested that HIV infection disrupts normal cellular splicing pathways^{446,485}. However, results have varied with many experimental parameters, including target cell type, HIV isolate and the duration of infection. Many previously published studies have focused on infections with lab-adapted HIV strains in transformed cell lines^{317,319,477,482,485,490}, and so results may not be fully reflective of infections in patients.

HIV infection also appears to induce the expression of human endogenous retroviruses

(HERVs)³³³, particularly HERV-K^{328–332}, and retrotransposons³³⁴. Immune responses to HERV proteins appear stronger in HIV-infected individuals suggesting candidate markers of infection and possible vaccine targets^{337–340}. In contrast, two recent RNA-Seq studies of expression during HIV infection did not report increases in HERV RNA^{319,482}. The origin of this discrepancy is unclear.

The suggestion that HIV integration may disrupt cellular cancer-associated genes and thereby promote cell proliferation^{491–494} has focused attention on the range of novel message types formed when HIV integrates within transcription units^{366,423,495–497}. Chimeric reads containing HIV and cellular sequence are also of interest due to the potential of lentiviral vectors to trigger oncogenesis in gene therapy patients through insertional mutagenesis^{498–501}. A better understanding of chimera formation would help clarify this phenomenon in both infected patients and gene therapy using lentiviral vectors.

In this study, we sought to generate data more representative of HIV replication in patients by using Illumina sequencing to analyze transcriptional responses after infection of primary T cells with HIV_{89.6}, a low passage patient isolate⁴⁴⁹. This represents a continuation of a long term effort to understand HIV-host cell interactions at the transcriptional level that began with analysis of transcription by HIV_{89.6} in primary T cells using Pacific Biosciences long read single molecule sequencing⁴¹⁹. Our strategy here was to analyze a single time after infection in depth with over 1 billion sequence reads from HIV_{89.6}-infected and uninfected host cells. These data were then combined with 147,281 unique integration site sequences from the same infections and the Pacific Biosciences data on HIV_{89.6} transcription to 1) elucidate effects of HIV infection on host cell mRNA abundances and splicing, 2) characterize viral message structure in detail and 3) probe the nature of the chimeras formed between host cell and viral RNAs.

4.3 Methods

4.3.1 Cell culture and viral infections

HIV_{89.6} stocks were generated by the University of Pennsylvania Center for AIDS Research. 293T cells were transfected with a plasmid encoding an HIV_{89.6} provirus, and harvested virus was passaged in SupT1 cells once. Viral stocks were quantified by measuring p24 antigen content. Primary CD4⁺ T cells were isolated by the University of Pennsylvania Center for AIDS Research Immunology Core from apheresis product from a single healthy male donor (ND365) using the RosetteSep Human CD4⁺ T Cell Enrichment Cocktail (StemCell Technologies). The Immunology Core maintains the IRB-approved protocol (IRB #705906) and receipt of these cells is considered secondary use of de-identified human specimens.

T cells were stimulated for 3 days at 0.5×10^6 cells per milliliter in R10 media (RPMI 1640 with GlutaMAX (Invitrogen) supplemented with 10% FBS (Sigma-Aldrich) with 100 units U/mL recombinant IL2 (Novartis) + 5 $\mu\text{g}/\text{mL}$ PHA-L (Sigma-Aldrich)). Cells were infected in triplicate and mock infections were performed in duplicate. For each infection, 6.6×10^6 cells were mixed with 1.32 μg HIV_{89.6} in a total volume of 2.25 mL. Infection mixtures was split into three wells of a 6 well plate for spinoculation at 1200 g for 2 hr at 37°C. Cells were incubated an additional 2 hr at 37°C. Cells were then pooled into flasks and volume was increased to a total of 12 mL. Spreading infection was allowed to proceed 48 hr at 37°C, after which cells were harvested. 1×10^6 cells were harvested for flow cytometry, and 6×10^6 cells were pelleted following two washes in PBS for nucleic acid extraction. Genomic DNA and total RNA were isolated from 6×10^6 T cells per infection using the AllPrep DNA/RNA Mini Kit (Qiagen) with Qiashreder columns (Qiagen) for homogenization according to the manufacturer's instructions. DNA was eluted in 140 μL elution buffer. RNA samples were treated with DNase prior to elution in 40 μL water.

4.3.2 Analysis of HIV_{89.6} integration sites in primary T cells

Integration site sequences were determined for DNA fractions from the above infections after ligation mediated PCR³⁹⁶. A total of 147,281 unique integration site sequences were determined. An analysis of integration site distributions for these samples was reported in Berry et al.³⁹⁶.

4.3.3 mRNA sequencing

Messenger RNA was isolated and amplified from purified total cellular RNA (3 μ L or approximately 9 μ g from each uninfected sample, 25 μ L or approximately 3 μ g from each infected sample) using the Illumina TruSeq RNA sample preparation kit according to manufacturer's protocol. SuperScript III (Invitrogen) was used for reverse transcription. Each sample was tagged with a separate barcode and sequenced on an Illumina HiSeq 2000 using 100-bp paired-end chemistry.

4.3.4 Flow cytometry

To assess percent infected cells, 1×10^6 cells per infection were stained for flow cytometry. All staining incubations were at room temperature. Cells were first washed in PBS and then twice in FACS wash buffer (PBS, 2.5% FBS, 2 mM EDTA). Cells were fixed and permeabilized with CytoFix/CytoPerm (BD) for 20 minutes and washed with Perm-Wash Buffer (BD) before staining with anti-HIV-Gag-PE (Beckman Coulter) for 60 min. Finally cells were washed in FACS wash buffer and resuspended in 3% PFA. Samples were run on a LSRII (BD) and analyzed with FlowJo 8.8.6 (Treestar). Cells were gated as follows: lymphocytes (SSC-A by FSC-A), then singlets (FSC-A by FSC-H), then by Gag expression (FSC-A by Gag).

4.3.5 Analysis

Reads were aligned to the human genome using a combination of BLAT³⁹⁵ and Bowtie⁵⁰² through the Rum pipeline⁵⁰³. Estimates of fragments per kilobase of transcript per million

mapped reads and changes in expression for cellular genes were calculated by Cufflinks³⁹⁷. Reads found to contain sequence similar to the HIV genome using a suffix tree algorithm were aligned against the HIV_{89.6} genome using BLAT³⁹⁵. All statistical analyses were performed in R 3.1.2³⁸⁸. RNA-Seq reads from Chang et al.³¹⁹ were downloaded from the Sequence Read Archive (SRP013224) and aligned using the Rum pipeline.

Gene lists were obtained from the supplementary materials of four other studies of differential gene expression during HIV infection^{319,482,483,486}. We called genes differentially expressed in Li et al.⁴⁸⁶ if they had a reported $p < 0.01$ or in Lefebvre et al.⁴⁸², Chang et al.³¹⁹ and Imbeault et al.⁴⁸³ if they had an adjusted $p < 0.05$. We called genes as differentially expressed in our own study if the adjusted $p < 0.01$. For the comparison of differentially expressed genes regardless of direction in figure 4.1 (below the diagonal), it was unclear exactly how many genes were studied in each study so we assumed a background of the 14,192 genes (the number of genes which could be tested for significance in our data).

We obtained transcriptional profiles comparing immune cell subsets from the Molecular Signatures Database⁵⁰⁴. MSigDB set names from the MSigDB used in Figure 4.2A were GSE10325 LUPUS CD4 TCELL VS LUPUS BCELL, GSE10325 CD4 TCELL VS MYELOID, GSE10325 CD4 TCELL VS BCELL, GSE10325 LUPUS CD4 TCELL VS LUPUS MYELOID, GSE3982 MEMORY CD4 TCELL VS TH1, GSE22886 CD4 TCELL VS BCELL NAIVE, GSE11057 CD4 CENT MEM VS PBMC, GSE11057 CD4 EFF MEM VS PBMC, GSE3982 MEMORY CD4 TCELL VS TH2 and GSE11057 PBMC VS MEM CD4 TCELL and in Figure 4.2B were GSE36476 CTRL VS TSST ACT 72H MEMORY CD4 TCELL OLD, GSE10325 CD4 TCELL VS LUPUS CD4 TCELL, GSE22886 NAIVE CD4 TCELL VS 12H ACT TH1, GSE3982 CENT MEMORY CD4 TCELL VS TH1, GSE17974 CTRL VS ACT IL4 AND ANTI IL12 48H CD4 TCELL, GSE24634 IL4 VS CTRL TREATED NAIVE CD4 TCELL DAY5, GSE24634 NAIVE CD4 TCELL VS DAY10 IL4 CONV TREG, GSE1460 CD4 THYMOCYTE VS THYMIC STROMAL CELL and GSE1460 INTRATHYMIC T PROGENITOR VS NAIVE CD4 TCELL ADULT BLOOD.

We downloaded the RepeatMasker⁴¹² track from the UCSC genome browser⁵⁰⁵ and used the SAMtools library⁵⁰⁶ to assign reads to the repeat regions. HERV-K age estimates were obtained from the supplementary materials of Subramanian et al.⁵⁰⁷.

We used a Bayesian estimate of the ratio of expression in uninfected and HIV-infected samples to account for sampling effort and differing expression in genomic regions. We modeled the observed counts as a binomial distribution with a flat beta prior ($\alpha = 1, \beta = 1$) separately for uninfected and infected samples. We then Monte Carlo sampled the two posterior distribution to estimate the posterior distribution of the ratio. For introns, the number of binomial successes was set to the number of reads mapped to the intron and the number of trials was the total number of reads observed in the genes overlapping that intron. For repeat regions, the number of binomial successes was set to the number of reads mapped to that region and the number of trials was the total number of reads mapped to the human genome.

To estimate determinants of LTR12C expression, we fit a logistic regression for which LTR12C increased in expression with HIV_{89.6} infection (95% Bayesian credible interval >1) on to characteristics of the LTR12C regions. We extracted all the LTR12C regions from the human genome and determined the U3-R boundary using a ends free alignment of the previously reported U3-R border^{508–512} against the sequences. Regions less than 1,000 bases long were discarded. Previous studies disagreed about the location of the LTR12C transcription start site and it appears that transcription may start in several places^{509,510}. We took the 5' most site that had agreement between studies (transcription starting with TGGCAACCC). We split the sequences into short, medium and long length classes based on an indel about 70 bases upstream from the transcription start site. For each length class, we generated a consensus sequence and counted the Levenshtein edit distance between the consensus and each corresponding sequence. We also counted the number of NFY motifs (CCAAT or ATTGG), MZF1 motifs (GTGGGGA) and GATA2 motifs (GATA or TATC) in the entire U3 region or checked in any of the three motifs was present in the 150 bases

Sample	Infection rate (%)	Reads	Human reads	HIV reads	% HIV	% HIV in infected
Uninfected-1	—	232,450,106	212,391,460	—	—	—
Uninfected-2	—	235,048,212	203,760,783	—	—	—
Infected-1	37.5	234,378,088	199,871,662	10,219,315	4.86	13.0
Infected-2	26	226,078,422	198,436,507	7,322,556	3.56	13.7
Infected-3	21	233,750,850	205,747,441	7,241,973	3.40	16.2

Table 4.1: Samples used in this study, their infection rates and sequencing depth. “% HIV in infected” is an estimate based on the assumption that infected and uninfected cells contain equal amounts of mRNA.

upstream of the TSS. A final regression model was selected using stepwise regression with an AIC cutoff of 5. For display, the LTR12C sequences were aligned with MUSCLE⁵¹³.

The abundance of the HIV RNA size classes was estimated as described in Figure 4.6. These estimates were then multiplied by the within size class proportions estimated by Ocwieja et al.⁴¹⁹ using PacBio sequencing of HIV_{89,6} to yield proportions over 78 measured HIV_{89,6} RNAs.

4.4 Results

4.4.1 Infections studied

Primary CD4⁺ T cells from a single human donor were infected with HIV_{89,6}, a clade B primary clinical isolate⁴⁴⁹, in three replicates. For comparison, two additional replicates from the same donor were mock infected. Samples were harvested 48 hours after viral inoculation, which allowed for widespread infection in the primary T cell cultures, though some cells may have been infected secondarily by viruses produced in the first round. Thus cultures probably were not tightly synchronized but did have extensive representation of infected primary T cells. From these samples, we obtained 1,161,705,678 101-bp reads from primary CD4⁺ T cells from a single donor; 1,021,207,853 were mapped to the human genome and 24,783,844 to the HIV_{89,6} provirus (Table 4.1). Below we first discuss the influence of infection on cellular gene activity and RNA splicing, then analyze HIV RNAs and lastly identify chimeras formed between HIV and cellular RNAs.

4.4.2 Changes in gene activity in primary T cells upon infection with HIV_{89.6}

We observed significant expression changes in 3,142 genes (false discovery rate of $q < 0.01$), which is 17.1% of expressed cellular genes. The genes with most extreme increases, all $>6\times$ fold higher, during HIV infection included IFI44L, RSAD2, HMOX1, MX1, USP18, IGJ, OAS1, CMPK2, DDX60, IFI44, IFI6, IFNG and CCL3. All of these have been reported to be involved in innate immunity⁵¹⁴ or are interferon-inducible⁵¹⁵, highlighting a strong innate immune response in the cells studied. Genes with the largest decreases, all $>3\times$ fold lower, were GNG4, GPA33, IL6R, CCR8, RORC, AFF2 and CCR2.

Many gene ontology categories were significantly enriched for differentially expressed genes. Notably upregulated with infection were genes involved in apoptosis, immune responses and cytokine production (all $q < 10^{-4}$) and down-regulated were genes involved in viral gene expression and translation elongation and termination (all $q < 10^{-19}$). These changes suggest that the cells responded to HIV infection with the induction of inflammatory, interferon-regulated and apoptotic responses, patterns posited from several previous studies^{319,477–484,490,516}. Expression significantly increased for several genes that are characteristic of other hematopoietic lineages, e.g. hemoglobin β , CD8, CD20 and CD117, while several CD4⁺ T cell specific genes, e.g. CD4 and CD3, were downregulated, potentially consistent with de-differentiation of infected or bystander cells. We return to this point in the discussion.

4.4.3 Comparison of transcriptional profiles from HIV_{89.6} infection of primary T cells to data on HIV infection in other cell types

We sought to identify the transcriptional responses that were most conserved upon HIV infection and so collected and analyzed data from four other studies of transcription in HIV-infected cells (Table 4.2). These included two studies of infection of the SupT1 cell line^{319,482}, a study of ex vivo infection of primary CD4⁺ T cells⁴⁸³ and a study of lymphatic tissue biopsies from acutely viremic patients⁴⁸⁶. Genes were scored as increased or decreased in activity in infected cell populations, and the amount of agreement was compared among

Cell type	HIV type	Differentially expressed genes (Up/Down)	Study
Primary CD4 ⁺ T	HIV _{89.6}	3393 (1756/1637)	This study
Primary CD4 ⁺ T	NL4-3 BAL-IRES-HSA	228 (182/46)	Imbeault et al. ⁴⁸³
Lymph node biopsies	Acute infection	448 (383/65)	Li et al. ⁴⁸⁶
SupT1	HIV _{LAI}	4997 (2666/2331)	Chang et al. ³¹⁹
SupT1	NL4-3Δenv-eGFP/VSV-G	579 (212/367)	Lefebvre et al. ⁴⁸²

Table 4.2: Data from this study and four others used for meta-analysis of human gene expression changes during HIV infection

the different studies.

No gene was called as differentially expressed in all five studies. Eight genes were differentially expressed in the same direction in 4 out of 5 studies; AQP3 and EPHX2 were down-regulated with HIV infection and CD70, EGR1, FOS, ISG20, RGS16 and SAMD9L were up-regulated. Several of the up-regulated genes are known to be interferon-inducible, again emphasizing the role of innate immune pathways.

For each pair of studies, we compared whether they agreed on the identities of differentially expressed genes and whether they agreed on the direction of change (Figure 4.1). The responses to infection in primary cells showed notable differences to responses in the SupT1 cell line. The two SupT1 studies were significantly similar to each other ($p < 10^{-15}$) but were not significantly associated or were negatively associated with data from ex vivo primary cells and from lymphatic tissue from acutely infected HIV patients. In contrast, our data was significantly associated with the primary cell ($p < 10^{-15}$) and lymphatic tissue data ($p = 0.003$). This documents significant differences in responses to HIV infection between infected primary cells and SupT1 cells and suggests that results of infections in primary cells more closely align with actual acute HIV infections in patients. SupT1 cells might be expected to respond to infection differently than primary cells since they have several nonsynonymous mutations in innate immunity genes⁵¹⁷, have blocks in immune signaling pathways⁵¹⁸ and fail to activate many interferon-stimulated genes during HIV infection⁴⁸⁴.

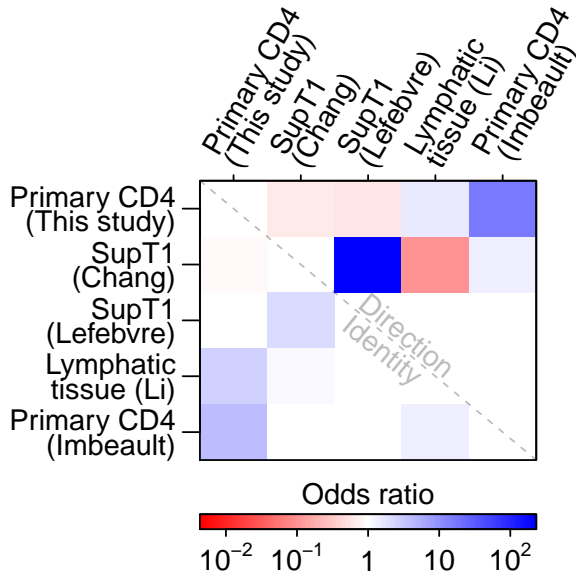


Figure 4.1: Comparisons among studies quantifying cellular gene expression after HIV infection. For each pair of studies, the association between up- and down-regulation calls was measured for genes identified by both studies as differentially expressed (above the diagonal). As another comparison, we also measured the agreement between studies for which genes were called differentially expressed regardless of direction (below the diagonal). The color scale shows the conservative (i.e. closest to 1) boundary of the confidence interval of the odds ratio with blue indicating a positive association and red a negative association between studies. For confidence intervals overlapping 1, the value was set to 1. Therefore all colored squares indicate significant associations.

4.4.4 Comparison of the HIV infected cell transcriptional profiles to additional experimental T cell profiles

To investigate the transcriptional changes in more depth, we compared the results of the five studies of HIV infection to transcriptional profiles comparing immune cell subsets available at the Molecular Signatures Database (MSigDB)⁵⁰⁴. The MSigDB reports genes that are increased or decreased in relative expression for 185 pairs of transcriptional profiles involving CD4⁺ T cells. We compared the lists of affected genes in each pair to genes altered in activity by HIV infection. Those pairs of studies with the most significant associations with HIV_{89,6} data are shown in Figure 4.2A. For comparison, the associations with the four other HIV transcriptional profiling studies mentioned above are shown as well.

The most significant associations for our data showed gene expression in HIV_{89,6}-infected cells moving away from typical T cell expression patterns and towards patterns more similar to B cells, myeloid cells and bulk peripheral blood mononuclear cells (all Fisher's exact test $p < 10^{-15}$) (Figure 4.2A). These changes were also seen, although to a lesser extent, in the Imbeault et al.⁵¹⁹ study which also used primary CD4⁺ T cells.

For comparison, we also extracted those profiles most strongly associated with the transcriptional data on lymphatic tissue of HIV patients⁴⁸⁶. The profiles showed patterns similar to strongly stimulated T cells, autoimmune disease and to the Th1 T cell subset (all $p < 0.01$) (Figure 4.2B). Our data in primary CD4⁺ T cells paralleled the changes seen in lymphatic tissue. These transcriptional changes again highlights the strong immune response generated by HIV infection in primary cells.

4.4.5 Intron retention

Cells respond to infection by shutting down macromolecular synthesis at multiple levels^{520–524}, so we investigated whether cells also showed perturbations in splicing efficiency after infection. As a probe, we created a database of cellular genomic regions annotated exclusively as exons or introns in all splice forms in the UCSC gene database⁴⁰⁷ and quantified expression in these regions in infected and uninfected cells. We found a significant increase in intronic sequences relative to exonic sequence (Wilcoxon $p < 10^{-15}$) (Figure 4.3A). This increase in intronic sequence was reproducible between replicates in our study (Kendall's $\tau = 0.42$, $p < 10^{-15}$) (Figure 4.3B). We reanalyzed RNA-Seq data from Chang et al.³¹⁹ and also documented intron retention which correlated with the changes seen in our data (Kendall's $\tau = 0.12$, $p < 10^{-15}$) (Figure 4.3C).

A possible artifactual explanation for enrichment of intronic sequences could involve greater DNA contamination in the infected cells samples. That is, if the relative amount of DNA differed between treatments, the amount of apparent intronic sequences could also differ due to sequencing of contaminating DNA. To examine whether DNA contamination was abundant in our samples, we compiled a collection of 27 large gene desert regions, defined here as 1) regions outside the centrosome and first and last cytoband, 2) containing less than 1% unknown sequence, 3) containing no genes annotated in UCSC genes⁴⁰⁷, 4) containing no repeats annotated in the repeatMasker database⁴¹² and 5) spanning more than 100 kb. No reads were mapped to these 41 Mb of gene deserts in any sample, arguing against explanations based on DNA contamination. Thus these data indicate that intron retention

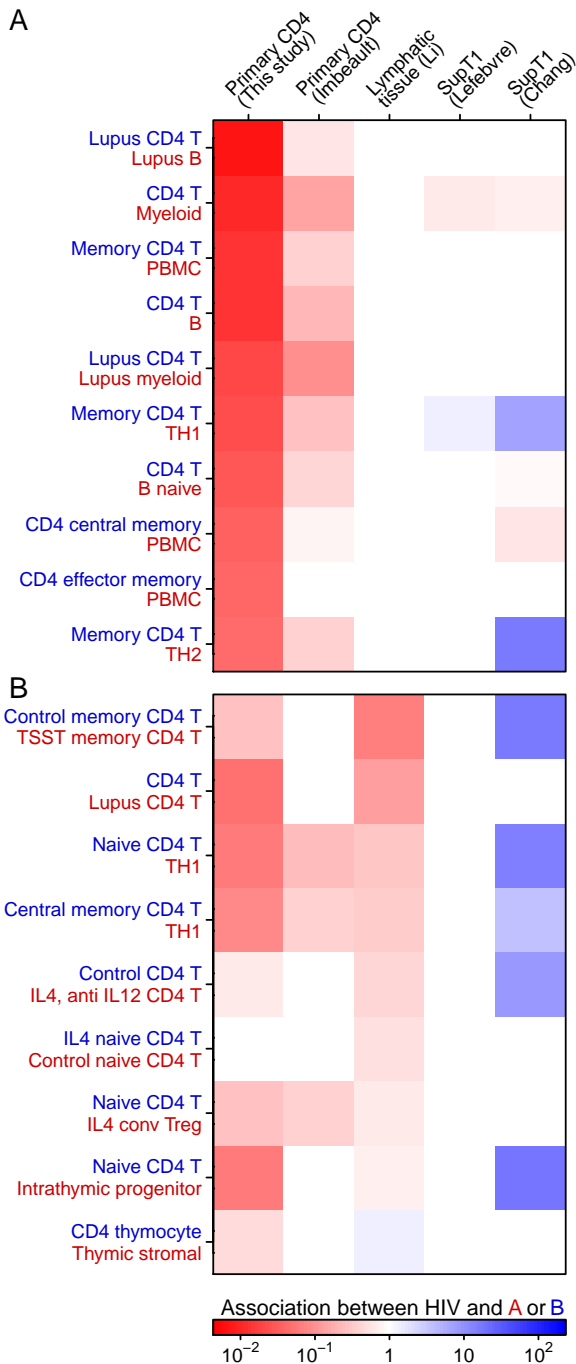


Figure 4.2: Comparisons of the effect of HIV infection on cellular gene expression to additional studies comparing transcription in subsets of immune cells. The MSigDB database was used to extract 185 sets of differentially expressed genes from pairs of transcriptional profiling studies of immune cell subsets involving CD4⁺ T cells. For each pair of studies, we used Fisher's exact test to measure the association between up- and down-regulation calls for genes identified as differentially expressed in both our HIV study and the comparator immune subsets. A) The transcriptional profiles with strongest associations with changes observed in our study of HIV_{89.6} infection of primary T cells. Blue indicates a positive association between changes seen in HIV-infected cells and the first immune subset (text colored blue) while red indicates a positive association with the second immune subset (text colored red). The color scale shows the conservative (i.e. closest to 1) boundary of the confidence interval of the odds ratio. For confidence intervals overlapping 1, the value was set to 1. Therefore all colored squares indicate significant associations. B) As in A, but showing the transcriptional profiles most strongly associated with changes observed in lymph node biopsies from acutely infected patients⁴⁸⁶.

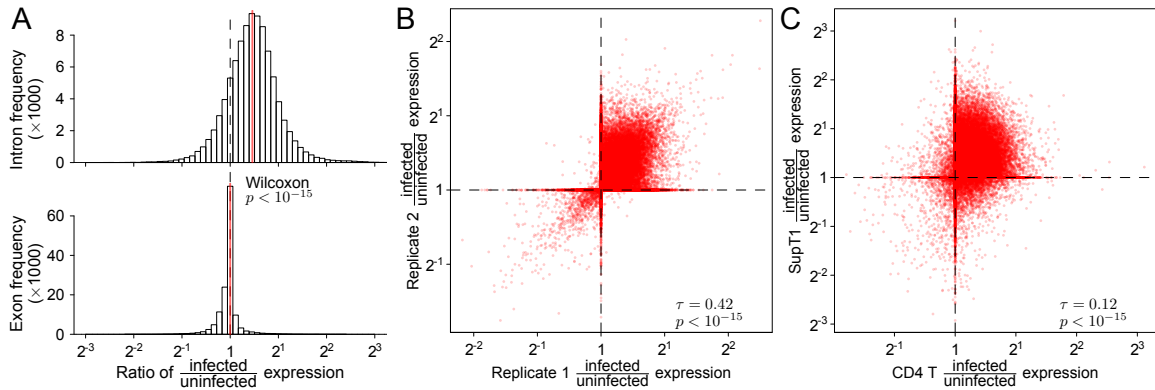


Figure 4.3: Changes in the abundance of intronic regions with HIV infection. Expression of intronic and exonic regions was quantified as the proportion of reads mapping within the intron/exon out of the total reads mapping to the transcription units overlapping that intron/exon. A) Comparison of the ratios of expression between infected and uninfected replicates in exclusively intronic or exonic regions of transcription units. B) Reproducibility of intron retention between replicates. Each point quantifies the change in expression with HIV infection for a specific intronic region. The x-axis shows changes in gene activity accompanying infection for one set of replicates (Infected-1 and Infected-2 vs. Uninfected-1) and the y-axis shows the same data for different replicates (Infected-3 vs. Uninfected-2). C) Reproducibility of intron retention between studies. The plot is arranged as in B but with all data from our study combined on the x-axis and corresponding data from Chang et al.³¹⁹ on the y-axis.

was increased in these cell populations upon HIV infection, revealing a previously undisclosed aspect of the host cell transcriptional response to infection.

4.4.6 Induction of transcription from HERVs and LINEs by HIV_{89.6} infection

In our data, several of the intronic regions with the greatest increases in expression contained HERVs. Thus we investigated the expression of HERVs, transposons and other repeated sequences. Figure 4.4A shows a comparison of the association between changes in expression with HIV_{89.6} infection and genomic repeat types annotated in the RepeatMasker database⁴¹² over varying levels of differential expression. At high levels of expression change, ERV-9 (odds ratio at 4× expression: 152, 95% CI:82.5–259) and its long terminal repeat LTR12C (odds ratio at 4× expression: 144, 95% CI: 98.2–207) are the only repeats highly associated with HIV infection. Looking at genomic repeats with any significant increase during HIV infection, the expression of many recently acquired genomic repeats, including L1HS, LTR5_Hs (a human specific LTR of HERV-K), AluYa5, AluYg6 and SVA_D and SVA_F, were associated

with HIV_{89.6} infection (Figure 4.4B).

We saw a relationship between the age of genomic repeats and its likelihood of being induced by HIV_{89.6} infection. The most highly enriched repeats were associated with relatively recent hominid-specific repeat classes as annotated by the RepeatMasker database (repeat classes with $p < 10^{-50}$ odds ratio: 31.6, 95% CI: 8.88–112). In HERV-K (HML-2), the most recently active endogenous retrovirus in the human genome^{507,525,526}, we saw that integrations unique to the human genome⁵⁰⁷ were more likely to be differentially expressed than older HERV-Ks (odds ratio: 5.38, 95% CI: 1.93–16.0).

Previous RNA-Seq studies of cellular expression during HIV infection in transformed cell lines did not report increases in HERV mRNA^{319,482}. To investigate this difference, we downloaded and analyzed the RNA-Seq data from Chang et al.³¹⁹, which quantified gene activity in transformed SupT1 cells infected with a lab-adapted strain of HIV. We found a much higher level of HERV expression in their data in both HIV-infected cells and uninfected controls than in primary cells (Figure 4.4C). We suspect that in SupT1 cells, as with many cancerous cells^{336,527–530}, the baseline expression of transposons and endogenous retroviruses is higher than in primary cells, masking further induction by HIV infection.

We observed heterogeneous expression among ERV-9/LTR12C sequences and so investigated the primary sequence determinants. We observed that ERV-9/LTR12C has three variants of differing length in the U3 region just upstream of the transcription start site (Figure 4.5A), an important region for transcription initiation⁵⁰⁹. The U3 region of LTR12C also contains multiple motifs for transcription factors NFY, GATA2 and MZF1⁵¹². To clarify factors affecting expression levels, we counted the number of motifs matching these transcription factors' binding motifs, assigned each LTR12C to one of the length classes, counted the number of mutations away from the consensus for that length class and checked for integration in a transcription unit. We then carried out a regression analysis to test the effects of these variables on LTR12C differential expression. We found that HIV_{89.6}-induced transcription was more likely with the fewer mutations away from consensus, the number of locations

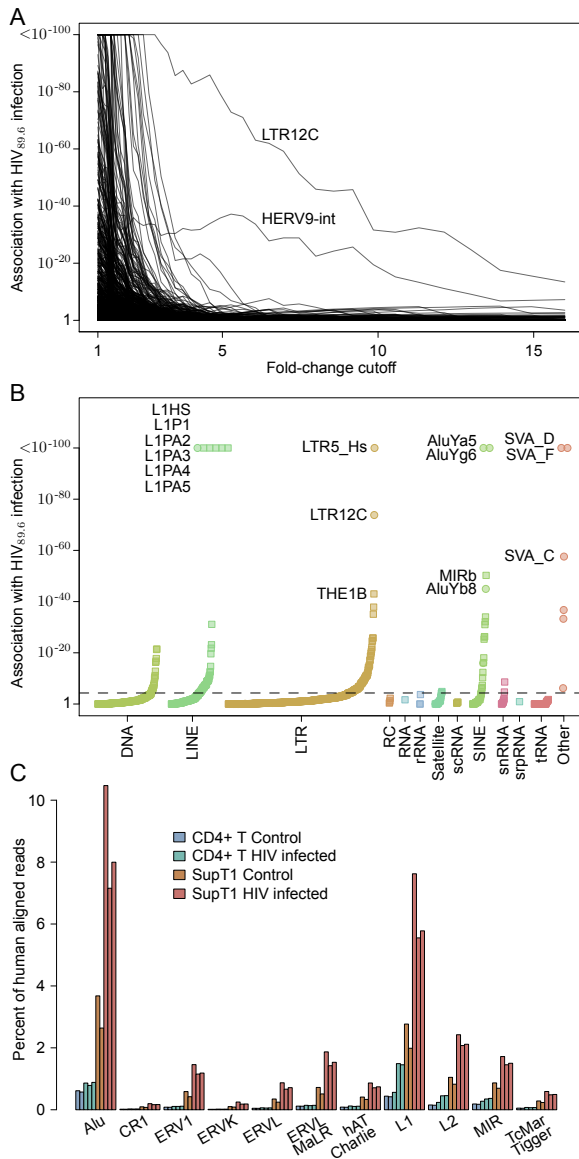


Figure 4.4: Repeat categories enriched upon infection with HIV. A) The association of repeat regions differentially expressed after HIV_{89.6} infection of primary T cells observed for varying thresholds of differential expression. The threshold used to call a gene differentially expressed based on the Bayesian posterior median was varied and Fisher's exact test was used to assess whether any genomic repeats had a significant association with this differential expression. Note that only ERV-9 (annotated as HERV9-int in the RepeatMasker database) and its corresponding long terminal repeat LTR12C were significantly associated with large changes in expression. B) Enrichment of repeat categories in regions differentially expressed (Bayesian 95% credible interval >1) between HIV-infected and control CD4⁺ T cells. The repeated sequences are ordered on the x-axis by the extent of induction within each class, the y-axis shows the p-value for upregulation after infection. The dashed line indicates a Bonferroni corrected *p* value of 0.05. C) The proportion of human mapped reads that align within classes of genomic repeats for data from primary CD4⁺ T cells from this study and SupT1 cells from Chang et al.³¹⁹. A single read mapping multiple times to a given category was only counted once.

matching the NFY transcription factor binding motif (CCAAT) and LTRs containing the short length variant of the 3' U3 region. The presence of a MZF1 motif near the transcription start site decreased transcription (Figure 4.5B).

4.4.7 HIV mRNA synthesis and splicing

Over 24 million Illumina reads mapped to HIV_{89.6}, yielding an average coverage of over 240,000-fold. Reads mapping to HIV_{89.6} comprised between 3.4–4.8% of mapped reads in the infected samples (Table 4.1). It is unclear whether HIV infection increases or decreases the amount of mRNA in infected cells but if we assume HIV-infected cells contain the same amount of mRNA as uninfected cells and adjust for rates of infection ranging between 21–37.5% (Table 4.1), we estimate that HIV transcripts comprise between 13.0–16.2% of the total polyadenylated mRNA nucleotides in infected cells 48 hours after initial infection. This parallels previous estimates of around 10%⁵³¹ at 48 hours postinfection, 38% at 24 hours³¹⁹ or 30% after 72 hours⁴⁷⁷.

Over 47,257 single reads spanned previously reported HIV splice junctions, allowing a quantitative assessment of donor and acceptor utilization (Figure 4.7A). As expected from previous studies^{419,425}, the most abundant junctions were D1-A5 and D4-A7. We confirmed the use of unusual splice acceptors A8c and A5a, previously reported in HIV_{89.6}⁴¹⁹. In the Illumina sequencing, we saw a higher abundance of D1-A1 and D1-A2 splice junctions than in PacBio sequencing⁴¹⁹, possibly indicative of recovery bias in PacBio sequencing.

A 3' bias is apparent in our sequencing data (Figure 4.6). This could be due to the poly-A capture step of the protocol where any break in the RNA would result in distal 5' sequences being lost⁵³². We used sequence reads from the large unspliced HIV intron 1 to measure this bias using a regression of the log of the number of fragments with a 5'-most end starting at a given position against the distance of that position from the viral polyadenylation site, yielding an estimated probability of breakage of 0.021% per base (Figure 4.6). Given this rate of truncation, there is only a 14% chance of reaching the 5' end of the 9171 nt unspliced

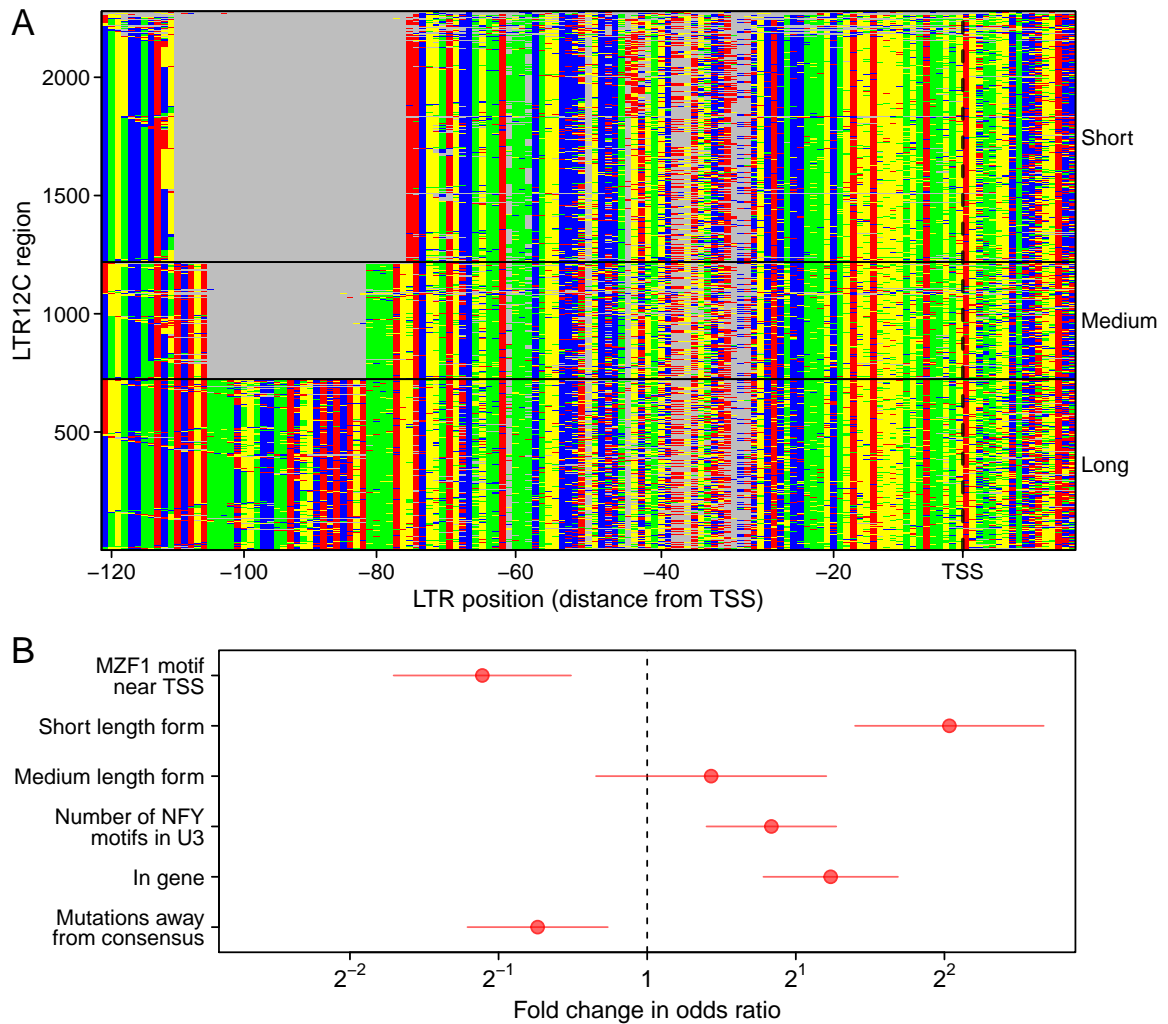


Figure 4.5: Characteristics of LTR12C sequences associated with induction upon infection of primary T cells with HIV_{89.6}. A) An alignment of the 3' end of the U3 region of repeats annotated as ERV-9 LTR12C. Each row is a LTR sequence and each column a base in that sequence colored by nucleotide identity (A: green, T: red, C: blue, G: yellow). Three distinct classes are visible with a short, medium and long form. Mutations away from the consensus can also be seen. B) The coefficients (points) and ± 1.96 standard errors (horizontal lines) of a logistic regression comparing differential expression of LTR12C to the presence of MZF1 and NFY motifs, short/medium/long length alternate forms of the U3-R region, mutations away from the consensus for each length form and integration inside a transcription unit. The coefficient shown for mutations away from consensus is for a 10 mutation difference and the coefficient shown for NFY motifs is for a change of 5 additional motifs. All other coefficients are for binary values.

HIV genome $((1 - 0.00021)^{9171})$.

Ocwieja et al.⁴¹⁹ determined the relative abundance of HIV_{89.6} of similarly sized transcripts using PacBio single molecule sequencing, but were not able to estimate the relative abundance of all transcripts due to a sequencing bias favoring shorter transcripts. For this reason, relative abundances could only be specified within message size classes (i.e. the 4 kb, 2 kb and unexpectedly a 1 kb size class as well) and the overall quantitative abundances were unknown. Our RNA-Seq data are unable to reconstruct the multiply spliced messages due to short read lengths but do permit estimation of size class abundances after correcting for 3' bias (Figure 4.6). Thus the PacBio data reported by Ocwieja et al.⁴¹⁹ and the Illumina data reported here can be combined together to determine complete relative abundance of 78 HIV_{89.6} transcripts (Figure 4.7B).

The most abundant HIV mRNAs were the unspliced HIV genome (37.6%), a transcript encoding Nef (D1-A5-D4-A7: 15.5%), two 1 kb size class transcripts (D1-A5-D4-A8c: 10.6%, D1-A8c: 4.9%) and two Rev-encoding transcripts (D1-A4c-D4-A7: 4.2%, D1-A4b-D4-A7: 3.1%).

Using these abundances, we can estimate the number of HIV_{89.6} genomes in these primary T cells 48 hours after infection. To determine the proportion of the mRNA nucleotides from viral transcripts, we multiplied the estimated abundances by their transcript lengths. Unspliced genome transcripts appear to form 79% of the mRNA nucleotides from HIV_{89.6} transcripts. Assuming T cells contain at least 0.1 pg of mRNA then an infected cell should contain at least 0.011 pg of unspliced HIV transcript $(0.1\text{pg} \times 0.14 \frac{\text{HIV mRNA nt}}{\text{cell mRNA nt}} \times 0.79 \frac{\text{unspliced mRNA nt}}{\text{HIV mRNA nt}})$ or, assuming 9171 bases of RNA weigh about 5×10^{-6} pg, at least 2200 HIV genomes at 48 hour post infection. This estimate roughly agrees with previous estimates of HIV production per cell^{531,533,534}.

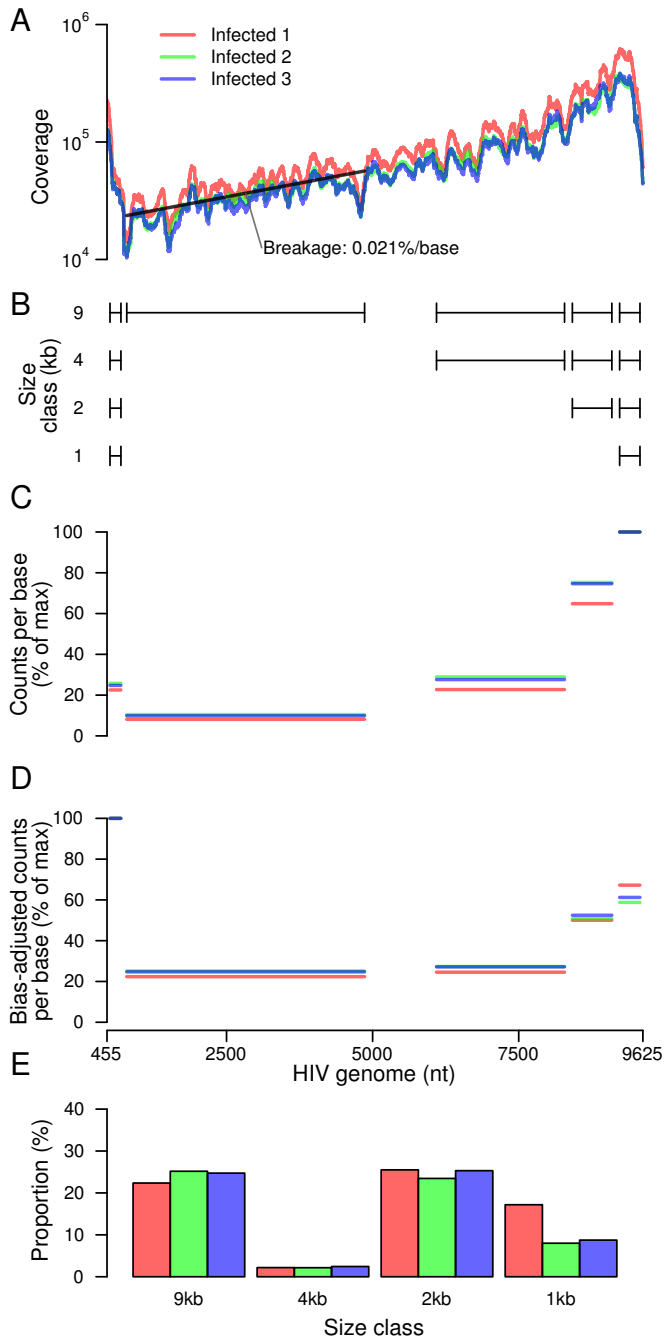


Figure 4.6: Estimating relative abundance of HIV_{89.6} message size classes using RNA-Seq data.

A) RNA-Seq coverage of the HIV_{89.6} genome for the replicates in this study. Each replicate is indicated by a different color. The HIV genome is shown on the x-axis and the number of reads that aligned to each position is shown on the y-axis. Black line indicates the 0.021% coverage decrease per base distance from the 3' end of the mRNA estimated from a least squares fit on the read counts in the first intron.

B) Diagram of the segments of the HIV_{89.6} RNA present in each of 9 kb, 4 kb, 2 kb and 1 kb size class.

C) The proportion of reads mapped to each of the segments of the HIV_{89.6} genome shown in B adjusted by the length of the segment. Each replicate is shown by a different color.

D) Corrected representation of RNA segments from the different size classes. Because cDNA synthesis was primed from the polyA tail, more 3' sequences are recovered preferentially. Using the bias estimate from A, we adjusted each genome segment by the inverse of the bias predicted based on its distance from the 3' end of the mRNA. Corrected proportions for the indicated RNA segments are shown colored by replicate.

E) The proportion of each size class was inferred using the estimates in D by calculating the difference between segments. Replicates are indicated by color.

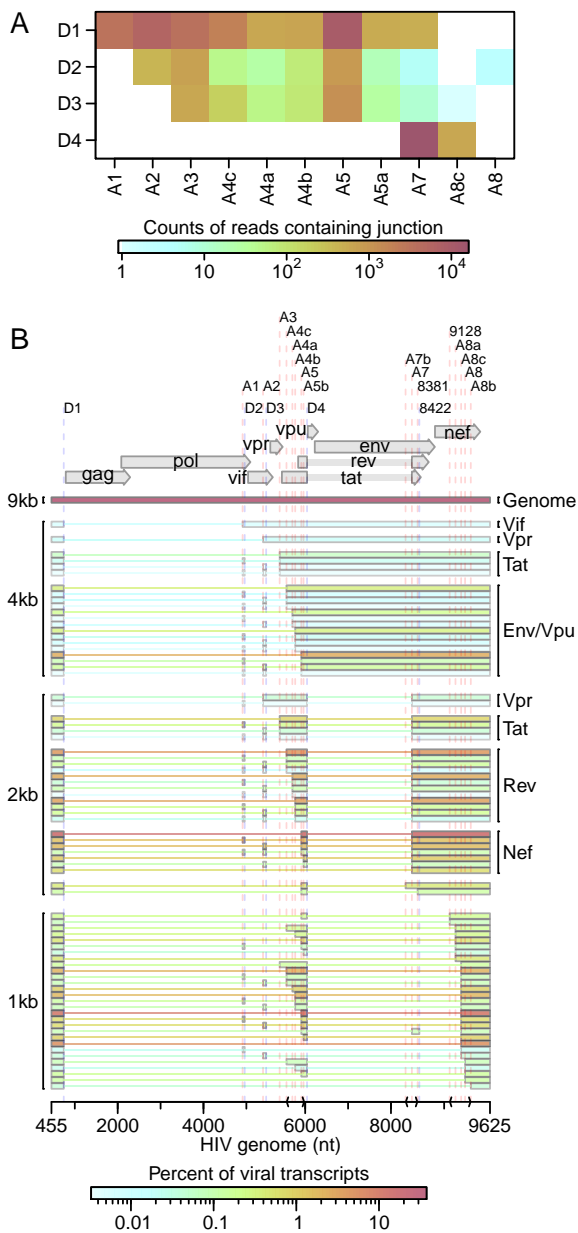


Figure 4.7: Transcription and splicing of the HIV_{89.6} RNA. A) Junctions between HIV splice donors and acceptors observed in the RNA-Seq data. Acceptors are shown as the columns and donors as the rows with the coloring indicating the frequency of each pairing. B) The relative abundance of 78 HIV_{89.6} transcripts as determined by a combination of PacBio sequencing⁴¹⁹ and Illumina sequencing. Message structures were generated by targeted long read single molecule sequencing, which allowed association of multiple splice junctions in single sequence reads. The Illumina short read sequencing allowed normalization of message abundances between size classes. The inferred HIV message population is shown colored by relative abundance.

4.4.8 Human-HIV chimeric reads

In our data, 80,045 reads contained sequences matching to both HIV and human genomic DNA, but a considerable complication arises because chimeras can be formed artifactually during the preparation of libraries for sequence analysis⁵³⁵⁻⁵⁴². Many of the chimeric sequences in our data contained junctions between the HIV and human sequence where the ends of the human and HIV sequence were similar and potentially complementary (Figure 4.8A). This raises the concern that some of these chimeras could be products of in vitro recombinations during the reverse transcription, amplification and sequencing processes. Template switching between sequences with shared similarity is a well established property of retroviral reverse transcriptase enzymes used in RNA-Seq library preparation⁵⁴³⁻⁵⁴⁵. Priming off incomplete transcripts during DNA synthesis is another potential source of chimeric transcripts^{535,536,546,547}. Failing to account for chimeras can hinder interpretation of deep sequencing data⁵³⁷⁻⁵⁴².

Also consistent with artifactual chimera formation, 7,354 reads (9.2% of chimeric messages) contained HIV sequences joined to human mitochondrial sequences, yet HIV proviruses have not previously been found integrated in mitochondrial DNA⁴²³. To probe this further, we used ligation-mediated PCR to recover integration site junctions from the same infected cell populations analyzed by RNA seq, yielding 147,281 unique integration sites (Figure 4.8B)³⁹⁶. No integrations in mitochondrial DNA were detected. We conclude that chimeric HIV-mitochondrial sequence reads in the RNA-seq data represent artifacts of library construction and so used these chimeras as an assay to evaluate subsequent data filtering steps. We reasoned that reads without sequence similarity at junctions between human and HIV mapping were less likely to be artifacts caused by template switching. Filtering to only reads where no overlap and no unknown intervening sequence was present between human and HIV portions left 2181 junctions and reduced the proportion of reads containing mitochondrial DNA to 2.4%. Of the remaining HIV-human chimeric reads, the HIV portion of 605 sequences bordered the 3' or 5' end of HIV or an HIV splice donor or acceptor. Filtering to these

more likely authentic junctions left only 2 (0.3%) chimeric reads containing mitochondrial sequence. This decrease in likely mitochondrial artifacts suggests that the filtering was effective. The high rate of mitochondrial chimeras in the unfiltered sequences raises the concern that artifacts may easily distort results in studies using similar amplification and sequencing techniques.

Chimeric messages composed of HIV and cellular RNA sequences can be formed by cellular gene transcription reading into the integrated provirus, by HIV transcription reading out through the viral polyadenylation site or by splicing between human and viral splice sites. In our filtered data, the predominant forms appear to be derived from reading through the HIV polyadenylation signal into the surrounding DNA (78%), splicing out of the viral D4 splice donor to join to human splice acceptors (17%) and reading into the HIV 5' LTR from human sequence (4.0%) (Figure 4.8C). No splice site other than D4 had more than two chimeric reads observed.

The filtered chimeric reads had many traits consistent with biological chimera formation. The reads containing HIV D4 joined to human sequences had the characteristics expected of splicing—72.1% of the chimeric junctions mapped to known human acceptors and 96.1% mapped to a location immediately preceded by the AG consensus of human mRNA acceptors. The reads containing the 5' or 3' LTR border were almost exclusively (93%) found in transcription units, with odds of being in a gene 2.3-fold (95% CI: 1.6–3.2 \times) higher than integration sites from the same sample. The readthrough chimeras were also more likely to be located in an exon than integration sites (odds ratio: 2.1 \times , 95% CI: 1.6–2.6 \times only considering integration sites and chimeras in transcription units).

Chimeric sequences have the potential to alter the expression of proto-oncogenes leading to proliferation of the host cell^{498–501}. In our data, we saw no significant enrichment of integrations in transcription units annotated as proto-oncogenes by the Uniprot Knowledgebase^{548,549} (Fisher's exact test $p = 0.15$). Chimeras were enriched relative to integration sites in genes annotated in a broader collection of cancer-related genes⁵⁵⁰ (odds ratio: 1.3, 95%

CI: 1.1–1.7). However, the expression of overlapping genes, as estimated by Cufflinks, was even more highly associated with chimeric reads (generalized linear model of chimera versus integration site on $\log(\text{FPKM})$: $p = 2 \times 10^{-9}$) and adding the cancer-related gene annotation was not significantly associated after accounting for expression (ANOVA: $p = 0.06$). This lack of enrichment might be expected since cells were infected for only 48 hours and it is unlikely that there would be time for any selection to occur.

We next compared whether the human and viral segments of chimeric reads agreed or disagreed in orientation (i.e. strand transcribed) for reads with the human portion mapped within annotated transcription units. The sequencing technique used here does not preserve strand information, but we can check whether the strand of a sequence read agrees or disagrees with the annotated gene strand and compare this to the observed strand of the HIV portion of the read. Chimeras involving HIV splice donor D4 were more highly enriched for matching orientations (odds ratio: 52.5 \times , 95% CI: 12.1–307 \times) suggesting that pairing with human splice acceptors constrains the orientation of D4 chimeric reads. We also found a strong association between the orientation of the human and HIV portions of chimeric reads within 3' and 5' chimeras (odds ratio: 6.2 \times , 95% CI: 3.9–10.2 \times). This highly significant enrichment of HIV and human genes in the same orientation (Fisher's exact test $p < 10^{-15}$) might indicate that antisense HIV RNA is rapidly degraded by a response to double-stranded RNA or that polymerases oriented in opposing directions interfere with one another during elongation.

Based on these data, we can propose a lower bound on the relative abundance of chimeras. If we assume that our filtering removed nearly all artifacts so that we have few false positives, then our estimate should be lower than the true proportion of chimeras. In our data, only $\frac{604}{12,689,879} = 0.0048\%$ of reads containing sequence mapping to HIV also contained identifiable chimeric junctions. However, this is an underestimate because in an HIV-derived mRNA, any fragment of the sequence will be mappable to HIV, while for a chimeric sequence only a read spanning the HIV-human junction will allow identification of a chimera. If we assume that

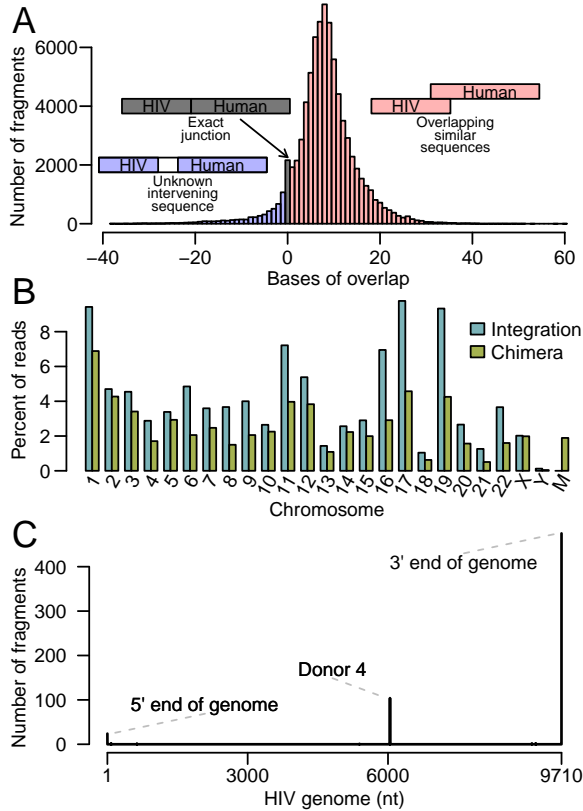


Figure 4.8: Analysis of chimeric RNA sequences containing both human and HIV sequences. A) The length of overlapping sequence (regions of complementarity potentially favoring chimera formation) matching both human and HIV at inferred chimeric junctions. The x-axis shows the length of the overlap and the y-axis shows the frequency of chimeric junctions with the indicated extent of overlap. B) Chromosomal distribution of uniquely mapping HIV integration sites from the same infections of primary T cells and comparison to uniquely mapping human sequences in chimeric reads observed in RNA-Seq. Note that the mitochondrial genome, denoted as M, has no authentic integration sites but does have extensive matches to chimeric junctions found in the RNA-Seq data. C) Counts of the location in the HIV genome of the HIV-human junctions in filtered chimeric reads.

25 bases of sequence are necessary to map to human or HIV sequence, then, with the 100-bp reads used here, only read fragments starting between 75- and 25-bp downstream of the chimeric junction will be identifiable. If we assume the average chimeric mRNA sequences is at least 2 kb long, then a read from a chimeric sequence has at most a $\frac{50}{2000} = 2.5\%$ chance of containing a mappable junction. Thus, a lower bound for the proportion of HIV mRNA that also contain human-derived sequences is 0.2% ($\frac{0.0048\%}{2.5\%}$). Looking only at splicing from HIV donor D4, we saw 16,843 reads containing a junction from D4 to an HIV acceptor and 104 reads from D4 to human sequence. Thus, in our data, 0.6% of D4 splice products form junctions with human acceptors instead of HIV acceptors.

4.5 Discussion

Here we used RNA-Seq to analyze mRNA accumulation and splicing in primary T cells infected with the low passage isolate HIV_{89.6}. We did not carry out dense time series analysis,

compare different human cell donors or compare different perturbations of the infections—instead, we focused on generating a dense data set at a single time point. We analyzed replicate infected cell and control samples to allow discrimination of within-condition versus between-condition variation and assessed differences using a series of bioinformatic approaches. Many previous studies have used microarray technology or RNA-Seq to study gene activity in HIV-infected cells^{317,319,477–485,490}, usually analyzing infections of transformed cell lines or laboratory adapted strains of HIV-1. Here we present what is to our knowledge the deepest RNA-Seq data set reported for infection in primary T cells using a low passage HIV isolate (HIV_{89.6}).

This RNA-Seq data set was paired with a set of 147,281 unique integration site sequences extracted from the same infections, which were critical to our ability to quality control chimeric reads. An advantage of studies using cell lines and laboratory adapted strains is that a high proportion of cells can be infected, whereas in this study we achieved only ~30% infection. In this study, T cells were activated using IL-2 and PHA-L. Further studies investigating the effects of cells activated in a more physiological way might provide further benefits. However, we report distinctive features of the transcriptional response not seen in studies of HIV infections in cell lines. Novel in this study are 1) identification of intron retention as a consequence of HIV infection, 2) the finding of activation of ERV-9/LTR12C after HIV infection, 3) generation of a quantitative account of the structures and abundances of over 70 HIV_{89.6} messages and 4) clarification of the predominant types of HIV-host transcriptional chimeras. These findings are discussed below.

Broad changes in host cell mRNA abundances were evident after infection, with over 17% of expressed genes changing significantly in activity. Changes included response to viral infection, apoptosis and T cell activation. Although it is not possible here to separate the response of infected and bystander cells, this study highlights the drastic changes in cellular expression caused by HIV-1 infection. In a meta-analysis including four previously published studies, no gene was detected as differentially expressed in all five studies and

only a handful of genes appeared in four out of five studies. Further analyses showed that expression changes appear to be cell type specific, raising concerns that studies using cell lines may not fully reflect host cell responses in *in vivo* infections.

Unexpectedly, intronic sequences were more common in the RNA-Seq data from cells after HIV_{89.6} infection than in mock infected cells. The mechanism is unclear. It is possible that the splicing machinery is reduced in activity after 48 hours of infection, perhaps as a part of the antiviral response of infected and bystander cells. HIV infection does appear to alter expression and localization of some splicing factors^{446,551,552} and genes involved in RNA splicing were more likely to be differentially expressed in our study (Benjamini-Hochberg corrected Fisher's exact test: $q = 2 \times 10^{-5}$). Alternatively, fully spliced mRNAs might be more rapidly degraded after infection, possibly by interferon-mediated induction of RNaseL⁵⁵³ or off-target binding of viral protein Rev might mediate export of incompletely spliced cellular transcripts^{226,227}. A speculative possibility is that HIV_{89.6} encodes a factor that alters cellular splicing or promotes mRNA degradation to optimize splicing and translation of viral messages.

Infection resulted in increased expression of specific cellular repeated sequences. HERVs, in particular HERV-K, have previously been observed to show increased RNA accumulation with HIV infection^{328-333,340} and possibly represent vaccine targets because of their production of distinctive proteins³³⁵⁻³⁴⁰. Here, though we saw modest increases in HERV-K expression, ERV-9 had the greatest change in expression (33 LTR12C and 14 ERV-9 annotated regions with greater than 4× change in expression). Previous RNA-Seq studies of HIV infection in cell lines did not report increases in HERV expression^{319,482} but this difference is likely due to a much higher baseline expression of HERVs in transformed cell lines. We also observed increases in LINE and Alu element transcription, as has been reported previously³³⁴, and expression changes in ERV-9/LTR12C expression associated with transcription factor motifs and U3 variants.

Many of the repeated sequence elements that were induced by HIV_{89.6} infection are relatively

recently integrated in the human genome. The reason for this pattern is unclear. It may be that older elements have accumulated more mutations, resulting in an inactivation of transcriptional signals. Alternatively, perhaps the elements that are induced have been recruited for transcriptional control of cellular functions, so that their transcriptional activity is preserved evolutionarily^{511,554-557}.

Comparison of the results of sequencing HIV_{89.6} messages using long-read single molecule sequencing (Pacific Biosciences) and dense short read sequencing (Illumina data reported here) allowed a full quantitative accounting of more than 70 HIV_{89.6} splice forms. The full length unspliced HIV RNA comprised 37.6% of all messages, corresponding to more than 2000 genomes per cell. Notably abundant messages included the full length genome and spliced transcripts encoding Nef and Rev transcripts. The full set of messages is summarized in Figure 4.7B.

Our previous analysis using PacBio sequencing⁴¹⁹ revealed an unusually prominent 1 kb size class. HIV_{89.6} encodes a splice acceptor (A8c) within Nef responsible for formation of the short messages. Our data indicated that two members of the 1-kb size class, D1-A5-D4-A8c and D1-A8c, accounted for 10.6% and 4.9% of all viral messages. The 1 kb size class as a whole accounted for fully 20% of messages. The function of this large amount of 1 kb transcript is unknown. The most abundant 1 kb transcripts do not appear to encode significant open reading frames although other 1 kb transcripts can encode a Rev-Nef fusion⁴¹⁹. Most HIV/SIV variants do appear to encode an acceptor near this position, suggesting a potential unknown function for these short spliced forms^{419,427,431}. This analysis also suggests a lower proportion of 4kb than has been seen for another isolate³²² suggesting that these ratios may vary with strain, time of infection or other conditions.

After filtering, we detected a sizeable number of apparently authentic chimeras containing both HIV and cellular sequences. Mechanisms of insertional activation have been studied intensively in animal models of transformation and in adverse events in human gene therapy. One of the most common mechanisms involves insertion of a retroviral enhancer near a

cellular promoter, so that transcription of a nearby gene is increased^{499,558–560}. However, another common mechanism involves formation of chimeric messages involving both cellular and viral/vector sequences^{498,499}. A targeted in vitro study of chimeric message formation by lentiviral vectors showed examples of multiple types of read-in and -out and splice-in and -out⁵⁰⁰, which may have been more frequent and more varied than for HIV_{89.6} proviruses studied here. The low level of splicing and reading into HIV in this study may be a reflection of the high rate HIV transcription in these infected cells—because HIV was so highly expressed, there would be more opportunities for polymerase to splice out of or read through the HIV genome than to read or splice in. The vast majority of HIV proviruses in expanded clones in well-suppressed patients appear to be defective⁴⁹⁴—going forward, it will be of interest to investigate whether these HIV proviruses are damaged in ways that promote formation of chimeric transcripts.

Lastly, we note that several features of the transcriptional response to HIV_{89.6} infection were suggestive of de-differentiation away from T cell specific expression patterns. The increase in expression of cellular HERVs and LINEs is characteristic of cells in early development. Specific HERVs and transposons, including ERV-9/LTR12C and HERV-K, have been implicated in regulating gene activity early in development^{511,554,557,561–564}. Several genes related to other hematopoietic cell types showed elevated RNA abundance after HIV_{89.6} infection. These data are of interest given the finding that patients undergoing long term ART can contain long lived T cell clones that may contribute to the latent reservoir^{494,565–568}. Possibly the transcriptional responses seen in infected primary T cells here are reflective of processes leading to formation of the long-lived latently-infected cells with stem-like properties.

4.6 Conclusions

Infections of primary T cells with a low passage HIV isolate showed several distinctive features compared to previously published data using T cell lines and/or lab-adapted HIV strains. We found strong changes in expression in genes related to immune response and

apoptosis similar to studies of HIV infection in patient samples and primary cells but different from studies performed in SupT1 cell lines. Notable changes after infection included intron retention and activation of recently integrated retrotransposons and endogenous retroviruses, in particular LTR12C/ERV-9. We also present complete absolute estimation of over 70 messages from HIV_{89.6} and specify the major virus-host chimeras as splicing from viral splice donor 4 to cellular acceptors and readthrough from the 5' and 3' ends of the provirus.

4.7 Availability of supporting data

RNA-Seq reads from this study are available at the Sequence Read Archive under accession number SRP055981. The integration site data is available at the Sequence Read Archive under accession number SRP057555.

4.8 Acknowledgements

We would like to thank the University of Pennsylvania Center for AIDS Research (P30 AI045008) for preparation of viral stocks and isolation of primary CD4⁺ T cells; Ronald G. Collman and members of the Bushman laboratory for reagents, helpful discussion and technical expertise. This work was funded by NIH grant R01 AI052845, the HIV Immune Networks Team (HINT) consortium P01 AI090935 and NRSA computational genomics training grant T32 HG000046.

CHAPTER 5: A reverse transcription loop-mediated isothermal amplification assay optimized to detect multiple HIV subtypes

This chapter was originally published as:

KE Ocwieja^{*}, S Sherrill-Mix^{*}, C Liu, J Song, H Bau and FD Bushman. 2015. A reverse transcription loop-mediated isothermal amplification assay optimized to detect multiple HIV subtypes. *PLoS One*, 10:e0117852. doi: 10.1371/journal.pone.0117852

KE Ocwieja, C Liu, H Bau, FD Bushman and I conceived the experiments. KE Ocwieja and I designed the assay. KE Ocwieja, C Liu and J Song performed the experiments. KE Ocwieja, J Song and I analyzed the data. I produced the figures. KE Ocwieja, C Liu, H Bau, FD Bushman and I wrote the paper.

Supporting information are available at <http://journals.plos.org/plosone/article?id=10.1371/journal.pone.0117852#sec011>

5.1 Abstract

Diagnostic methods for detecting and quantifying HIV RNA have been improving, but efficient methods for point-of-care analysis are still needed, particularly for applications in resource-limited settings. Detection based on reverse-transcription loop-mediated isothermal amplification (RT-LAMP) is particularly useful for this, because when combined with fluorescence-based DNA detection, RT-LAMP can be implemented with minimal equipment and expense. Assays have been developed to detect HIV RNA with RT-LAMP, but existing methods detect only a limited subset of HIV subtypes. Here we report a bioinformatic study to develop optimized primers, followed by empirical testing of 44 new primer designs. One primer set (ACeIN-26), targeting the HIV integrase coding region, consistently detected subtypes A, B, C, D, and G. The assay was sensitive to at least 5000 copies per reaction for

subtypes A, B, C, D, and G, with Z-factors of above 0.69 (detection of the minor subtype F was found to be unreliable). There are already rapid and efficient assays available for detecting HIV infection in a binary yes/no format, but the rapid RT-LAMP assay described here has additional uses, including 1) tracking response to medication by comparing longitudinal values for a subject, 2) detecting of infection in neonates unimpeded by the presence of maternal antibody, and 3) detecting infection prior to seroconversion.

5.2 Introduction

Despite the introduction of efficient antiretroviral therapy, HIV infection and AIDS continue to cause a worldwide health crisis⁵⁷⁰. Methods for detecting HIV infection have improved greatly with time⁵⁷¹—today rapid assays are available that can detect HIV infection in a yes-no format using a home test kit that detects antibodies in saliva. Viral load assays that quantify viral RNA with quick turn-around time are widely available in the developed world. However, quantitative viral load assays are not commonly available with actionable time scales in much of the developing world. This motivates the development of new rapid and quantitative assays that can be used at the point of care with minimal infrastructure^{572,573}.

One simple and quantitative detection method involves reverse transcription-based loop mediated isothermal amplification (RT-LAMP)⁵⁷⁴. In this method, a DNA copy of the viral RNA is generated by reverse transcriptase, and then isothermal amplification is carried out to increase the amount of total DNA. Primer binding sites are chosen so that a series of strand displacement steps allow continuous synthesis of DNA without requiring thermocycling. Reaction products can be detected by adding an intercalating dye to reaction mixtures that fluoresces only when bound to DNA, allowing quantification of product formation by measurement of fluorescence intensity. Such assays can potentially be packaged in simple self-contained devices and read out with no technology beyond a cell phone.

RT-LAMP assays for HIV-1 have been developed previously and reported to show high sensitivity and specificity for subtype B, the most common HIV strain in the developed

world^{573,575,576}. Another recent study reported RT-LAMP primer set optimized for the detection of HIV variants circulating in China⁵⁷⁷, and another on confirmatory RT-LAMP for group M viruses⁵⁷⁸. Assays have also been developed for HIV-2⁵⁷⁹. A complication arises in using available RT-LAMP assays due to the variation of HIV genomic sequences among the HIV subtypes^{580,581}, so that an RT-LAMP assay optimized for one viral subtype may not detect viral RNA of another subtype⁵⁸². Tests presented below show that many RT-LAMP assays are efficient for detecting subtype B, for which they were designed, but often performed poorly on other subtypes. Subtype C infects the greatest number of people worldwide, including in Sub-Saharan Africa, where such RT-LAMP assays would be most valuable, motivating optimization for subtype C. Several additional non-B subtypes are also responsible for significant burdens of disease world-wide⁵⁸³.

Here we present the development of an RT-LAMP assay capable of detecting HIV-1 subtypes A, B, C, D, and G. We first carried out a bioinformatic analysis to identify regions conserved in all the HIV subtypes. We then tested 44 different combinations of RT-LAMP primers targeting this region in over 700 individual assays, allowing identification of a primer set (ACeIN-26) that was suitable for detecting these subtypes. We propose that the optimized RT-LAMP assay may be useful for quantifying HIV RNA copy numbers in point-of-care applications in the developing world, where multiple different subtypes may be encountered.

5.3 Methods

5.3.1 Viral strains used in this study

Viral strains tested included HIV-1 92/UG/029 (Uganda) (subtype A, NIH AIDS Reagent program reagent number 1650), HIV-1 THRO (subtype B, plasmid derived, University of Pennsylvania CFAR)⁵⁸⁴, CH269 (subtype C, plasmid derived, University of Pennsylvania CFAR)⁵⁸⁴, UG0242 (subtype D, University of Pennsylvania CFAR), 93BRO20 (subtype F, University of Pennsylvania CFAR), HIV-1 G3 (subtype G, NIH AIDS Reagent program reagent number 3187)⁵⁸⁵.

Viral stocks were prepared by transfection and infection. Culture supernatants were cleared of cellular debris by centrifugation at 1500g for 10 min. The supernatant containing virus was then treated with 100 U DNase (Roche) per 450 uL virus for 15 min at 30°C. RNA was isolated using the QiaAmp Viral RNA mini kit (Qiagen GmbH, Hilden, Germany). RNA was eluted in 80 uL of the provided elution buffer and stored at -80°C.

Concentration of viral RNA copies was calculated from p24 capsid antigen capture assay results provided by the University of Pennsylvania CFAR or the NIH AIDS-reagent program. In calculating viral RNA copy numbers, we assumed that all p24 was incorporated in virions, all RNA was recovered completely from stocks, 2 genomes were present per virion, 2000 p24 molecules per viral particle, and the molecular weight of HIV-1 p24 was 25.6 kDa.

5.3.2 Assays

RT-LAMP reaction mixtures (15 μ L) contained 0.2 μ M each of primers F3 and B3 (if a primer set used multiple B3 primers, mixture contained 0.2 μ M of each); 1.6 μ M each of FIP and BIP primers (if a primer set had multiple FIP primes, reaction mixture contained 0.8 μ M of each FIP primer); and 0.8 μ M each of LoopF and LoopB primers; 7.5 μ L OptiGene Isothermal Mastermix ISO-100nd (Optigene, UK), ROX reference dye (0.15 μ L from a 50X stock), EvaGreen dye (0.4 μ L from a 20X stock; Biotium, Hayward, CA); HIV RNA in 4.7 μ L; AMV reverse transcriptase (10U/ μ L) 0.1 μ L and water to 15 μ L. In most cases where two primer sets were combined, the total primer concentration within the reaction was doubled such that the above individual primer molarities were maintained. For the mixture ACeIN-26+F-IN (S2 Table, line 46), the total primer concentration was not doubled—the F-IN primer set comprised 25% of the total primer concentration, and the ACeIN-26 primer set comprised 75% of the total primer concentration with the ratios of primers listed above preserved. This mixture was combined 1:1 with the ACe-PR primer set (S2 Table, line 47) such that total primer concentration in the final mixture was doubled.

Amplification was measured using the 7500-Fast Real Time PCR system from Applied

Biosystems with the following settings: 1 minute at 62°C; 60 cycles of 30 seconds at 62°C and 30 seconds at 63°C. Data was collected every minute. Product structure was assessed using dissociation curves which showed denaturation at 83°C. Products from selected amplification reactions were analyzed by agarose gel electrophoresis and showed a ladder of low molecular weight products (data not shown).

Product synthesis was quantified as the cycle of threshold for 10% amplification. Z-factors⁵⁸⁶ were calculated from tests of 24 replicates using the ACeIN-26 primer set in assays with viral RNA of each subtype. No detection after 60 min was given a value of 61 min in the Z-factor calculation.

5.4 Results

5.4.1 Testing published RT-LAMP primer sets against multiple HIV subtypes

We first assessed the performance of existing RT-LAMP assays on RNA samples from multiple HIV subtypes. We obtained viral stocks from HIV subtypes A, B, C, D, F, and G, estimated the numbers of virions per ml, and extracted RNA. RNAs were mixed with RT-LAMP reagents which included the six RT-LAMP primers, designated F3, B3, FIP, BIP, LF and LB⁵⁷⁴. Reactions also contained reverse transcriptase, DNA polymerase, nucleotides and the intercalating fluorescent EvaGreen dye, which yields a fluorescent signal upon DNA binding. DNA synthesis was quantified as the increase in fluorescence intensity over time, which yielded a typical curve describing exponential growth with saturation (examples are shown below). Results are expressed as threshold times (T_t) for achieving 10% of maximum fluorescence intensity at the HIV RNA template copy number tested.

In initial tests, published primer sets targeting the HIV-1 subtype B coding regions for capsid (CA), protease (PR), and reverse transcriptase (RT) (named B-CA, B-PR and B-RT) were assayed in reactions with RNAs from four of the subtypes. Results with each primer set tested are shown in Figure 5.1 in heat map format, where each tile summarizes the results of tests of 5000 RNA copies. Primers and their groupings into sets are summarized in S1 and

S2 Tables, average assay results are in S3 Table, and raw assay data is in S4 Table. Assays (Figure 5.1, top) with the B-CA, B-PR and B-RT primer sets detected subtypes B and D at 5000 RNA copies with threshold times less than 20 min. However, assays with B-CA and B-RT detected subtypes C and F with threshold times > 50 min, indicating inefficient amplification and the potential for poor separation between signal and noise. B-PR did not detect subtype C at all. In an effort to improve the breadth of detection, we first tried mixing the B-PR primers, which detected clade F (albeit with limited efficiency) with the B-CA and B-RT primers (Figure 5.1 and S3 and S4 Tables). In neither case did this provide coverage of all four clades tested. We thus did not test these primer sets on RNAs from the remaining subtypes and instead sought to develop primer sets targeting different regions of the HIV genome.

5.4.2 Primer design strategy

To design primers that detected multiple HIV subtypes efficiently, we analyzed alignments of HIV genomes (downloaded from the Los Alamos National Laboratory site⁵⁸⁰) for regions with similarity across most viruses, revealing that a segment of the pol gene encoding IN was particularly conserved (Figure 5.2A). A total of six primers are required for each RT-LAMP assay⁵⁷⁴. We used the EIKEN primer design tool to identify an initial primer set targeting this region. In further analysis, positions in the alignments were identified within primer landing sites that commonly contained multiple different bases. Primer positions were manually adjusted to avoid these bases when possible, and when necessary mixtures were formulated containing each of these commonly occurring bases (S1 and S2 Tables). An extensive series of variants targeting the IN coding region was tested empirically in assays containing RNAs from multiple subtypes (5000 RNA copies per reaction, over 700 total assays; S3 and S4 Tables). Based on initial results, primers were further modified by adjusting the primer position or addition of locked nucleic acids as described below.

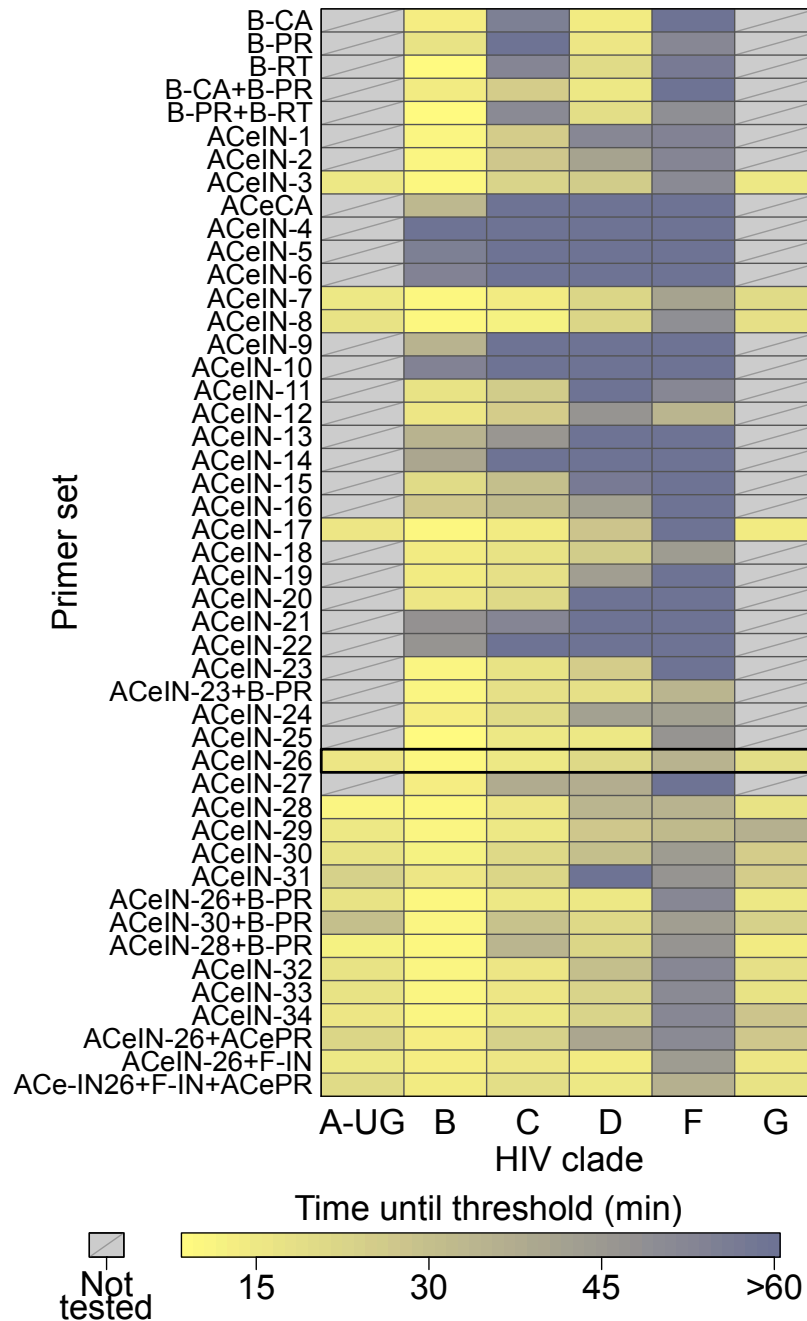


Figure 5.1: Summary of amplification results for all the RT-LAMP primer sets tested in this study. The data is shown as a heat map, with more intense yellow coloring indicating shorter amplification times (key at bottom). Primer sets tested are named along the left of the figure. Primer sequences, and their organization into LAMP primer sets, are cataloged in S1 and S2 Tables. The raw data and averaged data are collected in S3 and S4 Tables. ACeIN-26 primer set (highlighted) had one of the best performances across the subtypes and a relatively simple primer design.

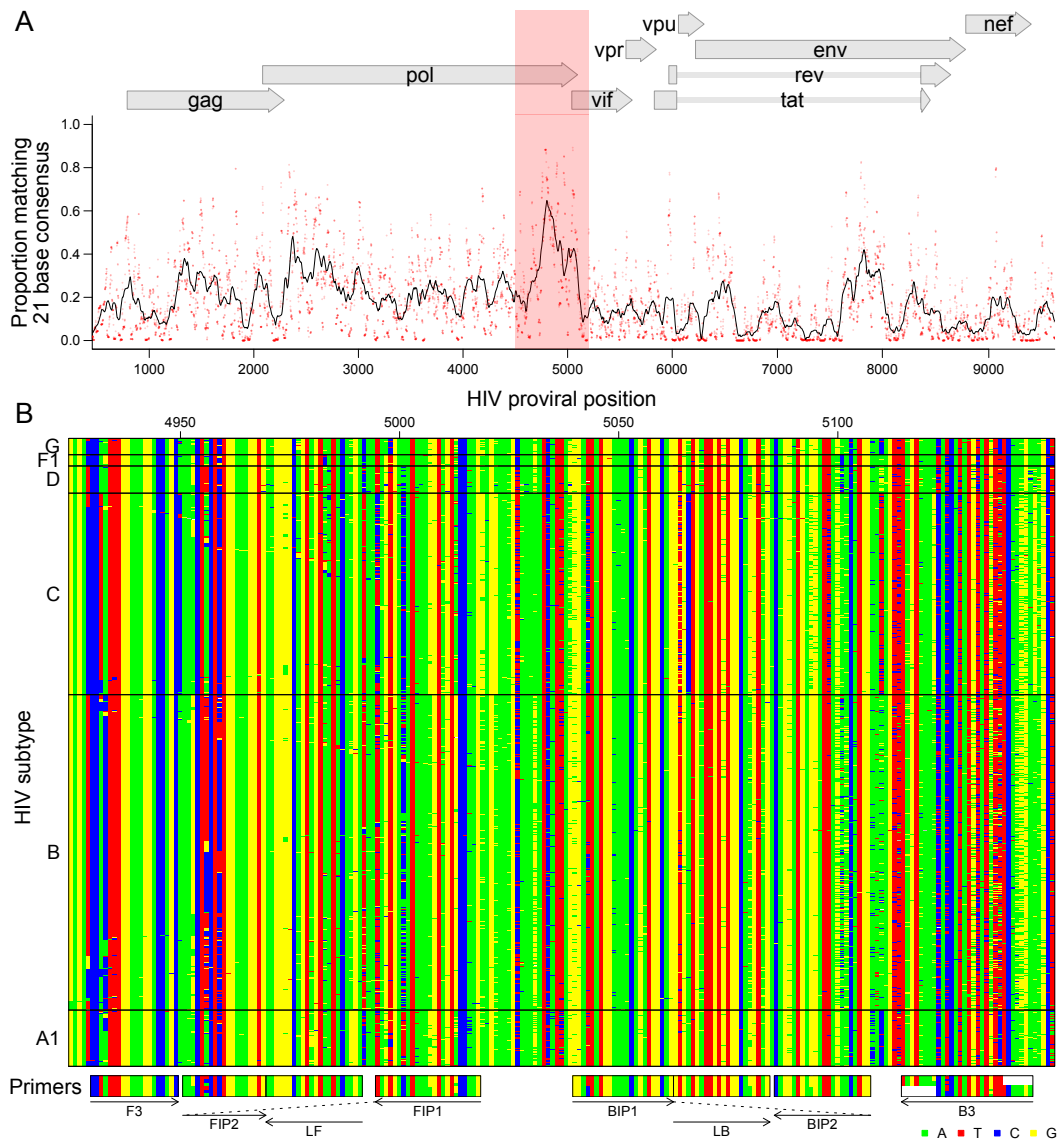


Figure 5.2: Bioinformatic analysis to design subtype-agnostic RT-LAMP primers. A) Conservation of sequence in HIV. HIV genomes ($n = 1340$) from the Los Alamos National Laboratory collection were aligned and conservation calculated. The x-axis shows the coordinate on the HIV genome, the y-axis shows the proportion of sequences matching the consensus for each 21 base segment of the genome (red points). The black line shows a 101 base sliding average over these proportions. The vertical red shading shows the region targeted for LAMP primer design that was used as input into the EIKEN primer design tool. Numbering is relative to the HIV_{89.6} sequence. B) Aligned genomes, showing the locations of the ACEIN-26 primers. Sequences are shown with DNA bases color-coded as shown at the lower right. Each row indicates an HIV sequence and each column a base in that sequence. Horizontal lines separate the HIV subtypes (labeled at left). Arrows indicate the strand targeted by each primer. Primers targeting the negative strand of the virus are shown as reverse complements for ease of viewing.

5.5 Testing different primer designs

Our first design, ACeIN-1 (“ACe” for “All Clade” and “IN” for “integrase”), targeted the HIV IN coding region and contained multiple bases at selected sites to broaden detection (Figure 5.1). ACeIN-2 and-3 have primers (B3) with slightly different landing sites. Tests showed that the mixture of primers allowed amplification with a shorter threshold time than did either alone (Figure 5.1).

We also tried to design a new primer set to the CA coding region (Figure 5.1, ACeCA) but found that the set only amplified clade B, and not efficiently. Thus this design was abandoned.

ACeIN-3 through-6 were altered by inserting a polyT sequence between the two different sections of FIP and BIP in various combinations, a modification introduced with the goal of improving primer folding, but these designs performed quite poorly (Figure 5.1).

Because the FIP primer appeared to bind the region with most variability among clades, we tried variations that bound to several nearby regions. These were tried with and without the polyT containing BIP and FIP primers in various combinations (Figure 5.1, ACeIN-7 through-22). We also tried mixing all of the variations of FIP together (ACeIN-23; S2 Table). The ACeIN-23 primer set was tried as a mixture with the B-PR set to try to capture clade F, yielding a relatively effective primer set (Figure 5.1, ACeIN-23+B-PR).

In an effort to increase affinity, an additional G/C pair was added to F3 and tested with various other IN primers (Figure 5.1, ACeIN-24 through-31). Testing showed improvement, with ACeIN-26 showing particularly robust amplification.

In a second effort to increase primer affinities, we substituted locked nucleic acids (LNAs) for selected bases that were particularly highly conserved among subtypes (Figure 5.1, ACeIN-30, -31, -32, -33, and-34). Some improvement was shown over the non-LNA containing bases. However, the ACeIN-26 primer set was as effective as or better than any LNA containing

Primer name	Sequence
ACeIN-F3.c	CCTATTTGGAAAGGACCAGC
ACeIN-B3a	TCTTTGAAAYATACATATGRTG
ACeIN-B3b	AACATACATATGRTGYTTTACTA
ACeIN-FIPe	CTTGGTACTACYTTTATGTCACTAAARCTACTCTGGAAAGGTG
ACeIN-FIPf	CTTGGCACTACYTTTATGTCACTAAARCTYCTCTGGAAAGGTG
ACeIN-BIP	GGAYTATGGAAAACAGATGGCAGCCATGTTCTAATCYTCATCCTG
ACeIN-LF	TCTTGTATTACTACTGCCCTT
ACeIN-LB	GTGATGATTGTGTGGCARGTAG

Table 5.1: The primers from the ACeIN-26 primer set selected for further study

primer sets.

In further tests, the ACeIN-26, -28 and -30 primers were tested combined with the ACePR primer set (a slightly modified version of the B-PR primer set, S2 Table, row 2, designed to accommodate a wider selection of HIV-1 subtypes) but no improvement was seen and efficiency may even have fallen for some subtypes. We also designed a primer set that matched exactly to the targeted sequences found in the problematic subtype F, and mixed this set with the ACeIN-26 primers. However, no improvement was seen (Figure 5.1, mixtures with F-IN set). Mixing the ACeIN-26 primers with both the ACePR and F-specific primers did yield effective primer sets (Figure 5.1, ACeIN-26+F-IN and ACeIN-26+F-IN+ACePR). However, amplification efficiency was not greatly improved over the ACeIN-26 primer set, so we proceeded with the simpler ACeIN-26 primer set (Figure 5.2B and Table 5.1) in further studies.

5.5.1 Performance of the optimized RT-LAMP assay

The ACeIN-26 RT-LAMP primer set was next tested to determine the minimum concentration of RNA detectable under the reaction conditions studied (Figure 5.3). RNA template amounts were titrated and time to detection quantified. Tests showed detection after less than 20 min of incubation for 50 copies of subtypes A or B, detection after less than 30 min for 5000 copies for C, D, and G, and detection after less than 20 min for 50,000 copies for F.

For clinical implementation the reliability of an assay is critical. This is commonly sum-

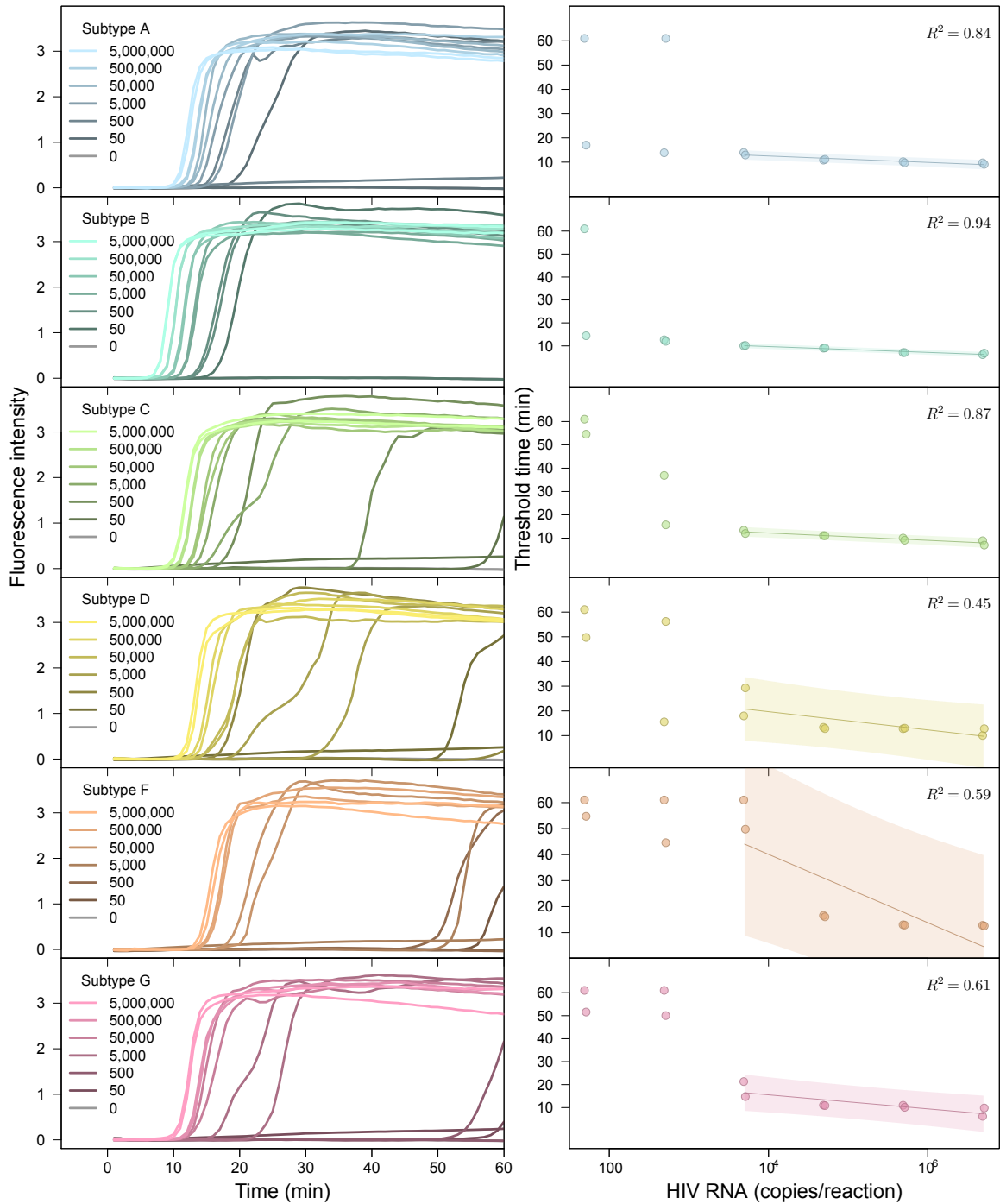


Figure 5.3: Performance of the AceIN-26 primer set with different starting RNA concentrations. Tests of each subtype are shown as rows. In each lettered panel, the left shows the raw accumulation of fluorescence signal (y-axis) as a function of time (x-axis); the right panel shows the threshold time (y-axis) as a function of log RNA copy number (x-axis) added to the reaction. In the right hand panels, values were dithered where two points overlapped to allow visualization of both.

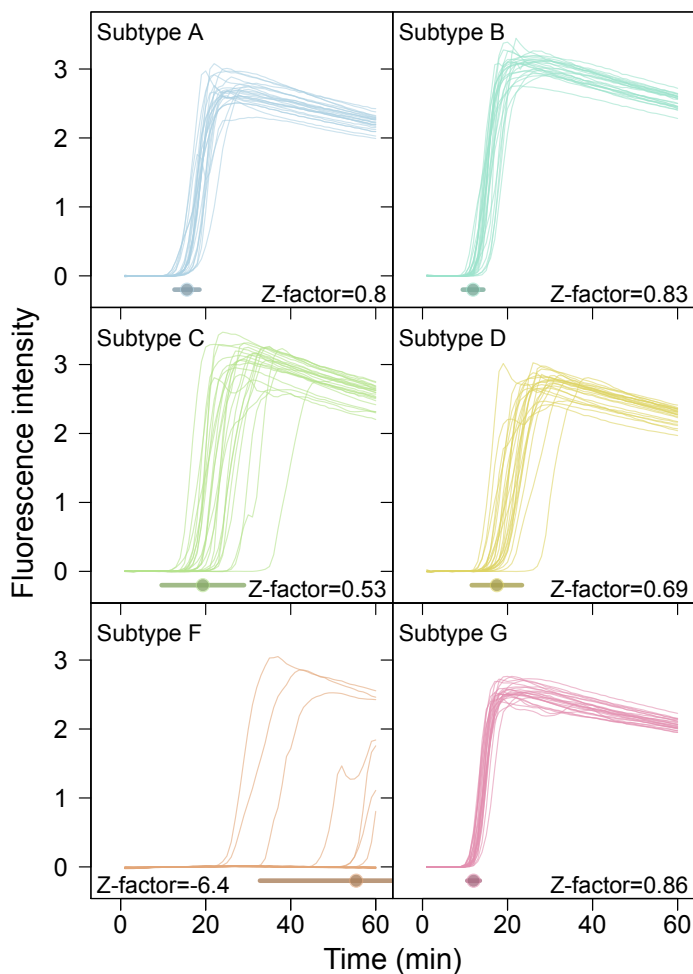


Figure 5.4: Examples of time course assays, displaying replicate tests of RT-LAMP primer set ACeIN-26 tested over six HIV subtypes, used in Z-factor calculations. A total of 5000 RNA copies were tested in each 15 μ L reaction. Time is shown on the x-axis, Fluorescence intensity on the y-axis. Replicates are distinguished using an arbitrary color code. Z-factor values and standard deviations are shown on each panel.

marized as a Z-factor⁵⁸⁶, which takes into account both the separation in means between positive and negative samples and the variance in measurement of each. An assay with a Z-factor above 0.5 is judged to be an excellent assay. Z-factors for detection of each of the subtypes at 5000 RNA copies per reaction were > 0.50 for subtypes A, B, C, D, and G, respectively (Figure 5.4, $n = 24$ replicates per test). Detection of subtype F at 5000 copies per reaction was sporadic, showing a much lower Z-factor. Therefore our ACeIN-26 RT-LAMP primer set appears well suited to detect 5000 copies of subtypes A, B, C, D and G.

5.6 Discussion

Here we present an RT-LAMP assay optimized to identify multiple HIV subtypes. Infections with subtype B predominate in most parts of the developed world, but elsewhere other subtypes are more common⁵⁸³. Thus nucleic acid-based assays for use in the developing world need to query HIV subtypes more broadly. Previously reported RT-LAMP assays, while effective at detecting subtype B, commonly showed poor ability to detect at least some of the HIV subtypes, including C, which is common in the developing world (Figure 5.1). Here we first carried out an initial bioinformatic survey to identify regions conserved across all HIV subtypes that could serve as binding sites for RT-LAMP primers. We then tested primer sets targeting these regions empirically for efficiency. Testing 44 different primer sets revealed that assays containing ACeIN-26 were effective in detecting 5000 copies of RNA from subtypes A, B, C, D, and G within 30 minutes of incubation. For these five subtypes, the times of incubation to reach the threshold times were not too different, which simplifies interpretation when the subtype in the sample is unknown. Regardless of the efficiency, these assays can be applied to longitudinal studies of changes in viral load within an individual. We propose that RT-LAMP assays based on the ACeIN-26 primer set can be useful world-wide for assaying HIV-1 viral loads in infected patients.

There are several limitations to our study. Subtypes A, B, C, D, and G were detected efficiently and showed Z-factors above 0.5, but subtype F was detected reliably only with higher template amounts, probably due to more extensive mismatches with the ACeIN-26 primer set. Subtype F is estimated, however, to comprise only 0.59% of all infections globally⁵⁸³, though it is common in some regions. For many of the common circulating recombinant forms, such as AE and BC, the target site for ACeIN-26 is from a subtype known to be efficiently detected, though in some cases the efficiency of detection is not easy to predict and will need to be tested. We did not test subtypes beyond A, B, C, D, F and G, and we did not attempt to assess multiple different variants within each subtype. Thus, while we do know that our RT-LAMP assays are more widely applicable than many of those

reported previously, we do not know whether they are able to detect all strains efficiently. In addition, although we carried out more than 700 assays in this study, there remain multiple parameters that could be optimized further, such as primer concentrations, salt type and concentration, temperature, and divalent metal concentrations, so there are likely further opportunities for improvement. Also, possible effects of RNA quality on assay performance were not tested rigorously.

A particularly important parameter for further optimization is primer sequence. Several groups have recently published primer sets optimized for broad detection of different HIV lineages^{577,578}, offering opportunities for creating sophisticated primer blends with increased breadth of detection. However, in developing such mixtures, it will be important to monitor for possible complicating interactions of primers with each other. As an example of ongoing development of mixtures, we found that addition of another primer to the ACeIN-26 set that was matched to a common subtype C lineage allowed improved detection of subtype C variants (S1 Report). In order to improve detection of subtype F, which was suboptimal with ACeIN-26, additional primer sets could be mixed to specifically target subtype F, though the ones we tried so far did not work well. It will be useful to explore the performance of broader primer mixtures in future work.

Today rapid assays are available that can report infection efficiently, for example by detecting anti-HIV antibodies in oral samples—however, the nucleic acid-based method presented here has additional potential uses. We envision combining the RT-LAMP assay with simple point-of-care devices for purifying blood plasma⁵⁷² and quantitative analysis of accumulation of fluorescent signals⁵⁸⁷. In one implementation of the technology, cell phones could be used to capture and analyze results, thereby minimizing equipment costs. Point-of-care devices are available facilitating the concentration of viral RNA from blood plasma or saliva⁵⁸⁷ to allow the detection of the 1000 RNA copy threshold that the WHO defines as virological treatment failure (World Health Organization, Consolidated ARV guidelines, June 2013). Together, these methods will allow assessment of parameters beyond just the presence/absence of

infection. Quantitative RT-LAMP assays should allow tracking of responses to medication, detection in neonates (where immunological tests are confounded by presence of maternal antibody), and early detection before seroconversion.

5.7 Acknowledgments

We are grateful to members of the Bushman and Bau laboratory for help and suggestions.

CHAPTER 6: Conclusions and future directions

In this dissertation, we described studies characterizing HIV-1 latency, expression and alternative splicing and host cell response to infection. We then developed point-of-care methods for the detection of infection and quantification of viral load. These projects suggest many avenues for continuing research.

6.1 Latency and integration location

In Chapter 2, we showed that the chromosomal location of integration affects proviral latency but the mechanisms appear to differ between cell culture models. Similarly a recent study of nine cell culture models found that no single model reliably predicted the performance of activating compounds in *ex vivo* tests of latently infected cells from HIV patients⁵⁸⁸. This suggests that either some cell culture models do not accurately reflect latency in patients or that there are diverse subsets of cells with differing mechanisms of latency within patients.

Cell culture models are currently used to screen potentially therapeutic compounds^{148,588}. If some cell culture models are not representative of *in vivo* conditions then potential treatments may be discarded or marked for development erroneously. Further comparisons between additional cell culture models and additional replicates of existing models might allow discrimination between batch/lab effects and reveal patterns between models. Comparison with cells extracted from patients or infected lab animals might offer a gold standard comparison although it is difficult to obtain large amounts of cells and difficult to distinguish defective provirus from latent provirus in such populations.

Various treatments are now being considered for the reactivation of latent provirus⁵⁸⁸. To further understand the mechanisms of these treatments, it would be informative to compare the features of latent provirus induced by a given treatment to latent viable provirus remaining uninduced. Repeated cell sorting and integration site sequencing might provide insight on mechanism. For example, one could first sort out cells with active provirus, then

treat with the potential latency modulator and sort out cells with newly active provirus and then treat with a strong inducer or alternative stimuli and sort out cell with newly activated provirus. This would give subsets of cells where latent proviruses had been activated by treatment and cells with provirus which were not activated by treatment but still inducible. Synergies between treatments could be assessed and the location of integration sites could be determined and used to locate patterns of genomic features correlated with induction for each treatment.

Current efforts at “shock and kill” therapy, inducing latent virus to activate and then eliminating infected cells, focus on histone deacetylase inhibitors. If there are diverse mechanisms of latency within patients then much of the latent reservoir may remain unactivated by single-target therapies. Clinical trials with histone deacetylase inhibitors have shown some small increases in viral RNA but little decrease in the latent reservoir of HIV^{383,589–591}. It appears that the majority of viable latent provirus from patient cells are not reactivated by current therapies⁵⁹². These results are particularly worrisome because a functional cure for HIV will likely require a greater than 10,000-fold reduction of the latent reservoir⁵⁹³.

In Chapter 2, we used publicly available genomic data. Perhaps there is some chromosomal feature with a strong association with latency but the data is not currently available or varies greatly between cell populations. More varieties of annotations are rapidly becoming available^{594–598}. Decreasing sequencing costs^{599–601} may also make it feasible to measure more epigenetic features in the exact cell population of interest. Repeating analyses similar to Chapter 2, perhaps by simply rerunning the reproducible report in Appendix A.2 with new data, would allow any new features to be monitored for correlations with latency.

6.2 HIV-1 alternative splicing

In Chapters 3 and 4, we showed that HIV RNA spliceforms are more diverse than previously appreciated and estimated the abundances of viral spliceforms. We also showed that splicing

at some splice sites vary between host subjects, between cell types and over the course of infection. Further characterization of viral splicing would be beneficial to the study and treatment of HIV-1 especially as there were some technical limitations to our research that might be improved upon using current techniques.

We studied HIV splicing using droplet PCR⁴⁵⁵ and a set of customized primer in Chapter 3 and bulk sequencing of cellular mRNA in Chapter 4. Sequencing biases and difficulties determining full length transcripts from short reads hindered characterization of HIV messages. One alternative to these techniques is the targeted capture and enrichment^{602,603} of HIV-specific sequences. Using probes targeted to conserved regions of HIV, similar to finding conserved regions for primers as in Chapter 5, would allow for enrichment of viral reads without the biases induced by primer-based PCR while still allowing for efficient use of sequencing effort.

The research in Chapter 3 was also limited by a short read bias in the PacBio sequencing. PacBio sequencing has improved⁶⁰⁴ and additional long read sequencers have been developed⁶⁰⁵⁻⁶⁰⁷. In addition, Illumina MiSeq sequencers can now produce 25 million paired 300 bp reads in a single run^{608,609} and better spliceform estimation methods are being developed^{610,611}. These improved sequencing techniques might allow for more straightforward analysis of new samples and verification of our previous results.

RNA transcribed antisense to the canonically expressed strand of HIV have been observed^{482,612-617}. These transcripts may be translated to proteins^{618,619} that trigger immune response in infected individuals^{617,618,620}. Our sequencing techniques were designed only for the HIV positive strand (Chapter 3) or did not preserve strand information (Chapter 4). Strand-specific sequencing^{621,622} of multiple HIV strains under varying cellular conditions would clarify the identity of these transcripts.

Cryptic polypeptides encoding epitopes recognized through major histocompatibility complex type I also appear to be generated from alternative reading frames in the sense strand of

the virus^{623,624}. Ribosome profiling^{625–627} of infected cells might reveal whether transcripts generated through alternative splicing or antisense expression are likely to be translated. These cryptic transcripts could offer new opportunities in vaccine design^{617,620,628,629} but first their abundance, identity and conservation across strains of HIV must be ascertained.

We observed that splicing varies over the course of infection, between human subjects and between cell types. Further sampling could reveal additional patterns in these splicing changes.

Long-lived reservoir of HIV infected cells exist in both macrophages^{630,631} and resting central memory CD4 T cells^{139,140,143,632,633}. It may be difficult to obtain enough viral RNA from resting CD4 cells⁶³² but macrophages provide an interesting target. Splicing changes due to differing abundances of splice factors have been reported in macrophages⁴⁴⁶. Characterization of splicing in these important reservoirs might aid in the understanding of latency.

We quantified the splicing of a single clinical isolate and showed unexpected diversity. Most previous studies of HIV splicing have been performed with lab-adapted strains⁴²⁵. Additional studies could determine if the high number of transcripts seen here is an anomaly and whether additional cryptic splice sites and novel proteins or epitopes exist. In addition, an important subset of HIV are the founder viruses transmitted between hosts^{634,635}. These viruses are not well studied and perhaps their splicing and gene expression differ from the rest of the viral swarm of infected patients. Comparisons to splicing in other retroviral taxa might highlight evolution and adaptation in this viral lineage.

Disruption of RNA processing can drastically reduce HIV replication^{288,636–639}. Inhibition of cellular splicing factors reduces the reproduction of HIV in many genome-wide siRNA screens^{433,435,640} and several members of the spliceosome interact with viral proteins in affinity pulldowns³¹⁰. Small molecules that inhibit cellular SR splicing proteins and disrupt viral splicing show promise as antiretroviral therapies^{432,641–643}. Characterization of splicing

in cells treated with splicing inhibitors could reveal potential escape pathways and optimal combinations of drug therapies.

6.3 Host expression during HIV infection

In Chapter 4, we saw many changes in host expression and splicing in HIV infected cells including intron retention and strong changes in apoptotic and innate immunity genes. We focused on generating a dense data set at a single time point and subject to allow discrimination of within-condition versus between-condition variation. Further sampling using more human subjects and time points, improved sequencing techniques, alternative culturing and extraction and more viral strains would clarify and extend these patterns.

In our primary cell infections, only about 25% of cells were infected with HIV. This makes it difficult to distinguish between the responses of bystander and infected cells. In addition, changes in expression due to cellular response to infection are confounded with changes due to hijacking of cellular controls by the virus. For example, bystander cell death has been suggested as a major driver of HIV pathogenesis^{644,645} but our data do not make it clear whether bystander or infected cells are undergoing apoptosis. Cell pull-down with a labelled HIV strain⁵¹⁹ or an anti-Env antibody⁶⁴⁶ or flow cytometry with a labelled antibody targeting HIV antigen^{152,647} might allow the separation of bystander and infected cells.

Additionally, abortive infections can drive cell death^{489,645} so our populations might be a mix of three responses; cells responding to a progressive infection, cells responding to an aborted infection and cells responding to neighbor cell infections. A useful control might be to infect cells with integrase-deficient virions to guarantee that all infections are aborted. This would provide a good measure of innate immune response and the effect of abortive infections undiluted by productive HIV infection and help to deconvolute the patterns seen in mixed populations.

HIV infection appeared to increase the abundance of intronic sequences. Perhaps these transcripts escape degradation due to decreased cellular RNA surveillance or mistargeted

export of incompletely spliced cellular transcripts by viral protein Rev. Alternatively, HIV Vpr protein has been reported to disrupt nuclear integrity and allow mixing of nuclear and cytoplasmic components²⁵³. These sequences might represent incompletely spliced mRNA that escaped into the cytoplasm before processing. Infection with a Vpr-deficient HIV virus and separate isolation of RNA from nuclear and cytoplasmic compartments^{648–650} would test these hypotheses.

We saw that chimeric sequences were almost entirely derived from read-in or -out from viral long terminal repeats or splicing from the viral splice donor D4 to human acceptors. With this knowledge, we could use targeted amplification of these three sites, analogous to integration site sequencing^{396,423,495}, on cellular cDNA to get a much deeper and cleaner sampling of chimera formation. Comparison of these data to deeply sequenced integration site data from the same samples might reveal associations between integration location and chimera formation.

MicroRNA are small RNAs that block translation through base pairing with complementary mRNA^{651–653}. Viral derived microRNA, perhaps in part from Dicer processing of the structured trans-activation response element of HIV^{614,654–656}, may suppress HIV expression^{217,657,658} and inhibit apoptosis⁶⁵⁶ but the presence of such microRNA is controversial^{219,659}. HIV may suppress silencing by microRNA^{216–218} but this is also controversial²¹⁹. Cellular microRNA may have antiviral effects^{660,661} or be exploited by HIV to enhance replication^{662–666} or promote latency^{667,668} but there seems to be disagreement on which microRNA are involved among different studies⁶⁶⁹. High-throughput genome-wide assays of small RNA^{482,516} from primary cells infected with patient isolates would help clarify these debates.

6.4 LAMP PCR and lab-on-a-chip

In Chapter 5, we report a loop-mediated isothermal amplification system using primers optimized to detect most subtypes of HIV-1. An alternative to a single broadly targeted

primer set would be to design separate primer sets targeted specifically to each subtype so that a positive amplification would then be able to discriminate viral subtype. Different viral subtypes can have different rates of disease progression^{670–673}, transmission dynamics^{674–676} and response to treatment^{677–679}. Simple low-cost devices with multiple reactions chambers could be used to both identify viral subtype, estimate viral load^{680,681} and allow more informed treatment decisions.

A LAMP chip with subtype-specific primers would also allow the detection of intersubtype superinfections. Superinfection of a single individual with multiple distinct strains of HIV is common in high risk individuals^{567,682–685} and the general population⁶⁸⁶. Superinfection with a phenotypically different strain of HIV can lead to disease progression^{687–692} or drug resistance⁶⁹³. Superinfection also allows recombination between divergent strains^{682,688,689,691,694} and this rapid exchange of genetic information can lead to more fit recombinant strains and worsen the global epidemic^{58,62,689,695,696}. LAMP detection of superinfection could allow early intervention and suppression in superinfected individuals.

The techniques described in Chapter 5 also allow for rapid development of detection assays for novel pathogens. For example, in a recent outbreak in West Africa, Zaire ebolavirus has infected over 26,000 confirmed, probable and suspected cases and caused over 11,000 reported deaths^{697–699}. Early detection and quarantine are essential to the control of this epidemic⁷⁰⁰. Amplification of Ebola virus nucleic acid through polymerase chain reaction is the best diagnostic test currently available but the necessary resources are often not available in these resource-poor regions^{701,702}. Antigen-based tests are quicker and available at the point-of-care but are not as accurate or sensitive as polymerase chain reaction tests and are still in limited supply⁷⁰². Loop-mediated isothermal amplification offers the potential for rapid, sensitive and efficient detection of Ebola virus RNA but available LAMP primers⁷⁰³ do not match the current outbreak strain. Using sequences from the recent outbreak^{697,704} and the methods described in Chapter 5, we designed primers to match all known Zaire ebolavirus (Figure 6.1). These primer combined with simple lab-on-a-chip devices for purifying blood

plasma⁵⁷² and imaging fluorescent signals^{587,680} could allow rapid point-of-care detection of Ebola virus.

6.4.1 Conclusions

These studies contribute to the study and treatment of HIV-1 by revealing aspects of latency, expression and host response. They highlight the importance of primary cell models and the effects that host cell can have on viral processes. With rapidly increasing sequencing throughput, further studies like those presented here offer the opportunity for a deeper and broader understanding of HIV-1 biology and host response and further development of diagnostics and therapeutics.

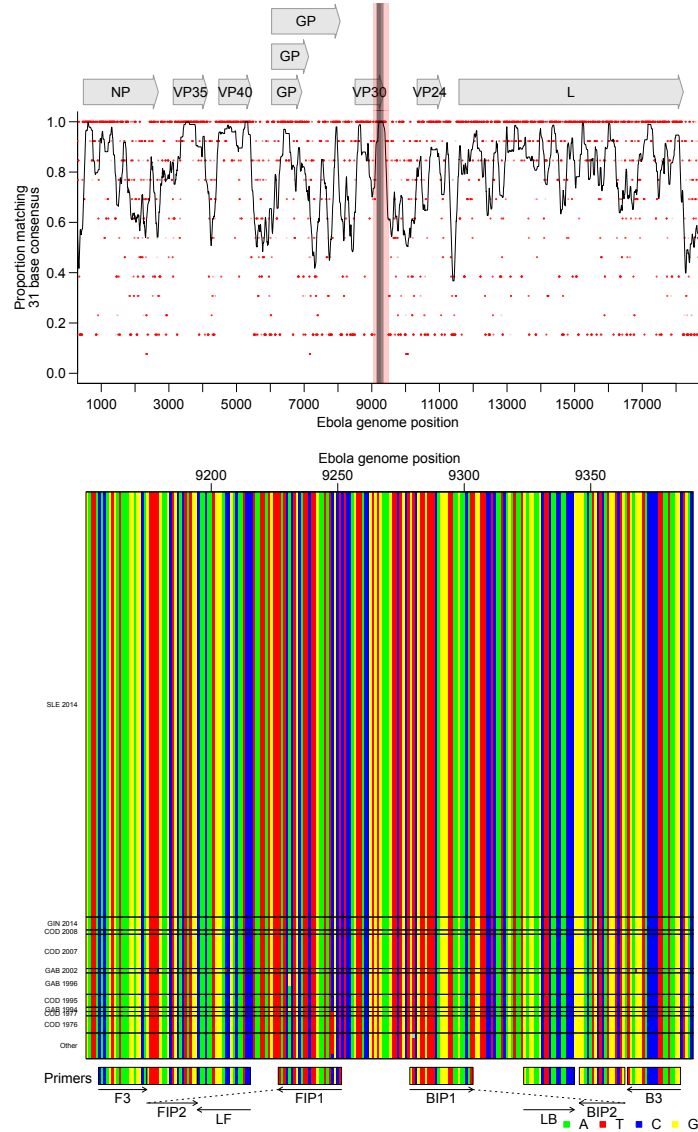


Figure 6.1: Bioinformatic analysis to design Ebola virus RT-LAMP primers. A) Conservation of sequence in Ebola virus. Ebola virus genomes ($n = 131$) from Genbank and sequences from the recent Zaire ebolavirus outbreak⁶⁹⁷ were aligned and conservation calculated. The x-axis shows the coordinate on the Ebola genome, the y-axis shows the proportion of sequences matching the consensus for each 21 base segment of the genome (red points). The black line shows a 101 base sliding average over these proportions. The vertical red shading shows the region targeted for LAMP primer design that was used as input into the EIKEN primer design tool and grey shading indicates the area covered by the optimized primer set. Numbering is relative to the Ebola Mayinga sequence. B) Aligned genomes, showing the locations of the LAMP primers. Sequences in the grey-shaded region in A are shown, with DNA bases color-coded as shown at the lower right. Each row indicates an Ebola virus sequence and each column a base in that sequence. Horizontal lines separate Ebola virus outbreaks (SLE: Sierra Leone, GIN: Guinea, COD: DR Congo, GAB: Gabon). Arrows indicate the strand targeted by each primer. Primers targeting the negative strand of the virus are shown as reverse compliments for ease of viewing.

APPENDIX A.1 : Generalized linear models of changes in use of mutually exclusive HIV-1 splice acceptors

Reads splicing from D1 to one of five mutually exclusive acceptors, D3, D4c, D4a, D4b, D5, and D5a, in three primers, 1.2, 1.3 and 1.4, were collected. Since these data are based on counts, we modeled them as Poisson distributed with an extra variance term allowing for additional variance using a quasi-Poisson generalized linear model with log link. We accounted for differences in sequencing effort by including the total number of D1 to mutually exclusive acceptors reads in each primer-sample as an offset. Differences in the read counts a) over time, b) between human donor and c) cell type were analyzed separately. A term was included for each acceptor and its interaction with the variable of interest. The models included primer and replicate terms and their individual interactions with acceptor to account for any confounding factors.

A.1.1 HOS vs T Cells

R command:

```
glm(count ~ offset(log(total)) + acceptor:primer + acceptor:isHos  
+ acceptor, data = mutEx[mutEx$time == 48,],  
family = 'quasipoisson')
```

Difference between HOS and T cells may be confounded by run differences between early sequencing and later sequencing. Verification by agarose gel (Figure 3.4B) suggest that these differences are likely biological.

Variable	Df	Deviance	Resid. Df	Resid. Dev	<i>F</i>	Pr(> <i>F</i>)
NULL	395	138 330				
acceptor	5	133 985	390	4345	9004	$<2.2 \times 10^{-16}$
acceptor:primer	12	751	378	3594	21.03	$<2.2 \times 10^{-16}$
acceptor:isHos	6	2466	372	1127	138.1	$<2.2 \times 10^{-16}$

So after accounting for primer-acceptor bias, the difference between HOS and T cells is significant.

The interesting terms in the model are:

Variable	Estimate	Std. Error	<i>t</i> value	Pr(> <i>t</i>)
acceptorA3:isHosTRUE	1.4717	0.065 86	22.35	$<2.2 \times 10^{-16}$
acceptorA4a:isHosTRUE	-0.9449	0.1246	-7.583	2.73×10^{-13}
acceptorA4b:isHosTRUE	-0.9285	0.1059	-8.767	$<2.2 \times 10^{-16}$
acceptorA4c:isHosTRUE	-1.228	0.1066	-11.51	$<2.2 \times 10^{-16}$
acceptorA5:isHosTRUE	0.090 82	0.026 08	3.483	0.000 555
acceptorA5a:isHosTRUE	0.6308	0.079 40	7.945	2.33×10^{-14}

So it appears A3 is up; A4c, A4a and A4b are down; A5 is up a little and A5a up in HOS.

A.1.2 HOS Over Time

R command:

```
glm(value~offset(log(total)) + acceptor + acceptor:primer
+ acceptor:time, data=mutEx[mutEx$isHos,],
family = 'quasipoisson')
```

Looking only within HOS, we see a significant linear effect of time:

Variable	Df	Deviance	Resid. Df	Resid. Dev	F	$\text{Pr}(>F)$
NULL	53	17962				
acceptor	5	17710	48	252.2	6698	$<2.2 \times 10^{-16}$
acceptor:primer	12	18.0	36	234.2	2.834	0.01018
acceptor:time	6	217.8	30	16.4	68.65	3.57×10^{-16}

We are assuming that a particular acceptor will have the same change in all three primers here.

The interesting terms are:

Variable	Estimate	Std. Error	t value	$\text{Pr}(> t)$
acceptorA3:time	0.02477	0.001778	13.93	1.22×10^{-14}
acceptorA4a:time	-0.01621	0.002812	-5.765	2.69×10^{-6}
acceptorA4b:time	-0.02526	0.002271	-11.12	3.62×10^{-12}
acceptorA4c:time	0.015867	0.003050	5.202	1.32×10^{-5}
acceptorA5:time	-0.001918	0.0006313	-3.038	0.00490
acceptorA5a:time	0.0049199	0.001969	2.499	0.0182

So A3, A4c and A5a increase over time and A4a, A4b and A5 decrease over time. All of these coefficients are with a log link and linear and so multiplicative. That means that for example A3 will increase 2.5%/hour ($\exp(.0247)$) or equivalently 81% (1.025^{24}) over 24hours.

A.1.3 Between Human Comparison

R command:

```
glm(value~offset(log(total)) + acceptor + acceptor:run
+ acceptor:primer + acceptor:subject,
data=mutEx[!mutEx$isHos,], family = 'quasipoisson')
```

In humans, we added a term to account for any potential run bias between the three replicates. Subject refers to the seven human blood donors from which T cells were collected:

Variable	Df	Deviance	Resid. Df	Resid. Dev	F	$\text{Pr}(> F)$
NULL	377	128 430				
acceptor	5	126 446	372	1985	19 598	$< 2.2 \times 10^{-16}$
acceptor:run	12	136	360	1849	8.792	1.77×10^{-14}
acceptor:primer	12	850	348	998	54.91	$< 2.2 \times 10^{-16}$
acceptor:subject	36	597	312	401	12.86	$< 2.2 \times 10^{-16}$

So after accounting for any run and primer bias, subject ID has a statistically significant effect on our observed counts. If we compare everything to subject 7, the interesting terms are:

Variable	Estimate	Std. Error	<i>t</i> value	Pr(> <i>t</i>)
acceptorA3:subject6	-0.001 399	0.072 86	-0.019	0.9847
acceptorA4a:subject6	-0.112 90	0.049 44	-2.284	0.023 07
acceptorA4b:subject6	-0.054 33	0.040 38	-1.345	0.1795
acceptorA4c:subject6	0.028 29	0.033 60	0.842	0.4005
acceptorA5:subject6	0.016 83	0.016 00	1.051	0.2939
acceptorA5a:subject6	-0.030 85	0.060 92	-0.506	0.6129
acceptorA3:subject5	-0.077 67	0.074 23	-1.046	0.2962
acceptorA4a:subject5	-0.1144	0.049 82	-2.296	0.0223
acceptorA4b:subject5	-0.0684	0.040 90	-1.672	0.0956
acceptorA4c:subject5	-0.085 85	0.034 75	-2.471	0.0140
acceptorA5:subject5	0.038 88	0.016 16	2.406	0.0167
acceptorA5a:subject5	0.078 77	0.060 38	1.304	0.1930
acceptorA3:subject4	-0.1849	0.095 78	-1.931	0.0544
acceptorA4a:subject4	0.071 86	0.057 91	1.241	0.2156
acceptorA4b:subject4	0.126 20	0.047 14	2.677	0.0078
acceptorA4c:subject4	-0.100 21	0.043 03	-2.329	0.0205
acceptorA5:subject4	-0.001 16	0.019 69	-0.059	0.9531
acceptorA5a:subject4	0.023 46	0.073 53	0.319	0.7499
acceptorA3:subject3	-0.003 51	0.086 65	-0.041	0.9677
acceptorA4a:subject3	0.071 07	0.055 64	1.277	0.2024
acceptorA4b:subject3	0.006 46	0.046 99	0.138	0.8907
acceptorA4c:subject3	-0.063 34	0.040 76	-1.554	0.1212
acceptorA5:subject3	0.010 52	0.018 87	0.557	0.5776
acceptorA5a:subject3	-0.070 95	0.072 85	-0.974	0.3309
acceptorA3:subject2	-0.2329	0.091 76	-2.539	0.0116
acceptorA4a:subject2	0.024 05	0.056 43	0.426	0.6702
acceptorA4b:subject2	0.1107	0.045 35	2.441	0.0152
acceptorA4c:subject2	0.021 76	0.039 52	0.551	0.5823
acceptorA5:subject2	-0.003 760	0.018 69	-0.201	0.8407
acceptorA5a:subject2	-0.1608	0.073 51	-2.187	0.0295
acceptorA3:subject1	0.095 36	0.065 56	1.454	0.1468
acceptorA4a:subject1	0.029 32	0.044 31	0.662	0.5087
acceptorA4b:subject1	-0.2144	0.038 43	-5.578	5.28×10^{-8}
acceptorA4c:subject1	-0.3974	0.033 85	-11.74	$<2.2 \times 10^{-16}$
acceptorA5:subject1	0.091 44	0.014 70	6.221	1.58×10^{-9}
acceptorA5a:subject1	0.027 47	0.055 94	0.491	0.6238

So there were small but significant effects between subjects especially between subject 1 and subjects 2–7. A potential confounder is that T cells were collected from apheresis product in

subject 1 and from whole blood in subjects 2–7 although why this would affect later assays is unknown.

APPENDIX A.2 : Reproducible report of HIV integration sites and latency analysis

A.2.1 Supplementary data

Additional File 2 is a gzipped csv file that includes a row for each uniquely mapped provirus and its surrounding genomic annotations. The csv file should have 12436 rows (excluding header) with 6252 expressed and 6184 latent proviruses.

```
integrationData <- read.csv("AdditionalFile2.csv.gz",
  stringsAsFactors = FALSE)

nrow(integrationData)

## [1] 12436

table(integrationData$isLatent)

##
## FALSE  TRUE
##  6252  6184
```

A.2.2 Lasso regression

The lasso regressions take a while to run so I've turned down the number of cross validations here (set `eval=FALSE` below to completely skip this step). Leave one out and 480-fold cross validation were used in the paper but processing may take a few days without parallel processing. Lasso regression requires the R `glmnet` package.

```

notFitColumns <- c("id", "chr", "pos", "strand", "sample", "isLatent
")

samples <- unique(as.character(integrationData$sample))

sampleMatrix <- do.call(cbind, lapply(samples, function(x)
  integrationData$sample == x))

colnames(sampleMatrix) <- gsub(" ", "_", samples)

interact <- function(predMatrix, columns, addNames = NULL) {
  out <- do.call(cbind, lapply(1:ncol(columns), function(x)
    predMatrix * columns[, x]))
  if (!is.null(addNames)) {
    if (length(addNames) != ncol(columns)) {
      stop(simpleError("Names not same length as columns"))
    }
    colnames(out) <- sprintf("%s_%s", rep(addNames, each = ncol(
      predMatrix)),
      rep(colnames(predMatrix), length(addNames)))
  }
  return(out)
}

fitData <- as.matrix(integrationData[, !colnames(integrationData) %in
% notFitColumns])

fitData2 <- as.matrix(cbind(interact(fitData, sampleMatrix, colnames(
sampleMatrix)),
  fitData, sampleMatrix))

```

```
library(glmnet)

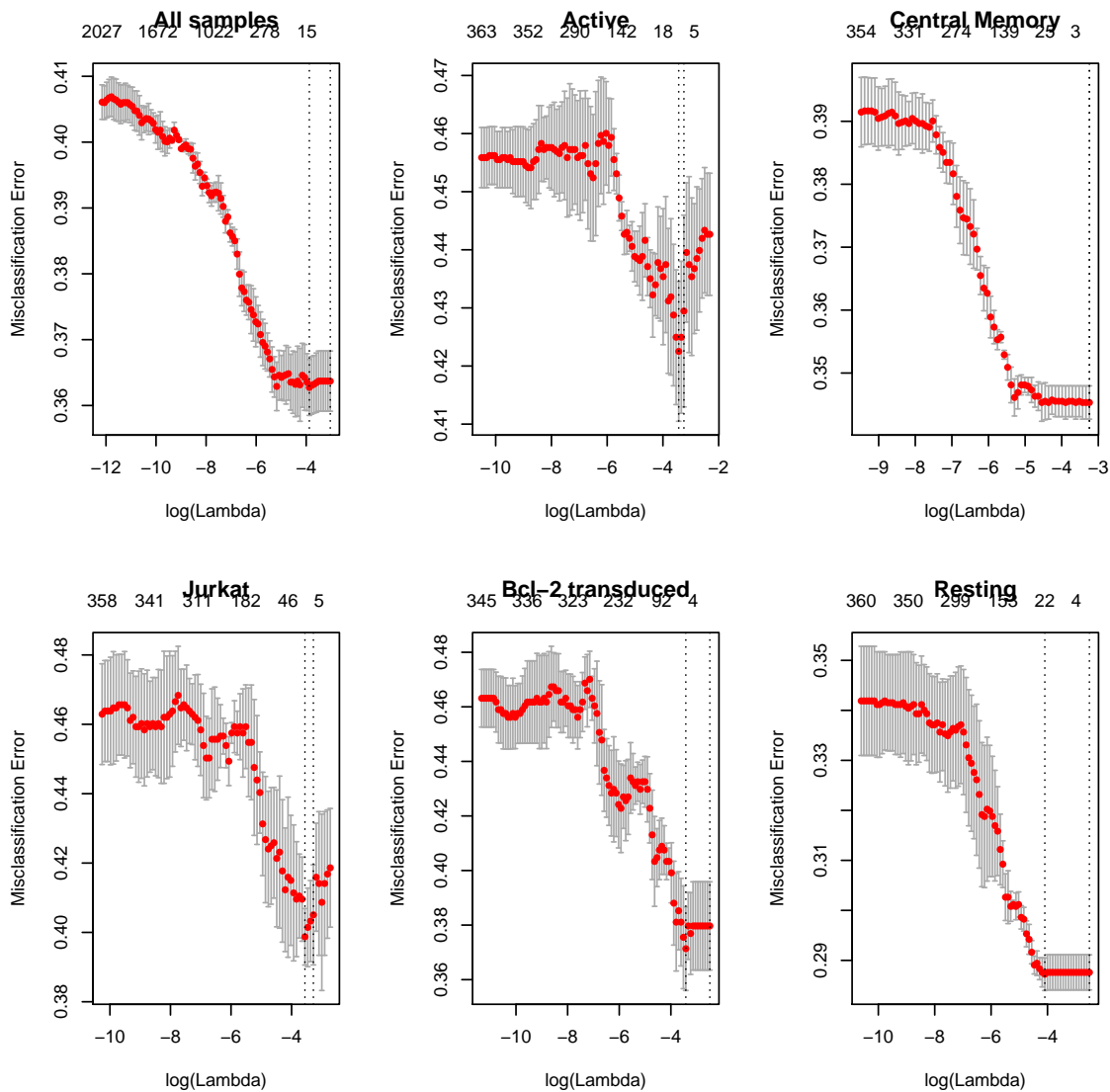
penalties <- rep(1, ncol(fitData2))

penalties[ncol(fitData2) - (ncol(sampleMatrix):1) + 1] <- 0

lassoFit <- cv.glmnet(fitData2, integrationData$isLatent, family = "
  binomial", type.measure = "class", nfolds = 3, penalty.factor =
  penalties)

seperateFits <- lapply(samples, function(x) cv.glmnet(fitData[
  integrationData$sample == x, ], integrationData$isLatent[
  integrationData$sample == x], family = "binomial", type.measure =
  "class", nfolds = 3))

names(seperateFits) <- samples
```



A.2.3 Correlation

We looked for correlation between the genomic variables and expression status of the proviruses.

```
corMat <- apply(fitData, 2, function(x) sapply(samples, function(y) {
  selector <- integrationData$sample == y
  if (sd(x[selector]) == 0)
```

```

        return(0)
        isLatent <- integrationData[selector, "isLatent"]
        cor(as.numeric(isLatent), x[selector], method = "spearman")
    )))

quantile(corMat, seq(0, 1, 0.1))

##           0%           10%           20%           30%
## -0.185223020 -0.081555830 -0.048938130 -0.030895834
##           40%           50%           60%           70%
## -0.018053321 -0.005613895  0.003580982  0.017822483
##           80%           90%           100%
##  0.036694554  0.062003356  0.170642314

```

If we looked for genomic variables consistently correlated or anti-correlated with proviral expression status with an FDR q-value less than 0.01, no variable was significantly correlated in more than 3 samples.

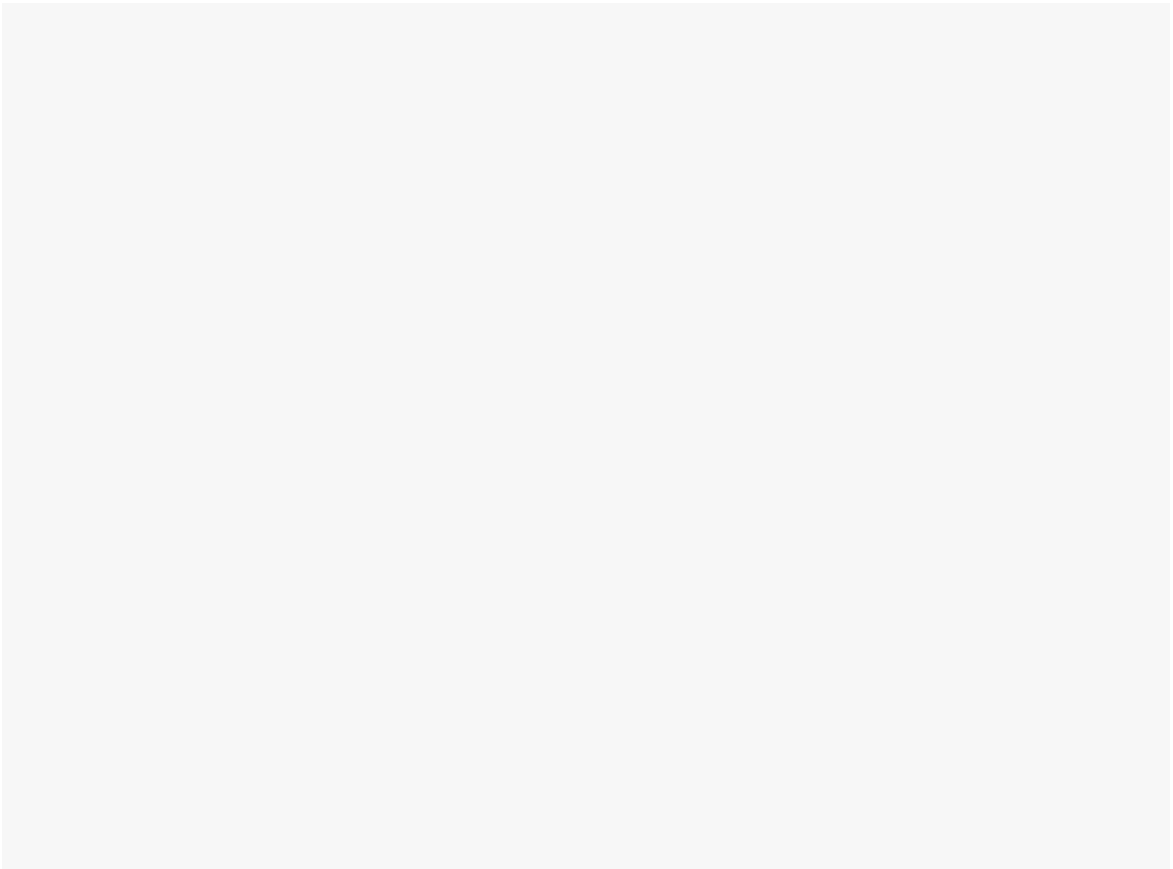
```

pMat <- apply(fitData, 2, function(x) sapply(samples, function(y) {
    selector <- integrationData$sample == y
    if (sd(x[selector]) == 0)
        return(NA)
    isLatent <- integrationData[selector, "isLatent"]
    cor.test(as.numeric(isLatent), x[selector], method = "spearman",
        exact = FALSE)$p.value
}))

adjustPMat <- pMat

adjustPMat[, ] <- p.adjust(pMat, "fdr")

```



A.2.4 RNA expression

We fit a logistic regression to a polynomial of log RNA-Seq reads within 5000 bases from Jurkat cells for the Jurkat sample and T cells for the rest.

```
rna <- ifelse(integrationData$sample == "Jurkat",  
             integrationData$log_jurkatRNA ,  
             integrationData$rna_5000)  
  
rna2 <- rna^2  
  
rna3 <- rna^3 #  
  
rna4 <- rna^4
```



```

glmData <- data.frame(isLatent = integrationData$isLatent, sample =
  integrationData$sample,
  rna, rna2, rna3, rna4)

glmMod <- glm(isLatent ~ sample * rna + sample * rna2 + sample *
  rna3 + sample * rna4, data = glmData, family = "binomial")

summary(glmMod)

##
## Call:
## glm(formula = isLatent ~ sample * rna + sample * rna2 + sample *
##     rna3 + sample * rna4, family = "binomial", data = glmData)
##
## Deviance Residuals:
##      Min       1Q   Median       3Q      Max
## -2.2899  -0.9864  -0.8676   1.0960   1.6007
##
## Coefficients:
##
##              Estimate Std. Error z value
## (Intercept)      1.7623655   0.2138859    8.240
## sampleBcl-2 transduced -2.1625912   0.7061524   -3.062
## sampleCentral Memory -2.5010063   0.2437685  -10.260
## sampleJurkat      -2.0800202   0.2836871   -7.332
## sampleResting      0.7840481   0.3312247    2.367
## rna               -0.6567268   0.2344422   -2.801
## rna2              0.1387703   0.0770589    1.801
## rna3             -0.0167219   0.0094076   -1.777
## rna4              0.0007572   0.0003845    1.969

```

```

## sampleBcl-2 transduced:rna      0.5750186  0.6366537  0.903
## sampleCentral Memory:rna      0.9067758  0.2750955  3.296
## sampleJurkat:rna              0.5294036  0.3867163  1.369
## sampleResting:rna             0.0366276  0.3436248  0.107
## sampleBcl-2 transduced:rna2   -0.0369353  0.1878816 -0.197
## sampleCentral Memory:rna2    -0.2106715  0.0915492 -2.301
## sampleJurkat:rna2            -0.0766215  0.1641153 -0.467
## sampleResting:rna2           -0.0760450  0.1086998 -0.700
## sampleBcl-2 transduced:rna3   0.0032503  0.0213743  0.152
## sampleCentral Memory:rna3    0.0237064  0.0112661  2.104
## sampleJurkat:rna3            0.0042183  0.0263910  0.160
## sampleResting:rna3           0.0153132  0.0128711  1.190
## sampleBcl-2 transduced:rna4  -0.0002532  0.0008267 -0.306
## sampleCentral Memory:rna4    -0.0009877  0.0004627 -2.135
## sampleJurkat:rna4            0.0001725  0.0014215  0.121
## sampleResting:rna4           -0.0008049  0.0005119 -1.572
##                                Pr(>|z|)
## (Intercept)                   < 2e-16 ***
## sampleBcl-2 transduced         0.00219 **
## sampleCentral Memory          < 2e-16 ***
## sampleJurkat                  2.27e-13 ***
## sampleResting                 0.01793 *
## rna                           0.00509 **
## rna2                           0.07173 .
## rna3                           0.07549 .
## rna4                           0.04891 *
## sampleBcl-2 transduced:rna    0.36643

```

```

## sampleCentral Memory:rna      0.00098 ***
## sampleJurkat:rna              0.17101
## sampleResting:rna            0.91511
## sampleBcl-2 transduced:rna2   0.84415
## sampleCentral Memory:rna2     0.02138 *
## sampleJurkat:rna2            0.64059
## sampleResting:rna2           0.48419
## sampleBcl-2 transduced:rna3   0.87913
## sampleCentral Memory:rna3     0.03536 *
## sampleJurkat:rna3            0.87301
## sampleResting:rna3           0.23415
## sampleBcl-2 transduced:rna4   0.75939
## sampleCentral Memory:rna4     0.03280 *
## sampleJurkat:rna4            0.90339
## sampleResting:rna4           0.11585
## ---
## Signif. codes:
## 0 '***' 0.001 '**' 0.01 '*' 0.05 '.' 0.1 ' ' 1
##
## (Dispersion parameter for binomial family taken to be 1)
##
##      Null deviance: 17240  on 12435  degrees of freedom
## Residual deviance: 15874  on 12411  degrees of freedom
## AIC: 15924
##
## Number of Fisher Scoring iterations: 4

```

A.2.5 Strand orientation

We used a Fisher's exact test to check if silent/inducible proviruses were enriched when integrated in the same strand orientation as cellular genes.

```
selector <- integrationData$inGene == 1

strandTable <- with(integrationData[selector, ], table(iffelse(
  isLatent, "Silent/Inducible", "Active"), iffelse(inGeneSameStrand
  == 1, "Same", "Diff"), sample))

apply(strandTable, 3, fisher.test)

## $Active
##
##      Fisher's Exact Test for Count Data
##
## data:  array(newX[, i], d.call, dn.call)
## p-value = 0.06061
## alternative hypothesis: true odds ratio is not equal to 1
## 95 percent confidence interval:
##  0.7219466 1.0081995
## sample estimates:
## odds ratio
##  0.8532127
##
##
## $`Bcl-2 transduced`
##
##      Fisher's Exact Test for Count Data
```

```

##
## data:  array(newX[, i], d.call, dn.call)
## p-value = 2.177e-05
## alternative hypothesis: true odds ratio is not equal to 1
## 95 percent confidence interval:
##  1.446896 2.872562
## sample estimates:
## odds ratio
##  2.036148
##
##
##  `$Central Memory`
##
##      Fisher's Exact Test for Count Data
##
## data:  array(newX[, i], d.call, dn.call)
## p-value = 0.2907
## alternative hypothesis: true odds ratio is not equal to 1
## 95 percent confidence interval:
##  0.9386167 1.2320238
## sample estimates:
## odds ratio
##  1.07529
##
##
##  $Jurkat
##

```

```

##      Fisher's Exact Test for Count Data
##
## data:  array(newX[, i], d.call, dn.call)
## p-value = 0.1674
## alternative hypothesis: true odds ratio is not equal to 1
## 95 percent confidence interval:
##  0.9207548 1.5699893
## sample estimates:
## odds ratio
##  1.202007
##
##
## $Resting
##
##      Fisher's Exact Test for Count Data
##
## data:  array(newX[, i], d.call, dn.call)
## p-value = 0.5732
## alternative hypothesis: true odds ratio is not equal to 1
## 95 percent confidence interval:
##  0.7825231 1.1405158
## sample estimates:
## odds ratio
##  0.9447415

```

A.2.6 Acetylation

To reduce correlation between acetylation marks, we generated the first ten principal components of the acetylation data and ran a logistic regression against them. We compared the cross validated performance of this regression with a base model only including which dataset the integration site came from. The cross-validation here has been reduced for efficiency but 480-fold cross-validation was used in the paper.

```
acetyl <- integrationData[, !grepl("logDist", colnames(
  integrationData)) & grepl("ac", colnames(integrationData))]

acetylPCA <- princomp(acetyl)

cumsum(acetylPCA$sdev[1:10]^2/sum(acetylPCA$sdev^2))

##      Comp.1      Comp.2      Comp.3      Comp.4      Comp.5      Comp.6
## 0.5947268 0.6786611 0.7267433 0.7610502 0.7833616 0.7964470
##      Comp.7      Comp.8      Comp.9      Comp.10
## 0.8093295 0.8215027 0.8299358 0.8372584

cv.glm <- function(model, K = nrow(thisData), subsets = NULL) {
  modelCall <- model$call
  thisData <- eval(modelCall$data)
  n <- nrow(thisData)
  if (is.null(subsets))
    subsets <- split(1:n, sample(rep(1:K, length.out = n)))
  preds <- lapply(subsets, function(outGroup) {
    subsetData <- thisData[-outGroup, , drop = FALSE]
    predData <- thisData[outGroup, , drop = FALSE]
    thisModel <- modelCall
    thisModel$data <- subsetData
```

```

        return(predict(eval(thisModel), predData))
    })
    pred <- unlist(preds)[order(unlist(subsets))]
    subsetId <- rep(1:K, sapply(subsets, length))[order(unlist(
        subsets))]
    return(data.frame(pred, subsetId))
}

inData <- data.frame(isLatent = integrationData$isLatent, sample = as
    .factor(integrationData$sample),
    acetylPCA$score[, 1:10])

modelPreds <- cv.glm(glm(isLatent ~ sample + Comp.1 + Comp.2 +
    Comp.3 + Comp.4 + Comp.5 + Comp.6 + Comp.7 + Comp.8 + Comp.9 +
    Comp.10, family = "binomial", data = inData), K = 5)

basePreds <- cv.glm(glm(isLatent ~ sample, family = "binomial",
    data = inData), subsets = split(1:nrow(inData),
    modelPreds$subsetId),
    K = 5)

modelCorrect <- sum((modelPreds$pred > 0) == integrationData$isLatent
    )
baseCorrect <- sum((basePreds$pred > 0) == integrationData$isLatent)

prop.test(c(baseCorrect, modelCorrect), rep(nrow(integrationData),
    2))

##
##      2-sample test for equality of proportions with

```



```
##      continuity correction
##
## data:  c(baseCorrect, modelCorrect) out of rep(nrow(
      integrationData), 2)
## X-squared = 0.00017372, df = 1, p-value = 0.9895
## alternative hypothesis: two.sided
## 95 percent confidence interval:
##  -0.01187726  0.01219890
## sample estimates:
##      prop 1      prop 2
## 0.6362978 0.6361370
```

A.2.7 Gene deserts

We used Fisher's exact test to look for an association between integration outside a gene and proviral expression status.

```
geneTable <- table(integrationData$isLatent, integrationData$inGene,
      integrationData$sample)
apply(geneTable, 3, fisher.test)

## $Active
##
##      Fisher's Exact Test for Count Data
##
## data:  array(newX[, i], d.call, dn.call)
## p-value < 2.2e-16
## alternative hypothesis: true odds ratio is not equal to 1
## 95 percent confidence interval:
```

```

## 0.3629548 0.5446204
## sample estimates:
## odds ratio
## 0.4452621
##
##
## $`Bcl-2 transduced`
##
##      Fisher's Exact Test for Count Data
##
## data:  array(newX[, i], d.call, dn.call)
## p-value = 0.1052
## alternative hypothesis: true odds ratio is not equal to 1
## 95 percent confidence interval:
## 0.9203418 2.3478599
## sample estimates:
## odds ratio
## 1.472224
##
##
## $`Central Memory`
##
##      Fisher's Exact Test for Count Data
##
## data:  array(newX[, i], d.call, dn.call)
## p-value = 0.7803
## alternative hypothesis: true odds ratio is not equal to 1

```

```

## 95 percent confidence interval:
## 0.8525329 1.1253952
## sample estimates:
## odds ratio
## 0.9791165
##
##
## $Jurkat
##
##      Fisher's Exact Test for Count Data
##
## data:  array(newX[, i], d.call, dn.call)
## p-value = 0.5443
## alternative hypothesis: true odds ratio is not equal to 1
## 95 percent confidence interval:
## 0.7909269 1.6167285
## sample estimates:
## odds ratio
## 1.127836
##
##
## $Resting
##
##      Fisher's Exact Test for Count Data
##
## data:  array(newX[, i], d.call, dn.call)
## p-value = 3.071e-08

```

```
## alternative hypothesis: true odds ratio is not equal to 1
## 95 percent confidence interval:
##  0.4384828 0.6864112
## sample estimates:
## odds ratio
##  0.5500205
```

We used a two-sample t-test to investigate whether there was a significant difference in distance to the nearest gene between expressed and silent/inducible proviruses integrated outside genes.

```
geneDistData <- integrationData[!integrationData$inGene, c("isLatent
", "logDist_nearest", "sample")]

by(geneDistData, geneDistData$sample, function(x) t.test(
  logDist_nearest ~ isLatent, data = x))

## geneDistData$sample: Active
##
##      Welch Two Sample t-test
##
## data:  logDist_nearest by isLatent
## t = -2.4539, df = 287.73, p-value = 0.01472
## alternative hypothesis: true difference in means is not equal to 0
## 95 percent confidence interval:
##  -0.80738340 -0.08867607
## sample estimates:
## mean in group FALSE  mean in group TRUE
##           9.608737           10.056767
```

```

##
## -----
## geneDistData$sample: Bcl-2 transduced
##
##      Welch Two Sample t-test
##
## data:  logDist_nearest by isLatent
## t = 0.40978, df = 86.2, p-value = 0.683
## alternative hypothesis: true difference in means is not equal to 0
## 95 percent confidence interval:
##  -0.6309351  0.9586004
## sample estimates:
## mean in group FALSE  mean in group TRUE
##           9.036872           8.873039
##
## -----
## geneDistData$sample: Central Memory
##
##      Welch Two Sample t-test
##
## data:  logDist_nearest by isLatent
## t = -0.07188, df = 861.61, p-value = 0.9427
## alternative hypothesis: true difference in means is not equal to 0
## 95 percent confidence interval:
##  -0.2371374  0.2203819
## sample estimates:
## mean in group FALSE  mean in group TRUE

```

```

##           10.19225           10.20063
##
## -----
## geneDistData$sample: Jurkat
##
##           Welch Two Sample t-test
##
## data:  logDist_nearest by isLatent
## t = -1.8217, df = 139.56, p-value = 0.07064
## alternative hypothesis: true difference in means is not equal to 0
## 95 percent confidence interval:
##  -1.26342086  0.05167979
## sample estimates:
## mean in group FALSE  mean in group TRUE
##           9.925782           10.531652
##
## -----
## geneDistData$sample: Resting
##
##           Welch Two Sample t-test
##
## data:  logDist_nearest by isLatent
## t = -5.1275, df = 193.49, p-value = 7.096e-07
## alternative hypothesis: true difference in means is not equal to 0
## 95 percent confidence interval:
##  -1.2687917 -0.5638568
## sample estimates:

```

```
## mean in group FALSE mean in group TRUE
##          9.489931          10.406255
```

To check for a relationship between silent/inducible status and distance to CpG islands, we used a two sample t-test on the logged distance and saw a significant difference between silent/inducible and expressed proviruses (before accounting for a correlation between being near CpG islands and in genes)

```
t.test(integrationData$logDist_cpg ~ integrationData$isLatent)

##
##      Welch Two Sample t-test
##
## data:  integrationData$logDist_cpg by integrationData$isLatent
## t = -2.0233, df = 12381, p-value = 0.04306
## alternative hypothesis: true difference in means is not equal to 0
## 95 percent confidence interval:
##  -0.105657514 -0.001675563
## sample estimates:
## mean in group FALSE mean in group TRUE
##          10.16362          10.21728

sapply(unique(integrationData$sample), function(x) with(
  integrationData[integrationData$sample ==
    x, ], p.adjust(t.test(logDist_cpg ~ isLatent)$p.value, method = "
    bonferroni",
    n = 5)))

##          Active      Central Memory          Jurkat
```

```
##      0.512040457      1.000000000      1.000000000
## Bcl-2 transduced      Resting
##      1.000000000      0.005866539
```

Many CpG islands are found near genes. To account for this relationship, we used an ANOVA test including whether the integration site was inside a gene prior to including CpG islands. After including integration inside genes, CpG islands were not significantly associated with silent/inducible status of the proviruses with all samples grouped or individually after Bonferonni correction for multiple comparisons.

```
anova(with(integrationData, glm(isLatent ~ I(logDist_nearest == 0) +
  logDist_cpg, family = "binomial")), test = "Chisq")

## Analysis of Deviance Table
##
## Model: binomial, link: logit
##
## Response: isLatent
##
## Terms added sequentially (first to last)
##
##
##              Df Deviance Resid. Df Resid. Dev
## NULL                    12435      17240
## I(logDist_nearest == 0)  1  26.2682   12434      17213
## logDist_cpg              1   1.1328   12433      17212
##
##              Pr(>Chi)
## NULL
```



```
## I(logDist_nearest == 0) 2.971e-07 ***
## logDist_cpg                0.2872
## ---
## Signif. codes:
## 0 '***' 0.001 '**' 0.01 '*' 0.05 '.' 0.1 ' ' 1

sapply(unique(integrationData$sample), function(x) {
  p.adjust(anova(with(integrationData[integrationData$sample == x,
    ], glm(isLatent ~ I(logDist_nearest == 0) + logDist_cpg,
    family = "binomial"))), test = "Chisq")["logDist_cpg", "Pr(>Chi
    )"], method = "bonferroni", n = 5)
})

##           Active      Central Memory           Jurkat
##           1.0000000           1.0000000           1.0000000
## Bcl-2 transduced           Resting
##           1.0000000           0.2007788
```

A.2.8 Alphoid repeats

When analyzing repetitive elements, we treated each read as an independent observation and included reads with multiple alignments to the genome. Additional File 3 is a gzipped csv file containing a row for each read with multiple alignments and one row for each dereplicated integration site with a single alignment with the count variable indicating the number of reads dereplicated to that integration site. There should be 26,190 rows (excluding header) with 14,494 rows of expressed provirus and 11,696 rows of silent/inducible provirus.

```
repeats <- read.csv("AdditionalFile3.csv.gz", check.names = FALSE,
  stringsAsFactors = FALSE)
```

To analyze whether there was an association between proviral expression status and integration within alphoid repeats, we used Fisher's exact test with a Bonferroni correction for five samples. For comparison, we looked at the association between proviral expression and the other repeats in the RepeatMasker database. We did not Bonferroni correct for the multiple repeat types so that the repeats could be compared with the analysis of alphoid repeats (for which we had an a priori hypothesis for an association with latency).

```
dummyX <- rep(c(TRUE, FALSE), 2)

dummyY <- rep(c(TRUE, FALSE), each = 2)

repeatData <- repeats[, !colnames(repeats) %in% notRepeatColumns]

repeatData <- repeatData[, apply(repeatData, 2, sum) > 0]

testRepeats <- function(x, repeats) {
  sapply(samples, function(thisSample, repeats) {
    selector <- repeats$sample == thisSample
    repLatent <- rep(repeats$isLatent[selector], repeats$count[
      selector])
    repRepeat <- rep(x[selector], repeats$count[selector])
```

```

        fisher.test(table(c(dummyX, repLatent), c(dummyY, repRepeat))
          - 1)$p.value
      }, repeats)
}

repeatPs <- apply(repeatData, 2, testRepeats, repeats[,
  notRepeatColumns])

table(apply(repeatPs * 5 < 0.05, 2, sum))

##
##  0  1  2  3
## 611 76 15  1

which(apply(repeatPs * 5 < 0.05, 2, sum) >= 3)

## ALR/Alpha
##      178

p.adjust(repeatPs[, "ALR/Alpha"], "bonferroni")

##           Active      Central Memory           Jurkat
## 5.026890e-02  3.940207e-03  1.027189e-08
## Bcl-2 transduced           Resting
## 1.000000e+00  2.424896e-02

```

A.2.9 Neighbors

We looked at all pairs of viruses on the same chromosome separated by no more than a given distance, e.g. 100 bases, either with all samples pooled or split between within sample pairs or between sample pairs.

```

allNeighbors <- data.frame(id1 = 0, id2 = 0)[0, ]

ids <- 1:nrow(integrationData)

for (chr in unique(integrationData$chr)) {
  chrSelector <- integrationData$chr == chr
  neighborPairs <- data.frame(id1 = rep(ids[chrSelector], sum(
    chrSelector)),
    id2 = rep(ids[chrSelector], each = sum(chrSelector)))
  neighborPairs <- neighborPairs[neighborPairs$id1 <
    neighborPairs$id2, ]
  allNeighbors <- rbind(allNeighbors, neighborPairs)
}

allNeighbors$dist <- abs(integrationData$pos[allNeighbors$id1] -
  integrationData$pos[allNeighbors$id2])

allNeighbors$latent1 <- integrationData$isLatent[allNeighbors$id1]

allNeighbors$latent2 <- integrationData$isLatent[allNeighbors$id2]

allNeighbors$sample1 <- integrationData$sample[allNeighbors$id1]

allNeighbors$sample2 <- integrationData$sample[allNeighbors$id2]

allNeighbors <- allNeighbors[allNeighbors$dist <= 1e+06, ]

```

The expected number of matching pairs was calculated as $\sum_{j \in \text{samples}} n_{j,d}(\theta_{j,d}\theta_{-j,d} + (1 - \theta_{j,d})(1 - \theta_{-j,d}))$ for between sample, $\sum_{j \in \text{samples}} n_{j,d}(\theta_{j,d}^2 + (1 - \theta_{j,d})^2)$ for within sample and $n_d(\theta_d^2 + (1 - \theta_d)^2)$ for all pairs, where $n_{j,d}$ is the number of pairs of proviruses separated by no more than d base pairs where the first provirus is from sample j , $\theta_{j,d}$ is the proportion of

silent/inducible proviruses in sample j appearing in at least one pair of proviruses separated by less than d base pairs and $\neg j$ means all samples except sample j .

```
dists <- unique(round(10^seq(1, 6, 1)))

pairings <- do.call(rbind, lapply(dists, function(x, allNeighbors) {
  inSelector <- allNeighbors$dist <= x & allNeighbors$sample1 ==
    allNeighbors$sample2
  outSelector <- allNeighbors$dist <= x & allNeighbors$sample1 !=
    allNeighbors$sample2
  allSelector <- allNeighbors$dist <= x
  out <- data.frame(dist = x, observedIn = sum(allNeighbors[
    inSelector, "latent1"] == allNeighbors[inSelector, "latent2"])
    , observedOut = sum(allNeighbors[outSelector,
    "latent1"] == allNeighbors[outSelector, "latent2"]),
    observedAll = sum(allNeighbors[allSelector, "latent1"] ==
    allNeighbors[allSelector, "latent2"]), totalIn = sum(
    inSelector),
    totalOut = sum(outSelector), totalAll = sum(allSelector))
  out$expectedIn <- sum(with(allNeighbors[inSelector, ], sapply(
    samples,
    function(x) {
      inLatent <- c(latent1[sample1 == x], latent2[sample2 ==
        x])[!duplicated(c(id1[sample1 == x], id2[sample2 ==
        x]))]
      if (length(inLatent) == 0) return(0)
      return(sum(sample1 == x) * (mean(inLatent)^2 + mean(!
        inLatent)^2))
    })))
}))
```

```

out$expectedOut <- sum(with(allNeighbors[outSelector, ],
  sapply(samples, function(x) {
    inLatent <- c(latent1[sample1 == x], latent2[sample2 ==
      x])![duplicated(c(id1[sample1 == x], id2[sample2 ==
      x]))]
    outLatent <- c(latent1[sample1 != x], latent2[sample2 !=
      x])![duplicated(c(id1[sample1 != x], id2[sample2 !=
      x]))]
    if (length(inLatent) == 0) return(0)
    return(sum(sample1 == x) * (mean(inLatent) * mean(
      outLatent) +
      mean(!inLatent) * mean(!outLatent)))
  })))
out$expectedAll <- sum(with(allNeighbors[allSelector, ],
  {
    allLatent <- c(latent1, latent2)[!duplicated(c(id1,
      id2))]
    return(length(latent1) * (mean(allLatent)^2 + mean(!
      allLatent)^2))
  })
  return(out)
}, allNeighbors))

rownames(pairings) <- pairings$dist

```

To look for more matches than expected by random pairing between neighboring proviruses, we used a one sample Z-test of proportion to compare the observed number of matching pairs with the expected proportion of pairs.

```

combinations <- c(All = "All", `Between sample` = "Out", `Within
  sample` = "In")

lapply(combinations, function(x, pairing) {
  vars <- sprintf(c("observed%s", "expected%s", "total%s"), x)
  expectedProb <- pairing[, vars[2]]/pairing[, vars[3]]
  prop.test(pairing[, vars[1]], pairing[, vars[3]], p =
    expectedProb)
}, pairings["100", ])

## $All
##
##      1-sample proportions test with continuity correction
##
## data:  pairing[, vars[1]] out of pairing[, vars[3]], null
  probability expectedProb
## X-squared = 13.002, df = 1, p-value = 0.0003111
## alternative hypothesis: true p is not equal to 0.5000141
## 95 percent confidence interval:
##  0.5586837 0.6962353
## sample estimates:
##      p
## 0.63
##
##
## $`Between sample`
##
##      1-sample proportions test with continuity correction
##

```

```

## data:  pairing[, vars[1]] out of pairing[, vars[3]], null
      probability expectedProb
## X-squared = 0.21919, df = 1, p-value = 0.6397
## alternative hypothesis: true p is not equal to 0.4836763
## 95 percent confidence interval:
##  0.3570532 0.5572662
## sample estimates:
##           p
## 0.4554455
##
##
## $`Within sample`
##
##      1-sample proportions test with continuity correction
##
## data:  pairing[, vars[1]] out of pairing[, vars[3]], null
      probability expectedProb
## X-squared = 24.446, df = 1, p-value = 7.644e-07
## alternative hypothesis: true p is not equal to 0.5561437
## 95 percent confidence interval:
##  0.7140170 0.8776751
## sample estimates:
##           p
## 0.8080808

```


A.2.10 Compiling this document

This document was generated using R's Sweave function (<http://en.wikipedia.org/wiki/Sweave>). If you would like to regenerate this document, download Additional Files 2, 3 and 4 from Sherrill-Mix et al.³⁶⁶ and make sure the files are all in the same directory and named AdditionalFile2.csv.gz, AdditionalFile3.csv.gz and AdditionalFile4.Rnw. Then compile by going to that directory and using the commands:

```
R CMD Sweave AdditionalFile4.Rnw  
pdflatex AdditionalFile4.tex
```

Note that you will need R and L^AT_EX (and the R package glmnet if you would like to rerun the lasso regressions) installed.

BIBLIOGRAPHY

- [1] MS Gottlieb, HM Schanker, PT Fan, A Saxon, JD Weisman and I Pozalski. 1981. Pneumocystis pneumonia—Los Angeles. *MMWR Morb Mortal Wkly Rep*, 30:250–252
- [2] A Friedman-Kien, L Laubenstein, M Marmor, K Hymes, J Green, A Ragaz, J Gottlieb, F Muggia, R Demopoulos and M Weintraub. 1981. Kaposi's sarcoma and Pneumocystis pneumonia among homosexual men—New York City and California. *MMWR Morb Mortal Wkly Rep*, 30:305–308
- [3] KB Hymes, T Cheung, JB Greene, NS Prose, A Marcus, H Ballard, DC William and LJ Laubenstein. 1981. Kaposi's sarcoma in homosexual men—a report of eight cases. *Lancet*, 2:598–600. doi: 10.1016/S0140-6736(81)92740-9
- [4] H Masur, MA Michelis, JB Greene, I Onorato, RA Stouwe, RS Holzman, G Wormser, L Brettman, M Lange et al. 1981. An outbreak of community-acquired Pneumocystis carinii pneumonia: initial manifestation of cellular immune dysfunction. *N Engl J Med*, 305:1431–1438. doi: 10.1056/NEJM198112103052402
- [5] FP Siegal, C Lopez, GS Hammer, AE Brown, SJ Kornfeld, J Gold, J Hassett, SZ Hirschman, C Cunningham-Rundles and BR Adelsberg. 1981. Severe acquired immunodeficiency in male homosexuals, manifested by chronic perianal ulcerative herpes simplex lesion. *N Engl J Med*, 305:1439–1444. doi: 10.1056/NEJM198112103052403
- [6] MS Gottlieb, R Schroff, HM Schanker, JD Weisman, PT Fan, RA Wolf and A Saxon. 1981. Pneumocystis carinii pneumonia and mucosal candidiasis in previously healthy homosexual men: evidence of a new acquired cellular immunodeficiency. *N Engl J Med*, 305:1425–1431. doi: 10.1056/NEJM198112103052401
- [7] Y Laor and RA Schwartz. 1979. Epidemiologic aspects of American Kaposi's sarcoma. *J Surg Oncol*, 12:299–303. doi: 10.1002/jso.2930120403
- [8] MB Klein, FA Pereira and I Kantor. 1974. Kaposi Sarcoma complicating systemic lupus erythematosus treated with immunosuppression. *Arch Dermatol*, 110:602–604. doi: 10.1001/archderm.1974.01630100058014
- [9] BD Myers, E Kessler, J Levi, A Pick, JB Rosenfeld and P Tikvah. 1974. Kaposi sarcoma in kidney transplant recipients. *Arch Intern Med*, 133:307–311. doi: 10.1001/archinte.1974.00320140145017
- [10] SB Kapadia and JR Krause. 1977. Kaposi's sarcoma after long-term alkylating agent therapy for multiple myeloma. *South Med J*, 70:1011–1013
- [11] B Safai and RA Good. 1981. Kaposi's sarcoma: a review and recent developments. *CA Cancer J Clin*, 31:2–12. doi: 10.3322/canjclin.31.1.2

- [12] Y Chang, E Cesarman, MS Pessin, F Lee, J Culpepper, DM Knowles and PS Moore. 1994. Identification of herpesvirus-like DNA sequences in AIDS-associated Kaposi's sarcoma. *Science*, 266:1865–1869. doi: 10.1126/science.7997879
- [13] F Sitas, H Carrara, V Beral, R Newton, G Reeves, D Bull, U Jentsch, R Pacella-Norman, D Bourboulia et al. 1999. Antibodies against human herpesvirus 8 in black South African patients with cancer. *N Engl J Med*, 340:1863–1871. doi: 10.1056/NEJM199906173402403
- [14] BA Burke and RA Good. 1973. Pneumocystis carinii infection. *Medicine (Baltimore)*, 52:23–51
- [15] WT Hughes. 1977. Pneumocystis carinii pneumonia. *N Engl J Med*, 297:1381–1383. doi: 10.1056/NEJM197712222972505
- [16] J Gerstoft, A Malchow-Møller, I Bygbjerg, E Dickmeiss, C Enk, P Halberg, S Haahr, M Jacobsen, K Jensen et al. 1982. Severe acquired immunodeficiency in European homosexual men. *Br Med J (Clin Res Ed)*, 285:17–19
- [17] H Masur, MA Michelis, GP Wormser, S Lewin, J Gold, ML Tapper, J Giron, CW Lerner, D Armstrong et al. 1982. Opportunistic infection in previously healthy women. Initial manifestations of a community-acquired cellular immunodeficiency. *Ann Intern Med*, 97:533–539
- [18] A Ammann, M Cowan, D Wara, H Goldman, H Perkins, R Lanzerotti, J Gullett, A Duff, S Dritz and J Chin. 1982. Possible transfusion-associated acquired immune deficiency syndrome (AIDS) — California. *MMWR Morb Mortal Wkly Rep*, 31:652–654
- [19] N Ehrenkranz, J Rubini, R Gunn, C Horsburgh, T Collins, U Hasiba, W Hathaway, W Doig, R Hopkins and J Elliott. 1982. Pneumocystis carinii pneumonia among persons with hemophilia A. *MMWR Morb Mortal Wkly Rep*, 31:365–367
- [20] MC Poon, A Landay, J Alexander, W Birch, M Eyster, H Al-Mondhiry, J Ballard, E Witte, C Hayes et al. 1982. Update on acquired immune deficiency syndrome (AIDS) among patients with hemophilia A. *MMWR Morb Mortal Wkly Rep*, 31:644–6, 652
- [21] JB Greene, GS Sidhu, S Lewin, JF Levine, H Masur, MS Simberkoff, P Nicholas, RC Good, SB Zolla-Pazner et al. 1982. Mycobacterium avium-intracellulare: a cause of disseminated life-threatening infection in homosexuals and drug abusers. *Ann Intern Med*, 97:539–546
- [22] R O'Reilly, D Kirkpatrick, CB Small, R Klein, H Keltz, G Friedland, K Bromberg, S Fikrig, H Mendez et al. 1982. Unexplained immunodeficiency and opportunistic infections in infants—New York, New Jersey, California. *MMWR Morb Mortal Wkly Rep*, 31:665–667
- [23] S Fannin, M Gottlieb, J Weisman, E Rogolsky, T Prendergast, J Chin, A Friedman-

- Kien, L Laubenstein, S Friedman and R Rothenberg. 1982. A cluster of Kaposi's sarcoma and *Pneumocystis carinii* pneumonia among homosexual male residents of Los Angeles and Orange Counties, California. *MMWR Morb Mortal Wkly Rep*, 31: 305–307
- [24] C Harris, CB Small, G Friedland, R Klein, B Moll, E Emeson, I Spigland, N Steigbigel, R Reiss et al. 1983. Immunodeficiency among female sexual partners of males with acquired immune deficiency syndrome (AIDS) — New York. *MMWR Morb Mortal Wkly Rep*, 31:697–698
- [25] F Barré-Sinoussi, JC Chermann, F Rey, MT Nugeyre, S Chamaret, J Gruest, C Dautoguet, C Axler-Blin, F Vézinet-Brun et al. 1983. Isolation of a T-lymphotropic retrovirus from a patient at risk for acquired immune deficiency syndrome (AIDS). *Science*, 220: 868–871
- [26] RC Gallo, PS Sarin, EP Gelmann, M Robert-Guroff, E Richardson, VS Kalyanaraman, D Mann, GD Sidhu, RE Stahl et al. 1983. Isolation of human T-cell leukemia virus in acquired immune deficiency syndrome (AIDS). *Science*, 220:865–867. doi: 10.1126/science.6601823
- [27] M Popovic, MG Sarngadharan, E Read and RC Gallo. 1984. Detection, isolation, and continuous production of cytopathic retroviruses (HTLV-III) from patients with AIDS and pre-AIDS. *Science*, 224:497–500. doi: 10.1126/science.6200935
- [28] JA Levy, AD Hoffman, SM Kramer, JA Landis, JM Shimabukuro and LS Oshiro. 1984. Isolation of lymphocytopathic retroviruses from San Francisco patients with AIDS. *Science*, 225:840–842. doi: 10.1126/science.6206563
- [29] RC Gallo, SZ Salahuddin, M Popovic, GM Shearer, M Kaplan, BF Haynes, TJ Palker, R Redfield, J Oleske and B Safai. 1984. Frequent detection and isolation of cytopathic retroviruses (HTLV-III) from patients with AIDS and at risk for AIDS. *Science*, 224: 500–503. doi: 10.1126/science.6200936
- [30] MG Sarngadharan, M Popovic, L Bruch, J Schüpbach and RC Gallo. 1984. Antibodies reactive with human T-lymphotropic retroviruses (HTLV-III) in the serum of patients with AIDS. *Science*, 224:506–508. doi: 10.1126/science.6324345
- [31] B Safai, MG Sarngadharan, JE Groopman, K Arnett, M Popovic, A Sliski, J Schüpbach and RC Gallo. 1984. Seroepidemiological studies of human T-lymphotropic retrovirus type III in acquired immunodeficiency syndrome. *Lancet*, 1:1438–1440. doi: 10.1016/S0140-6736(84)91933-0
- [32] N Clumeck, F Mascart-Lemone, J de Maubeuge, D Brenez and L Marcelis. 1983. Acquired immune deficiency syndrome in Black Africans. *Lancet*, 1:642. doi: 10.1016/S0140-6736(83)91808-1
- [33] N Clumeck, J Sonnet, H Taelman, S Cran and P Henrivaux. 1984. Acquired immune

- deficiency syndrome in Belgium and its relation to Central Africa. *Ann N Y Acad Sci*, 437:264–269. doi: 10.1111/j.1749-6632.1984.tb37144.x
- [34] P Van de Perre, D Rouvroy, P Lepage, J Bogaerts, P Kestelyn, J Kayihigi, AC Hekker, JP Butzler and N Clumeck. 1984. Acquired immunodeficiency syndrome in Rwanda. *Lancet*, 2:62–65. doi: 10.1016/S0140-6736(84)90240-X
- [35] P Piot, TC Quinn, H Taelman, FM Feinsod, KB Minlangu, O Wobin, N Mbendi, P Mazebo, K Ndangi and W Stevens. 1984. Acquired immunodeficiency syndrome in a heterosexual population in Zaire. *Lancet*, 2:65–69. doi: 10.1016/S0140-6736(84)90241-1
- [36] JN Nkengasong, W Janssens, L Heyndrickx, K Fransen, PM Ndumbe, J Motte, A Leonaers, M Ngolle, J Ayuk and P Piot. 1994. Genotypic subtypes of HIV-1 in Cameroon. *AIDS*, 8:1405–1412
- [37] J Louwagie, W Janssens, J Mascola, L Heyndrickx, P Hegerich, G van der Groen, FE McCutchan and DS Burke. 1995. Genetic diversity of the envelope glycoprotein from human immunodeficiency virus type 1 isolates of African origin. *J Virol*, 69: 263–271
- [38] N Vidal, M Peeters, C Mulanga-Kabeya, N Nzilambi, D Robertson, W Ilunga, H Sema, K Tshimanga, B Bongo and E Delaporte. 2000. Unprecedented degree of human immunodeficiency virus type 1 (HIV-1) group M genetic diversity in the Democratic Republic of Congo suggests that the HIV-1 pandemic originated in Central Africa. *J Virol*, 74:10498–10507. doi: 10.1128/JVI.74.22.10498-10507.2000
- [39] A Rambaut, DL Robertson, OG Pybus, M Peeters and EC Holmes. 2001. Human immunodeficiency virus. Phylogeny and the origin of HIV-1. *Nature*, 410:1047–1048. doi: 10.1038/35074179
- [40] C Yang, B Dash, SL Hanna, HS Frances, N Nzilambi, RC Colebunders, M St Louis, TC Quinn, TM Folks and RB Lal. 2001. Predominance of HIV type 1 subtype G among commercial sex workers from Kinshasa, Democratic Republic of Congo. *AIDS Res Hum Retroviruses*, 17:361–365. doi: 10.1089/08892220150503726
- [41] ML Kalish, KE Robbins, D Pieniazek, A Schaefer, N Nzilambi, TC Quinn, ME St Louis, AS Youngpairoj, J Phillips et al. 2004. Recombinant viruses and early global HIV-1 epidemic. *Emerg Infect Dis*, 10:1227–1234. doi: 10.3201/eid1007.030904
- [42] SS Frøland, P Jenum, CF Lindboe, KW Wefring, PJ Linnestad and T Böhmer. 1988. HIV-1 infection in Norwegian family before 1970. *Lancet*, 1:1344–1345. doi: 10.1016/S0140-6736(88)92164-2
- [43] RF Garry, MH Witte, AA Gottlieb, M Elvin-Lewis, MS Gottlieb, CL Witte, SS Alexander, WR Cole and W Drake, Jr. 1988. Documentation of an AIDS virus infection in the United States in 1968. *JAMA*, 260:2085–2087. doi: 10.1001/jama.1988.03410140097031

- [44] IC Bygbjerg. 1983. AIDS in a Danish surgeon (Zaire, 1976). *Lancet*, 1:925. doi: 10.1016/S0140-6736(83)91348-X
- [45] J Vandepitte, R Verwilghen and P Zachee. 1983. AIDS and cryptococcosis (Zaire, 1977). *Lancet*, 1:925–926. doi: 10.1016/S0140-6736(83)91349-1
- [46] AJ Nahmias, J Weiss, X Yao, F Lee, R Kodosi, M Schanfield, T Matthews, D Bolognesi, D Durack and A Motulsky. 1986. Evidence for human infection with an HTLV III/LAV-like virus in Central Africa, 1959. *Lancet*, 1:1279–1280. doi: 10.1016/S0140-6736(86)91422-4
- [47] T Zhu, BT Korber, AJ Nahmias, E Hooper, PM Sharp and DD Ho. 1998. An African HIV-1 sequence from 1959 and implications for the origin of the epidemic. *Nature*, 391:594–597. doi: 10.1038/35400
- [48] M Worobey, M Gemmel, DE Teuwen, T Haselkorn, K Kunstman, M Bunce, JJ Muyembe, JMM Kabongo, RM Kalengayi et al. 2008. Direct evidence of extensive diversity of HIV-1 in Kinshasa by 1960. *Nature*, 455:661–664. doi: 10.1038/nature07390
- [49] B Korber, M Muldoon, J Theiler, F Gao, R Gupta, A Lapedes, BH Hahn, S Wolinsky and T Bhattacharya. 2000. Timing the ancestor of the HIV-1 pandemic strains. *Science*, 288:1789–1796. doi: 10.1126/science.288.5472.1789
- [50] M Salemi, K Strimmer, WW Hall, M Duffy, E Delaporte, S Mboup, M Peeters and AM Vandamme. 2001. Dating the common ancestor of SIVcpz and HIV-1 group M and the origin of HIV-1 subtypes using a new method to uncover clock-like molecular evolution. *FASEB J*, 15:276–278. doi: 10.1096/fj.00-0449fje
- [51] PM Sharp, E Bailes, RR Chaudhuri, CM Rodenburg, MO Santiago and BH Hahn. 2001. The origins of acquired immune deficiency syndrome viruses: where and when? *Philos Trans R Soc Lond B Biol Sci*, 356:867–876. doi: 10.1098/rstb.2001.0863
- [52] K Yusim, M Peeters, OG Pybus, T Bhattacharya, E Delaporte, C Mulanga, M Muldoon, J Theiler and B Korber. 2001. Using human immunodeficiency virus type 1 sequences to infer historical features of the acquired immune deficiency syndrome epidemic and human immunodeficiency virus evolution. *Philos Trans R Soc Lond B Biol Sci*, 356: 855–866. doi: 10.1098/rstb.2001.0859
- [53] NR Faria, A Rambaut, MA Suchard, G Baele, T Bedford, MJ Ward, AJ Tatem, JD Sousa, N Arinaminpathy et al. 2014. The early spread and epidemic ignition of HIV-1 in human populations. *Science*, 346:56–61. doi: 10.1126/science.1256739
- [54] MD Daniel, NL Letvin, NW King, M Kannagi, PK Sehgal, RD Hunt, PJ Kanki, M Essex and RC Desrosiers. 1985. Isolation of T-cell tropic HTLV-III-like retrovirus from macaques. *Science*, 228:1201–1204. doi: 10.1126/science.3159089
- [55] M Peeters, C Honoré, T Huet, L Bedjabaga, S Ossari, P Bussi, RW Cooper and

- E Delaporte. 1989. Isolation and partial characterization of an HIV-related virus occurring naturally in chimpanzees in Gabon. *AIDS*, 3:625–630
- [56] M Peeters, V Courgnaud and B Abela. 2001. Genetic diversity of lentiviruses in non-human primates. *AIDS Rev*, 3:3–10
- [57] T Huet, R Cheynier, A Meyerhans, G Roelants and S Wain-Hobson. 1990. Genetic organization of a chimpanzee lentivirus related to HIV-1. *Nature*, 345:356–359. doi: 10.1038/345356a0
- [58] F Gao, E Bailes, DL Robertson, Y Chen, CM Rodenburg, SF Michael, LB Cummins, LO Arthur, M Peeters et al. 1999. Origin of HIV-1 in the chimpanzee *Pan troglodytes troglodytes*. *Nature*, 397:436–441. doi: 10.1038/17130
- [59] BF Keele, F Van Heuverswyn, Y Li, E Bailes, J Takehisa, ML Santiago, F Bibollet-Ruche, Y Chen, LV Wain et al. 2006. Chimpanzee reservoirs of pandemic and nonpandemic HIV-1. *Science*, 313:523–526. doi: 10.1126/science.1126531
- [60] F Van Heuverswyn, Y Li, E Bailes, C Neel, B Lafay, BF Keele, KS Shaw, J Takehisa, MH Kraus et al. 2007. Genetic diversity and phylogeographic clustering of SIVcpzPtt in wild chimpanzees in Cameroon. *Virology*, 368:155–171. doi: 10.1016/j.virol.2007.06.018
- [61] E Bowen-Jones and S Pendry. 1999. The threat to primates and other mammals from the bushmeat trade in Africa, and how this threat could be diminished. *Oryx*, 33: 233–246. doi: 10.1046/j.1365-3008.1999.00066.x
- [62] BH Hahn, GM Shaw, KM De Cock and PM Sharp. 2000. AIDS as a zoonosis: scientific and public health implications. *Science*, 287:607–614. doi: 10.1126/science.287.5453.607
- [63] M Peeters, V Courgnaud, B Abela, P Auzel, X Pourrut, F Bibollet-Ruche, S Loul, F Liegeois, C Butel et al. 2002. Risk to human health from a plethora of simian immunodeficiency viruses in primate bushmeat. *Emerg Infect Dis*, 8:451–457. doi: 10.3201/eid0805.010522
- [64] ND Wolfe, TA Prosser, JK Carr, U Tamoufe, E Mpoudi-Ngole, JN Torimiro, M LeBreton, FE McCutchan, DL Birx and DS Burke. 2004. Exposure to nonhuman primates in rural Cameroon. *Emerg Infect Dis*, 10:2094–2099. doi: 10.3201/eid1012.040062
- [65] ND Wolfe, W Heneine, JK Carr, AD Garcia, V Shanmugam, U Tamoufe, JN Torimiro, AT Prosser, M Lebreton et al. 2005. Emergence of unique primate T-lymphotropic viruses among central African bushmeat hunters. *Proc Natl Acad Sci U S A*, 102: 7994–7999. doi: 10.1073/pnas.0501734102
- [66] ML Kalish, ND Wolfe, CB Ndongmo, J McNicholl, KE Robbins, M Aidoo, PN Fonjungo, G Alemnji, C Zeh et al. 2005. Central African hunters exposed to simian immunodeficiency virus. *Emerg Infect Dis*, 11:1928–1930. doi: 10.3201/eid1112.050394

- [67] PM Sharp and BH Hahn. 2008. AIDS: prehistory of HIV-1. *Nature*, 455:605–606. doi: 10.1038/455605a
- [68] D Vangroenweghe. 2001. The earliest cases of human immunodeficiency virus type 1 group M in Congo-Kinshasa, Rwanda and Burundi and the origin of acquired immune deficiency syndrome. *Philos Trans R Soc Lond B Biol Sci*, 356:923–925. doi: 10.1098/rstb.2001.0876
- [69] A Chitnis, D Rawls and J Moore. 2000. Origin of HIV type 1 in colonial French Equatorial Africa? *AIDS Res Hum Retroviruses*, 16:5–8. doi: 10.1089/088922200309548
- [70] JD de Sousa, V Müller, P Lemey and AM Vandamme. 2010. High GUD incidence in the early 20 century created a particularly permissive time window for the origin and initial spread of epidemic HIV strains. *PLoS One*, 5:e9936. doi: 10.1371/journal.pone.0009936
- [71] JD de Sousa, C Alvarez, AM Vandamme and V Müller. 2012. Enhanced heterosexual transmission hypothesis for the origin of pandemic HIV-1. *Viruses*, 4:1950–1983. doi: 10.3390/v4101950
- [72] MTP Gilbert, A Rambaut, G Wlasiuk, TJ Spira, AE Pitchenik and M Worobey. 2007. The emergence of HIV/AIDS in the Americas and beyond. *Proc Natl Acad Sci U S A*, 104:18566–18570. doi: 10.1073/pnas.0705329104
- [73] UNAIDS Communications and Global Advocacy. 2014. Fact sheet 2014. URL <http://www.unaids.org/en/resources/campaigns/2014/2014gapreport/factsheet>
- [74] RD Moore and RE Chaisson. 1996. Natural history of opportunistic disease in an HIV-infected urban clinical cohort. *Ann Intern Med*, 124:633–642. doi: 10.7326/0003-4819-124-7-199604010-00003
- [75] R Rothenberg, M Woelfel, R Stoneburner, J Milberg, R Parker and B Truman. 1987. Survival with the acquired immunodeficiency syndrome. Experience with 5833 cases in New York City. *N Engl J Med*, 317:1297–1302. doi: 10.1056/NEJM198711193172101
- [76] S Vella, M Giuliano, P Pezzotti, MG Agresti, C Tomino, M Floridia, D Greco, M Moroni, G Visco and F Milazzo. 1992. Survival of zidovudine-treated patients with AIDS compared with that of contemporary untreated patients. *JAMA*, 267:1232–1236. doi: 10.1001/jama.1992.03480090080031
- [77] KJ Lui, DN Lawrence, WM Morgan, TA Peterman, HW Haverkos and DJ Bregman. 1986. A model-based approach for estimating the mean incubation period of transfusion-associated acquired immunodeficiency syndrome. *Proc Natl Acad Sci U S A*, 83: 3051–3055
- [78] MM Deschamps, DW Fitzgerald, JW Pape and W Johnson, Jr. 2000. HIV infection in Haiti: natural history and disease progression. *AIDS*, 14:2515–2521

- [79] KM Harrison, R Song and X Zhang. 2010. Life expectancy after HIV diagnosis based on national HIV surveillance data from 25 states, United States. *J Acquir Immune Defic Syndr*, 53:124–130. doi: 10.1097/QAI.0b013e3181b563e7
- [80] Collaborative Group on AIDS Incubation and HIV Survival. 2000. Time from HIV-1 seroconversion to AIDS and death before widespread use of highly-active antiretroviral therapy: a collaborative re-analysis. *Lancet*, 355:1131–1137. doi: 10.1016/S0140-6736(00)02061-4
- [81] MA Fischl, DD Richman, MH Grieco, MS Gottlieb, PA Volberding, OL Laskin, JM Leedom, JE Groopman, D Mildvan and RT Schooley. 1987. The efficacy of azidothymidine (AZT) in the treatment of patients with AIDS and AIDS-related complex. A double-blind, placebo-controlled trial. *N Engl J Med*, 317:185–191. doi: 10.1056/NEJM198707233170401
- [82] MA Fischl, DD Richman, DM Causey, MH Grieco, Y Bryson, D Mildvan, OL Laskin, JE Groopman, PA Volberding and RT Schooley. 1989. Prolonged zidovudine therapy in patients with AIDS and advanced AIDS-related complex. *JAMA*, 262:2405–2410. doi: 10.1001/jama.1989.03430170067030
- [83] PA Volberding, SW Lagakos, MA Koch, C Pettinelli, MW Myers, DK Booth, H Balfour, Jr, RC Reichman, JA Bartlett et al. 1990. Zidovudine in asymptomatic human immunodeficiency virus infection. A controlled trial in persons with fewer than 500 CD4-positive cells per cubic millimeter. *N Engl J Med*, 322:941–949. doi: 10.1056/NEJM199004053221401
- [84] BH Hahn, GM Shaw, ME Taylor, RR Redfield, PD Markham, SZ Salahuddin, F Wong-Staal, RC Gallo, ES Parks and WP Parks. 1986. Genetic variation in HTLV-III/LAV over time in patients with AIDS or at risk for AIDS. *Science*, 232:1548–1553. doi: 10.1126/science.3012778
- [85] BD Preston, BJ Poiesz and LA Loeb. 1988. Fidelity of HIV-1 reverse transcriptase. *Science*, 242:1168–1171. doi: 10.1126/science.2460924
- [86] JD Roberts, K Bebenek and TA Kunkel. 1988. The accuracy of reverse transcriptase from HIV-1. *Science*, 242:1171–1173. doi: 10.1126/science.2460925
- [87] LM Mansky and HM Temin. 1995. Lower in vivo mutation rate of human immunodeficiency virus type 1 than that predicted from the fidelity of purified reverse transcriptase. *J Virol*, 69:5087–5094
- [88] LM Mansky. 1996. The mutation rate of human immunodeficiency virus type 1 is influenced by the vpr gene. *Virology*, 222:391–400. doi: 10.1006/viro.1996.0436
- [89] ME Abram, AL Ferris, W Shao, WG Alvord and SH Hughes. 2010. Nature, position, and frequency of mutations made in a single cycle of HIV-1 replication. *J Virol*, 84: 9864–9878. doi: 10.1128/JVI.00915-10

- [90] V Achuthan, BJ Keith, BA Connolly and JJ DeStefano. 2014. Human immunodeficiency virus reverse transcriptase displays dramatically higher fidelity under physiological magnesium conditions in vitro. *J Virol*, 88:8514–8527. doi: 10.1128/JVI.00752-14
- [91] BA Larder, G Darby and DD Richman. 1989. HIV with reduced sensitivity to zidovudine (AZT) isolated during prolonged therapy. *Science*, 243:1731–1734. doi: 10.1126/science.2467383
- [92] BA Larder and SD Kemp. 1989. Multiple mutations in HIV-1 reverse transcriptase confer high-level resistance to zidovudine (AZT). *Science*, 246:1155–1158. doi: 10.1126/science.2479983
- [93] S Land, G Terloar, D McPhee, C Birch, R Doherty, D Cooper and I Gust. 1990. Decreased in vitro susceptibility to zidovudine of HIV isolates obtained from patients with AIDS. *J Infect Dis*, 161:326–329. doi: 10.1093/infdis/161.2.326
- [94] CA Boucher, M Tersmette, JM Lange, P Kellam, RE de Goede, JW Mulder, G Darby, J Goudsmit and BA Larder. 1990. Zidovudine sensitivity of human immunodeficiency viruses from high-risk, symptom-free individuals during therapy. *Lancet*, 336:585–590. doi: 10.1016/0140-6736(90)93391-2
- [95] DD Richman, JM Grimes and SW Lagakos. 1990. Effect of stage of disease and drug dose on zidovudine susceptibilities of isolates of human immunodeficiency virus. *J Acquir Immune Defic Syndr*, 3:743–746
- [96] DD Richman, JC Guatelli, J Grimes, A Tsiatis and T Gingeras. 1991. Detection of mutations associated with zidovudine resistance in human immunodeficiency virus by use of the polymerase chain reaction. *J Infect Dis*, 164:1075–1081. doi: 10.1093/infdis/164.6.1075
- [97] JE Fitzgibbon, RM Howell, CA Habertzettl, SJ Sperber, DJ Gocke and DT Dubin. 1992. Human immunodeficiency virus type 1 pol gene mutations which cause decreased susceptibility to 2',3'-dideoxycytidine. *Antimicrob Agents Chemother*, 36:153–157. doi: 10.1128/AAC.36.1.153
- [98] DD Richman, D Havlir, J Corbeil, D Looney, C Ignacio, SA Spector, J Sullivan, S Cheeseman, K Barringer and D Pauletti. 1994. Nevirapine resistance mutations of human immunodeficiency virus type 1 selected during therapy. *J Virol*, 68:1660–1666
- [99] R Schuurman, M Nijhuis, R van Leeuwen, P Schipper, D de Jong, P Collis, SA Danner, J Mulder, C Loveday and C Christopherson. 1995. Rapid changes in human immunodeficiency virus type 1 RNA load and appearance of drug-resistant virus populations in persons treated with lamivudine (3TC). *J Infect Dis*, 171:1411–1419. doi: 10.1093/infdis/171.6.1411
- [100] JC Schmit, L Ruiz, B Clotet, A Raventos, J Tor, J Leonard, J Desmyter, E De Clercq and AM Vandamme. 1996. Resistance-related mutations in the HIV-1 protease gene

- of patients treated for 1 year with the protease inhibitor ritonavir (ABT-538). *AIDS*, 10:995–999
- [101] T Creagh-Kirk, P Doi, E Andrews, S Nusinoff-Lehrman, H Tilson, D Hoth and DW Barry. 1988. Survival experience among patients with AIDS receiving zidovudine. Follow-up of patients in a compassionate plea program. *JAMA*, 260:3009–3015. doi: 10.1001/jama.1988.03410200065027
- [102] RD Moore, J Keruly, DD Richman, T Creagh-Kirk and RE Chaisson. 1992. Natural history of advanced HIV disease in patients treated with zidovudine. *AIDS*, 6:671–677
- [103] S Vella, B Schwartländer, SP Sow, SP Eholie and RL Murphy. 2012. The history of antiretroviral therapy and of its implementation in resource-limited areas of the world. *AIDS*, 26:1231–1241. doi: 10.1097/QAD.0b013e32835521a3
- [104] JO Kahn, SW Lagakos, DD Richman, A Cross, C Pettinelli, SH Liou, M Brown, PA Volberding, CS Crumpacker and G Beall. 1992. A controlled trial comparing continued zidovudine with didanosine in human immunodeficiency virus infection. *N Engl J Med*, 327:581–587. doi: 10.1056/NEJM199208273270901
- [105] G Skowron, SA Bozzette, L Lim, CB Pettinelli, HH Schaumburg, J Arezzo, MA Fischl, WG Powderly, DJ Gocke et al. 1993. Alternating and intermittent regimens of zidovudine and dideoxycytidine in patients with AIDS or AIDS-related complex. *Ann Intern Med*, 118:321–330
- [106] DI Abrams, AI Goldman, C Launer, JA Korvick, JD Neaton, LR Crane, M Grodesky, S Wakefield, K Muth and S Kornegay. 1994. A comparative trial of didanosine or zalcitabine after treatment with zidovudine in patients with human immunodeficiency virus infection. *N Engl J Med*, 330:657–662. doi: 10.1056/NEJM199403103301001
- [107] MD de Jong, M Loewenthal, CA Boucher, I van der Ende, D Hall, P Schipper, A Imrie, HM Weigel, RH Kauffmann and R Koster. 1994. Alternating nevirapine and zidovudine treatment of human immunodeficiency virus type 1-infected persons does not prolong nevirapine activity. *J Infect Dis*, 169:1346–1350. doi: 10.1093/infdis/169.6.1346
- [108] JC Schmit, J Cogniaux, P Hermans, C Van Vaeck, S Sprecher, B Van Remoortel, M Witvrouw, J Balzarini, J Desmyter et al. 1996. Multiple drug resistance to nucleoside analogues and nonnucleoside reverse transcriptase inhibitors in an efficiently replicating human immunodeficiency virus type 1 patient strain. *J Infect Dis*, 174:962–968. doi: 10.1093/infdis/174.5.962
- [109] AC Collier, RW Coombs, MA Fischl, PR Skolnik, D Northfelt, P Boutin, CJ Hooper, LD Kaplan, PA Volberding et al. 1993. Combination therapy with zidovudine and didanosine compared with zidovudine alone in HIV-1 infection. *Ann Intern Med*, 119:786–793. doi: 10.7326/0003-4819-119-8-199310150-00003
- [110] SM Hammer, DA Katzenstein, MD Hughes, H Gundacker, RT Schooley, RH Haubrich,

- WK Henry, MM Lederman, JP Phair et al. 1996. A trial comparing nucleoside monotherapy with combination therapy in HIV-infected adults with CD4 cell counts from 200 to 500 per cubic millimeter. *N Engl J Med*, 335:1081–1090. doi: 10.1056/NEJM199610103351501
- [111] JJ Eron, SL Benoit, J Jemsek, RD MacArthur, J Santana, JB Quinn, DR Kuritzkes, MA Fallon and M Rubin. 1995. Treatment with lamivudine, zidovudine, or both in HIV-positive patients with 200 to 500 CD4+ cells per cubic millimeter. *N Engl J Med*, 333:1662–1669. doi: 10.1056/NEJM199512213332502
- [112] LD Saravolatz, DL Winslow, G Collins, JS Hodges, C Pettinelli, DS Stein, N Markowitz, R Reves, MO Loveless et al. 1996. Zidovudine alone or in combination with didanosine or zalcitabine in HIV-infected patients with the acquired immunodeficiency syndrome or fewer than 200 CD4 cells per cubic millimeter. *N Engl J Med*, 335:1099–1106. doi: 10.1056/NEJM199610103351503
- [113] J Darbyshire, Delta Coordinating Committee et al. 1996. Delta: a randomised double-blind controlled trial comparing combinations of zidovudine plus didanosine or zalcitabine with zidovudine alone in HIV-infected individuals. *Lancet*, 348:283–291. doi: 10.1016/S0140-6736(96)05387-1
- [114] RE Dornsife, MH St Clair, AT Huang, TJ Panella, GW Kozsalka, CL Burns and DR Averett. 1991. Anti-human immunodeficiency virus synergism by zidovudine (3'-azidothymidine) and didanosine (dideoxyinosine) contrasts with their additive inhibition of normal human marrow progenitor cells. *Antimicrob Agents Chemother*, 35:322–328. doi: 10.1128/AAC.35.2.322
- [115] VA Johnson, DP Merrill, JA Videler, TC Chou, RE Byington, JJ Eron, RT D'Aquila and MS Hirsch. 1991. Two-drug combinations of zidovudine, didanosine, and recombinant interferon-alpha A inhibit replication of zidovudine-resistant human immunodeficiency virus type 1 synergistically in vitro. *J Infect Dis*, 164:646–655. doi: 10.1093/infdis/164.4.646
- [116] SW Cox, K Apéria, J Albert and B Wahren. 1994. Comparison of the sensitivities of primary isolates of HIV type 2 and HIV type 1 to antiviral drugs and drug combinations. *AIDS Res Hum Retroviruses*, 10:1725–1729. doi: 10.1177/095632029300400407
- [117] JY Feng, JK Ly, F Myrick, D Goodman, KL White, ES Svarovskaia, K Borroto-Esoda and MD Miller. 2009. The triple combination of tenofovir, emtricitabine and efavirenz shows synergistic anti-HIV-1 activity in vitro: a mechanism of action study. *Retrovirology*, 6:44. doi: 10.1186/1742-4690-6-44
- [118] BL Jilek, M Zarr, ME Sampah, SA Rabi, CK Bullen, J Lai, L Shen and RF Siliciano. 2012. A quantitative basis for antiretroviral therapy for HIV-1 infection. *Nat Med*, 18: 446–451. doi: 10.1038/nm.2649
- [119] R Kulkarni, R Hluhanich, DM McColl, MD Miller and KL White. 2014. The com-

- bined anti-HIV-1 activities of emtricitabine and tenofovir plus the integrase inhibitor elvitegravir or raltegravir show high levels of synergy in vitro. *Antimicrob Agents Chemother*, 58:6145–6150. doi: 10.1128/AAC.03591-14
- [120] YK Chow, MS Hirsch, DP Merrill, LJ Bechtel, JJ Eron, JC Kaplan and RT D’Aquila. 1993. Use of evolutionary limitations of HIV-1 multidrug resistance to optimize therapy. *Nature*, 361:650–654. doi: 10.1038/361650a0
- [121] BA Larder, SD Kemp and PR Harrigan. 1995. Potential mechanism for sustained antiretroviral efficacy of AZT-3TC combination therapy. *Science*, 269:696–699. doi: 10.1126/science.7542804
- [122] AC Collier, RW Coombs, DA Schoenfeld, RL Bassett, J Timpone, A Baruch, M Jones, K Facey, C Whitacre et al. 1996. Treatment of human immunodeficiency virus infection with saquinavir, zidovudine, and zalcitabine. *N Engl J Med*, 334:1011–1017. doi: 10.1056/NEJM199604183341602
- [123] SM Hammer, KE Squires, MD Hughes, JM Grimes, LM Demeter, JS Currier, J Eron, Jr, JE Feinberg, H Balfour, Jr et al. 1997. A controlled trial of two nucleoside analogues plus indinavir in persons with human immunodeficiency virus infection and CD4 cell counts of 200 per cubic millimeter or less. *N Engl J Med*, 337:725–733. doi: 10.1056/NEJM199709113371101
- [124] RM Gulick, JW Mellors, D Havlir, JJ Eron, C Gonzalez, D McMahon, DD Richman, FT Valentine, L Jonas et al. 1997. Treatment with indinavir, zidovudine, and lamivudine in adults with human immunodeficiency virus infection and prior antiretroviral therapy. *N Engl J Med*, 337:734–739. doi: 10.1056/NEJM199709113371102
- [125] JS Montaner, P Reiss, D Cooper, S Vella, M Harris, B Conway, MA Wainberg, D Smith, P Robinson et al. 1998. A randomized, double-blind trial comparing combinations of nevirapine, didanosine, and zidovudine for HIV-infected patients: the INCAS Trial. Italy, The Netherlands, Canada and Australia Study. *JAMA*, 279:930–937. doi: 10.1001/jama.279.12.930
- [126] RD Moore and RE Chaisson. 1999. Natural history of HIV infection in the era of combination antiretroviral therapy. *AIDS*, 13:1933–1942
- [127] Antiretroviral Therapy Cohort Collaboration, M Zwahlen, R Harris, M May, R Hogg, D Costagliola, F de Wolf, J Gill, G Fätkenheuer et al. 2009. Mortality of HIV-infected patients starting potent antiretroviral therapy: comparison with the general population in nine industrialized countries. *Int J Epidemiol*, 38:1624–1633. doi: 10.1093/ije/dyp306
- [128] AI van Sighem, LAJ Gras, P Reiss, K Brinkman, F de Wolf and ATHENAoccs . 2010. Life expectancy of recently diagnosed asymptomatic HIV-infected patients approaches that of uninfected individuals. *AIDS*, 24:1527–1535. doi: 10.1097/QAD.0b013e32833a3946

- [129] F Nakagawa, RK Lodwick, CJ Smith, R Smith, V Cambiano, JD Lundgren, V Delpuch and AN Phillips. 2012. Projected life expectancy of people with HIV according to timing of diagnosis. *AIDS*, 26:335–343. doi: 10.1097/QAD.0b013e32834dcec9
- [130] F Nakagawa, M May and A Phillips. 2013. Life expectancy living with HIV: recent estimates and future implications. *Curr Opin Infect Dis*, 26:17–25. doi: 10.1097/QCO.0b013e32835ba6b1
- [131] LF Johnson, J Mossong, RE Dorrington, M Schomaker, CJ Hoffmann, O Keiser, MP Fox, R Wood, H Prozesky et al. 2013. Life expectancies of South African adults starting antiretroviral treatment: collaborative analysis of cohort studies. *PLoS Med*, 10:e1001418. doi: 10.1371/journal.pmed.1001418
- [132] G Hütter, D Nowak, M Mossner, S Ganepola, A Müssig, K Allers, T Schneider, J Hofmann, C Kücherer et al. 2009. Long-term control of HIV by CCR5 Delta32/Delta32 stem-cell transplantation. *N Engl J Med*, 360:692–698. doi: 10.1056/NEJMoa0802905
- [133] E Check Hayden. 2013. Hopes of HIV cure in ‘Boston patients’ dashed. *Nature*, 785: 6–8. doi: 10.1038/nature.2013.14324
- [134] RT Davey, N Bhat, C Yoder, TW Chun, JA Metcalf, R Dewar, V Natarajan, RA Lempicki, JW Adelsberger et al. 1999. HIV-1 and T cell dynamics after interruption of highly active antiretroviral therapy (HAART) in patients with a history of sustained viral suppression. *Proc Natl Acad Sci U S A*, 96:15109–15114
- [135] E Hamlyn, FM Ewings, K Porter, DA Cooper, G Tambussi, M Schechter, C Pedersen, JF Okulicz, M McClure et al. 2012. Plasma HIV viral rebound following protocol-indicated cessation of ART commenced in primary and chronic HIV infection. *PLoS One*, 7:e43754. doi: 10.1371/journal.pone.0043754
- [136] W Stöhr, S Fidler, M McClure, J Weber, D Cooper, G Ramjee, P Kaleebu, G Tambussi, M Schechter et al. 2013. Duration of HIV-1 viral suppression on cessation of antiretroviral therapy in primary infection correlates with time on therapy. *PLoS One*, 8:e78287. doi: 10.1371/journal.pone.0078287
- [137] TW Chun, D Engel, MM Berrey, T Shea, L Corey and AS Fauci. 1998. Early establishment of a pool of latently infected, resting CD4(+) T cells during primary HIV-1 infection. *Proc Natl Acad Sci U S A*, 95:8869–8873
- [138] JB Whitney, AL Hill, S Sanisetty, P Penalzoza-MacMaster, J Liu, M Shetty, L Parenteau, C Cabral, J Shields et al. 2014. Rapid seeding of the viral reservoir prior to SIV viraemia in rhesus monkeys. *Nature*, 512:74–77. doi: 10.1038/nature13594
- [139] D Finzi, M Hermankova, T Pierson, LM Carruth, C Buck, RE Chaisson, TC Quinn, K Chadwick, J Margolick et al. 1997. Identification of a reservoir for HIV-1 in patients on highly active antiretroviral therapy. *Science*, 278:1295–1300. doi: 10.1126/science.278.5341.1295

- [140] TW Chun, L Carruth, D Finzi, X Shen, JA DiGiuseppe, H Taylor, M Hermankova, K Chadwick, J Margolick et al. 1997. Quantification of latent tissue reservoirs and total body viral load in HIV-1 infection. *Nature*, 387:183–188. doi: 10.1038/387183a0
- [141] D Finzi, J Blankson, JD Siliciano, JB Margolick, K Chadwick, T Pierson, K Smith, J Lisziewicz, F Lori et al. 1999. Latent infection of CD4+ T cells provides a mechanism for lifelong persistence of HIV-1, even in patients on effective combination therapy. *Nat Med*, 5:512–517. doi: 10.1038/8394
- [142] JD Siliciano, J Kajdas, D Finzi, TC Quinn, K Chadwick, JB Margolick, C Kovacs, SJ Gange and RF Siliciano. 2003. Long-term follow-up studies confirm the stability of the latent reservoir for HIV-1 in resting CD4+ T cells. *Nat Med*, 9:727–728. doi: 10.1038/nm880
- [143] TW Chun, D Finzi, J Margolick, K Chadwick, D Schwartz and RF Siliciano. 1995. In vivo fate of HIV-1-infected T cells: quantitative analysis of the transition to stable latency. *Nat Med*, 1:1284–1290
- [144] JK Wong, M Hezareh, HF Günthard, DV Havlir, CC Ignacio, CA Spina and DD Richman. 1997. Recovery of replication-competent HIV despite prolonged suppression of plasma viremia. *Science*, 278:1291–1295. doi: 10.1126/science.278.5341.1291
- [145] DD Richman, DM Margolis, M Delaney, WC Greene, D Hazuda and RJ Pomerantz. 2009. The challenge of finding a cure for HIV infection. *Science*, 323:1304–1307. doi: 10.1126/science.1165706
- [146] NM Archin, A Espeseth, D Parker, M Cheema, D Hazuda and DM Margolis. 2009. Expression of latent HIV induced by the potent HDAC inhibitor suberoylanilide hydroxamic acid. *AIDS Res Hum Retroviruses*, 25:207–212. doi: 10.1089/aid.2008.0191
- [147] J Kulkosky, DM Culnan, J Roman, G Dornadula, M Schnell, MR Boyd and RJ Pomerantz. 2001. Prostratin: activation of latent HIV-1 expression suggests a potential inductive adjuvant therapy for HAART. *Blood*, 98:3006–3015. doi: 10.1182/blood.V98.10.3006
- [148] S Xing, CK Bullen, NS Shroff, L Shan, HC Yang, JL Manucci, S Bhat, H Zhang, JB Margolick et al. 2011. Disulfiram reactivates latent HIV-1 in a Bcl-2-transduced primary CD4+ T cell model without inducing global T cell activation. *J Virol*, 85: 6060–6064. doi: 10.1128/JVI.02033-10
- [149] DG Wei, V Chiang, E Fyne, M Balakrishnan, T Barnes, M Graupe, J Hesselgesser, A Irrinki, JP Murry et al. 2014. Histone deacetylase inhibitor romidepsin induces HIV expression in CD4 T cells from patients on suppressive antiretroviral therapy at concentrations achieved by clinical dosing. *PLoS Pathog*, 10:e1004071. doi: 10.1371/journal.ppat.1004071
- [150] MK Lewinski, D Bisgrove, P Shinn, H Chen, C Hoffmann, S Hannenhalli, E Verdin,

- CC Berry, JR Ecker and FD Bushman. 2005. Genome-wide analysis of chromosomal features repressing human immunodeficiency virus transcription. *J Virol*, 79:6610–6619. doi: 10.1128/JVI.79.11.6610-6619.2005
- [151] L Shan, HC Yang, SA Rabi, HC Bravo, NS Shroff, RA Irizarry, H Zhang, JB Margolick, JD Siliciano and RF Siliciano. 2011. Influence of host gene transcription level and orientation on HIV-1 latency in a primary-cell model. *J Virol*, 85:5384–5393. doi: 10.1128/JVI.02536-10
- [152] MJ Pace, EH Graf, LM Agosto, AM Mexas, F Male, T Brady, FD Bushman and U O’Doherty. 2012. Directly infected resting CD4+ T cells can produce HIV Gag without spreading infection in a model of HIV latency. *PLoS Pathog*, 8:e1002818. doi: 10.1371/journal.ppat.1002818
- [153] AG Dalgleish, PC Beverley, PR Clapham, DH Crawford, MF Greaves and RA Weiss. 1984. The CD4 (T4) antigen is an essential component of the receptor for the AIDS retrovirus. *Nature*, 312:763–767. doi: 10.1038/312763a0
- [154] D Klatzmann, E Champagne, S Chamaret, J Gruest, D Guetard, T Hercend, JC Gluckman and L Montagnier. 1984. T-lymphocyte T4 molecule behaves as the receptor for human retrovirus LAV. *Nature*, 312:767–768. doi: 10.1038/312767a0
- [155] JD Lifson, MB Feinberg, GR Reyes, L Rabin, B Banapour, S Chakrabarti, B Moss, F Wong-Staal, KS Steimer and EG Engleman. 1986. Induction of CD4-dependent cell fusion by the HTLV-III/LAV envelope glycoprotein. *Nature*, 323:725–728. doi: 10.1038/323725a0
- [156] JD Lifson, GR Reyes, MS McGrath, BS Stein and EG Engleman. 1986. AIDS retrovirus induced cytopathology: giant cell formation and involvement of CD4 antigen. *Science*, 232:1123–1127. doi: 10.1126/science.3010463
- [157] PJ Maddon, AG Dalgleish, JS McDougal, PR Clapham, RA Weiss and R Axel. 1986. The T4 gene encodes the AIDS virus receptor and is expressed in the immune system and the brain. *Cell*, 47:333–348. doi: 10.1016/0092-8674(86)90590-8
- [158] Y Feng, CC Broder, PE Kennedy and EA Berger. 1996. HIV-1 entry cofactor: functional cDNA cloning of a seven-transmembrane, G protein-coupled receptor. *Science*, 272:872–877. doi: 10.1126/science.272.5263.872
- [159] H Choe, M Farzan, Y Sun, N Sullivan, B Rollins, PD Ponath, L Wu, CR Mackay, G LaRosa et al. 1996. The beta-chemokine receptors CCR3 and CCR5 facilitate infection by primary HIV-1 isolates. *Cell*, 85:1135–1148. doi: 10.1016/S0092-8674(00)81313-6
- [160] J He, Y Chen, M Farzan, H Choe, A Ohagen, S Gartner, J Busciglio, X Yang, W Hofmann et al. 1997. CCR3 and CCR5 are co-receptors for HIV-1 infection of microglia. *Nature*, 385:645–649. doi: 10.1038/385645a0

- [161] D Baltimore. 1970. RNA-dependent DNA polymerase in virions of RNA tumour viruses. *Nature*, 226:1209–1211. doi: 10.1038/2261209a0
- [162] HM Temin and S Mizutani. 1970. RNA-dependent DNA polymerase in virions of Rous sarcoma virus. *Nature*, 226:1211–1213. doi: 10.1038/2261211a0
- [163] DP Grandgenett, AC Vora and RD Schiff. 1978. A 32,000-dalton nucleic acid-binding protein from avian reovirus cores possesses DNA endonuclease activity. *Virology*, 89: 119–132. doi: 10.1016/0042-6822(78)90046-6
- [164] FD Bushman, T Fujiwara and R Craigie. 1990. Retroviral DNA integration directed by HIV integration protein in vitro. *Science*, 249:1555–1558. doi: 10.1126/science.2171144
- [165] CP Hill, D Worthylake, DP Bancroft, AM Christensen and WI Sundquist. 1996. Crystal structures of the trimeric human immunodeficiency virus type 1 matrix protein: implications for membrane association and assembly. *Proc Natl Acad Sci U S A*, 93: 3099–3104
- [166] NK Heinzinger, MI Bukrinsky, SA Haggerty, AM Ragland, V Kewalramani, MA Lee, HE Gendelman, L Ratner, M Stevenson and M Emerman. 1994. The Vpr protein of human immunodeficiency virus type 1 influences nuclear localization of viral nucleic acids in nondividing host cells. *Proc Natl Acad Sci U S A*, 91:7311–7315
- [167] MI Bukrinsky, N Sharova, TL McDonald, T Pushkarskaya, WG Tarpley and M Stevenson. 1993. Association of integrase, matrix, and reverse transcriptase antigens of human immunodeficiency virus type 1 with viral nucleic acids following acute infection. *Proc Natl Acad Sci U S A*, 90:6125–6129
- [168] BK Ganser, S Li, VY Klishko, JT Finch and WI Sundquist. 1999. Assembly and analysis of conical models for the HIV-1 core. *Science*, 283:80–83. doi: 10.1126/science.283.5398.80
- [169] S Li, CP Hill, WI Sundquist and JT Finch. 2000. Image reconstructions of helical assemblies of the HIV-1 CA protein. *Nature*, 407:409–413. doi: 10.1038/35030177
- [170] IJL Byeon, X Meng, J Jung, G Zhao, R Yang, J Ahn, J Shi, J Concel, C Aiken et al. 2009. Structural convergence between Cryo-EM and NMR reveals intersubunit interactions critical for HIV-1 capsid function. *Cell*, 139:780–790. doi: 10.1016/j.cell.2009.10.010
- [171] G Zhao, JR Perilla, EL Yufenyuy, X Meng, B Chen, J Ning, J Ahn, AM Gronenborn, K Schulten et al. 2013. Mature HIV-1 capsid structure by cryo-electron microscopy and all-atom molecular dynamics. *Nature*, 497:643–646. doi: 10.1038/nature12162
- [172] K Lee, Z Ambrose, TD Martin, I Oztop, A Mulky, JG Julias, N Vandegraaff, JG Baumann, R Wang et al. 2010. Flexible use of nuclear import pathways by HIV-1. *Cell Host Microbe*, 7:221–233. doi: 10.1016/j.chom.2010.02.007

- [173] M Thali, A Bukovsky, E Kondo, B Rosenwirth, CT Walsh, J Sodroski and HG Göttinger. 1994. Functional association of cyclophilin A with HIV-1 virions. *Nature*, 372:363–365. doi: 10.1038/372363a0
- [174] TR Gamble, FF Vajdos, S Yoo, DK Worthylake, M Houseweart, WI Sundquist and CP Hill. 1996. Crystal structure of human cyclophilin A bound to the amino-terminal domain of HIV-1 capsid. *Cell*, 87:1285–1294. doi: 10.1016/S0092-8674(00)81823-1
- [175] T Schaller, KE Ocwieja, J Rasaiyaah, AJ Price, TL Brady, SL Roth, S Hué, AJ Fletcher, K Lee et al. 2011. HIV-1 capsid-cyclophilin interactions determine nuclear import pathway, integration targeting and replication efficiency. *PLoS Pathog*, 7:e1002439. doi: 10.1371/journal.ppat.1002439
- [176] KE Ocwieja, TL Brady, K Ronen, A Huegel, SL Roth, T Schaller, LC James, GJ Towers, JAT Young et al. 2011. HIV integration targeting: a pathway involving Transportin-3 and the nuclear pore protein RanBP2. *PLoS Pathog*, 7:e1001313. doi: 10.1371/journal.ppat.1001313
- [177] J Rasaiyaah, CP Tan, AJ Fletcher, AJ Price, C Blondeau, L Hilditch, DA Jacques, DL Selwood, LC James et al. 2013. HIV-1 evades innate immune recognition through specific cofactor recruitment. *Nature*, 503:402–405. doi: 10.1038/nature12769
- [178] GP Harrison and AM Lever. 1992. The human immunodeficiency virus type 1 packaging signal and major splice donor region have a conserved stable secondary structure. *J Virol*, 66:4144–4153
- [179] J Dannull, A Surovoy, G Jung and K Moelling. 1994. Specific binding of HIV-1 nucleocapsid protein to PSI RNA in vitro requires N-terminal zinc finger and flanking basic amino acid residues. *EMBO J*, 13:1525–1533
- [180] FD Veronese, R Rahman, TD Copeland, S Oroszlan, RC Gallo and MG Sarngadharan. 1987. Immunological and chemical analysis of P6, the carboxyl-terminal fragment of HIV P15. *AIDS Res Hum Retroviruses*, 3:253–264. doi: 10.1089/aid.1987.3.253
- [181] HG Göttinger, T Dorfman, JG Sodroski and WA Haseltine. 1991. Effect of mutations affecting the p6 gag protein on human immunodeficiency virus particle release. *Proc Natl Acad Sci U S A*, 88:3195–3199. doi: 10.1073/pnas.88.8.3195
- [182] B Strack, A Calistri, S Craig, E Popova and HG Göttinger. 2003. AIP1/ALIX is a binding partner for HIV-1 p6 and EIAV p9 functioning in virus budding. *Cell*, 114: 689–699. doi: 10.1016/S0092-8674(03)00653-6
- [183] W Paxton, RI Connor and NR Landau. 1993. Incorporation of Vpr into human immunodeficiency virus type 1 virions: requirement for the p6 region of gag and mutational analysis. *J Virol*, 67:7229–7237
- [184] NT Parkin, M Chamorro and HE Varmus. 1992. Human immunodeficiency virus

type 1 gag-pol frameshifting is dependent on downstream mRNA secondary structure: demonstration by expression in vivo. *J Virol*, 66:5147–5151

- [185] T Jacks, MD Power, FR Masiarz, PA Luciw, PJ Barr and HE Varmus. 1988. Characterization of ribosomal frameshifting in HIV-1 gag-pol expression. *Nature*, 331:280–283. doi: 10.1038/331280a0
- [186] H Reil and H Hauser. 1990. Test system for determination of HIV-1 frameshifting efficiency in animal cells. *Biochim Biophys Acta*, 1050:288–292. doi: 10.1016/0167-4781(90)90183-3
- [187] LA Kohlstaedt, J Wang, JM Friedman, PA Rice and TA Steitz. 1992. Crystal structure at 3.5 Å resolution of HIV-1 reverse transcriptase complexed with an inhibitor. *Science*, 256:1783–1790. doi: 10.1126/science.1377403
- [188] AR Bellamy, SC Gillies and JD Harvey. 1974. Molecular weight of two oncornavirus genomes: derivation from particle molecular weights and RNA content. *J Virol*, 14:1388–1393
- [189] HJ Kung, JM Bailey, N Davidson, MO Nicolson and RM McAllister. 1975. Structure, subunit composition, and molecular weight of RD-114 RNA. *J Virol*, 16:397–411
- [190] HJ Kung, S Hu, W Bender, JM Bailey, N Davidson, MO Nicolson and RM McAllister. 1976. RD-114, baboon, and woolly monkey viral RNA's compared in size and structure. *Cell*, 7:609–620. doi: 10.1016/0092-8674(76)90211-7
- [191] AT Panganiban and D Fiore. 1988. Ordered interstrand and intrastrand DNA transfer during reverse transcription. *Science*, 241:1064–1069. doi: 10.1126/science.2457948
- [192] WS Hu and HM Temin. 1990. Genetic consequences of packaging two RNA genomes in one retroviral particle: pseudodiploidy and high rate of genetic recombination. *Proc Natl Acad Sci U S A*, 87:1556–1560. doi: 10.1073/pnas.87.4.1556
- [193] WS Hu and HM Temin. 1990. Retroviral recombination and reverse transcription. *Science*, 250:1227–1233. doi: 10.1126/science.1700865
- [194] A Engelman, K Mizuuchi and R Craigie. 1991. HIV-1 DNA integration: mechanism of viral DNA cleavage and DNA strand transfer. *Cell*, 67:1211–1221. doi: 10.1016/0092-8674(91)90297-C
- [195] AT Panganiban and HM Temin. 1984. The retrovirus pol gene encodes a product required for DNA integration: identification of a retrovirus int locus. *Proc Natl Acad Sci U S A*, 81:7885–7889
- [196] GN Maertens, S Hare and P Cherepanov. 2010. The mechanism of retroviral integration from X-ray structures of its key intermediates. *Nature*, 468:326–329. doi: 10.1038/nature09517

- [197] S Hare, SS Gupta, E Valkov, A Engelman and P Cherepanov. 2010. Retroviral intasome assembly and inhibition of DNA strand transfer. *Nature*, 464:232–236. doi: 10.1038/nature08784
- [198] FD Bushman and R Craigie. 1991. Activities of human immunodeficiency virus (HIV) integration protein in vitro: specific cleavage and integration of HIV DNA. *Proc Natl Acad Sci U S A*, 88:1339–1343. doi: 10.1073/pnas.88.4.1339
- [199] A Wlodawer, M Miller, M Jaskólski, BK Sathyanarayana, E Baldwin, IT Weber, LM Selk, L Clawson, J Schneider and SB Kent. 1989. Conserved folding in retroviral proteases: crystal structure of a synthetic HIV-1 protease. *Science*, 245:616–621. doi: 10.1126/science.2548279
- [200] HG Krüsslich, RH Ingraham, MT Skoog, E Wimmer, PV Pallai and CA Carter. 1989. Activity of purified biosynthetic proteinase of human immunodeficiency virus on natural substrates and synthetic peptides. *Proc Natl Acad Sci U S A*, 86:807–811
- [201] NE Kohl, EA Emini, WA Schleif, LJ Davis, JC Heimbach, RA Dixon, EM Scolnick and IS Sigal. 1988. Active human immunodeficiency virus protease is required for viral infectivity. *Proc Natl Acad Sci U S A*, 85:4686–4690
- [202] FD Veronese, AL DeVico, TD Copeland, S Oroszlan, RC Gallo and MG Sarngadharan. 1985. Characterization of gp41 as the transmembrane protein coded by the HTLV-III/LAV envelope gene. *Science*, 229:1402–1405. doi: 10.1126/science.2994223
- [203] S Hallenberger, V Bosch, H Angliker, E Shaw, HD Klenk and W Garten. 1992. Inhibition of furin-mediated cleavage activation of HIV-1 glycoprotein gp160. *Nature*, 360:358–361. doi: 10.1038/360358a0
- [204] X Wei, JM Decker, S Wang, H Hui, JC Kappes, X Wu, JF Salazar-Gonzalez, MG Salazar, JM Kilby et al. 2003. Antibody neutralization and escape by HIV-1. *Nature*, 422:307–312. doi: 10.1038/nature01470
- [205] P Zhu, J Liu, J Bess, Jr, E Chertova, JD Lifson, H Grisé, GA Ofek, KA Taylor and KH Roux. 2006. Distribution and three-dimensional structure of AIDS virus envelope spikes. *Nature*, 441:847–852. doi: 10.1038/nature04817
- [206] EC Holmes, LQ Zhang, P Simmonds, CA Ludlam and AJ Brown. 1992. Convergent and divergent sequence evolution in the surface envelope glycoprotein of human immunodeficiency virus type 1 within a single infected patient. *Proc Natl Acad Sci U S A*, 89:4835–4839
- [207] R Shankarappa, JB Margolick, SJ Gange, AG Rodrigo, D Upchurch, H Farzadegan, P Gupta, CR Rinaldo, GH Learn et al. 1999. Consistent viral evolutionary changes associated with the progression of human immunodeficiency virus type 1 infection. *J Virol*, 73:10489–10502

- [208] S Bonhoeffer, EC Holmes and MA Nowak. 1995. Causes of HIV diversity. *Nature*, 376:125. doi: 10.1038/376125a0
- [209] SM Wolinsky, BT Korber, AU Neumann, M Daniels, KJ Kunstman, AJ Whetsell, MR Furtado, Y Cao, DD Ho and JT Safrit. 1996. Adaptive evolution of human immunodeficiency virus-type 1 during the natural course of infection. *Science*, 272: 537–542. doi: 10.1126/science.272.5261.537
- [210] HA Ross and AG Rodrigo. 2002. Immune-mediated positive selection drives human immunodeficiency virus type 1 molecular variation and predicts disease duration. *J Virol*, 76:11715–11720. doi: 10.1128/JVI.76.22.11715-11720.2002
- [211] J Sodroski, C Rosen, F Wong-Staal, SZ Salahuddin, M Popovic, S Arya, RC Gallo and WA Haseltine. 1985. Trans-acting transcriptional regulation of human T-cell leukemia virus type III long terminal repeat. *Science*, 227:171–173. doi: 10.1126/science.2981427
- [212] J Sodroski, R Patarca, C Rosen, F Wong-Staal and W Haseltine. 1985. Location of the trans-activating region on the genome of human T-cell lymphotropic virus type III. *Science*, 229:74–77. doi: 10.1126/science.2990041
- [213] BR Cullen. 1986. Trans-activation of human immunodeficiency virus occurs via a bimodal mechanism. *Cell*, 46:973–982. doi: 10.1016/0092-8674(86)90696-3
- [214] AI Dayton, JG Sodroski, CA Rosen, WC Goh and WA Haseltine. 1986. The trans-activator gene of the human T cell lymphotropic virus type III is required for replication. *Cell*, 44:941–947. doi: 10.1016/0092-8674(86)90017-6
- [215] TK Howcroft, K Strebler, MA Martin and DS Singer. 1993. Repression of MHC class I gene promoter activity by two-exon Tat of HIV. *Science*, 260:1320–1322. doi: 10.1126/science.8493575
- [216] Y Bennasser, SY Le, M Benkirane and KT Jeang. 2005. Evidence that HIV-1 encodes an siRNA and a suppressor of RNA silencing. *Immunity*, 22:607–619. doi: 10.1016/j.immuni.2005.03.010
- [217] R Triboulet, B Mari, YL Lin, C Chable-Bessia, Y Bennasser, K Lebrigand, B Cardinaud, T Maurin, P Barbry et al. 2007. Suppression of microRNA-silencing pathway by HIV-1 during virus replication. *Science*, 315:1579–1582. doi: 10.1126/science.1136319
- [218] S Qian, X Zhong, L Yu, B Ding, P de Haan and K Boris-Lawrie. 2009. HIV-1 Tat RNA silencing suppressor activity is conserved across kingdoms and counteracts translational repression of HIV-1. *Proc Natl Acad Sci U S A*, 106:605–610. doi: 10.1073/pnas.0806822106
- [219] J Lin and BR Cullen. 2007. Analysis of the interaction of primate retroviruses with the human RNA interference machinery. *J Virol*, 81:12218–12226. doi: 10.1128/JVI.01390-07

- [220] BE Meyer and MH Malim. 1994. The HIV-1 Rev trans-activator shuttles between the nucleus and the cytoplasm. *Genes Dev*, 8:1538–1547. doi: 10.1101/gad.8.13.1538
- [221] J Sodroski, WC Goh, C Rosen, A Dayton, E Terwilliger and W Haseltine. 1986. A second post-transcriptional trans-activator gene required for HTLV-III replication. *Nature*, 321:412–417. doi: 10.1038/321412a0
- [222] MB Feinberg, RF Jarrett, A Aldovini, RC Gallo and F Wong-Staal. 1986. HTLV-III expression and production involve complex regulation at the levels of splicing and translation of viral RNA. *Cell*, 46:807–817. doi: 10.1016/0092-8674(86)90062-0
- [223] DM Knight, FA Flomerfelt and J Ghrayeb. 1987. Expression of the art/trs protein of HIV and study of its role in viral envelope synthesis. *Science*, 236:837–840. doi: 10.1126/science.3033827
- [224] MH Malim, J Hauber, R Fenrick and BR Cullen. 1988. Immunodeficiency virus rev trans-activator modulates the expression of the viral regulatory genes. *Nature*, 335:181–183. doi: 10.1038/335181a0
- [225] D Gutman and CJ Goldenberg. 1988. Virus-specific splicing inhibitor in extracts from cells infected with HIV-1. *Science*, 241:1492–1495. doi: 10.1126/science.3047873
- [226] MH Malim, J Hauber, SY Le, JV Maizel and BR Cullen. 1989. The HIV-1 rev trans-activator acts through a structured target sequence to activate nuclear export of unspliced viral mRNA. *Nature*, 338:254–257. doi: 10.1038/338254a0
- [227] MH Malim, S Bhnlein, J Hauber and BR Cullen. 1989. Functional dissection of the HIV-1 Rev trans-activator—derivation of a trans-dominant repressor of Rev function. *Cell*, 58:205–214. doi: 10.1016/0092-8674(89)90416-9
- [228] G Yu and RL Felsted. 1992. Effect of myristoylation on p27 nef subcellular distribution and suppression of HIV-LTR transcription. *Virology*, 187:46–55. doi: 10.1016/0042-6822(92)90293-X
- [229] JV Garcia and AD Miller. 1991. Serine phosphorylation-independent downregulation of cell-surface CD4 by nef. *Nature*, 350:508–511. doi: 10.1038/350508a0
- [230] RE Benson, A Sanfridson, JS Ottinger, C Doyle and BR Cullen. 1993. Downregulation of cell-surface CD4 expression by simian immunodeficiency virus Nef prevents viral super infection. *J Exp Med*, 177:1561–1566. doi: 10.1084/jem.177.6.1561
- [231] C Aiken, J Konner, NR Landau, ME Lenburg and D Trono. 1994. Nef induces CD4 endocytosis: requirement for a critical dileucine motif in the membrane-proximal CD4 cytoplasmic domain. *Cell*, 76:853–864. doi: 10.1016/0092-8674(94)90360-3
- [232] J Lama, A Mangasarian and D Trono. 1999. Cell-surface expression of CD4 reduces HIV-1 infectivity by blocking Env incorporation in a Nef- and Vpu-inhibitable manner. *Curr Biol*, 9:622–631. doi: 10.1016/S0960-9822(99)80284-X

- [233] TM Ross, AE Oran and BR Cullen. 1999. Inhibition of HIV-1 progeny virion release by cell-surface CD4 is relieved by expression of the viral Nef protein. *Curr Biol*, 9: 613–621. doi: 10.1016/S0960-9822(99)80283-8
- [234] N Michel, I Allespach, S Venzke, OT Fackler and OT Keppler. 2005. The Nef protein of human immunodeficiency virus establishes superinfection immunity by a dual strategy to downregulate cell-surface CCR5 and CD4. *Curr Biol*, 15:714–723. doi: 10.1016/j.cub.2005.02.058
- [235] O Schwartz, V Maréchal, S Le Gall, F Lemonnier and JM Heard. 1996. Endocytosis of major histocompatibility complex class I molecules is induced by the HIV-1 Nef protein. *Nat Med*, 2:338–342. doi: 10.1038/nm0396-338
- [236] KL Collins, BK Chen, SA Kalams, BD Walker and D Baltimore. 1998. HIV-1 Nef protein protects infected primary cells against killing by cytotoxic T lymphocytes. *Nature*, 391:397–401. doi: 10.1038/34929
- [237] P Stumptner-Cuvelette, S Morchoisne, M Dugast, S Le Gall, G Raposo, O Schwartz and P Benaroch. 2001. HIV-1 Nef impairs MHC class II antigen presentation and surface expression. *Proc Natl Acad Sci U S A*, 98:12144–12149. doi: 10.1073/pnas.221256498
- [238] AD Blagoveshchenskaya, L Thomas, SF Feliciangeli, CH Hung and G Thomas. 2002. HIV-1 Nef downregulates MHC-I by a PACS-1- and PI3K-regulated ARF6 endocytic pathway. *Cell*, 111:853–866. doi: 10.1016/S0092-8674(02)01162-5
- [239] XN Xu, B Laffert, GR Screaton, M Kraft, D Wolf, W Kolanus, J Mongkolsapay, AJ McMichael and AS Baur. 1999. Induction of Fas ligand expression by HIV involves the interaction of Nef with the T cell receptor zeta chain. *J Exp Med*, 189:1489–1496. doi: 10.1084/jem.189.9.1489
- [240] JA Schragar and JW Marsh. 1999. HIV-1 Nef increases T cell activation in a stimulus-dependent manner. *Proc Natl Acad Sci U S A*, 96:8167–8172. doi: 10.1073/pnas.96.14.8167
- [241] JK Wang, E Kiyokawa, E Verdin and D Trono. 2000. The Nef protein of HIV-1 associates with rafts and primes T cells for activation. *Proc Natl Acad Sci U S A*, 97: 394–399. doi: 10.1073/pnas.97.1.394
- [242] A Simmons, V Aluvihare and A McMichael. 2001. Nef triggers a transcriptional program in T cells imitating single-signal T cell activation and inducing HIV virulence mediators. *Immunity*, 14:763–777. doi: 10.1016/S1074-7613(01)00158-3
- [243] JA Schragar, V Der Minassian and JW Marsh. 2002. HIV Nef increases T cell ERK MAP kinase activity. *J Biol Chem*, 277:6137–6142. doi: 10.1074/jbc.M107322200
- [244] M Schindler, J Münch, O Kutsch, H Li, ML Santiago, F Bibollet-Ruche, MC Müller-Trutwin, FJ Novembre, M Peeters et al. 2006. Nef-mediated suppression of T cell

- activation was lost in a lentiviral lineage that gave rise to HIV-1. *Cell*, 125:1055–1067. doi: 10.1016/j.cell.2006.04.033
- [245] F Kirchhoff, M Schindler, A Specht, N Arhel and J Münch. 2008. Role of Nef in primate lentiviral immunopathogenesis. *Cell Mol Life Sci*, 65:2621–2636. doi: 10.1007/s00018-008-8094-2
- [246] F Kirchhoff. 2009. Is the high virulence of HIV-1 an unfortunate coincidence of primate lentiviral evolution? *Nat Rev Microbiol*, 7:467–476. doi: 10.1038/nrmicro2111
- [247] F Wong-Staal, PK Chanda and J Ghrayeb. 1987. Human immunodeficiency virus: the eighth gene. *AIDS Res Hum Retroviruses*, 3:33–39. doi: 10.1089/aid.1987.3.33
- [248] EA Cohen, EF Terwilliger, Y Jalinoos, J Proulx, JG Sodroski and WA Haseltine. 1990. Identification of HIV-1 vpr product and function. *J Acquir Immune Defic Syndr*, 3: 11–18
- [249] JB Jowett, V Planelles, B Poon, NP Shah, ML Chen and IS Chen. 1995. The human immunodeficiency virus type 1 vpr gene arrests infected T cells in the G2 + M phase of the cell cycle. *J Virol*, 69:6304–6313
- [250] F Re, D Braaten, EK Franke and J Luban. 1995. Human immunodeficiency virus type 1 Vpr arrests the cell cycle in G2 by inhibiting the activation of p34cdc2-cyclin B. *J Virol*, 69:6859–6864
- [251] J He, S Choe, R Walker, P Di Marzio, DO Morgan and NR Landau. 1995. Human immunodeficiency virus type 1 viral protein R (Vpr) arrests cells in the G2 phase of the cell cycle by inhibiting p34cdc2 activity. *J Virol*, 69:6705–6711
- [252] ME Rogel, LI Wu and M Emerman. 1995. The human immunodeficiency virus type 1 vpr gene prevents cell proliferation during chronic infection. *J Virol*, 69:882–888
- [253] CM de Noronha, MP Sherman, HW Lin, MV Cavois, RD Moir, RD Goldman and WC Greene. 2001. Dynamic disruptions in nuclear envelope architecture and integrity induced by HIV-1 Vpr. *Science*, 294:1105–1108. doi: 10.1126/science.1063957
- [254] WC Goh, ME Rogel, CM Kinsey, SF Michael, PN Fultz, MA Nowak, BH Hahn and M Emerman. 1998. HIV-1 Vpr increases viral expression by manipulation of the cell cycle: a mechanism for selection of Vpr in vivo. *Nat Med*, 4:65–71. doi: 10.1038/nm0198-065
- [255] RA Subbramanian, A Kessous-Elbaz, R Lodge, J Forget, XJ Yao, D Bergeron and EA Cohen. 1998. Human immunodeficiency virus type 1 Vpr is a positive regulator of viral transcription and infectivity in primary human macrophages. *J Exp Med*, 187: 1103–1111. doi: 10.1084/jem.187.7.1103
- [256] SA Stewart, B Poon, JB Jowett and IS Chen. 1997. Human immunodeficiency virus type 1 Vpr induces apoptosis following cell cycle arrest. *J Virol*, 71:5579–5592

- [257] LD Shostak, J Ludlow, J Fisk, S Pursell, BJ Rimel, D Nguyen, JD Rosenblatt and V Planelles. 1999. Roles of p53 and caspases in the induction of cell cycle arrest and apoptosis by HIV-1 vpr. *Exp Cell Res*, 251:156–165. doi: 10.1006/excr.1999.4568
- [258] EA Cohen, G Dehni, JG Sodroski and WA Haseltine. 1990. Human immunodeficiency virus vpr product is a virion-associated regulatory protein. *J Virol*, 64:3097–3099
- [259] X Yuan, Z Matsuda, M Matsuda, M Essex and TH Lee. 1990. Human immunodeficiency virus vpr gene encodes a virion-associated protein. *AIDS Res Hum Retroviruses*, 6: 1265–1271. doi: 10.1089/aid.1990.6.1265
- [260] AM Sheehy, NC Gaddis, JD Choi and MH Malim. 2002. Isolation of a human gene that inhibits HIV-1 infection and is suppressed by the viral Vif protein. *Nature*, 418: 646–650. doi: 10.1038/nature00939
- [261] R Mariani, D Chen, B Schröfelbauer, F Navarro, R König, B Bollman, C Münk, H Nymark-McMahon and NR Landau. 2003. Species-specific exclusion of APOBEC3G from HIV-1 virions by Vif. *Cell*, 114:21–31. doi: 10.1016/S0092-8674(03)00515-4
- [262] AM Sheehy, NC Gaddis and MH Malim. 2003. The antiretroviral enzyme APOBEC3G is degraded by the proteasome in response to HIV-1 Vif. *Nat Med*, 9:1404–1407. doi: 10.1038/nm945
- [263] M Marin, KM Rose, SL Kozak and D Kabat. 2003. HIV-1 Vif protein binds the editing enzyme APOBEC3G and induces its degradation. *Nat Med*, 9:1398–1403. doi: 10.1038/nm946
- [264] X Yu, Y Yu, B Liu, K Luo, W Kong, P Mao and XF Yu. 2003. Induction of APOBEC3G ubiquitination and degradation by an HIV-1 Vif-Cul5-SCF complex. *Science*, 302:1056–1060. doi: 10.1126/science.1089591
- [265] RS Harris, KN Bishop, AM Sheehy, HM Craig, SK Petersen-Mahrt, IN Watt, MS Neuberger and MH Malim. 2003. DNA deamination mediates innate immunity to retroviral infection. *Cell*, 113:803–809. doi: 10.1016/S0092-8674(03)00423-9
- [266] B Mangeat, P Turelli, G Caron, M Friedli, L Perrin and D Trono. 2003. Broad antiretroviral defence by human APOBEC3G through lethal editing of nascent reverse transcripts. *Nature*, 424:99–103. doi: 10.1038/nature01709
- [267] H Zhang, B Yang, RJ Pomerantz, C Zhang, SC Arunachalam and L Gao. 2003. The cytidine deaminase CEM15 induces hypermutation in newly synthesized HIV-1 DNA. *Nature*, 424:94–98. doi: 10.1038/nature01707
- [268] D Lecossier, F Bouchonnet, F Clavel and AJ Hance. 2003. Hypermutation of HIV-1 DNA in the absence of the Vif protein. *Science*, 300:1112. doi: 10.1126/science.1083338
- [269] EA Cohen, EF Terwilliger, JG Sodroski and WA Haseltine. 1988. Identification of a protein encoded by the vpu gene of HIV-1. *Nature*, 334:532–534. doi: 10.1038/334532a0

- [270] K Strebel, T Klimkait and MA Martin. 1988. A novel gene of HIV-1, vpu, and its 16-kilodalton product. *Science*, 241:1221–1223. doi: 10.1126/science.3261888
- [271] RL Willey, F Maldarelli, MA Martin and K Strebel. 1992. Human immunodeficiency virus type 1 Vpu protein induces rapid degradation of CD4. *J Virol*, 66:7193–7200
- [272] S Bour, U Schubert and K Strebel. 1995. The human immunodeficiency virus type 1 Vpu protein specifically binds to the cytoplasmic domain of CD4: implications for the mechanism of degradation. *J Virol*, 69:1510–1520
- [273] WL Marshall, DC Diamond, MM Kowalski and RW Finberg. 1992. High level of surface CD4 prevents stable human immunodeficiency virus infection of T-cell transfectants. *J Virol*, 66:5492–5499
- [274] MJ Cortés, F Wong-Staal and J Lama. 2002. Cell surface CD4 interferes with the infectivity of HIV-1 particles released from T cells. *J Biol Chem*, 277:1770–1779. doi: 10.1074/jbc.M109807200
- [275] B Crise, L Buonocore and JK Rose. 1990. CD4 is retained in the endoplasmic reticulum by the human immunodeficiency virus type 1 glycoprotein precursor. *J Virol*, 64:5585–5593
- [276] S Bour, F Boulerice and MA Wainberg. 1991. Inhibition of gp160 and CD4 maturation in U937 cells after both defective and productive infections by human immunodeficiency virus type 1. *J Virol*, 65:6387–6396
- [277] SJD Neil, T Zang and PD Bieniasz. 2008. Tetherin inhibits retrovirus release and is antagonized by HIV-1 Vpu. *Nature*, 451:425–430. doi: 10.1038/nature06553
- [278] N Van Damme, D Goff, C Katsura, RL Jorgenson, R Mitchell, MC Johnson, EB Stephens and J Guatelli. 2008. The interferon-induced protein BST-2 restricts HIV-1 release and is downregulated from the cell surface by the viral Vpu protein. *Cell Host Microbe*, 3:245–252. doi: 10.1016/j.chom.2008.03.001
- [279] K Strebel, T Klimkait, F Maldarelli and MA Martin. 1989. Molecular and biochemical analyses of human immunodeficiency virus type 1 vpu protein. *J Virol*, 63:3784–3791
- [280] C Gélinas and HM Temin. 1986. Nondefective spleen necrosis virus-derived vectors define the upper size limit for packaging reticuloendotheliosis viruses. *Proc Natl Acad Sci USA*, 83:9211–9215
- [281] SA Herman and JM Coffin. 1987. Efficient packaging of readthrough RNA in ALV: implications for oncogene transduction. *Science*, 236:845–848. doi: 10.1126/science.3033828
- [282] NH Shin, D Hartigan-O'Connor, JK Pfeiffer and A Telesnitsky. 2000. Replication of lengthened Moloney murine leukemia virus genomes is impaired at multiple stages. *J Virol*, 74:2694–2702

- [283] S Kammler, M Otte, I Hauber, J Kjems, J Hauber and H Schaal. 2006. The strength of the HIV-1 3' splice sites affects Rev function. *Retrovirology*, 3:89. doi: 10.1186/1742-4690-3-89
- [284] CM Stoltzfus. 2009. Chapter 1. Regulation of HIV-1 alternative RNA splicing and its role in virus replication. *Adv Virus Res*, 74:1–40. doi: 10.1016/S0065-3527(09)74001-1
- [285] MM O'Reilly, MT McNally and KL Beemon. 1995. Two strong 5' splice sites and competing, suboptimal 3' splice sites involved in alternative splicing of human immunodeficiency virus type 1 RNA. *Virology*, 213:373–385. doi: 10.1006/viro.1995.0010
- [286] BA Amendt, D Hesslein, LJ Chang and CM Stoltzfus. 1994. Presence of negative and positive cis-acting RNA splicing elements within and flanking the first tat coding exon of human immunodeficiency virus type 1. *Mol Cell Biol*, 14:3960–3970. doi: 10.1128/MCB.14.6.3960
- [287] JD Levensgood, C Rollins, CHJ Mishler, CA Johnson, G Miner, P Rajan, BM Znosko and BS Tolbert. 2012. Solution structure of the HIV-1 exon splicing silencer 3. *J Mol Biol*, 415:680–698. doi: 10.1016/j.jmb.2011.11.034
- [288] M Caputi, M Freund, S Kammler, C Asang and H Schaal. 2004. A bidirectional SF2/ASF- and SRp40-dependent splicing enhancer regulates human immunodeficiency virus type 1 rev, env, vpu, and nef gene expression. *J Virol*, 78:6517–6526. doi: 10.1128/JVI.78.12.6517-6526.2004
- [289] C Asang, I Hauber and H Schaal. 2008. Insights into the selective activation of alternatively used splice acceptors by the human immunodeficiency virus type-1 bidirectional splicing enhancer. *Nucleic Acids Res*, 36:1450–1463. doi: 10.1093/nar/gkm1147
- [290] TO Tange, CK Damgaard, S Guth, J Valcreel and J Kjems. 2001. The hnRNP A1 protein regulates HIV-1 tat splicing via a novel intron silencer element. *EMBO J*, 20: 5748–5758. doi: 10.1093/emboj/20.20.5748
- [291] JA Jablonski, E Buratti, C Stuanani and M Caputi. 2008. The secondary structure of the human immunodeficiency virus type 1 transcript modulates viral splicing and infectivity. *J Virol*, 82:8038–8050. doi: 10.1128/JVI.00721-08
- [292] A Tranell, EM Feny and S Schwartz. 2010. Serine- and arginine-rich proteins 55 and 75 (SRp55 and SRp75) induce production of HIV-1 vpr mRNA by inhibiting the 5'-splice site of exon 3. *J Biol Chem*, 285:31537–31547. doi: 10.1074/jbc.M109.077453
- [293] CM Stoltzfus and JM Madsen. 2006. Role of viral splicing elements and cellular RNA binding proteins in regulation of HIV-1 alternative RNA splicing. *Curr HIV Res*, 4: 43–55. doi: 10.2174/157016206775197655

- [294] E Buratti and FE Baralle. 2004. Influence of RNA secondary structure on the pre-mRNA splicing process. *Mol Cell Biol*, 24:10505–10514. doi: 10.1128/MCB.24.24.10505-10514.2004
- [295] PJ Shepard and KJ Hertel. 2008. Conserved RNA secondary structures promote alternative splicing. *RNA*, 14:1463–1469. doi: 10.1261/rna.1069408
- [296] M Alló, V Buggiano, JP Fededa, E Petrillo, I Schor, M de la Mata, E Agirre, M Plass, E Eyraas et al. 2009. Control of alternative splicing through siRNA-mediated transcriptional gene silencing. *Nat Struct Mol Biol*, 16:717–724. doi: 10.1038/nsmb.1620
- [297] H Tilgner, C Nikolaou, S Althammer, M Sammeth, M Beato, J Valcárcel and R Guig. 2009. Nucleosome positioning as a determinant of exon recognition. *Nat Struct Mol Biol*, 16:996–1001. doi: 10.1038/nsmb.1658
- [298] S Schwartz, E Meshorer and G Ast. 2009. Chromatin organization marks exon-intron structure. *Nat Struct Mol Biol*, 16:990–995. doi: 10.1038/nsmb.1659
- [299] TL Crabb, BJ Lam and KJ Hertel. 2010. Retention of spliceosomal components along ligated exons ensures efficient removal of multiple introns. *RNA*, 16:1786–1796. doi: 10.1261/rna.2186510
- [300] K Takahara, U Schwarze, Y Imamura, GG Hoffman, H Toriello, LT Smith, PH Byers and DS Greenspan. 2002. Order of intron removal influences multiple splice outcomes, including a two-exon skip, in a COL5A1 acceptor-site mutation that results in abnormal pro-alpha1(V) N-propeptides and Ehlers-Danlos syndrome type I. *Am J Hum Genet*, 71:451–465. doi: 10.1086/342099
- [301] M de la Mata, C Lafaille and AR Kornblihtt. 2010. First come, first served revisited: factors affecting the same alternative splicing event have different effects on the relative rates of intron removal. *RNA*, 16:904–912. doi: 10.1261/rna.1993510
- [302] AM Zahler, KM Neugebauer, WS Lane and MB Roth. 1993. Distinct functions of SR proteins in alternative pre-mRNA splicing. *Science*, 260:219–222. doi: 10.1126/science.8385799
- [303] CW Smith and J Valcárcel. 2000. Alternative pre-mRNA splicing: the logic of combinatorial control. *Trends Biochem Sci*, 25:381–388. doi: 10.1016/S0968-0004(00)01604-2
- [304] J Ule, G Stefani, A Mele, M Ruggiu, X Wang, B Taneri, T Gaasterland, BJ Blencowe and RB Darnell. 2006. An RNA map predicting Nova-dependent splicing regulation. *Nature*, 444:580–586. doi: 10.1038/nature05304
- [305] Y Barash, JA Calarco, W Gao, Q Pan, X Wang, O Shai, BJ Blencowe and BJ Frey. 2010. Deciphering the splicing code. *Nature*, 465:53–59. doi: 10.1038/nature09000

- [306] HY Xiong, Y Barash and BJ Frey. 2011. Bayesian prediction of tissue-regulated splicing using RNA sequence and cellular context. *Bioinformatics*, 27:2554–2562. doi: 10.1093/bioinformatics/btr444
- [307] JT Witten and J Ule. 2011. Understanding splicing regulation through RNA splicing maps. *Trends Genet*, 27:89–97. doi: 10.1016/j.tig.2010.12.001
- [308] TO Tange, TH Jensen and J Kjems. 1996. In vitro interaction between human immunodeficiency virus type 1 Rev protein and splicing factor ASF/SF2-associated protein, p32. *J Biol Chem*, 271:10066–10072. doi: 10.1074/jbc.271.17.10066
- [309] R Berro, K Kehn, C de la Fuente, A Pumfery, R Adair, J Wade, AM Colberg-Poley, J Hiscott and F Kashanchi. 2006. Acetylated Tat regulates human immunodeficiency virus type 1 splicing through its interaction with the splicing regulator p32. *J Virol*, 80:3189–3204. doi: 10.1128/JVI.80.7.3189-3204.2006
- [310] S Jäger, P Cimercanic, N Gulbahce, JR Johnson, KE McGovern, SC Clarke, M Shales, G Mercenne, L Pache et al. 2012. Global landscape of HIV-human protein complexes. *Nature*, 481:365–370. doi: 10.1038/nature10719
- [311] J Bohne, A Schambach and D Zychlinski. 2007. New way of regulating alternative splicing in retroviruses: the promoter makes a difference. *J Virol*, 81:3652–3656. doi: 10.1128/JVI.02105-06
- [312] JA Jablonski, AL Amelio, M Giacca and M Caputi. 2010. The transcriptional transactivator Tat selectively regulates viral splicing. *Nucleic Acids Res*, 38:1249–1260. doi: 10.1093/nar/gkp1105
- [313] M Kuramitsu, C Hashizume, N Yamamoto, A Azuma, M Kamata, N Yamamoto, Y Tanaka and Y Aida. 2005. A novel role for Vpr of human immunodeficiency virus type 1 as a regulator of the splicing of cellular pre-mRNA. *Microbes Infect*, 7:1150–1160. doi: 10.1016/j.micinf.2005.03.022
- [314] C Hashizume, M Kuramitsu, X Zhang, T Kurosawa, M Kamata and Y Aida. 2007. Human immunodeficiency virus type 1 Vpr interacts with spliceosomal protein SAP145 to mediate cellular pre-mRNA splicing inhibition. *Microbes Infect*, 9:490–497. doi: 10.1016/j.micinf.2007.01.013
- [315] MT Vahey, ME Nau, LL Jagodzinski, J Yalley-Ogunro, M Taubman, NL Michael and MG Lewis. 2002. Impact of viral infection on the gene expression profiles of proliferating normal human peripheral blood mononuclear cells infected with HIV type 1 RF. *AIDS Res Hum Retroviruses*, 18:179–192. doi: 10.1089/08892220252781239
- [316] AB van 't Wout, GK Lehrman, SA Mikheeva, GC O'Keeffe, MG Katze, RE Bumgarner, GK Geiss and JI Mullins. 2003. Cellular gene expression upon human immunodeficiency virus type 1 infection of CD4(+)-T-cell lines. *J Virol*, 77:1392–1402. doi: 10.1128/JVI.77.2.1392-1402.2003

- [317] R Mitchell, CY Chiang, C Berry and F Bushman. 2003. Global analysis of cellular transcription following infection with an HIV-based vector. *Mol Ther*, 8:674–687. doi: 10.1016/S1525-0016(03)00215-6
- [318] M Rotger, KK Dang, J Fellay, EL Heizen, S Feng, P Descombes, KV Shianna, D Ge, HF Gnthard et al. 2010. Genome-wide mRNA expression correlates of viral control in CD4+ T-cells from HIV-1-infected individuals. *PLoS Pathog*, 6:e1000781. doi: 10.1371/journal.ppat.1000781
- [319] ST Chang, P Sova, X Peng, J Weiss, GL Law, RE Palermo and MG Katze. 2011. Next-generation sequencing reveals HIV-1-mediated suppression of T cell activation and RNA processing and regulation of noncoding RNA expression in a CD4+ T cell line. *MBio*, 2. doi: 10.1128/mBio.00134-11
- [320] P Legrain and M Rosbash. 1989. Some cis- and trans-acting mutants for splicing target pre-mRNA to the cytoplasm. *Cell*, 57:573–583. doi: 10.1016/0092-8674(89)90127-X
- [321] U Fischer, S Meyer, M Teufel, C Heckel, R Lhrmann and G Rautmann. 1994. Evidence that HIV-1 Rev directly promotes the nuclear export of unspliced RNA. *EMBO J*, 13: 4105–4112
- [322] VW Pollard and MH Malim. 1998. The HIV-1 Rev protein. *Annu Rev Microbiol*, 52: 491–532. doi: 10.1146/annurev.micro.52.1.491
- [323] KA Jones and BM Peterlin. 1994. Control of RNA initiation and elongation at the HIV-1 promoter. *Annu Rev Biochem*, 63:717–743. doi: 10.1146/annurev.bi.63.070194.003441
- [324] TW McCloskey, M Ott, E Tribble, SA Khan, S Teichberg, MO Paul, S Pahwa, E Verdin and N Chirmule. 1997. Dual role of HIV Tat in regulation of apoptosis in T cells. *J Immunol*, 158:1014–1019
- [325] GR Campbell, E Pasquier, J Watkins, V Bourgarel-Rey, V Peyrot, D Esquieu, P Barbier, J de Mareuil, D Braguer et al. 2004. The glutamine-rich region of the HIV-1 Tat protein is involved in T-cell apoptosis. *J Biol Chem*, 279:48197–48204. doi: 10.1074/jbc.M406195200
- [326] HB Miller, TJ Robinson, R Gordn, AJ Hartemink and MA Garcia-Blanco. 2011. Identification of Tat-SF1 cellular targets by exon array analysis reveals dual roles in transcription and splicing. *RNA*, 17:665–674. doi: 10.1261/rna.2462011
- [327] AK Gubitz, W Feng and G Dreyfuss. 2004. The SMN complex. *Exp Cell Res*, 296: 51–56. doi: 10.1016/j.yexcr.2004.03.022
- [328] R Contreras-Galindo, MH Kaplan, DM Markovitz, E Lorenzo and Y Yamamura. 2006. Detection of HERV-K(HML-2) viral RNA in plasma of HIV type 1-infected individuals. *AIDS Res Hum Retroviruses*, 22:979–984. doi: 10.1089/aid.2006.22.979

- [329] MP Laderoute, A Giulivi, L Larocque, D Bellfooy, Y Hou, HX Wu, K Fowke, J Wu and F Diaz-Mitoma. 2007. The replicative activity of human endogenous retrovirus K102 (HERV-K102) with HIV viremia. *AIDS*, 21:2417–2424. doi: 10.1097/QAD.0b013e3282f14d64
- [330] R Contreras-Galindo, P López, R Vélez and Y Yamamura. 2007. HIV-1 infection increases the expression of human endogenous retroviruses type K (HERV-K) in vitro. *AIDS Res Hum Retroviruses*, 23:116–122. doi: 10.1089/aid.2006.0117
- [331] R Contreras-Galindo, MH Kaplan, S He, AC Contreras-Galindo, MJ Gonzalez-Hernandez, F Kappes, D Dube, SM Chan, D Robinson et al. 2013. HIV infection reveals widespread expansion of novel centromeric human endogenous retroviruses. *Genome Res*, 23:1505–1513. doi: 10.1101/gr.144303.112
- [332] N Bhardwaj, F Maldarelli, J Mellors and JM Coffin. 2014. HIV-1 infection leads to increased transcription of human endogenous retrovirus HERV-K (HML-2) proviruses in vivo but not to increased virion production. *J Virol*, 88:11108–11120. doi: 10.1128/JVI.01623-14
- [333] M Vincendeau, I Göttesdorfer, JMH Schreml, AGN Wetie, J Mayer, AD Greenwood, M Helfer, S Kramer, W Seifarth et al. 2015. Modulation of human endogenous retrovirus (HERV) transcription during persistent and de novo HIV-1 infection. *Retrovirology*, 12:27. doi: 10.1186/s12977-015-0156-6
- [334] RB Jones, H Song, Y Xu, KE Garrison, AA Buzdin, N Anwar, DV Hunter, S Mujib, V Mihajlovic et al. 2013. LINE-1 retrotransposable element DNA accumulates in HIV-1-infected cells. *J Virol*, 87:13307–13320. doi: 10.1128/JVI.02257-13
- [335] K Boller, O Janssen, H Schuldes, RR Tönjes and R Kurth. 1997. Characterization of the antibody response specific for the human endogenous retrovirus HTDV/HERV-K. *J Virol*, 71:4581–4588
- [336] K Büscher, U Trefzer, M Hofmann, W Sterry, R Kurth and J Denner. 2005. Expression of human endogenous retrovirus K in melanomas and melanoma cell lines. *Cancer Res*, 65:4172–4180. doi: 10.1158/0008-5472.CAN-04-2983
- [337] KE Garrison, RB Jones, DA Meiklejohn, N Anwar, LC Ndhlovu, JM Chapman, AL Erickson, A Agrawal, G Spotts et al. 2007. T cell responses to human endogenous retroviruses in HIV-1 infection. *PLoS Pathog*, 3:e165. doi: 10.1371/journal.ppat.0030165
- [338] R Tandon, D SenGupta, LC Ndhlovu, RGS Vieira, RB Jones, VA York, VA Vieira, ER Sharp, AA Wiznia et al. 2011. Identification of human endogenous retrovirus-specific T cell responses in vertically HIV-1-infected subjects. *J Virol*, 85:11526–11531. doi: 10.1128/JVI.05418-11
- [339] D SenGupta, R Tandon, RGS Vieira, LC Ndhlovu, R Lown-Hecht, CE Ormsby, L Loh,

- RB Jones, KE Garrison et al. 2011. Strong human endogenous retrovirus-specific T cell responses are associated with control of HIV-1 in chronic infection. *J Virol*, 85: 6977–6985. doi: 10.1128/JVI.00179-11
- [340] RB Jones, KE Garrison, S Mujib, V Mihajlovic, N Aidarus, DV Hunter, E Martin, VM John, W Zhan et al. 2012. HERV-K-specific T cells eliminate diverse HIV-1/2 and SIV primary isolates. *J Clin Invest*, 122:4473–4489. doi: 10.1172/JCI64560
- [341] RS Yalow and SA Berson. 1960. Immunoassay of endogenous plasma insulin in man. *J Clin Invest*, 39:1157–1175. doi: 10.1172/JCI104130
- [342] E Engvall and P Perlmann. 1971. Enzyme-linked immunosorbent assay (ELISA). Quantitative assay of immunoglobulin G. *Immunochemistry*, 8:871–874. doi: 10.1016/0019-2791(71)90454-X
- [343] BK Van Weemen and AH Schuurs. 1971. Immunoassay using antigen-enzyme conjugates. *FEBS Lett*, 15:232–236. doi: 10.1016/0014-5793(71)80319-8
- [344] JW Ward, AJ Grindon, PM Feorino, C Schable, M Parvin and JR Allen. 1986. Laboratory and epidemiologic evaluation of an enzyme immunoassay for antibodies to HTLV-III. *JAMA*, 256:357–361. doi: 10.1001/jama.1986.03380030059028
- [345] H Towbin, T Staehelin and J Gordon. 1979. Electrophoretic transfer of proteins from polyacrylamide gels to nitrocellulose sheets: procedure and some applications. *Proc Natl Acad Sci U S A*, 76:4350–4354
- [346] Centers for Disease Control. 1985. Provisional Public Health Service inter-agency recommendations for screening donated blood and plasma for antibody to the virus causing acquired immunodeficiency syndrome. *MMWR Morb Mortal Wkly Rep*, 34:1–5
- [347] DS Burke and RR Redfield. 1986. False-positive Western blot tests for antibodies to HTLV-III. *JAMA*, 256:347. doi: 10.1001/jama.1986.03380030049013
- [348] DS Burke, JF Brundage, RR Redfield, JJ Damato, CA Schable, P Putman, R Visintine and HI Kim. 1988. Measurement of the false positive rate in a screening program for human immunodeficiency virus infections. *N Engl J Med*, 319:961–964. doi: 10.1056/NEJM198810133191501
- [349] RJ Chappel, KM Wilson and EM Dax. 2009. Immunoassays for the diagnosis of HIV: meeting future needs by enhancing the quality of testing. *Future Microbiol*, 4:963–982. doi: 10.2217/fmb.09.77
- [350] B Weber, EH Fall, A Berger and HW Doerr. 1998. Reduction of diagnostic window by new fourth-generation human immunodeficiency virus screening assays. *J Clin Microbiol*, 36:2235–2239
- [351] B Weber, L Gürtler, R Thorstensson, U Michl, A Mühlbacher, P Bürgisser, R Villaescusa, A Eiras, C Gabriel et al. 2002. Multicenter evaluation of a new automated

- fourth-generation human immunodeficiency virus screening assay with a sensitive antigen detection module and high specificity. *J Clin Microbiol*, 40:1938–1946. doi: 10.1128/JCM.40.6.1938-1946.2002
- [352] WJ Kassler, C Haley, WK Jones, AR Gerber, EJ Kennedy and JR George. 1995. Performance of a rapid, on-site human immunodeficiency virus antibody assay in a public health setting. *J Clin Microbiol*, 33:2899–2902
- [353] Centers for Disease Control and Prevention. 1998. Update: HIV counseling and testing using rapid tests—United States, 1995. *MMWR Morb Mortal Wkly Rep*, 47:211–215
- [354] Centers for Disease Control and Prevention. 2002. Approval of a new rapid test for HIV antibody. *MMWR Morb Mortal Wkly Rep*, 51:1051–1052
- [355] D Gallo, JR George, JH Fitchen, AS Goldstein and MS Hindahl. 1997. Evaluation of a system using oral mucosal transudate for HIV-1 antibody screening and confirmatory testing. *JAMA*, 277:254–258. doi: 10.1001/jama.1997.03540270080030
- [356] KP Delaney, BM Branson, A Uniyal, PR Kerndt, PA Keenan, K Jafa, AD Gardner, DJ Jamieson and M Bulterys. 2006. Performance of an oral fluid rapid HIV-1/2 test: experience from four CDC studies. *AIDS*, 20:1655–1660. doi: 10.1097/01.aids.0000238412.75324.82
- [357] C Semá Baltazar, C Raposo, IV Jani, D Shodell, D Correia, C Gonçalves da Silva, M Kalou, H Patel and B Parekh. 2014. Evaluation of performance and acceptability of two rapid oral fluid tests for HIV detection in Mozambique. *J Clin Microbiol*, 52: 3544–3548. doi: 10.1128/JCM.01098-14
- [358] TC Granade, BS Parekh, SK Phillips and JS McDougal. 2004. Performance of the OraQuick and Hema-Strip rapid HIV antibody detection assays by non-laboratorians. *J Clin Virol*, 30:229–232. doi: 10.1016/j.jcv.2003.12.006
- [359] N Pant Pai, J Sharma, S Shivkumar, S Pillay, C Vadnais, L Joseph, K Dheda and RW Peeling. 2013. Supervised and unsupervised self-testing for HIV in high- and low-risk populations: a systematic review. *PLoS Med*, 10:e1001414. doi: 10.1371/journal.pmed.1001414
- [360] M Usdin, M Guillermin and A Calmy. 2010. Patient needs and point-of-care requirements for HIV load testing in resource-limited settings. *J Infect Dis*, 201 Suppl 1:S73–S77. doi: 10.1086/650384
- [361] SA Fiscus, B Cheng, SM Crowe, L Demeter, C Jennings, V Miller, R Respass, W Stevens and FfCHIVRAVLAWG . 2006. HIV-1 viral load assays for resource-limited settings. *PLoS Med*, 3:e417. doi: 10.1371/journal.pmed.0030417
- [362] S Wang, F Xu and U Demirci. 2010. Advances in developing HIV-1 viral load assays

- for resource-limited settings. *Biotechnol Adv*, 28:770–781. doi: 10.1016/j.biotechadv.2010.06.004
- [363] P Mee, KL Fielding, S Charalambous, GJ Churchyard and AD Grant. 2008. Evaluation of the WHO criteria for antiretroviral treatment failure among adults in South Africa. *AIDS*, 22:1971–1977. doi: 10.1097/QAD.0b013e32830e4cd8
- [364] JJG van Oosterhout, L Brown, R Weigel, JJ Kumwenda, D Mzinganjira, N Saukila, B Mhango, T Hartung, S Phiri and MC Hosseinipour. 2009. Diagnosis of antiretroviral therapy failure in Malawi: poor performance of clinical and immunological WHO criteria. *Trop Med Int Health*, 14:856–861. doi: 10.1111/j.1365-3156.2009.02309.x
- [365] MC Hosseinipour, JJG van Oosterhout, R Weigel, S Phiri, D Kamwendo, N Parkin, SA Fiscus, JAE Nelson, JJ Eron and J Kumwenda. 2009. The public health approach to identify antiretroviral therapy failure: high-level nucleoside reverse transcriptase inhibitor resistance among Malawians failing first-line antiretroviral therapy. *AIDS*, 23:1127–1134. doi: 10.1097/QAD.0b013e32832ac34e
- [366] S Sherrill-Mix, MK Lewinski, M Famiglietti, A Bosque, N Malani, KE Ocwieja, CC Berry, D Looney, L Shan et al. 2013. HIV latency and integration site placement in five cell-based models. *Retrovirology*, 10:90. doi: 10.1186/1742-4690-10-90
- [367] LS Weinberger, RD Dar and ML Simpson. 2008. Transient-mediated fate determination in a transcriptional circuit of HIV. *Nat Genet*, 40:466–470. doi: 10.1038/ng.116
- [368] A Singh, B Razooky, CD Cox, ML Simpson and LS Weinberger. 2010. Transcriptional bursting from the HIV-1 promoter is a significant source of stochastic noise in HIV-1 gene expression. *Biophys J*, 98:L32–L34. doi: 10.1016/j.bpj.2010.03.001
- [369] BS Razooky and LS Weinberger. 2011. Mapping the architecture of the HIV-1 Tat circuit: A decision-making circuit that lacks bistability and exploits stochastic noise. *Methods*, 53:68–77. doi: 10.1016/j.ymeth.2010.12.006
- [370] HJ Muller. 1930. Types of visible variations induced by X-rays in *Drosophila*. *J Genet*, 22:299–334
- [371] M Gaszner and G Felsenfeld. 2006. Insulators: exploiting transcriptional and epigenetic mechanisms. *Nat Rev Genet*, 7:703–713. doi: 10.1038/nrg1925
- [372] A Jordan, P Defechereux and E Verdin. 2001. The site of HIV-1 integration in the human genome determines basal transcriptional activity and response to Tat transactivation. *EMBO J*, 20:1726–1738. doi: 10.1093/emboj/20.7.1726
- [373] A Jordan, D Bisgrove and E Verdin. 2003. HIV reproducibly establishes a latent infection after acute infection of T cells in vitro. *EMBO J*, 22:1868–1877. doi: 10.1093/emboj/cdg188

- [374] R Pearson, YK Kim, J Hokello, K Lassen, J Friedman, M Tyagi and J Karn. 2008. Epigenetic silencing of human immunodeficiency virus (HIV) transcription by formation of restrictive chromatin structures at the viral long terminal repeat drives the progressive entry of HIV into latency. *J Virol*, 82:12291–12303. doi: 10.1128/JVI.01383-08
- [375] F Romerio, MN Gabriel and DM Margolis. 1997. Repression of human immunodeficiency virus type 1 through the novel cooperation of human factors YY1 and LSF. *J Virol*, 71:9375–9382
- [376] JJ Coull, F Romerio, JM Sun, JL Volker, KM Galvin, JR Davie, Y Shi, U Hansen and DM Margolis. 2000. The human factors YY1 and LSF repress the human immunodeficiency virus type 1 long terminal repeat via recruitment of histone deacetylase 1. *J Virol*, 74:6790–6799. doi: 10.1128/JVI.74.15.6790-6799.2000
- [377] G He and DM Margolis. 2002. Counterregulation of chromatin deacetylation and histone deacetylase occupancy at the integrated promoter of human immunodeficiency virus type 1 (HIV-1) by the HIV-1 repressor YY1 and HIV-1 activator Tat. *Mol Cell Biol*, 22:2965–2973. doi: 10.1128/MCB.22.9.2965-2973.2002
- [378] T Lenasi, X Contreras and BM Peterlin. 2008. Transcriptional interference antagonizes proviral gene expression to promote HIV latency. *Cell Host Microbe*, 4:123–133. doi: 10.1016/j.chom.2008.05.016
- [379] Y Han, YB Lin, W An, J Xu, HC Yang, K O’Connell, D Dordai, JD Boeke, JD Siliciano and RF Siliciano. 2008. Orientation-dependent regulation of integrated HIV-1 expression by host gene transcriptional readthrough. *Cell Host Microbe*, 4:134–146. doi: 10.1016/j.chom.2008.06.008
- [380] L Shan, K Deng, NS Shroff, CM Durand, SA Rabi, HC Yang, H Zhang, JB Margolick, JN Blankson and RF Siliciano. 2012. Stimulation of HIV-1-specific cytolytic T lymphocytes facilitates elimination of latent viral reservoir after virus reactivation. *Immunity*, 36:491–501. doi: 10.1016/j.immuni.2012.01.014
- [381] D Boehm, V Calvanese, RD Dar, S Xing, S Schroeder, L Martins, K Aull, PC Li, V Planelles et al. 2013. BET bromodomain-targeting compounds reactivate HIV from latency via a Tat-independent mechanism. *Cell Cycle*, 12:452–462. doi: 10.4161/cc.23309
- [382] A Savarino, A Mai, S Norelli, SE Daker, S Valente, D Rotili, L Altucci, AT Palamara and E Garaci. 2009. “Shock and kill” effects of class I-selective histone deacetylase inhibitors in combination with the glutathione synthesis inhibitor buthionine sulfoximine in cell line models for HIV-1 quiescence. *Retrovirology*, 6:52. doi: 10.1186/1742-4690-6-52
- [383] NM Archin, AL Liberty, AD Kashuba, SK Choudhary, JD Kuruc, AM Crooks, DC Parker, EM Anderson, MF Kearney et al. 2012. Administration of vorinostat

- disrupts HIV-1 latency in patients on antiretroviral therapy. *Nature*, 487:482–485. doi: 10.1038/nature11286
- [384] A Bosque and V Planelles. 2009. Induction of HIV-1 latency and reactivation in primary memory CD4+ T cells. *Blood*, 113:58–65. doi: 10.1182/blood-2008-07-168393
- [385] A Bosque and V Planelles. 2011. Studies of HIV-1 latency in an ex vivo model that uses primary central memory T cells. *Methods*, 53:54–61. doi: 10.1016/j.ymeth.2010.10.002
- [386] X Wu, Y Li, B Crise and SM Burgess. 2003. Transcription start regions in the human genome are favored targets for MLV integration. *Science*, 300:1749–1751. doi: 10.1126/science.1083413
- [387] RS Mitchell, BF Beitzel, ARW Schroder, P Shinn, H Chen, CC Berry, JR Ecker and FD Bushman. 2004. Retroviral DNA integration: ASLV, HIV, and MLV show distinct target site preferences. *PLoS Biol*, 2:e234. doi: 10.1371/journal.pbio.0020234
- [388] R Core Team. *R: A Language and Environment for Statistical Computing*. R Foundation for Statistical Computing, Vienna, Austria, 2012
- [389] C Berry, S Hannenhalli, J Leipzig and FD Bushman. 2006. Selection of target sites for mobile DNA integration in the human genome. *PLoS Comput Biol*, 2:e157. doi: 10.1371/journal.pcbi.0020157
- [390] GP Wang, A Ciuffi, J Leipzig, CC Berry and FD Bushman. 2007. HIV integration site selection: analysis by massively parallel pyrosequencing reveals association with epigenetic modifications. *Genome Res*, 17:1186–1194. doi: 10.1101/gr.6286907
- [391] H Mochizuki, JP Schwartz, K Tanaka, RO Brady and J Reiser. 1998. High-titer human immunodeficiency virus type 1-based vector systems for gene delivery into nondividing cells. *J Virol*, 72:8873–8883
- [392] Y Han, K Lassen, D Monie, AR Sedaghat, S Shimoji, X Liu, TC Pierson, JB Margolick, RF Siliciano and JD Siliciano. 2004. Resting CD4+ T cells from human immunodeficiency virus type 1 (HIV-1)-infected individuals carry integrated HIV-1 genomes within actively transcribed host genes. *J Virol*, 78:6122–6133. doi: 10.1128/JVI.78.12.6122-6133.2004
- [393] G Plesa, J Dai, C Baytop, JL Riley, CH June and U O’Doherty. 2007. Addition of deoxynucleosides enhances human immunodeficiency virus type 1 integration and 2LTR formation in resting CD4+ T cells. *J Virol*, 81:13938–13942. doi: 10.1128/JVI.01745-07
- [394] N Malani. hiReadsProcessor R package. URL <http://github.com/malnirav/hiReadsProcessor>
- [395] WJ Kent. 2002. BLAT—the BLAST-like alignment tool. *Genome Res*, 12:656–664. doi: 10.1101/gr.229202

- [396] CC Berry, K Ocwieja, N Malani and FD Bushman. 2014. Comparing DNA integration site clusters with Scan Statistics. *Bioinformatics*, 30:1493–1500. doi: 10.1093/bioinformatics/btu035
- [397] C Trapnell, BA Williams, G Pertea, A Mortazavi, G Kwan, MJ van Baren, SL Salzberg, BJ Wold and L Pachter. 2010. Transcript assembly and quantification by RNA-Seq reveals unannotated transcripts and isoform switching during cell differentiation. *Nat Biotechnol*, 28:511–515. doi: 10.1038/nbt.1621
- [398] J Ernst and M Kellis. 2010. Discovery and characterization of chromatin states for systematic annotation of the human genome. *Nat Biotechnol*, 28:817–825. doi: 10.1038/nbt.1662
- [399] AS Hinrichs, D Karolchik, R Baertsch, GP Barber, G Bejerano, H Clawson, M Diekhans, TS Furey, RA Harte et al. 2006. The UCSC Genome Browser Database: update 2006. *Nucleic Acids Res*, 34:D590–D598. doi: 10.1093/nar/gkj144
- [400] KR Rosenbloom, CA Sloan, VS Malladi, TR Dreszer, K Learned, VM Kirkup, MC Wong, M Maddren, R Fang et al. 2013. ENCODE data in the UCSC Genome Browser: year 5 update. *Nucleic Acids Res*, 41:D56–D63. doi: 10.1093/nar/gks1172
- [401] J Han, SG Park, JB Bae, J Choi, JM Lyu, SH Park, HS Kim, YJ Kim, S Kim and TY Kim. 2012. The characteristics of genome-wide DNA methylation in naïve CD4+ T cells of patients with psoriasis or atopic dermatitis. *Biochem Biophys Res Commun*, 422:157–163. doi: 10.1016/j.bbrc.2012.04.128
- [402] LR Meyer, AS Zweig, AS Hinrichs, D Karolchik, RM Kuhn, M Wong, CA Sloan, KR Rosenbloom, G Roe et al. 2013. The UCSC Genome Browser database: extensions and updates 2013. *Nucleic Acids Res*, 41:D64–D69. doi: 10.1093/nar/gks1048
- [403] Z Wang, C Zang, JA Rosenfeld, DE Schones, A Barski, S Cuddapah, K Cui, TY Roh, W Peng et al. 2008. Combinatorial patterns of histone acetylations and methylations in the human genome. *Nat Genet*, 40:897–903. doi: 10.1038/ng.154
- [404] A Barski, S Cuddapah, K Cui, TY Roh, DE Schones, Z Wang, G Wei, I Chepelev and K Zhao. 2007. High-resolution profiling of histone methylations in the human genome. *Cell*, 129:823–837. doi: 10.1016/j.cell.2007.05.009
- [405] Z Wang, C Zang, K Cui, DE Schones, A Barski, W Peng and K Zhao. 2009. Genome-wide mapping of HATs and HDACs reveals distinct functions in active and inactive genes. *Cell*, 138:1019–1031. doi: 10.1016/j.cell.2009.06.049
- [406] DE Schones, K Cui, S Cuddapah, TY Roh, A Barski, Z Wang, G Wei and K Zhao. 2008. Dynamic regulation of nucleosome positioning in the human genome. *Cell*, 132: 887–898. doi: 10.1016/j.cell.2008.02.022

- [407] F Hsu, WJ Kent, H Clawson, RM Kuhn, M Diekhans and D Haussler. 2006. The UCSC Known Genes. *Bioinformatics*, 22:1036–1046. doi: 10.1093/bioinformatics/btl048
- [408] J Friedman, T Hastie and R Tibshirani. 2010. Regularization paths for generalized linear models via coordinate descent. *J Stat Softw*, 33:1–22
- [409] IH Greger, F Demarchi, M Giacca and NJ Proudfoot. 1998. Transcriptional interference perturbs the binding of Sp1 to the HIV-1 promoter. *Nucleic Acids Res*, 26:1294–1301
- [410] A De Marco, C Biancotto, A Knezevich, P Maiuri, C Vardabasso and A Marcello. 2008. Intragenic transcriptional cis-activation of the human immunodeficiency virus 1 does not result in allele-specific inhibition of the endogenous gene. *Retrovirology*, 5:98. doi: 10.1186/1742-4690-5-98
- [411] JS Waye and HF Willard. 1987. Nucleotide sequence heterogeneity of alpha satellite repetitive DNA: a survey of alphoid sequences from different human chromosomes. *Nucleic Acids Res*, 15:7549–7569. doi: 10.1093/nar/15.18.7549
- [412] J Jurka, VV Kapitonov, A Pavlicek, P Klonowski, O Kohany and J Walichiewicz. 2005. Repbase Update, a database of eukaryotic repetitive elements. *Cytogenet Genome Res*, 110:462–467. doi: 10.1159/000084979
- [413] E Verdin, P Paras and C Van Lint. 1993. Chromatin disruption in the promoter of human immunodeficiency virus type 1 during transcriptional activation. *EMBO J*, 12: 3249–3259
- [414] C Van Lint, S Emiliani, M Ott and E Verdin. 1996. Transcriptional activation and chromatin remodeling of the HIV-1 promoter in response to histone acetylation. *EMBO J*, 15:1112–1120
- [415] KG Lassen, KX Ramyar, JR Bailey, Y Zhou and RF Siliciano. 2006. Nuclear retention of multiply spliced HIV-1 RNA in resting CD4+ T cells. *PLoS Pathog*, 2:e68. doi: 10.1371/journal.ppat.0020068
- [416] M Dieudonné, P Maiuri, C Biancotto, A Knezevich, A Kula, M Lusic and A Marcello. 2009. Transcriptional competence of the integrated HIV-1 provirus at the nuclear periphery. *EMBO J*, 28:2231–2243. doi: 10.1038/emboj.2009.141
- [417] RF Siliciano and WC Greene. 2011. HIV Latency. *Cold Spring Harb Perspect Med*, 1: a007096. doi: 10.1101/cshperspect.a007096
- [418] M Lusic, B Marini, H Ali, B Lucic, R Luzzati and M Giacca. 2013. Proximity to PML nuclear bodies regulates HIV-1 latency in CD4+ T cells. *Cell Host Microbe*, 13: 665–677. doi: 10.1016/j.chom.2013.05.006
- [419] KE Ocwieja, S Sherrill-Mix, R Mukherjee, R Custers-Allen, P David, M Brown, S Wang, DR Link, J Olson et al. 2012. Dynamic regulation of HIV-1 mRNA populations

- analyzed by single-molecule enrichment and long-read sequencing. *Nucleic Acids Res*, 40:10345–10355. doi: 10.1093/nar/gks753
- [420] Q Pan, O Shai, LJ Lee, BJ Frey and BJ Blencowe. 2008. Deep surveying of alternative splicing complexity in the human transcriptome by high-throughput sequencing. *Nature Genetics*, 40:1413–1415. doi: 10.1038/ng.259
- [421] ET Wang, R Sandberg, S Luo, I Khrebtkova, L Zhang, C Mayr, SF Kingsmore, GP Schroth and CB Burge. 2008. Alternative isoform regulation in human tissue transcriptomes. *Nature*, 456:470–476. doi: 10.1038/nature07509
- [422] F Pagani, M Raponi and FE Baralle. 2005. Synonymous mutations in CFTR exon 12 affect splicing and are not neutral in evolution. *Proc Natl Acad Sci U S A*, 102: 6368–6372. doi: 10.1073/pnas.0502288102
- [423] C Wang, Y Mitsuya, B Gharizadeh, M Ronaghi and SR W. 2007. Characterization of mutation spectra with ultra-deep pyrosequencing: Application to HIV-1 drug resistance. *Genome Research*, 17:1195–1201. doi: 10.1101/gr.6468307
- [424] K Wang, R Wernersson and S Brunak. 2011. The strength of intron donor splice sites in human genes displays a bell-shaped pattern. *Bioinformatics*, 27:3079–3084. doi: 10.1093/bioinformatics/btr532
- [425] DF Purcell and MA Martin. 1993. Alternative splicing of human immunodeficiency virus type 1 mRNA modulates viral protein expression, replication, and infectivity. *J Virol*, 67:6365–6378
- [426] DM Benko, S Schwartz, GN Pavlakis and BK Felber. 1990. A novel human immunodeficiency virus type 1 protein, tev, shares sequences with tat, env, and rev proteins. *J Virol*, 64:2505–2518
- [427] C Carrera, M Pinilla, L Pérez-Alvarez and MM Thomson. 2010. Identification of unusual and novel HIV type 1 spliced transcripts generated in vivo. *AIDS Res Hum Retroviruses*, 26:815–820. doi: 10.1089/aid.2010.0011
- [428] M Lützelberger, LS Reinert, AT Das, B Berkhout and J Kijms. 2006. A novel splice donor site in the gag-pol gene is required for HIV-1 RNA stability. *J Biol Chem*, 281: 18644–18651. doi: 10.1074/jbc.M513698200
- [429] J Salfeld, HG Gttlinger, RA Sia, RE Park, JG Sodroski and WA Haseltine. 1990. A tripartite HIV-1 tat-env-rev fusion protein. *EMBO J*, 9:965–970
- [430] S Schwartz, BK Felber, DM Benko, EM Fenyö and GN Pavlakis. 1990. Cloning and functional analysis of multiply spliced mRNA species of human immunodeficiency virus type 1. *J Virol*, 64:2519–2529
- [431] J Smith, A Azad and N Deacon. 1992. Identification of two novel human immunodeficiency

- ciency virus type 1 splice acceptor sites in infected T cell lines. *J Gen Virol*, 73 (Pt 7):1825–1828
- [432] N Bakkour, YL Lin, S Maire, L Ayadi, F Mahuteau-Betzer, CH Nguyen, C Mettling, P Portales, D Grierson et al. 2007. Small-molecule inhibition of HIV pre-mRNA splicing as a novel antiretroviral therapy to overcome drug resistance. *PLoS Pathog*, 3: 1530–1539. doi: 10.1371/journal.ppat.0030159
- [433] AL Brass, DM Dykxhoorn, Y Benita, N Yan, A Engelman, RJ Xavier, J Lieberman and SJ Elledge. 2008. Identification of host proteins required for HIV infection through a functional genomic screen. *Science*, 319:921–926. doi: 10.1126/science.1152725
- [434] JA Jablonski and M Caputi. 2009. Role of cellular RNA processing factors in human immunodeficiency virus type 1 mRNA metabolism, replication, and infectivity. *J Virol*, 83:981–992. doi: 10.1128/JVI.01801-08
- [435] R König, Y Zhou, D Elleder, TL Diamond, GMC Bonamy, JT Ireland, CY Chiang, BP Tu, PDD Jesus et al. 2008. Global analysis of host-pathogen interactions that regulate early-stage HIV-1 replication. *Cell*, 135:49–60. doi: 10.1016/j.cell.2008.07.032
- [436] A Tranell, S Tingsborg, EM Feny and S Schwartz. 2011. Inhibition of splicing by serine-arginine rich protein 55 (SRp55) causes the appearance of partially spliced HIV-1 mRNAs in the cytoplasm. *Virus Res*, 157:82–91. doi: 10.1016/j.virusres.2011.02.010
- [437] H Zhou, M Xu, Q Huang, AT Gates, XD Zhang, JC Castle, E Stec, M Ferrer, B Strulovici et al. 2008. Genome-scale RNAi screen for host factors required for HIV replication. *Cell Host Microbe*, 4:495–504. doi: 10.1016/j.chom.2008.10.004
- [438] Y Zhu, G Chen, F Lv, X Wang, X Ji, Y Xu, J Sun, L Wu, YT Zheng and G Gao. 2011. Zinc-finger antiviral protein inhibits HIV-1 infection by selectively targeting multiply spliced viral mRNAs for degradation. *Proc Natl Acad Sci U S A*, 108:15834–15839. doi: 10.1073/pnas.1101676108
- [439] MJ Saltarelli, E Hadziyannis, CE Hart, JV Harrison, BK Felber, TJ Spira and GN Pavlakis. 1996. Analysis of human immunodeficiency virus type 1 mRNA splicing patterns during disease progression in peripheral blood mononuclear cells from infected individuals. *AIDS Res Hum Retroviruses*, 12:1443–1456. doi: 10.1089/aid.1996.12.1443
- [440] E Delgado, C Carrera, P Nebreda, A Fernandez-Garca, M Pinilla, V Garca, L Prezlvarez and MM Thomson. 2012. Identification of new splice sites used for generation of rev transcripts in human immunodeficiency virus type 1 subtype C primary isolates. *PLoS One*, 7:e30574. doi: 10.1371/journal.pone.0030574
- [441] P Grabowski. 2011. Alternative splicing takes shape during neuronal development. *Curr Opin Genet Dev*, 21:388–394. doi: 10.1016/j.gde.2011.03.005

- [442] M Llorian and CWJ Smith. 2011. Decoding muscle alternative splicing. *Curr Opin Genet Dev*, 21:380–387. doi: 10.1016/j.gde.2011.03.006
- [443] JY Ip, A Tong, Q Pan, JD Topp, BJ Blencowe and KW Lynch. 2007. Global analysis of alternative splicing during T-cell activation. *RNA*, 13:563–572. doi: 10.1261/rna.457207
- [444] JD Topp, J Jackson, AA Melton and KW Lynch. 2008. A cell-based screen for splicing regulators identifies hnRNP LL as a distinct signal-induced repressor of CD45 variable exon 4. *RNA*, 14:2038–2049. doi: 10.1261/rna.1212008
- [445] S Sonza, HP Mutimer, K O'Brien, P Ellery, JL Howard, JH Axelrod, NJ Deacon, SM Crowe and DFJ Purcell. 2002. Selectively reduced tat mRNA heralds the decline in productive human immunodeficiency virus type 1 infection in monocyte-derived macrophages. *J Virol*, 76:12611–12621
- [446] D Dowling, S Nasr-Esfahani, CH Tan, K O'Brien, JL Howard, DA Jans, DF j Purcell, CM Stoltzfus and S Sonza. 2008. HIV-1 infection induces changes in expression of cellular splicing factors that regulate alternative viral splicing and virus production in macrophages. *Retrovirology*, 5:18. doi: 10.1186/1742-4690-5-18
- [447] J Hull, S Campino, K Rowlands, MS Chan, RR Copley, MS Taylor, K Rockett, G Elvidge, B Keating et al. 2007. Identification of common genetic variation that modulates alternative splicing. *PLoS Genet*, 3:e99. doi: 10.1371/journal.pgen.0030099
- [448] T Kwan, D Benovoy, C Dias, S Gurd, D Serre, H Zuzan, TA Clark, A Schweitzer, MK Staples et al. 2007. Heritability of alternative splicing in the human genome. *Genome Res*, 17:1210–1218. doi: 10.1101/gr.6281007
- [449] R Collman, JW Balliet, SA Gregory, H Friedman, DL Kolson, N Nathanson and A Srinivasan. 1992. An infectious molecular clone of an unusual macrophage-tropic and highly cytopathic strain of human immunodeficiency virus type 1. *J Virol*, 66:7517–7521
- [450] J Eid, A Fehr, J Gray, K Luong, J Lyle, G Otto, P Peluso, D Rank, P Baybayan et al. 2009. Real-time DNA sequencing from single polymerase molecules. *Science*, 323:133–138. doi: 10.1126/science.1162986
- [451] H Deng, R Liu, W Ellmeier, S Choe, D Unutmaz, M Burkhart, P Di Marzio, S Marmon, RE Sutton et al. 1996. Identification of a major co-receptor for primary isolates of HIV-1. *Nature*, 381:661–666. doi: 10.1038/381661a0
- [452] NR Landau and DR Littman. 1992. Packaging system for rapid production of murine leukemia virus vectors with variable tropism. *J Virol*, 66:5110–5113
- [453] N Srinivasakumar, N Chazal, C Helga-Maria, S Prasad, ML Hammarskjöld and D Rekosh. 1997. The effect of viral regulatory protein expression on gene delivery by

- human immunodeficiency virus type 1 vectors produced in stable packaging cell lines. *J Virol*, 71:5841–5848
- [454] DC Shugars, MS Smith, DH Glueck, PV Nantermet, F Seillier-Moiseiwitsch and R Swanstrom. 1993. Analysis of human immunodeficiency virus type 1 nef gene sequences present in vivo. *J Virol*, 67:4639–4650
- [455] R Tewhey, JB Warner, M Nakano, B Libby, M Medkova, PH David, SK Kotsopoulos, ML Samuels, JB Hutchison et al. 2009. Microdroplet-based PCR enrichment for large-scale targeted sequencing. *Nat Biotechnol*, 27:1025–1031. doi: 10.1038/nbt.1583
- [456] KJ Travers, CS Chin, DR Rank, JS Eid and SW Turner. 2010. A flexible and efficient template format for circular consensus sequencing and SNP detection. *Nucleic Acids Res*, 38:e159. doi: 10.1093/nar/gkq543
- [457] TA Thanaraj and F Clark. 2001. Human GC-AG alternative intron isoforms with weak donor sites show enhanced consensus at acceptor exon positions. *Nucleic Acids Res*, 29:2581–2593. doi: 10.1093/nar/29.12.2581
- [458] M Aebi, H Hornig, RA Padgett, J Reiser and C Weissmann. 1986. Sequence requirements for splicing of higher eukaryotic nuclear pre-mRNA. *Cell*, 47:555–565
- [459] M Buset, IA Seledtsov and VV Solovyev. 2000. Analysis of canonical and non-canonical splice sites in mammalian genomes. *Nucleic Acids Res*, 28:4364–4375. doi: 10.1093/nar/28.21.4364
- [460] M Buset, IA Seledtsov and VV Solovyev. 2001. SpliceDB: database of canonical and non-canonical mammalian splice sites. *Nucleic Acids Res*, 29:255–259. doi: 10.1093/nar/29.1.255
- [461] N Sheth, X Roca, ML Hastings, T Roeder, AR Krainer and R Sachidanandam. 2006. Comprehensive splice-site analysis using comparative genomics. *Nucleic Acids Res*, 34:3955–3967. doi: 10.1093/nar/gkl556
- [462] JC Guatelli, TR Gingeras and DD Richman. 1990. Alternative splice acceptor utilization during human immunodeficiency virus type 1 infection of cultured cells. *J Virol*, 64:4093–4098
- [463] C Kuiken, B Foley, T Leitner, C Apetrei, B Hahn, I Mizrachi, J Mullins, A Rambaut, S Wolinsky and B Korber. 2010. HIV Sequence Compendium 2010. Theoretical Biology and Biophysics Group, Los Alamos National Laboratory, New Mexico. URL <http://www.hiv.lanl.gov/content/sequence/HIV/COMPENDIUM/2010compendium.html>
- [464] C Burge, T Tuschl and P Sharp. 1999. Splicing of precursors to mRNAs by the spliceosomes. *Cold Spring Harbor Monograph Archive*, 37. doi: 10.1101/087969589.37.525

- [465] TEM Abbink and B Berkhout. 2008. RNA structure modulates splicing efficiency at the human immunodeficiency virus type 1 major splice donor. *J Virol*, 82:3090–3098. doi: 10.1128/JVI.01479-07
- [466] K Verhoef, PS Bilodeau, JL van Wamel, J Kjemis, CM Stoltzfus and B Berkhout. 2001. Repair of a Rev-minus human immunodeficiency virus type 1 mutant by activation of a cryptic splice site. *J Virol*, 75:3495–3500. doi: 10.1128/JVI.75.7.3495-3500.2001
- [467] AM Zahler, CK Damgaard, J Kjemis and M Caputi. 2004. SC35 and heterogeneous nuclear ribonucleoprotein A/B proteins bind to a juxtaposed exonic splicing enhancer/exonic splicing silencer element to regulate HIV-1 tat exon 2 splicing. *J Biol Chem*, 279:10077–10084. doi: 10.1074/jbc.M312743200
- [468] S Sherrill-Mix, K Ocwieja and F Bushman. Under Review. Gene activity in primary T cells infected with HIV89.6: intron retention and induction of distinctive genomic repeats. *Retrovirology*
- [469] S Wain-Hobson, P Sonigo, O Danos, S Cole and M Alizon. 1985. Nucleotide sequence of the AIDS virus, LAV. *Cell*, 40:9–17. doi: 10.1016/0092-8674(85)90303-4
- [470] SK Arya, C Guo, SF Josephs and F Wong-Staal. 1985. Trans-activator gene of human T-lymphotropic virus type III (HTLV-III). *Science*, 229:69–73
- [471] RA Marciniak and PA Sharp. 1991. HIV-1 Tat protein promotes formation of more-processive elongation complexes. *EMBO J*, 10:4189–4196
- [472] P Wei, ME Garber, SM Fang, WH Fischer and KA Jones. 1998. A novel CDK9-associated C-type cyclin interacts directly with HIV-1 Tat and mediates its high-affinity, loop-specific binding to TAR RNA. *Cell*, 92:451–462. doi: 10.1016/S0092-8674(00)80939-3
- [473] S Kanazawa, T Okamoto and BM Peterlin. 2000. Tat competes with CIITA for the binding to P-TEFb and blocks the expression of MHC class II genes in HIV infection. *Immunity*, 12:61–70. doi: 10.1016/S1074-7613(00)80159-4
- [474] M Barboric, JHN Yik, N Czudnochowski, Z Yang, R Chen, X Contreras, M Geyer, B Matija Peterlin and Q Zhou. 2007. Tat competes with HEXIM1 to increase the active pool of P-TEFb for HIV-1 transcription. *Nucleic Acids Res*, 35:2003–2012. doi: 10.1093/nar/gkm063
- [475] SK O’Brien, H Cao, R Nathans, A Ali and TM Rana. 2010. P-TEFb kinase complex phosphorylates histone H1 to regulate expression of cellular and HIV-1 genes. *J Biol Chem*, 285:29713–29720. doi: 10.1074/jbc.M110.125997
- [476] L Muniz, S Egloff, B Ughy, BE Jády and T Kiss. 2010. Controlling cellular P-TEFb activity by the HIV-1 transcriptional transactivator Tat. *PLoS Pathog*, 6:e1001152. doi: 10.1371/journal.ppat.1001152

- [477] J Corbeil, D Sheeter, D Genini, S Rought, L Leoni, P Du, M Ferguson, DR Masys, JB Welsh et al. 2001. Temporal gene regulation during HIV-1 infection of human CD4+ T cells. *Genome Res*, 11:1198–1204. doi: 10.1101/gr.180201
- [478] CH Woelk, F Ottonnes, CR Plotkin, P Du, CD Royer, SE Rought, J Lozach, R Sasik, RS Kornbluth et al. 2004. Interferon gene expression following HIV type 1 infection of monocyte-derived macrophages. *AIDS Res Hum Retroviruses*, 20:1210–1222. doi: 10.1089/0889222042545009
- [479] MD Hycza, C Kovacs, M Loutfy, R Halpenny, L Heisler, S Yang, O Wilkins, M Ostrowski and SD Der. 2007. Distinct transcriptional profiles in ex vivo CD4+ and CD8+ T cells are established early in human immunodeficiency virus type 1 infection and are characterized by a chronic interferon response as well as extensive transcriptional changes in CD8+ T cells. *J Virol*, 81:3477–3486. doi: 10.1128/JVI.01552-06
- [480] JQ Wu, DE Dwyer, WB Dyer, YH Yang, B Wang and NK Saksena. 2008. Transcriptional profiles in CD8+ T cells from HIV+ progressors on HAART are characterized by coordinated up-regulation of oxidative phosphorylation enzymes and interferon responses. *Virology*, 380:124–135. doi: 10.1016/j.virol.2008.06.039
- [481] AJ Smith, Q Li, SW Wietgreffe, TW Schacker, CS Reilly and AT Haase. 2010. Host genes associated with HIV-1 replication in lymphatic tissue. *J Immunol*, 185:5417–5424. doi: 10.4049/jimmunol.1002197
- [482] G Lefebvre, S Desfarges, F Uyttebroeck, M Muoz, N Beerenwinkel, J Rougemont, A Telenti and A Ciuffi. 2011. Analysis of HIV-1 expression level and sense of transcription by high-throughput sequencing of the infected cell. *J Virol*, 85:6205–6211. doi: 10.1128/JVI.00252-11
- [483] M Imbeault, K Giguère, M Ouellet and MJ Tremblay. 2012. Exon level transcriptomic profiling of HIV-1-infected CD4(+) T cells reveals virus-induced genes and host environment favorable for viral replication. *PLoS Pathog*, 8:e1002861. doi: 10.1371/journal.ppat.1002861
- [484] P Mohammadi, S Desfarges, I Bartha, B Joos, N Zangger, M Muoz, HF Gnthard, N Beerenwinkel, A Telenti and A Ciuffi. 2013. 24 hours in the life of HIV-1 in a T cell line. *PLoS Pathog*, 9:e1003161. doi: 10.1371/journal.ppat.1003161
- [485] X Peng, P Sova, RR Green, MJ Thomas, MJ Korth, S Proll, J Xu, Y Cheng, K Yi et al. 2014. Deep sequencing of HIV-infected cells: insights into nascent transcription and host-directed therapy. *J Virol*, 88:8768–8782. doi: 10.1128/JVI.00768-14
- [486] Q Li, AJ Smith, TW Schacker, JV Carlis, L Duan, CS Reilly and AT Haase. 2009. Microarray analysis of lymphatic tissue reveals stage-specific, gene expression signatures in HIV-1 infection. *J Immunol*, 183:1975–1982. doi: 10.4049/jimmunol.0803222
- [487] M Rotger, J Dalmau, A Rauch, P McLaren, SE Bosinger, R Martinez, NG Sandler,

- A Roque, J Liebner et al. 2011. Comparative transcriptomics of extreme phenotypes of human HIV-1 infection and SIV infection in sooty mangabey and rhesus macaque. *J Clin Invest*, 121:2391–2400. doi: 10.1172/JCI45235
- [488] D Gao, J Wu, YT Wu, F Du, C Aroh, N Yan, L Sun and ZJ Chen. 2013. Cyclic GMP-AMP synthase is an innate immune sensor of HIV and other retroviruses. *Science*, 341:903–906. doi: 10.1126/science.1240933
- [489] KM Monroe, Z Yang, JR Johnson, X Geng, G Doitsh, NJ Krogan and WC Greene. 2014. IFI16 DNA sensor is required for death of lymphoid CD4 T cells abortively infected with HIV. *Science*, 343:428–432. doi: 10.1126/science.1243640
- [490] C de la Fuente, F Santiago, L Deng, C Eadie, I Zilberman, K Kehn, A Maddukuri, S Baylor, K Wu et al. 2002. Gene expression profile of HIV-1 Tat expressing cells: a close interplay between proliferative and differentiation signals. *BMC Biochem*, 3:14. doi: 10.1186/1471-2091-3-14
- [491] T Ikeda, J Shibata, K Yoshimura, A Koito and S Matsushita. 2007. Recurrent HIV-1 integration at the BACH2 locus in resting CD4+ T cell populations during effective highly active antiretroviral therapy. *J Infect Dis*, 195:716–725. doi: 10.1086/510915
- [492] TA Wagner, S McLaughlin, K Garg, CYK Cheung, BB Larsen, S Styrchak, HC Huang, PT Edlefsen, JI Mullins and LM Frenkel. 2014. Proliferation of cells with HIV integrated into cancer genes contributes to persistent infection. *Science*, 345:570–573. doi: 10.1126/science.1256304
- [493] F Maldarelli, X Wu, L Su, FR Simonetti, W Shao, S Hill, J Spindler, AL Ferris, JW Mellors et al. 2014. Specific HIV integration sites are linked to clonal expansion and persistence of infected cells. *Science*, 345:179–183. doi: 10.1126/science.1254194
- [494] LB Cohn, IT Silva, TY Oliveira, RA Rosales, EH Parrish, GH Learn, BH Hahn, JL Czartoski, MJ McElrath et al. 2015. HIV-1 integration landscape during latent and active infection. *Cell*, 160:420–432. doi: 10.1016/j.cell.2015.01.020
- [495] ARW Schröder, P Shinn, H Chen, C Berry, JR Ecker and F Bushman. 2002. HIV-1 integration in the human genome favors active genes and local hotspots. *Cell*, 110: 521–529. doi: 10.1016/S0092-8674(02)00864-4
- [496] T Brady, YN Lee, K Ronen, N Malani, CC Berry, PD Bieniasz and FD Bushman. 2009. Integration target site selection by a resurrected human endogenous retrovirus. *Genes Dev*, 23:633–642. doi: 10.1101/gad.1762309
- [497] B Marini, A Kertesz-Farkas, H Ali, B Lucic, K Lisek, L Manganaro, S Pongor, R Luzzati, A Recchia et al. 2015. Nuclear architecture dictates HIV-1 integration site selection. *Nature*. doi: 10.1038/nature14226
- [498] M Cavazzana-Calvo, E Payen, O Negre, G Wang, K Hehir, F Fusil, J Down, M Denaro,

- T Brady et al. 2010. Transfusion independence and HMGA2 activation after gene therapy of human β -thalassaemia. *Nature*, 467:318–322. doi: 10.1038/nature09328
- [499] S Hacein-Bey-Abina, A Garrigue, GP Wang, J Soulier, A Lim, E Morillon, E Clappier, L Caccavelli, E Delabesse et al. 2008. Insertional oncogenesis in 4 patients after retrovirus-mediated gene therapy of SCID-X1. *J Clin Invest*, 118:3132–3142. doi: 10.1172/JCI35700
- [500] A Moiani, Y Paleari, D Sartori, R Mezzadra, A Miccio, C Cattoglio, F Cocchiarella, MR Lidonnici, G Ferrari and F Mavilio. 2012. Lentiviral vector integration in the human genome induces alternative splicing and generates aberrant transcripts. *J Clin Invest*, 122:1653–1666. doi: 10.1172/JCI61852
- [501] D Cesana, J Sgualdino, L Rudilosso, S Merella, L Naldini and E Montini. 2012. Whole transcriptome characterization of aberrant splicing events induced by lentiviral vector integrations. *J Clin Invest*, 122:1667–1676. doi: 10.1172/JCI62189
- [502] B Langmead, C Trapnell, M Pop and SL Salzberg. 2009. Ultrafast and memory-efficient alignment of short DNA sequences to the human genome. *Genome Biology*, 10:R25. doi: 10.1186/gb-2009-10-3-r25
- [503] GR Grant, MH Farkas, AD Pizarro, NF Lahens, J Schug, BP Brunk, CJ Stoeckert, JB Hogenesch and EA Pierce. 2011. Comparative analysis of RNA-Seq alignment algorithms and the RNA-Seq unified mapper (RUM). *Bioinformatics*, 27:2518–2528. doi: 10.1093/bioinformatics/btr427
- [504] A Subramanian, P Tamayo, VK Mootha, S Mukherjee, BL Ebert, MA Gillette, A Paulovich, SL Pomeroy, TR Golub et al. 2005. Gene set enrichment analysis: a knowledge-based approach for interpreting genome-wide expression profiles. *Proc Natl Acad Sci U S A*, 102:15545–15550. doi: 10.1073/pnas.0506580102
- [505] WJ Kent, CW Sugnet, TS Furey, KM Roskin, TH Pringle, AM Zahler and D Haussler. 2002. The human genome browser at UCSC. *Genome Res*, 12:996–1006. doi: 10.1101/gr.229102
- [506] H Li, B Handsaker, A Wysoker, T Fennell, J Ruan, N Homer, G Marth, G Abecasis, R Durbin and GPDPS . 2009. The Sequence Alignment/Map format and SAMtools. *Bioinformatics*, 25:2078–2079. doi: 10.1093/bioinformatics/btp352
- [507] RP Subramanian, JH Wildschutte, C Russo and JM Coffin. 2011. Identification, characterization, and comparative genomic distribution of the HERV-K (HML-2) group of human endogenous retroviruses. *Retrovirology*, 8:90. doi: 10.1186/1742-4690-8-90
- [508] G La Mantia, D Maglione, G Pengue, A Di Cristofano, A Simeone, L Lanfrancone and L Lania. 1991. Identification and characterization of novel human endogenous retroviral sequences preferentially expressed in undifferentiated embryonal carcinoma cells. *Nucleic Acids Res*, 19:1513–1520

- [509] G La Mantia, B Majello, A Di Cristofano, M Strazzullo, G Minchiotti and L Lania. 1992. Identification of regulatory elements within the minimal promoter region of the human endogenous ERV9 proviruses: accurate transcription initiation is controlled by an Inr-like element. *Nucleic Acids Res*, 20:4129–4136. doi: 10.1093/nar/20.16.4129
- [510] KE Plant, SJ Routledge and NJ Proudfoot. 2001. Intergenic transcription in the human beta-globin gene cluster. *Mol Cell Biol*, 21:6507–6514. doi: 10.1128/MCB.21.19.6507-6514.2001
- [511] J Ling, W Pi, R Bollag, S Zeng, M Keskinetepe, H Saliman, S Krantz, B Whitney and D Tuan. 2002. The solitary long terminal repeats of ERV-9 endogenous retrovirus are conserved during primate evolution and possess enhancer activities in embryonic and hematopoietic cells. *J Virol*, 76:2410–2423. doi: 10.1128/jvi.76.5.2410-2423.2002
- [512] X Yu, X Zhu, W Pi, J Ling, L Ko, Y Takeda and D Tuan. 2005. The long terminal repeat (LTR) of ERV-9 human endogenous retrovirus binds to NF-Y in the assembly of an active LTR enhancer complex NF-Y/MZF1/GATA-2. *J Biol Chem*, 280:35184–35194. doi: 10.1074/jbc.M508138200
- [513] RC Edgar. 2004. MUSCLE: a multiple sequence alignment method with reduced time and space complexity. *BMC Bioinformatics*, 5:113. doi: 10.1186/1471-2105-5-113
- [514] K Breuer, AK Foroushani, MR Laird, C Chen, A Sribnaia, R Lo, GL Winsor, REW Hancock, FSL Brinkman and DJ Lynn. 2013. InnateDB: systems biology of innate immunity and beyond—recent updates and continuing curation. *Nucleic Acids Res*, 41: D1228–D1233. doi: 10.1093/nar/gks1147
- [515] I Rusinova, S Forster, S Yu, A Kannan, M Masse, H Cumming, R Chapman and PJ Hertzog. 2013. Interferome v2.0: an updated database of annotated interferon-regulated genes. *Nucleic Acids Res*, 41:D1040–D1046. doi: 10.1093/nar/gks1215
- [516] ST Chang, MJ Thomas, P Sova, RR Green, RE Palermo and MG Katze. 2013. Next-generation sequencing of small RNAs from HIV-infected cells identifies phased microRNA expression patterns and candidate novel microRNAs differentially expressed upon infection. *MBio*, 4:e00549–e00512. doi: 10.1128/mBio.00549-12
- [517] Z Kalender Atak, K De Keersmaecker, V Gianfelici, E Geerdens, R Vandepoel, D Pauwels, M Porcu, I Lahortiga, V Brys et al. 2012. High accuracy mutation detection in leukemia on a selected panel of cancer genes. *PLoS One*, 7:e38463. doi: 10.1371/journal.pone.0038463
- [518] ES Patel and LJ Chang. 2012. Synergistic effects of interleukin-7 and pre-T cell receptor signaling in human T cell development. *J Biol Chem*, 287:33826–33835. doi: 10.1074/jbc.M112.380113
- [519] M Imbeault, M Ouellet and MJ Tremblay. 2009. Microarray study reveals that HIV-1

- induces rapid type-I interferon-dependent p53 mRNA up-regulation in human primary CD4+ T cells. *Retrovirology*, 6:5. doi: 10.1186/1742-4690-6-5
- [520] S Iwase, Y Furukawa, J Kikuchi, M Nagai, Y Terui, M Nakamura and H Yamada. 1997. Modulation of E2F activity is linked to interferon-induced growth suppression of hematopoietic cells. *J Biol Chem*, 272:12406–12414. doi: 10.1074/jbc.272.19.12406
- [521] RW Johnstone, JA Kerry and JA Trapani. 1998. The human interferon-inducible protein, IFI 16, is a repressor of transcription. *J Biol Chem*, 273:17172–17177. doi: 10.1074/jbc.273.27.17172
- [522] BR Williams. 1999. PKR; a sentinel kinase for cellular stress. *Oncogene*, 18:6112–6120. doi: 10.1038/sj.onc.1203127
- [523] CV Ramana, N Grammatikakis, M Chernov, H Nguyen, KC Goh, BR Williams and GR Stark. 2000. Regulation of c-myc expression by IFN-gamma through Stat1-dependent and -independent pathways. *EMBO J*, 19:263–272. doi: 10.1093/emboj/19.2.263
- [524] SL Liang, D Quirk and A Zhou. 2006. RNase L: its biological roles and regulation. *IUBMB Life*, 58:508–514. doi: 10.1080/15216540600838232
- [525] P Medstrand and DL Mager. 1998. Human-specific integrations of the HERV-K endogenous retrovirus family. *J Virol*, 72:9782–9787
- [526] C Macfarlane and P Simmonds. 2004. Allelic variation of HERV-K(HML-2) endogenous retroviral elements in human populations. *J Mol Evol*, 59:642–656. doi: 10.1007/s00239-004-2656-1
- [527] G Howard, R Eiges, F Gaudet, R Jaenisch and A Eden. 2008. Activation and transposition of endogenous retroviral elements in hypomethylation induced tumors in mice. *Oncogene*, 27:404–408. doi: 10.1038/sj.onc.1210631
- [528] RC Iskow, MT McCabe, RE Mills, S Torene, WS Pittard, AF Neuwald, EG Van Meir, PM Vertino and SE Devine. 2010. Natural mutagenesis of human genomes by endogenous retrotransposons. *Cell*, 141:1253–1261. doi: 10.1016/j.cell.2010.05.020
- [529] E Lee, R Iskow, L Yang, O Gokcumen, P Haseley, LJ Luquette, 3rd, JG Lohr, CC Harris, L Ding et al. 2012. Landscape of somatic retrotransposition in human cancers. *Science*, 337:967–971. doi: 10.1126/science.1222077
- [530] SW Criscione, Y Zhang, W Thompson, JM Sedivy and N Neretti. 2014. Transcriptional landscape of repetitive elements in normal and cancer human cells. *BMC Genomics*, 15:583. doi: 10.1186/1471-2164-15-583
- [531] AW Whisnant, HP Bogerd, O Flores, P Ho, JG Powers, N Sharova, M Stevenson, CH Chen and BR Cullen. 2013. In-depth analysis of the interaction of HIV-1

- with cellular microRNA biogenesis and effector mechanisms. *MBio*, 4:e000193. doi: 10.1128/mBio.00193-13
- [532] NF Lahens, IH Kavakli, R Zhang, K Hayer, MB Black, H Dueck, A Pizarro, J Kim, R Irizarry et al. 2014. IVT-seq reveals extreme bias in RNA sequencing. *Genome Biol*, 15:R86. doi: 10.1186/gb-2014-15-6-r86
- [533] RD Hockett, JM Kilby, CA Derdeyn, MS Saag, M Sillers, K Squires, S Chiz, MA Nowak, GM Shaw and RP Bucy. 1999. Constant mean viral copy number per infected cell in tissues regardless of high, low, or undetectable plasma HIV RNA. *J Exp Med*, 189: 1545–1554. doi: 10.1084/jem.189.10.1545
- [534] RJ De Boer, RM Ribeiro and AS Perelson. 2010. Current estimates for HIV-1 production imply rapid viral clearance in lymphoid tissues. *PLoS Comput Biol*, 6: e1000906. doi: 10.1371/journal.pcbi.1000906
- [535] S Pääbo, DM Irwin and AC Wilson. 1990. DNA damage promotes jumping between templates during enzymatic amplification. *J Biol Chem*, 265:4718–4721
- [536] SJ Odelberg, RB Weiss, A Hata and R White. 1995. Template-switching during DNA synthesis by *Thermus aquaticus* DNA polymerase I. *Nucleic Acids Res*, 23:2049–2057. doi: 10.1093/nar/23.11.2049
- [537] XC Zeng and SX Wang. 2002. Evidence that BmTXK beta-BmKCT cDNA from Chinese scorpion *Buthus martensii* Karsch is an artifact generated in the reverse transcription process. *FEBS Lett*, 520:183–4; author reply 185
- [538] B Tasic, CE Nabholz, KK Baldwin, Y Kim, EH Rueckert, SA Ribich, P Cramer, Q Wu, R Axel and T Maniatis. 2002. Promoter choice determines splice site selection in protocadherin alpha and gamma pre-mRNA splicing. *Mol Cell*, 10:21–33
- [539] M Geiszt, K Lekstrom and TL Leto. 2004. Analysis of mRNA transcripts from the NAD(P)H oxidase 1 (Nox1) gene. Evidence against production of the NADPH oxidase homolog-1 short (NOH-1S) transcript variant. *J Biol Chem*, 279:51661–51668. doi: 10.1074/jbc.M409325200
- [540] J Cocquet, A Chong, G Zhang and RA Veitia. 2006. Reverse transcriptase template switching and false alternative transcripts. *Genomics*, 88:127–131. doi: 10.1016/j.ygeno.2005.12.013
- [541] CJ McManus, JD Coolon, MO Duff, J Eipper-Mains, BR Graveley and PJ Wittkopp. 2010. Regulatory divergence in *Drosophila* revealed by mRNA-seq. *Genome Res*, 20: 816–825. doi: 10.1101/gr.102491.109
- [542] B Cogné, R Snyder, P Lindenbaum, JB Dupont, R Redon, P Moullier and A Leger. 2014. NGS library preparation may generate artifactual integration sites of AAV vectors. *Nat Med*, 20:577–578. doi: 10.1038/nm.3578

- [543] E Gilboa, SW Mitra, S Goff and D Baltimore. 1979. A detailed model of reverse transcription and tests of crucial aspects. *Cell*, 18:93–100. doi: 10.1016/0092-8674(79)90357-X
- [544] GX Luo and J Taylor. 1990. Template switching by reverse transcriptase during DNA synthesis. *J Virol*, 64:4321–4328
- [545] J Houseley and D Tollervey. 2010. Apparent non-canonical trans-splicing is generated by reverse transcriptase in vitro. *PLoS One*, 5:e12271. doi: 10.1371/journal.pone.0012271
- [546] A Meyerhans, JP Vartanian and S Wain-Hobson. 1990. DNA recombination during PCR. *Nucleic Acids Res*, 18:1687–1691
- [547] DJG Lahr and LA Katz. 2009. Reducing the impact of PCR-mediated recombination in molecular evolution and environmental studies using a new-generation high-fidelity DNA polymerase. *Biotechniques*, 47:857–866. doi: 10.2144/000113219
- [548] M Magrane and UniProt Consortium. 2011. UniProt Knowledgebase: a hub of integrated protein data. *Database (Oxford)*, 2011:bar009. doi: 10.1093/database/bar009
- [549] UniProt Consortium. 2015. UniProt: a hub for protein information. *Nucleic Acids Res*, 43:D204–D212. doi: 10.1093/nar/gku989
- [550] EP Papapetrou, G Lee, N Malani, M Setty, I Riviere, LMS Tirunagari, K Kadota, SL Roth, P Giardina et al. 2011. Genomic safe harbors permit high β -globin transgene expression in thalassemia induced pluripotent stem cells. *Nat Biotechnol*, 29:73–78. doi: 10.1038/nbt.1717
- [551] F Maldarelli, C Xiang, G Chamoun and SL Zeichner. 1998. The expression of the essential nuclear splicing factor SC35 is altered by human immunodeficiency virus infection. *Virus Res*, 53:39–51
- [552] A Monette, L Ajamian, M López-Lastra and AJ Mouland. 2009. Human immunodeficiency virus type 1 (HIV-1) induces the cytoplasmic retention of heterogeneous nuclear ribonucleoprotein A1 by disrupting nuclear import: implications for HIV-1 gene expression. *J Biol Chem*, 284:31350–31362. doi: 10.1074/jbc.M109.048736
- [553] W Al-Ahmadi, L Al-Haj, FA Al-Mohanna, RH Silverman and KSA Khabar. 2009. RNase L downmodulation of the RNA-binding protein, HuR, and cellular growth. *Oncogene*, 28:1782–1791. doi: 10.1038/onc.2009.16
- [554] W Pi, Z Yang, J Wang, L Ruan, X Yu, J Ling, S Krantz, C Isales, SJ Conway et al. 2004. The LTR enhancer of ERV-9 human endogenous retrovirus is active in oocytes and progenitor cells in transgenic zebrafish and humans. *Proc Natl Acad Sci U S A*, 101:805–810. doi: 10.1073/pnas.0307698100
- [555] XHF Zhang and LA Chasin. 2006. Comparison of multiple vertebrate genomes reveals

- the birth and evolution of human exons. *Proc Natl Acad Sci USA*, 103:13427–13432. doi: 10.1073/pnas.0603042103
- [556] M Zeng, Z Hu, X Shi, X Li, X Zhan, XD Li, J Wang, JH Choi, Kw Wang et al. 2014. MAVS, cGAS, and endogenous retroviruses in T-independent B cell responses. *Science*, 346:1486–1492. doi: 10.1126/science.346.6216.1486
- [557] EJ Grow, RA Flynn, SL Chavez, NL Bayless, M Wossidlo, DJ Wesche, L Martin, CB Ware, CA Blish et al. 2015. Intrinsic retroviral reactivation in human preimplantation embryos and pluripotent cells. *Nature*, 522:221–225. doi: 10.1038/nature14308
- [558] N Rosenberg and P Jolicoeur. *Retroviruses*, chapter Retroviral Pathogenesis. Cold Spring Harbor Laboratory Press, 1997
- [559] MG Ott, M Schmidt, K Schwarzwaelder, S Stein, U Siler, U Koehl, H Glimm, K Kühlcke, A Schilz et al. 2006. Correction of X-linked chronic granulomatous disease by gene therapy, augmented by insertional activation of MDS1-EVI1, PRDM16 or SETBP1. *Nat Med*, 12:401–409. doi: 10.1038/nm1393
- [560] CJ Braun, K Boztug, A Paruzynski, M Witzel, A Schwarzer, M Rothe, U Modlich, R Beier, G Göhring et al. 2014. Gene therapy for Wiskott-Aldrich syndrome—long-term efficacy and genotoxicity. *Sci Transl Med*, 6:227ra33. doi: 10.1126/scitranslmed.3007280
- [561] FA Santoni, J Guerra and J Luban. 2012. HERV-H RNA is abundant in human embryonic stem cells and a precise marker for pluripotency. *Retrovirology*, 9:111. doi: 10.1186/1742-4690-9-111
- [562] NV Fuchs, S Loewer, GQ Daley, Z Izsvák, J Löwer and R Löwer. 2013. Human endogenous retrovirus K (HML-2) RNA and protein expression is a marker for human embryonic and induced pluripotent stem cells. *Retrovirology*, 10:115. doi: 10.1186/1742-4690-10-115
- [563] A Fort, K Hashimoto, D Yamada, M Salimullah, CA Keya, A Saxena, A Bonetti, I Voineagu, N Bertin et al. 2014. Deep transcriptome profiling of mammalian stem cells supports a regulatory role for retrotransposons in pluripotency maintenance. *Nat Genet*, 46:558–566. doi: 10.1038/ng.2965
- [564] J Wang, G Xie, M Singh, AT Ghanbarian, T Raskó, A Szvetnik, H Cai, D Besser, A Prigione et al. 2014. Primate-specific endogenous retrovirus-driven transcription defines naive-like stem cells. *Nature*, 516:405–409. doi: 10.1038/nature13804
- [565] B Joos, M Fischer, H Kuster, SK Pillai, JK Wong, J Böni, B Hirschel, R Weber, A Trkola et al. 2008. HIV rebounds from latently infected cells, rather than from continuing low-level replication. *Proc Natl Acad Sci U S A*, 105:16725–16730. doi: 10.1073/pnas.0804192105
- [566] TP Brennan, JO Woods, AR Sedaghat, JD Siliciano, RF Siliciano and CO Wilke.

2009. Analysis of human immunodeficiency virus type 1 viremia and provirus in resting CD4+ T cells reveals a novel source of residual viremia in patients on antiretroviral therapy. *J Virol*, 83:8470–8481. doi: 10.1128/JVI.02568-08
- [567] TA Wagner, JL McKernan, NH Tobin, KA Tapia, JI Mullins and LM Frenkel. 2013. An increasing proportion of monotypic HIV-1 DNA sequences during antiretroviral treatment suggests proliferation of HIV-infected cells. *J Virol*, 87:1770–1778. doi: 10.1128/JVI.01985-12
- [568] MF Kearney, J Spindler, W Shao, S Yu, EM Anderson, A O’Shea, C Rehm, C Poethke, N Kovacs et al. 2014. Lack of detectable HIV-1 molecular evolution during suppressive antiretroviral therapy. *PLoS Pathog*, 10:e1004010. doi: 10.1371/journal.ppat.1004010
- [569] KE Ocwieja*, S Sherrill-Mix*, C Liu, J Song, H Bau and FD Bushman. 2015. A reverse transcription loop-mediated isothermal amplification assay optimized to detect multiple HIV subtypes. *PLoS One*, 10:e0117852. doi: 10.1371/journal.pone.0117852
- [570] CJL Murray, KF Ortblad, C Guinovart, SS Lim, TM Wolock, DA Roberts, EA Dansereau, N Graetz, RM Barber et al. 2014. Global, regional, and national incidence and mortality for HIV, tuberculosis, and malaria during 1990-2013: a systematic analysis for the Global Burden of Disease Study 2013. *Lancet*, 384:1005–1070. doi: 10.1016/S0140-6736(14)60844-8
- [571] KA Sollis, PW Smit, S Fiscus, N Ford, M Vitoria, S Essajee, D Barnett, B Cheng, SM Crowe et al. 2014. Systematic review of the performance of HIV viral load technologies on plasma samples. *PLoS One*, 9:e85869. doi: 10.1371/journal.pone.0085869
- [572] C Liu, M Mauk, R Gross, FD Bushman, PH Edelstein, RG Collman and HH Bau. 2013. Membrane-based, sedimentation-assisted plasma separator for point-of-care applications. *Anal Chem*, 85:10463–10470. doi: 10.1021/ac402459h
- [573] KA Curtis, DL Rudolph, I Nejad, J Singleton, A Beddoe, B Weigl, P LaBarre and SM Owen. 2012. Isothermal amplification using a chemical heating device for point-of-care detection of HIV-1. *PLoS One*, 7:e31432. doi: 10.1371/journal.pone.0031432
- [574] T Notomi, H Okayama, H Masubuchi, T Yonekawa, K Watanabe, N Amino and T Hase. 2000. Loop-mediated isothermal amplification of DNA. *Nucleic Acids Res*, 28:E63
- [575] KA Curtis, DL Rudolph and SM Owen. 2008. Rapid detection of HIV-1 by reverse-transcription, loop-mediated isothermal amplification (RT-LAMP). *J Virol Methods*, 151:264–270. doi: 10.1016/j.jviromet.2008.04.011
- [576] KA Curtis, DL Rudolph and SM Owen. 2009. Sequence-specific detection method for reverse transcription, loop-mediated isothermal amplification of HIV-1. *J Med Virol*, 81:966–972. doi: 10.1002/jmv.21490

- [577] Y Zeng, X Zhang, K Nie, X Ding, BZ Ring, L Xu, L Dai, X Li, W Ren et al. 2014. Rapid quantitative detection of Human immunodeficiency virus type 1 by a reverse transcription-loop-mediated isothermal amplification assay. *Gene*, 541:123–128. doi: 10.1016/j.gene.2014.03.015
- [578] N Hosaka, N Ndembi, A Ishizaki, S Kageyama, K Numazaki and H Ichimura. 2009. Rapid detection of human immunodeficiency virus type 1 group M by a reverse transcription-loop-mediated isothermal amplification assay. *J Virol Methods*, 157: 195–199. doi: 10.1016/j.jviromet.2009.01.004
- [579] KA Curtis, PL Niedzwiedz, AS Youngpairoj, DL Rudolph and SM Owen. 2014. Real-time detection of HIV-2 by reverse transcription-loop-mediated isothermal amplification. *J Clin Microbiol*, 52:2674–2676. doi: 10.1128/JCM.00935-14
- [580] C Kuiken, H Yoon, W Abfalterer, B Gaschen, C Lo and B Korber. 2013. Viral genome analysis and knowledge management. *Methods Mol Biol*, 939:253–261. doi: 10.1007/978-1-62703-107-3_16
- [581] M Manak, S Sina, B Anekella, I Hewlett, E Sanders-Buell, V Ragupathy, J Kim, M Vermeulen, SL Stramer et al. 2012. Pilot studies for development of an HIV subtype panel for surveillance of global diversity. *AIDS Res Hum Retroviruses*, 28:594–606. doi: 10.1089/AID.2011.0271
- [582] J Louwagie, FE McCutchan, M Peeters, TP Brennan, E Sanders-Buell, GA Eddy, G van der Groen, K Fransen, GM Gershy-Damet and R Deleys. 1993. Phylogenetic analysis of gag genes from 70 international HIV-1 isolates provides evidence for multiple genotypes. *AIDS*, 7:769–780
- [583] L Buonaguro, ML Tornesello and FM Buonaguro. 2007. Human immunodeficiency virus type 1 subtype distribution in the worldwide epidemic: pathogenetic and therapeutic implications. *J Virol*, 81:10209–10219. doi: 10.1128/JVI.00872-07
- [584] NF Parrish, F Gao, H Li, EE Giorgi, HJ Barbian, EH Parrish, L Zajic, SS Iyer, JM Decker et al. 2013. Phenotypic properties of transmitted founder HIV-1. *Proc Natl Acad Sci U S A*, 110:6626–6633. doi: 10.1073/pnas.1304288110
- [585] AG Abimiku, TL Stern, A Zwandor, PD Markham, C Calef, S Kyari, WC Saxinger, RC Gallo, M Robert-Guroff and MS Reitz. 1994. Subgroup G HIV type 1 isolates from Nigeria. *AIDS Res Hum Retroviruses*, 10:1581–1583
- [586] Zhang, Chung and Oldenburg. 1999. A simple statistical parameter for use in evaluation and validation of high throughput screening assays. *J Biomol Screen*, 4:67–73. doi: 10.1177/108705719900400206
- [587] C Liu, E Geva, M Mauk, X Qiu, WR Abrams, D Malamud, K Curtis, SM Owen and HH Bau. 2011. An isothermal amplification reactor with an integrated isolation

- membrane for point-of-care detection of infectious diseases. *Analyst*, 136:2069–2076. doi: 10.1039/c1an00007a
- [588] CA Spina, J Anderson, NM Archin, A Bosque, J Chan, M Famiglietti, WC Greene, A Kashuba, SR Lewin et al. 2013. An in-depth comparison of latent HIV-1 reactivation in multiple cell model systems and resting CD4+ T cells from aviremic patients. *PLoS Pathog*, 9:e1003834. doi: 10.1371/journal.ppat.1003834
- [589] G Lehrman, IB Hogue, S Palmer, C Jennings, CA Spina, A Wiegand, AL Landay, RW Coombs, DD Richman et al. 2005. Depletion of latent HIV-1 infection in vivo: a proof-of-concept study. *Lancet*, 366:549–555. doi: 10.1016/S0140-6736(05)67098-5
- [590] NM Archin, M Cheema, D Parker, A Wiegand, RJ Bosch, JM Coffin, J Eron, M Cohen and DM Margolis. 2010. Antiretroviral intensification and valproic acid lack sustained effect on residual HIV-1 viremia or resting CD4+ cell infection. *PLoS One*, 5:e9390. doi: 10.1371/journal.pone.0009390
- [591] AM Spivak, A Andrade, E Eisele, R Hoh, P Bacchetti, NN Bumpus, F Emad, R Buckheit, 3rd, EF McCance-Katz et al. 2014. A pilot study assessing the safety and latency-reversing activity of disulfiram in HIV-1-infected adults on antiretroviral therapy. *Clin Infect Dis*, 58:883–890. doi: 10.1093/cid/cit813
- [592] AR Cillo, MD Sobolewski, RJ Bosch, E Fyne, M Piatak, Jr, JM Coffin and JW Mellors. 2014. Quantification of HIV-1 latency reversal in resting CD4+ T cells from patients on suppressive antiretroviral therapy. *Proc Natl Acad Sci U S A*, 111:7078–7083. doi: 10.1073/pnas.1402873111
- [593] AL Hill, DIS Rosenbloom, F Fu, MA Nowak and RF Siliciano. 2014. Predicting the outcomes of treatment to eradicate the latent reservoir for HIV-1. *Proc Natl Acad Sci U S A*, 111:13475–13480. doi: 10.1073/pnas.1406663111
- [594] ENCODE Project Consortium. 2012. An integrated encyclopedia of DNA elements in the human genome. *Nature*, 489:57–74. doi: 10.1038/nature11247
- [595] T Barrett, SE Wilhite, P Ledoux, C Evangelista, IF Kim, M Tomashevsky, KA Marshall, KH Phillippy, PM Sherman et al. 2013. NCBI GEO: archive for functional genomics data sets–update. *Nucleic Acids Res*, 41:D991–D995. doi: 10.1093/nar/gks1193
- [596] D Karolchik, GP Barber, J Casper, H Clawson, MS Cline, M Diekhans, TR Dreszer, PA Fujita, L Guruvadoo et al. 2014. The UCSC Genome Browser database: 2014 update. *Nucleic Acids Res*, 42:D764–D770. doi: 10.1093/nar/gkt1168
- [597] M Goldman, B Craft, T Swatloski, M Cline, O Morozova, M Diekhans, D Haussler and J Zhu. 2015. The UCSC Cancer Genomics Browser: update 2015. *Nucleic Acids Res*, 43:D812–D817. doi: 10.1093/nar/gku1073
- [598] F Cunningham, MR Amode, D Barrell, K Beal, K Billis, S Brent, D Carvalho-Silva,

- P Clapham, G Coates et al. 2015. Ensembl 2015. *Nucleic Acids Res*, 43:D662–D669. doi: 10.1093/nar/gku1010
- [599] ML Metzker. 2010. Sequencing technologies - the next generation. *Nat Rev Genet*, 11: 31–46. doi: 10.1038/nrg2626
- [600] ER Mardis. 2011. A decade’s perspective on DNA sequencing technology. *Nature*, 470: 198–203. doi: 10.1038/nature09796
- [601] K Wetterstrand. 2015. DNA Sequencing Costs: Data from the NHGRI Genome Sequencing Program (GSP). URL www.genome.gov/sequencingcosts
- [602] DP Depledge, AL Palser, SJ Watson, IYC Lai, ER Gray, P Grant, RK Kanda, E Leproust, P Kellam and J Breuer. 2011. Specific capture and whole-genome sequencing of viruses from clinical samples. *PLoS One*, 6:e27805. doi: 10.1371/journal.pone.0027805
- [603] TR Mercer, MB Clark, J Crawford, ME Brunck, DJ Gerhardt, RJ Taft, LK Nielsen, ME Dinger and JS Mattick. 2014. Targeted sequencing for gene discovery and quantification using RNA CaptureSeq. *Nat Protoc*, 9:989–1009. doi: 10.1038/nprot.2014.058
- [604] JJ Mosher, B Bowman, EL Bernberg, O Shevchenko, J Kan, J Korlach and LA Kaplan. 2014. Improved performance of the PacBio SMRT technology for 16S rDNA sequencing. *J Microbiol Methods*, 104:59–60. doi: 10.1016/j.mimet.2014.06.012
- [605] AS Mikheyev and MMY Tin. 2014. A first look at the Oxford Nanopore MinION sequencer. *Mol Ecol Resour*, 14:1097–1102. doi: 10.1111/1755-0998.12324
- [606] M Jain, IT Fiddes, KH Miga, HE Olsen, B Paten and M Akeson. 2015. Improved data analysis for the MinION nanopore sequencer. *Nat Methods*, 12:351–356. doi: 10.1038/nmeth.3290
- [607] A Kilianski, JL Haas, EJ Corriveau, AT Liem, KL Willis, DR Kadavy, CN Rosenzweig and SS Minot. 2015. Bacterial and viral identification and differentiation by amplicon sequencing on the MinION nanopore sequencer. *Gigascience*, 4:12. doi: 10.1186/s13742-015-0051-z
- [608] S Jünemann, FJ Sedlazeck, K Prior, A Albersmeier, U John, J Kalinowski, A Mellmann, A Goesmann, A von Haeseler et al. 2013. Updating benchtop sequencing performance comparison. *Nat Biotechnol*, 31:294–296. doi: 10.1038/nbt.2522
- [609] Illumina, Inc. 2015. System specification sheet: MiSeq system. URL <http://www.illumina.com/products/miseq-reagent-kit-v3.html>
- [610] D Rossell, C Stephan-Otto Attolini, M Kroiss and A Stöcker. 2014. Quantifying alternative splicing from paired-end RNA-sequencing data. *Ann Appl Stat*, 8:309–330. doi: 10.1214/13-AOAS687

- [611] N Bray, H Pimentel, P Melsted and L Pachter. 2015. Near-optimal RNA-Seq quantification. *arXiv preprint*, page 1505.02710
- [612] NL Michael, MT Vahey, L d’Arcy, PK Ehrenberg, JD Mosca, J Rappaport and RR Redfield. 1994. Negative-strand RNA transcripts are produced in human immunodeficiency virus type 1-infected cells and patients by a novel promoter downregulated by Tat. *J Virol*, 68:979–987
- [613] S Landry, M Halin, S Lefort, B Audet, C Vaquero, JM Mesnard and B Barbeau. 2007. Detection, characterization and regulation of antisense transcripts in HIV-1. *Retrovirology*, 4:71. doi: 10.1186/1742-4690-4-71
- [614] NCT Schopman, M Willemsen, YP Liu, T Bradley, A van Kampen, F Baas, B Berkhout and J Haasnoot. 2012. Deep sequencing of virus-infected cells reveals HIV-encoded small RNAs. *Nucleic Acids Res*, 40:414–427. doi: 10.1093/nar/gkr719
- [615] M Kobayashi-Ishihara, M Yamagishi, T Hara, Y Matsuda, R Takahashi, A Miyake, K Nakano, T Yamochi, T Ishida and T Watanabe. 2012. HIV-1-encoded antisense RNA suppresses viral replication for a prolonged period. *Retrovirology*, 9:38. doi: 10.1186/1742-4690-9-38
- [616] S Saayman, A Ackley, AMW Turner, M Famiglietti, A Bosque, M Clemson, V Planelles and KV Morris. 2014. An HIV-encoded antisense long noncoding RNA epigenetically regulates viral transcription. *Mol Ther*, 22:1164–1175. doi: 10.1038/mt.2014.29
- [617] CT Berger, A Llano, JM Carlson, ZL Brumme, MA Brockman, S Cedeño, PR Harrigan, DE Kaufmann, D Heckerman et al. 2015. Immune screening identifies novel T cell targets encoded by antisense reading frames of HIV-1. *J Virol*, 89:4015–4019. doi: 10.1128/JVI.03435-14
- [618] LB Ludwig, JL Ambrus, KA Krawczyk, S Sharma, S Brooks, CB Hsiao and SA Schwartz. 2006. Human Immunodeficiency Virus-Type 1 LTR DNA contains an intrinsic gene producing antisense RNA and protein products. *Retrovirology*, 3:80. doi: 10.1186/1742-4690-3-80
- [619] C Torresilla, É Larocque, S Landry, M Halin, Y Coulombe, JY Masson, JM Mesnard and B Barbeau. 2013. Detection of the HIV-1 minus-strand-encoded antisense protein and its association with autophagy. *J Virol*, 87:5089–5105. doi: 10.1128/JVI.00225-13
- [620] A Bansal, J Carlson, J Yan, OT Akinsiku, M Schaefer, S Sabbaj, A Bet, DN Levy, S Heath et al. 2010. CD8 T cell response and evolutionary pressure to HIV-1 cryptic epitopes derived from antisense transcription. *J Exp Med*, 207:51–59. doi: 10.1084/jem.20092060
- [621] JZ Levin, M Yassour, X Adiconis, C Nusbaum, DA Thompson, N Friedman, A Gnirke and A Regev. 2010. Comprehensive comparative analysis of strand-specific RNA sequencing methods. *Nat Methods*, 7:709–715. doi: 10.1038/nmeth.1491

- [622] J Podnar, H Deiderick, G Huerta and S Hunicke-Smith. 2014. Next-generation sequencing RNA-Seq library construction. *Curr Protoc Mol Biol*, 106:4.21.1–4.21.19. doi: 10.1002/0471142727.mb0421s106
- [623] S Cardinaud, A Moris, M Février, PS Rohrlich, L Weiss, P Langlade-Demoyen, FA Lemonnier, O Schwartz and A Habel. 2004. Identification of cryptic MHC I-restricted epitopes encoded by HIV-1 alternative reading frames. *J Exp Med*, 199: 1053–1063. doi: 10.1084/jem.20031869
- [624] CT Berger, JM Carlson, CJ Brumme, KL Hartman, ZL Brumme, LM Henry, PC Rosato, A Piechocka-Trocha, MA Brockman et al. 2010. Viral adaptation to immune selection pressure by HLA class I-restricted CTL responses targeting epitopes in HIV frameshift sequences. *J Exp Med*, 207:61–75. doi: 10.1084/jem.20091808
- [625] NT Ingolia, S Ghaemmaghami, JRS Newman and JS Weissman. 2009. Genome-wide analysis in vivo of translation with nucleotide resolution using ribosome profiling. *Science*, 324:218–223. doi: 10.1126/science.1168978
- [626] NT Ingolia, LF Lareau and JS Weissman. 2011. Ribosome profiling of mouse embryonic stem cells reveals the complexity and dynamics of mammalian proteomes. *Cell*, 147: 789–802. doi: 10.1016/j.cell.2011.10.002
- [627] NT Ingolia. 2014. Ribosome profiling: new views of translation, from single codons to genome scale. *Nat Rev Genet*, 15:205–213. doi: 10.1038/nrg3645
- [628] NJ Maness, AD Walsh, SM Piaskowski, J Furlott, HL Kolar, AT Bean, NA Wilson and DI Watkins. 2010. CD8+ T cell recognition of cryptic epitopes is a ubiquitous feature of AIDS virus infection. *J Virol*, 84:11569–11574. doi: 10.1128/JVI.01419-10
- [629] A Bet, EA Maze, A Bansal, S Sterrett, A Gross, S Graff-Dubois, A Samri, A Guihot, C Katlama et al. 2015. The HIV-1 antisense protein (ASP) induces CD8 T cell responses during chronic infection. *Retrovirology*, 12:15. doi: 10.1186/s12977-015-0135-y
- [630] S Koenig, HE Gendelman, JM Orenstein, MC Dal Canto, GH Pezeshkpour, M Yungbluth, F Janotta, A Aksamit, MA Martin and AS Fauci. 1986. Detection of AIDS virus in macrophages in brain tissue from AIDS patients with encephalopathy. *Science*, 233:1089–1093. doi: 10.1126/science.3016903
- [631] S Sonza, HP Mutimer, R Oelrichs, D Jardine, K Harvey, A Dunne, DF Purcell, C Birch and SM Crowe. 2001. Monocytes harbour replication-competent, non-latent HIV-1 in patients on highly active antiretroviral therapy. *AIDS*, 15:17–22
- [632] M Hermankova, JD Siliciano, Y Zhou, D Monie, K Chadwick, JB Margolick, TC Quinn and RF Siliciano. 2003. Analysis of human immunodeficiency virus type 1 gene expression in latently infected resting CD4+ T lymphocytes in vivo. *J Virol*, 77: 7383–7392. doi: 10.1128/JVI.77.13.7383-7392.2003

- [633] N Soriano-Sarabia, RE Bateson, NP Dahl, AM Crooks, JD Kuruc, DM Margolis and NM Archin. 2014. Quantitation of replication-competent HIV-1 in populations of resting CD4+ T cells. *J Virol*, 88:14070–14077. doi: 10.1128/JVI.01900-14
- [634] BF Keele, EE Giorgi, JF Salazar-Gonzalez, JM Decker, KT Pham, MG Salazar, C Sun, T Grayson, S Wang et al. 2008. Identification and characterization of transmitted and early founder virus envelopes in primary HIV-1 infection. *Proc Natl Acad Sci USA*, 105:7552–7557. doi: 10.1073/pnas.0802203105
- [635] JF Salazar-Gonzalez, MG Salazar, BF Keele, GH Learn, EE Giorgi, H Li, JM Decker, S Wang, J Baalwa et al. 2009. Genetic identity, biological phenotype, and evolutionary pathways of transmitted/founder viruses in acute and early HIV-1 infection. *J Exp Med*, 206:1273–1289. doi: 10.1084/jem.20090378
- [636] MP Wentz, BE Moore, MW Cloyd, SM Berget and LA Donehower. 1997. A naturally arising mutation of a potential silencer of exon splicing in human immunodeficiency virus type 1 induces dominant aberrant splicing and arrests virus production. *J Virol*, 71:8542–8551
- [637] JM Madsen and CM Stoltzfus. 2005. An exonic splicing silencer downstream of the 3' splice site A2 is required for efficient human immunodeficiency virus type 1 replication. *J Virol*, 79:10478–10486. doi: 10.1128/JVI.79.16.10478-10486.2005
- [638] S Paca-Uccaralertkun, CK Damgaard, P Auewarakul, A Thitithanyanont, P Suphaphiphat, M Essex, J Kjemis and TH Lee. 2006. The effect of a single nucleotide substitution in the splicing silencer in the tat/rev intron on HIV type 1 envelope expression. *AIDS Research & Human Retroviruses*, 22:76–82. doi: 10.1089/aid.2006.22.76
- [639] D Mandal, Z Feng and CM Stoltzfus. 2008. Gag-processing defect of human immunodeficiency virus type 1 integrase E246 and G247 mutants is caused by activation of an overlapping 5' splice site. *J Virol*, 82:1600–1604. doi: 10.1128/JVI.02295-07
- [640] FD Bushman, N Malani, J Fernandes, I D'Orso, G Cagney, TL Diamond, H Zhou, DJ Hazuda, AS Espeseth et al. 2009. Host cell factors in HIV replication: meta-analysis of genome-wide studies. *PLoS Pathog*, 5:e1000437. doi: 10.1371/journal.ppat.1000437
- [641] T Fukuhara, T Hosoya, S Shimizu, K Sumi, T Oshiro, Y Yoshinaka, M Suzuki, N Yamamoto, LA Herzenberg et al. 2006. Utilization of host SR protein kinases and RNA-splicing machinery during viral replication. *Proc Natl Acad Sci USA*, 103:11329–11333. doi: 10.1073/pnas.0604616103
- [642] R Wong, A Balachandran, AY Mao, W Dobson, S Gray-Owen and A Cochrane. 2011. Differential effect of CLK SR Kinases on HIV-1 gene expression: potential novel targets for therapy. *Retrovirology*, 8:47. doi: 10.1186/1742-4690-8-47
- [643] RW Wong, A Balachandran, MA Ostrowski and A Cochrane. 2013. Digoxin suppresses

- HIV-1 replication by altering viral RNA processing. *PLoS Pathog*, 9:e1003241. doi: 10.1371/journal.ppat.1003241
- [644] TH Finkel, G Tudor-Williams, NK Banda, MF Cotton, T Curiel, C Monks, TW Baba, RM Ruprecht and A Kupfer. 1995. Apoptosis occurs predominantly in bystander cells and not in productively infected cells of HIV- and SIV-infected lymph nodes. *Nat Med*, 1:129–134. doi: 10.1038/nm0295-129
- [645] G Doitsh, NLK Galloway, X Geng, Z Yang, KM Monroe, O Zepeda, PW Hunt, H Hatano, S Sowinski et al. 2014. Cell death by pyroptosis drives CD4 T-cell depletion in HIV-1 infection. *Nature*, 505:509–514. doi: 10.1038/nature12940
- [646] B Bahbouhi and L al Harthi. 2004. Enriching for HIV-infected cells using anti-gp41 antibodies indirectly conjugated to magnetic microbeads. *Biotechniques*, 36:139–147
- [647] S Hrvatin, F Deng, CW O’Donnell, DK Gifford and DA Melton. 2014. MARIS: method for analyzing RNA following intracellular sorting. *PLoS One*, 9:e89459. doi: 10.1371/journal.pone.0089459
- [648] M Wilkinson. 1988. A rapid and convenient method for isolation of nuclear, cytoplasmic and total cellular RNA. *Nucleic Acids Res*, 16:10934. doi: 10.1093/nar/16.22.1093
- [649] HW Trask, R Cowper-Sal-lari, MA Sartor, J Gui, CV Heath, J Renuka, AJ Higgins, P Andrews, M Korc et al. 2009. Microarray analysis of cytoplasmic versus whole cell RNA reveals a considerable number of missed and false positive mRNAs. *RNA*, 15: 1917–1928. doi: 10.1261/rna.1677409
- [650] BW Solnestam, H Stranneheim, J Hällman, M Käller, E Lundberg, J Lundeberg and P Akan. 2012. Comparison of total and cytoplasmic mRNA reveals global regulation by nuclear retention and miRNAs. *BMC Genomics*, 13:574. doi: 10.1186/1471-2164-13-574
- [651] M Lagos-Quintana, R Rauhut, W Lendeckel and T Tuschl. 2001. Identification of novel genes coding for small expressed RNAs. *Science*, 294:853–858. doi: 10.1126/science.1064921
- [652] V Ambros. 2004. The functions of animal microRNAs. *Nature*, 431:350–355. doi: 10.1038/nature02871
- [653] P Landgraf, M Rusu, R Sheridan, A Sewer, N Iovino, A Aravin, S Pfeffer, A Rice, AO Kamphorst et al. 2007. A mammalian microRNA expression atlas based on small RNA library sequencing. *Cell*, 129:1401–1414. doi: 10.1016/j.cell.2007.04.040
- [654] Z Klase, P Kale, R Winograd, MV Gupta, M Heydarian, R Berro, T McCaffrey and F Kashanchi. 2007. HIV-1 TAR element is processed by Dicer to yield a viral micro-RNA involved in chromatin remodeling of the viral LTR. *BMC Mol Biol*, 8:63. doi: 10.1186/1471-2199-8-63

- [655] DL Ouellet, I Plante, P Landry, C Barat, ME Janelle, L Flamand, MJ Tremblay and P Provost. 2008. Identification of functional microRNAs released through asymmetrical processing of HIV-1 TAR element. *Nucleic Acids Res*, 36:2353–2365. doi: 10.1093/nar/gkn076
- [656] Z Klase, R Winograd, J Davis, L Carpio, R Hildreth, M Heydarian, S Fu, T McCaffrey, E Meiri et al. 2009. HIV-1 TAR miRNA protects against apoptosis by altering cellular gene expression. *Retrovirology*, 6:18. doi: 10.1186/1742-4690-6-18
- [657] S Omoto, M Ito, Y Tsutsumi, Y Ichikawa, H Okuyama, EA Brisibe, NK Saksena and YR Fujii. 2004. HIV-1 nef suppression by virally encoded microRNA. *Retrovirology*, 1: 44. doi: 10.1186/1742-4690-1-44
- [658] C Chable-Bessia, O Meziane, D Latreille, R Triboulet, A Zamborlini, A Wagschal, JM Jacquet, J Reynes, Y Levy et al. 2009. Suppression of HIV-1 replication by microRNA effectors. *Retrovirology*, 6:26. doi: 10.1186/1742-4690-6-26
- [659] S Pfeffer, A Sewer, M Lagos-Quintana, R Sheridan, C Sander, FA Grässer, LF van Dyk, CK Ho, S Shuman et al. 2005. Identification of microRNAs of the herpesvirus family. *Nat Methods*, 2:269–276. doi: 10.1038/nmeth746
- [660] TL Sung and AP Rice. 2009. miR-198 inhibits HIV-1 gene expression and replication in monocytes and its mechanism of action appears to involve repression of cyclin T1. *PLoS Pathog*, 5:e1000263. doi: 10.1371/journal.ppat.1000263
- [661] G Swaminathan, F Rossi, LJ Sierra, A Gupta, S Navas-Martín and J Martín-García. 2012. A role for microRNA-155 modulation in the anti-HIV-1 effects of Toll-like receptor 3 stimulation in macrophages. *PLoS Pathog*, 8:e1002937. doi: 10.1371/journal.ppat.1002937
- [662] HS Zhang, TC Wu, WW Sang and Z Ruan. 2012. MiR-217 is involved in Tat-induced HIV-1 long terminal repeat (LTR) transactivation by down-regulation of SIRT1. *Biochim Biophys Acta*, 1823:1017–1023. doi: 10.1016/j.bbamcr.2012.02.014
- [663] HS Zhang, XY Chen, TC Wu, WW Sang and Z Ruan. 2012. MiR-34a is involved in Tat-induced HIV-1 long terminal repeat (LTR) transactivation through the SIRT1/NFκB pathway. *FEBS Lett*, 586:4203–4207. doi: 10.1016/j.febslet.2012.10.023
- [664] K Chiang, H Liu and AP Rice. 2013. miR-132 enhances HIV-1 replication. *Virology*, 438:1–4. doi: 10.1016/j.virol.2012.12.016
- [665] E Orecchini, M Doria, A Michienzi, E Giuliani, L Vassena, SA Ciafrè, MG Farace and S Galardi. 2014. The HIV-1 Tat protein modulates CD4 expression in human T cells through the induction of miR-222. *RNA Biol*, 11:334–338. doi: 10.4161/rna.28372
- [666] L Farberov, E Herzig, S Modai, O Isakov, A Hizi and N Shomron. 2015. MicroRNA-

- mediated regulation of p21 and TASK1 cellular restriction factors enhances HIV-1 infection. *J Cell Sci*, 128:1607–1616. doi: 10.1242/jcs.167817
- [667] J Huang, F Wang, E Argyris, K Chen, Z Liang, H Tian, W Huang, K Squires, G Verlinghieri and H Zhang. 2007. Cellular microRNAs contribute to HIV-1 latency in resting primary CD4+ T lymphocytes. *Nat Med*, 13:1241–1247. doi: 10.1038/nm1639
- [668] K Chiang, TL Sung and AP Rice. 2012. Regulation of cyclin T1 and HIV-1 Replication by microRNAs in resting CD4+ T lymphocytes. *J Virol*, 86:3244–3252. doi: 10.1128/JVI.05065-11
- [669] K Chiang and AP Rice. 2012. MicroRNA-mediated restriction of HIV-1 in resting CD4+ T cells and monocytes. *Viruses*, 4:1390–1409. doi: 10.3390/v4091390
- [670] PJ Kanki, DJ Hamel, JL Sankalé, C Hsieh, I Thior, F Barin, SA Woodcock, A Guèye-Ndiaye, E Zhang et al. 1999. Human immunodeficiency virus type 1 subtypes differ in disease progression. *J Infect Dis*, 179:68–73. doi: 10.1086/314557
- [671] P Kaleebu, N French, C Mahe, D Yirrell, C Watera, F Lyagoba, J Nakiyingi, A Rutebemberwa, D Morgan et al. 2002. Effect of human immunodeficiency virus (HIV) type 1 envelope subtypes A and D on disease progression in a large cohort of HIV-1-positive persons in Uganda. *J Infect Dis*, 185:1244–1250. doi: 10.1086/340130
- [672] JM Baeten, B Chohan, L Lavreys, V Chohan, RS McClelland, L Certain, K Mandaliya, W Jaoko and J Overbaugh. 2007. HIV-1 subtype D infection is associated with faster disease progression than subtype A in spite of similar plasma HIV-1 loads. *J Infect Dis*, 195:1177–1180. doi: 10.1086/512682
- [673] N Kiwanuka, O Laeyendecker, M Robb, G Kigozi, M Arroyo, F McCutchan, LA Eller, M Eller, F Makumbi et al. 2008. Effect of human immunodeficiency virus Type 1 (HIV-1) subtype on disease progression in persons from Rakai, Uganda, with incident HIV-1 infection. *J Infect Dis*, 197:707–713. doi: 10.1086/527416
- [674] B Renjifo, P Gilbert, B Chaplin, G Msamanga, D Mwakagile, W Fawzi, M Essex, TV and HIVS Group. 2004. Preferential in-utero transmission of HIV-1 subtype C as compared to HIV-1 subtype A or D. *AIDS*, 18:1629–1636
- [675] GC John-Stewart, RW Nduati, CM Rousseau, DA Mbori-Ngacha, BA Richardson, S Rainwater, DD Panteleeff and J Overbaugh. 2005. Subtype C Is associated with increased vaginal shedding of HIV-1. *J Infect Dis*, 192:492–496. doi: 10.1086/431514
- [676] W Huang, SH Eshleman, J Toma, S Fransen, E Stawiski, EE Paxinos, JM Whitcomb, AM Young, D Donnell et al. 2007. Coreceptor tropism in human immunodeficiency virus type 1 subtype D: high prevalence of CXCR4 tropism and heterogeneous composition of viral populations. *J Virol*, 81:7885–7893. doi: 10.1128/JVI.00218-07
- [677] J Snoeck, R Kantor, RW Shafer, K Van Laethem, K Deforche, AP Carvalho, B Wyn-

- hoven, MA Soares, P Cane et al. 2006. Discordances between interpretation algorithms for genotypic resistance to protease and reverse transcriptase inhibitors of human immunodeficiency virus are subtype dependent. *Antimicrob Agents Chemother*, 50: 694–701. doi: 10.1128/AAC.50.2.694-701.2006
- [678] PJ Easterbrook, M Smith, J Mullen, S O’Shea, I Chrystie, A de Ruiter, ID Tatt, AM Geretti and M Zuckerman. 2010. Impact of HIV-1 viral subtype on disease progression and response to antiretroviral therapy. *J Int AIDS Soc*, 13:4. doi: 10.1186/1758-2652-13-4
- [679] AU Scherrer, B Ledergerber, V von Wyl, J Böni, S Yerly, T Klimkait, P Bürgisser, A Rauch, B Hirschel et al. 2011. Improved virological outcome in White patients infected with HIV-1 non-B subtypes compared to subtype B. *Clin Infect Dis*, 53: 1143–1152. doi: 10.1093/cid/cir669
- [680] C Liu, MM Sadik, MG Mauk, PH Edelstein, FD Bushman, R Gross and HH Bau. 2014. Nuclemeter: a reaction-diffusion based method for quantifying nucleic acids undergoing enzymatic amplification. *Sci Rep*, 4:7335. doi: 10.1038/srep07335
- [681] MG Mauk, C Liu, M Sadik and HH Bau. 2015. Microfluidic devices for nucleic acid (NA) isolation, isothermal NA amplification, and real-time detection. *Methods Mol Biol*, 1256:15–40. doi: 10.1007/978-1-4939-2172-0_2
- [682] A Piantadosi, B Chohan, V Chohan, RS McClelland and J Overbaugh. 2007. Chronic HIV-1 infection frequently fails to protect against superinfection. *PLoS Pathog*, 3:e177. doi: 10.1371/journal.ppat.0030177
- [683] RLR Powell, MM Urbanski, S Burda, T Kinge and PN Nyambi. 2009. High frequency of HIV-1 dual infections among HIV-positive individuals in Cameroon, West Central Africa. *J Acquir Immune Defic Syndr*, 50:84–92. doi: 10.1097/QAI.0b013e31818d5a40
- [684] K Ronen, CO McCoy, FA Matsen, DF Boyd, S Emery, K Odem-Davis, W Jaoko, K Mandaliya, RS McClelland et al. 2013. HIV-1 superinfection occurs less frequently than initial infection in a cohort of high-risk Kenyan women. *PLoS Pathog*, 9:e1003593. doi: 10.1371/journal.ppat.1003593
- [685] AD Redd, D Ssemwanga, J Vandepitte, SK Wendel, N Ndembu, J Bukonya, S Nakubulwa, H Grosskurth, CM Parry et al. 2014. Rates of HIV-1 superinfection and primary HIV-1 infection are similar in female sex workers in Uganda. *AIDS*, 28:2147–2152. doi: 10.1097/QAD.0000000000000365
- [686] AD Redd, CE Mullis, D Serwadda, X Kong, C Martens, SM Ricklefs, AAR Tobian, C Xiao, MK Grabowski et al. 2012. The rates of HIV superinfection and primary HIV incidence in a general population in Rakai, Uganda. *J Infect Dis*, 206:267–274. doi: 10.1093/infdis/jis325
- [687] S Jost, MC Bernard, L Kaiser, S Yerly, B Hirschel, A Samri, B Autran, LE Goh and

- L Perrin. 2002. A patient with HIV-1 superinfection. *N Engl J Med*, 347:731–736. doi: 10.1056/NEJMoa020263
- [688] G Fang, B Weiser, C Kuiken, SM Philpott, S Rowland-Jones, F Plummer, J Kimani, B Shi, R Kaul et al. 2004. Recombination following superinfection by HIV-1. *AIDS*, 18:153–159
- [689] G Blick, RM Kagan, E Coakley, C Petropoulos, L Maroldo, P Greiger-Zanlungo, S Gretz and T Garton. 2007. The probable source of both the primary multidrug-resistant (MDR) HIV-1 strain found in a patient with rapid progression to AIDS and a second recombinant MDR strain found in a chronically HIV-1-infected patient. *J Infect Dis*, 195:1250–1259. doi: 10.1086/512240
- [690] GS Gottlieb, DC Nickle, MA Jensen, KG Wong, RA Kaslow, JC Shepherd, JB Margolick and JI Mullins. 2007. HIV type 1 superinfection with a dual-tropic virus and rapid progression to AIDS: a case report. *Clin Infect Dis*, 45:501–509. doi: 10.1086/520024
- [691] H Streeck, B Li, AFY Poon, A Schneidewind, AD Gladden, KA Power, D Daskalakis, S Bazner, R Zuniga et al. 2008. Immune-driven recombination and loss of control after HIV superinfection. *J Exp Med*, 205:1789–1796. doi: 10.1084/jem.20080281
- [692] O Clerc, S Colombo, S Yerly, A Telenti and M Cavassini. 2010. HIV-1 elite controllers: beware of super-infections. *J Clin Virol*, 47:376–378. doi: 10.1016/j.jcv.2010.01.013
- [693] DM Smith, JK Wong, GK Hightower, CC Ignacio, KK Koelsch, CJ Petropoulos, DD Richman and SJ Little. 2005. HIV drug resistance acquired through superinfection. *AIDS*, 19:1251–1256
- [694] M Pernas, C Casado, R Fuentes, MJ Pérez-Elías and C López-Galíndez. 2006. A dual superinfection and recombination within HIV-1 subtype B 12 years after primoinfection. *J Acquir Immune Defic Syndr*, 42:12–18. doi: 10.1097/01.qai.0000214810.65292.73
- [695] DL Robertson, PM Sharp, FE McCutchan and BH Hahn. 1995. Recombination in HIV-1. *Nature*, 374:124–126. doi: 10.1038/374124b0
- [696] MH Malim and M Emerman. 2001. HIV-1 sequence variation: drift, shift, and attenuation. *Cell*, 104:469–472. doi: 10.1016/S0092-8674(01)00234-3
- [697] SK Gire, A Goba, KG Andersen, RSG Sealfon, DJ Park, L Kanneh, S Jalloh, M Momoh, M Fullah et al. 2014. Genomic surveillance elucidates Ebola virus origin and transmission during the 2014 outbreak. *Science*, 345:1369–1372. doi: 10.1126/science.1259657
- [698] WHO Ebola Response Team. 2014. Ebola virus disease in West Africa—the first 9 months of the epidemic and forward projections. *N Engl J Med*, 371:1481–1495. doi: 10.1056/NEJMoa1411100

- [699] World Health Organization. 2015. Ebola situation report: 13 May 2014. URL <http://apps.who.int/ebola/en/current-situation/ebola-situation-report-13-may-2015>
- [700] G Chowell and H Nishiura. 2014. Transmission dynamics and control of Ebola virus disease (EVD): a review. *BMC Med*, 12:196. doi: 10.1186/s12916-014-0196-0
- [701] AS Fauci. 2014. Ebola—underscoring the global disparities in health care resources. *N Engl J Med*, 371:1084–1086. doi: 10.1056/NEJMp1409494
- [702] World Health Organization. 2015. Interim guidance on the use of rapid Ebola antigen detection tests. URL <http://www.who.int/csr/resources/publications/ebola/ebola-antigen-detection/en/>
- [703] Y Kurosaki, A Takada, H Ebihara, A Grolla, N Kamo, H Feldmann, Y Kawaoka and J Yasuda. 2007. Rapid and simple detection of Ebola virus by reverse transcription-loop-mediated isothermal amplification. *J Virol Methods*, 141:78–83. doi: 10.1016/j.jviromet.2006.11.031
- [704] T Hoenen, D Safronetz, A Groseth, KR Wollenberg, OA Koita, B Diarra, IS Fall, FC Haidara, F Diallo et al. 2015. Mutation rate and genotype variation of Ebola virus from Mali case sequences. *Science*, 348:117–119. doi: 10.1126/science.aaa5646